An-Najah National University

Faculty of Graduate Study

Influence of Bearing Non-Reinforced Parameter Walls with Stone Cladding on Fundamental Period Computation

By

Mohammad O. Halahla

Supervisor

Dr. Abdul Razzaq A. Touqan

Co-Supervisor

Dr. Munther D. Ibrahim

This Thesis is Submitted in Partial Fulfillment of the Requirements for the Degree of Master of Construction Engineering, Faculty of Graduate Studies, An-Najah National University, Nablus, Palestine.

2019

Influence of Bearing Non-Reinforced Parameter Walls with Stone Cladding on Fundamental Period Computation

By

Mohammad O. Halahla

This thesis was Defended successfully on 21/8/2019, and approved by:

Defense Committee Members	**Signature**
1. Dr. Abdul Razzaq A. Touqan / Supervisor	Abdul Razzaq Touqan
2. Dr. Munther D. Ibrahim / Co-Supervisor	....
3. Dr. Abdulsamee Halahla / External Examiner	....
4. Dr. Mohammad Samaneh / Internal Examiner	....

Dedication

To My Parents, Brother, Sister, and My Beloved Wife

ACKNOWLEDGMENT

Praise be to Allah, Lord of the World's, first of all

I would like to thank whoever participated in this effort

Many thanks and regards to Dr. Abdul-Razaq Touqan, and Dr. Munther Ibrahim for their valuable efforts in completing this work.

الإقرار

أنا الموقع أدناه مقدم الرسالة التي تحمل عنوان

Influence of Bearing Non-Reinforced Parameter Walls with Stone Cladding on Fundamental Period Computation

أقر بأن ما اشتملت عليه هذه الرسالة إنما هو نتاج جهدي الخاص، باستثناء ما تمت الإشارة اليه حيثما ورد، وأن هذه الرسالة ككل، أو أي جزء منها لم يقدم من قبل لنيل أية درجة علمية أو بحث علمي أو بحثي لدى أية مؤسسة تعليمية أو بحثية أخرى.

Declaration

The work provided in this thesis, unless otherwise referenced, is the researcher's own work, and has not been submitted elsewhere for any other degree or qualification.

Student's Name: **اسم الطالب: محمد عمر حلاحلة**

Signature: **التوقيع:**

Date: **التاريخ:**

Table of Contents

Table of Figures

List of Tables

List of Symbols

T_n = Natural Period

A_B = area of base of structure, (ft^2)

A_i = web area of shear wall i , (ft^2)

D_i = length of shear wall i in ft

h_i = height of shear wall i in ft

x = number of shear walls in the building effective in resisting lateral forces in the direction under consideration

m = Mass of structural system

k = Lateral stiffness

d_{inf} = Diagonal length of the infill wall

h_{inf} = Height of infill wall

λ_h =horizontal contact length between the frame and the diagonal strut

E_c = Modulus of Elasticity of Concrete

Ac = Gross Area of Column in a frame

G_{inf} = Shear modulus of infill walls

A_{inf} = Area of infill is the product of infill length by strut thickness

L = Center to center spacing between columns in frame

h = Center to center frame height

θ = Angle between diagonal and horizontal projection of the diagonal

t = thickness of infill panel

E_{inf} = Modulus of Elasticity of infill walls

I_c = Moment of intertia for column in the frame

I_b = Moment of intertia for beam in the frame

α_h =contact length between infill wall and column at the time of initial failure of wall.

α_L =the contact length between infill wall and beam respectively at the time of initial failure of wall.

v_{inf} = Poisson's ratio of infill wall

A_b = Beam's area

t_e=sum of the thickness of the two face shells for hollow or semi-solid block units and the thickness of the wall for solid or fully grouted hollow or semi-solid block units.

l_s = Diagonal length of the equivalent strut

α_w = infill wall opening percentage (area of opening to the area of infill wall)

ρ_w = Width reduction factor

$$\alpha_{co} = \text{Opening Area Ratio} = \frac{\text{Area of Opening } (A_{op})}{\text{Area of Infill } (A_{inf})}$$

w = width of equivalent strut

N = Number of stories above the base

t_{inf}=strut thickness

l_n = Clear distance between columns

Vu = Ultimate shear strength

Vc = Shear capacity

f'_c = compressive strength of concrete

b_0 =Perimeter of the critical section taken at (d/2) from the loaded area

d = effective depth of slab

λ = factor to determine wether concrete is normal weight or not

I_g = Gross moment of interia of the section (non − cracked)

T_a = Approximate fundamental period

w_i = The portion of the total seismic dead load located at or assigned to level i

δ_i = the horizontal displacement at level i relative to the base due to applied lateral forces

g = the acceleration due to gravity

f_i = the lateral force at level i

C_s = The seismic response coeffi cient determined in accordance with Section 12.8.1.1 in ASCE7 − 10

W = the effective seismic weight per Section 12.7.2 in ASCE7 − 10

S_{DS}= the design spectral response acceleration parameter in the short period range as determined from Section 11.4.4 or 11.4.7 in ASCE7-10.

R=the response modification factor in Table 12.2-1 in ASCE7-10.

I_e=the importance factor determined in accordance with Section 11.5.1 in ASCE7-10

Influence of Bearing Non-Reinforced Parameter Walls with Stone Cladding on Fundamental Period Computation

By
Mohammad O. Halahla
Supervisor
Dr. Abdul Razzaq A. Touqan
Co-Supervisor
Dr. Munther D. Ibrahim

Abstract

The behavior of the majority of structures in Palestine against earthquakes cannot be confidently predicted; as the construction methodology usually includes constructing framing system, where gaps in the frames are filled by panels of non-reinforced layers of either plain concrete or a layer of voided bricks.

Usually a natural stone cladding is attached to infill walls forming facades. The main questions that affect the analysis of this type of structures are how to model these walls in order to have an accurate simulation? And whether including these walls in the modeling affect the behavior of structures against earthquakes?

The understanding of the response of structures to earthquake loads depends mainly on the computed value of the fundamental period. A reliable estimation of the fundamental period is considered as an essential step in earthquake analysis and design procedures.

This Study aims to enhance the reliability of computed fundamental periods for majority of structures built in Palestine; as the common practice in analysis is by ignoring the contribution of non-reinforced walls in modeling, which will not truly simulate the real behavior of structures, leading to inaccurate prediction of earthquake response, and therefore, inaccurate seismic design.

Modeling of infill walls has been an interest for researchers since more than sixty years. Methods of analysis are diverse and degree of complexity is not the same; as some modeling methods deals with infill walls components, where other methods replace infill wall with an equivalent compression strut.

A single strut is found to be the simplest and the most applicable method of modeling; therefore, this study focuses on comparing different approaches of single strut method. The study concludes that the strut width as computed using NBCC code may be the best choice.

Methods of infill walls construction also differ in a way that affect analysis. Therefore, variable methods of construction as being applied in Palestine is introduced, and three types of cross sections are defined and analyzed to give a clear conclusion about infill walls role in affecting the behavior of structures against earthquakes.

Study shows that existence of infill walls contributes in defining the lateral stiffness of the structure, where this contribution may be critical when infill walls are not distributed uniformly, or when infill walls does not start from base level.

Impact of infill walls is a serious subject that needs consideration, as the impact is direct on both the fundamental period and on regularity of structures. This study gives recommendations about developing the computation of fundamental period for structures with infill walls with cladding system, in order to improve both earthquake design and assessment for structures in Palestine

Chapter One

Introduction

1.1 General

Seismological and historical studies in Palestine show that occurrence probability of damaging earthquakes is high. Records show that an earthquake of a strength of 6.2 on the Richter scale had occurred in1927. Later on in 2004, another earthquake of 5.2 Richter had occurred but without causing any severe damages. (Al-Dabbeek et. al, 2008).

The development of constructing multi-story structures in west bank and Gaza strip in Palestine can be justified due to many factors. One of the main factors is the fact that Palestinians are only allowed to build in about 40% of their land without having the Israeli permission, unlike the remaining 60% where Israeli permission is mandatory (The Applied Research Institute in Jerusalem).

Low rise buildings (one to two stories) is hardly found inside the major large cities in in Palestine; as most structures are constructed to the maximum allowed by the local authorities, in order to effectively use the available lands in providing housings and services.

The awareness of the importance of designing structures regarding earthquakes forces has been developed lately in Palestine. Moreover, the Palestinian engineering association developed rules that enforce structural engineers to analyze and design structures to resist earthquake forces.

Most practiced method of construction in Palestine for different functional uses is through constructing framed concrete structures with infill walls, where infill walls may be either a layer of brick or a non-reinforced concrete layer. For cases of cladding Palestinians usually use natural stone facades.

Infill walls that fill gaps in frames are either starting from foundation level, or from upper levels (walls are not reaching foundation level).

The local practice in most of the engineering offices is to analyze and design structures using 3D finite element model. Moreover, the engineering association does not confirm structural drawings without submission of structural calculations that show 3D model with earthquake force calculations based on the uniform building code (UBC97).

1.2 Problem Statement

Although the increase rate of using light decorative cladding systems, infill walls still preserve popularity in Palestine, as it is the main cladding system for many governmental, commercial, and residential buildings.

Modeling procedures that deal with infill walls as structural elements are not well understood or practiced for majority of design engineers. The common practice is to model these infill walls as nonstructural elements; by representing their existence by only line loads. Such modeling procedure means that infill walls contribution in lateral stiffness are not being considered; leading to wrong estimate of many parameters such as:

fundamental time period, drift calculations, and checking irregularities specified in building codes.

Infill walls don’t have a uniform pattern, some of these walls start from foundation level, while other walls may start from higher levels. Moreover, infill walls layout may change from one story to another based on the architectural design. Indeed, the fact that infill walls are decorative walls increase the risk and the level of complication, and ignoring them in modeling will avoid studying possible critical irregularities.

Existence of infill walls affect the behavior of frame systems under lateral forces. Both lateral strength and stiffness regarding frame will increase when subjected to earthquake forces (Bertero et. al 1983).

A dynamic vital parameter known as the natural period “T_n” defines the needed time to complete one cycle during oscillation. For a single degree of freedom structure a unique natural period can be obtained through Equation 1-1 (Murthy et al. 2012).

$$T_n = 2\pi\sqrt{\frac{m}{k}} \quad \text{[Equation 1-1]}$$

As can be concluded from Equation 1-1, two parameters mainly control the value of the fundamental period, the first parameter is the mass of the structure, where any increase in mass with keeping lateral stiffness constant increases the natural period. On the other hand, any increases in the lateral stiffness with keeping the same mass will decrease the natural period value.

A case of single degree of freedom is a theoretical case, where structures in reality are multi-degree freedom systems. In multi degree structural systems structures have number of natural periods equal to the number of degrees of freedom. Indeed, the least value of those natural periods is known as the fundamental natural period, where fundamental natural period is associated with a specific pattern of motion (frequency) (Murty et al., 2012).

Design procedures for earthquake resistance depend on computing developed forces in structures, while developed forces in structures change based on the mode that is related to the natural period of the mode.

According to ASCE code, base shear in a given direction shall be determined in accordance with the following equation:

$$V = C_s W \quad \text{[Equation 1-2]}$$

Value of C_s is calculated based on the following formulas:

$$C_s = \frac{S_{DS}}{\left(\frac{R}{I_e}\right)} \quad \leq 0.044 S_{DS} I_e$$

$$\geq 0.01$$

$$\leq \frac{S_{D1}}{T\left(\frac{R}{I_e}\right)} \quad for\ T \leq T_L$$

$$\leq \frac{S_{D1} T_L}{T\left(\frac{R}{I_e}\right)} \quad for\ T \geq T_L$$

As can be concluded from C_s formulas a change by decreasing in fundamental natural period may increase the value of C_s causing an increase in the computed base shear value. Therefore, role of Infill walls as structural element is suspected to increase the lateral stiffness that will decrease the fundamental period that leading to a considerable increase in the computed base shear value.

Another important point that need attention is the lateral stiffness of infill walls, and the impact of this lateral stiffness on the regularity of the structure; as in many cases infill walls are distributed noon-uniformly causing un balance in the horizontal irregularity.

As can be concluded two main concerns need focusing when talking about infill walls, those two main concerns are as following:

1- Impact of change of fundamental period on the computed base shear value, and therefore the design forces for the structure.
2- Impact of infill walls on the regularity of structures based on infill walls distributions.

1.3 Scope of the Research

It is agreed that effect of infill walls on the performance of structures need to be evaluated in order to safely design structures against lateral forces. In this research the outer walls that represent facades for buildings in Palestine will be evaluated, first by reviewing common methods of construction, then by providing modeling procedure to take effect of such walls in seismic analysis.

To study effect of infill walls, a specific shape of structure is chosen with variation in materials specifications, and with variation in type of infill wall; some infill walls are constructed using layer of brick, and in other cases infill walls are composed of bricks and plain concrete layers.

The main parameter that will be investigated is the fundamental period, where it is suspected that the fundamental period will decrease due to including infill walls in analysis. The impact of decreasing fundamental period will be reflected in the base shear value; therefore, suggested value of base shear as provided by the ASCE code based on the approximate fundamental period will be evaluated to check if design is conservative or not.

The change of lateral stiffness will also be considered but with less details; as it is expected that including infill walls in analysis will increase the lateral stiffness. Such change may be critical on both the structure horizontal and vertical regularity when walls are distributed in unbalanced pattern.

1.4 Research Methodology

Uncertainties regarding the performance of buildings with infill walls need serious research; in order to enhance the predictions of local Palestinian structures performance against any suspected earthquake.

The fact of not having local code forced Palestinians engineers to adopt the American code. Indeed, the American methodology of constructing buildings are totally different from what is being applied in Palestine; thus –as an example- the suggested formulas for fundamental periods may not be conservative.

Due to complication in understanding the behavior of infill walls, two-time period boundaries will be defined. Lower limit represents including a full stiffness of infill walls, with an assumption of reinforced infill walls. While the upper boundary will be formed when neglecting the lateral stiffness of infill walls.

The philosophy of computing base shear is based on the fact of the complication of earthquake science. The many uncertainties in this science lead codes to create lower limit of the value of time period. In other words, codes require to design structures on higher forces to increase the reliability, and to enhance structures response due to any suspected earthquake.

Codes such as American and Canadian suggests methods of modeling infill walls. These methods depend on treating infill walls as compression only members using equivalent strut that replaces infill walls. The existence of both upper and lower boundary must give a good indication regarding the reliability of these formulas; as the true value must lie between those limits.

Chapter Two

Literature Review

2.1 Introduction

Understanding role of infill walls in the response of structures due to earthquakes is a common topic in the field of research. Through years many researchers around the world studied modeling of such walls in a way that enhance our expectations of performance against earthquakes.

Reliable estimation of the natural period of vibration is a vital step in the understanding of the global demands of structures under lateral forces such as earthquakes. Indeed, Estimation of seismic response depends mainly on the natural period of vibration (Eleftheriadou et. al, 2011).

Literature review focuses on exploring the most updates related to this topic, including experimental researches that examine theoretical approaches of infill walls modeling techniques.

2.2 Approximation of Fundamental Period

Since the parameter of fundamental period is a vital parameter in earthquake analysis, codes usually suggest many empirical formulas for the estimation of an approximate value of the fundamental period. These formulas have been usually derived through application of regression analysis on empirical data of measured fundamental period, after subjecting seismic actions to existing buildings. Empirical formulas suggested by codes don’t take in consideration several parameters that affect the value of period of vibrations (construction practices, seismicity, and soil conditions) (A.K. Eleftheriadou et. al, 2013).

Suggested formulas by codes developed in a way that make design conservative; therefore, codes formulas are supposed to under estimate the value of fundamental period in a way that increases the computed base shear.

2.2.1 Approximating Fundamental Period of Reinforced Concrete Frames

Reliable estimation of the fundamental period is essential step in predicting structures response due to earthquake forces. For design purposes codes usually suggest formulas that relate the fundamental period with structure type and height.

Fundamental time period mainly depends on both the mass and the stiffness of the structure. Equation 2-1 is used in the determination of the natural period of a single degree of freedom system.

$$T_n = 2\pi\sqrt{\frac{m}{k}} \qquad \text{[Equation 2-1]}$$

Empirical formulas provided in codes are usually derived based on empirical data and using regression analysis. Although the fact that many parameters play role in forming the fundamental periods such as soil conditions, and seismicity, and practices of construction, empirical formulas are considering only structural typology and the height of the structure (Chopra et. al, 2000).

ASCE Formulas

Section 12.8.2.1 in the ASCE7-10 states that the approximate fundamental period (Ta) (American Society of Civil Engineers 2010), shall be determined from the following equation:

$$Ta = C_t h_n{}^x \quad \text{[Equation 2- 2]}$$

Where h_n is the structural height as defined in Section 11.2 and the coefficients C_t and x are determined from Tables 12.8-1(Table 2-1) 12.8-2 in the code (see Table 2-2).

Table 2-1: Table 12.8-1 in the ASCE7-10 code, Coefficient for upper limit on calculated period

Design Spectral Response Acceleration Parameter at 1 s, SD_1	Coefficient C_u
≥ 0.4	1.4
0.3	1.4
0.2	1.5
0.15	1.6
≤ 0.1	1.7

Table 2-2: Part of 12.8-2 in metric units

Structure Type	C_t (metric units)	X (metric units)
Moment-resisting frame systems in which the frames resist 100% of the required seismic force and are not enclosed or adjoined by components that are more rigid and will prevent the frames from deflecting where subjected to seismic forces: Concrete moment resisting frames	0.0466	0.9
Steel eccentrically braced frames in accordance with Table 12.2-1 lines B1 or D1	0.0731	0.75
Steel buckling-restrained braced frames	0.0731	0.75
All other structural systems	0.0488	0.75

Therefore, ASCE code formulas for reinforced concrete moment frames can be written as following.

$$Ta = 0.0466{h_n}^{0.9} \quad \text{[Equation 2-3]}$$

And for other concrete structures equation is as follows:

$$Ta = 0.0488{h_n}^{0.75} \quad \text{[Equation 2-4]}$$

Uniform building code (UBC 97) suggests following formula (equation 2-5) for time period:

$$T = 2\pi\sqrt{(\sum_{i=1}^{n} w_i{\delta_i}^2) \div (g\sum_{i=1}^{n} f_i\delta_i)} \quad \text{[Equation 2-5]}$$

Although equation 2-5is more accurate it is use is rare as the computation requires horizontal displacement calculations. (J. Hsiao,2009).

According to ASCE it is permitted to determine the approximate fundamental period (Ta), from the equation 2-6 for structures not exceeding 12 stories above the base as defined in Section 11.2 (in ASCE) where the seismic force-resisting system consists entirely of concrete or steel moment resisting frames and the average story height is at least 3 meters height:

$$T_a = 0.1 \times \mathrm{N} \quad \text{[Equation 2-6]}$$

For masonry or concrete shear wall structures ASCE permits to determine the approximate fundamental period from equation 2-7:

$$T_a = \frac{0.0019}{\sqrt{C_w}}\ \mathrm{h}_n \quad \text{[Equation 2-7]}$$

Where C_w is calculated from equation 2-8:

$$C_w = \frac{100}{A_B}\sum_{i=1}^{x}\left(\frac{h_n}{h_i}\right)^2 \frac{A_i}{\left[1+0.83\left(\frac{h_i}{D_i}\right)^2\right]} \text{[Equation 2-8]}$$

2.3 Definition of Infill Walls

According to FEMA 356-2000 definition of concrete frames with infills is related to structural system where a frame system is designed to fully carry gravity loads, in the same time infill walls are constructed in a way that permits interaction between frames and infills against both vertical and lateral loads.

On the other hand, infills can be isolated if gaps with minimum space as required by section 7.5.1 in FEMA are provided (FEMA 2000).

FEMA divides infill walls to two types as following:

1- Masonry Infill Walls.
2- Concrete Infill Walls.

In the local practice the construction of concrete infill walls is much known specially for buildings with stone cladding. According to FEMA the construction of concrete infill walls is very similar to masonry. FEMA states that in concrete frames concrete is likely to be of lower quality if compared to frame’s concrete, therefore, concrete of infill walls needs separate investigation.

Determining accurate fundamental period has been always an essential step in the procedure of analysis and design for earthquakes. Fundamental period is a vital dynamic parameter that gives a clear indication of the suspected behavior of structures under motional loads like earthquakes. Time period value affect base shear, drift, and displacements values of structures.

Accurate value of fundamental period depends mainly on the assumptions the analyzer suggests; thus, the accuracy of earthquake analysis depend on how much the model is similar to reality.

2.4 Infill Walls Modeling Common Practice

In the majority of cases of designing structures to resist earthquakes, masonry infill walls in reinforced concrete structures are treated as non-structural elements.

The inadequate knowledge of behavior of reinforced concrete frames with infill walls may be the main reason why engineers ignore such elements in modeling. Another reason that explain this ignorance is the uncertainty about the non-integral action between reinforced frames and infill walls (Maidiawati, 2013).

2.5 Infill Walls Structural Role

One of the challenges in fundamental period calculation is the existence of infill walls between framed structures. These walls are not reinforced, and it is capacity in tension is neglected. Moreover, these walls include openings for both windows and doors.

Previous research has demonstrated through both experiments and numerical approaches the importance of infill walls in the dynamic behavior of the structure. Although the importance of infill walls in the behavior of structures, such walls are neglected from analysis for the following reasons (Panagiotis et. al, 2015):

1- Higher computational time.
2- Variable response of walls during an earthquake: beneficial at the beginning but adverse after being damaged.
3- lack of reliability in infill wall brittle materials behavior.
4- Effect of the construction practices.
5- Openings existence in the infill reduces their stiffness and affects the interaction with the frame, altering the overall dynamic characteristics of the structure.
6- The assumption that such walls are not structural increase the probability of walls removal and replacement by a light system that considerably change the behavior of the system.
7- Accurate modeling of infill walls shall take in consideration the components forming the infill walls. These components include bricks, mortar, and friction surfaces between frame elements and infill wall (Ugur Albayarak, 2017).

One of the main challenges in the modeling of infill walls is the fact of the many probable failure modes that need to be evaluated. Existing of openings, and large variance in the applied construction practices may totally change the behavior of the infill panel. Moreover, the removal of such walls is possible as it is widely believed in both analysis and design that infill walls are not structural elements. Such removal may be followed by replacement with light partitions (such as curtain walls) changing the overall behavior of the structure. Therefore, it is not surprising that no unified approach for infill walls modeling is developed, in spite of more than fifty years of intensive research. It is worth mentioning that infill walls contribution in the frame's lateral stiffness is significantly reduced when structure is subjected to reverse cyclic loading (Asteris et al. 2016). Research is constrained with external infill walls.

Turkish Seismic Code 2007 states that infill walls between frame systems of beams and columns have a significant role under seismic loads. "Infill walls in framed structures affect the dynamic characteristics of building such as stiffness, strength, and ductility of the entire structure and response to earthquakes" (Albayrak et. al, 2017).

Damages investigations post-earthquakes showed that infill walls suffered large residual deformations. These cracks took place at the first moments of earthquakes, causing reduction of earthquake forces on frames. (Albayrak, 2016).

Albayrak in his paper (published in 2017) states that in earthquake analysis the effect of infill walls must be considered for the expected performance under earthquakes.

Under minor seismic forces, research shows that these infill walls will be displaced with frames, similar to the behavior of shear walls.

In seismic area it is not considered conservative ignoring the effect of infill walls, as the existence of these walls will dramatically increase the lateral stiffness, and thus decreasing the fundamental period and increasing the seismic demand for the system. (Panagiotis et. al, 2012).

Infill panels may radically change response of structures under lateral loads. “The lateral stiffness can become ten times higher and the strength can increase four times if compared with the conventionally designed ones in which the presence of the infill is not considered.” (Amato et al. 2008).

It is important to note that interaction between the reinforced frame and the infill wall may be beneficial or not regarding structure performance against earthquakes; this may happen when such panels are not uniformly distributed horizontally and vertically. (G. Amato et. al, 2008).

A PHD thesis by Maidiawati in 2013 (Toyohashi University of Technology) about brick masonry walls includes a study site observation on two 3 story structures subjected to the same earthquake. The two buildings are with similar structural characteristics, but under earthquake one of them totally collapsed while the other was moderately damaged.

Analysis neglecting infill walls stated that both building has the same seismic capacity. Actually, the structure that survived had more brick walls than the other totally damaged; and this leaded the author to conclude that infill walls played a positive role in increasing the strength of the structure. This conclusion was supported in the end of the research as results of analysis considering infill walls proved that the existence of infill walls effectively increases the seismic capacity of the structure.

A paper published in 2019 was prepared after the strong earthquake that took place on April, 2015 in Nepal. A filed study was performed in one of the most affected areas in the capital region of Kathmandu. Paper focused on evaluating damage in a 15-story infilled reinforced concrete structure.

According to paper, failure in infill walls structures has three mechanisms; the first mechanism is the short column, where short column is taking place where an infill wall is not reaching the bottom of slab. The second failure mechanism is also short column, where short column happens by the influence of stair-slabs connection to columns.

Final mechanism is related to vertical stiffness irregularity due to non-uniform distribution of infill walls, as a common practice in Nepal is to reduce infill walls in the ground level for commercial purposes, where such reduction increases seismic vulnerability.

Observations post Nepal earthquake proved that damage related to high-rise reinforced concrete structures (ranges between 10-18 stories) was mainly in infill walls. Figure 2-1 shows damages in infill walls in a 15-story building, and as can be noted damages are concentrated at the first seven floors, where damages are composed by detachment of infill walls from the frame. Moreover, diagonal cracks and out-of-plane detachment can be observed clearly.

a) b) c)

Figure 2-1: 14-story RC structure with masonry infill wall damages after the Gorkha earthquake: a) damages distribution from 1st to 7th story; b) detachment of the walls from the frame; c) diagonal cracking with slight out-of-plane detachment of the wall. (Furtado et. al, 2019)

2.6 Modeling of Infill Walls

For more than sixty years of work and research regarding infill systems, no uniform approach is developed for analysis procedure. This is due to the complication of many factors, such as many possible failure modes that need to be evaluated with high degree of uncertainty (Swarnkar et. al, 2015).

Codes usually are suggesting formulas derived from empirical data using regression analysis for data recorded on existing building due seismic actions. Although fundamental period is subjected to many factors as soil type, methods of construction, codes suggest formula proportional to buildings heights. (A.K Eleftheriadou,2012).

Many codes suggest modeling infill walls using strut infill model. The ASCE/SEI 41-06, and NBCC 2005 code suggest modeling of infill walls. Tarek Alguhane and others in 2015 evaluate both methods and came to a conclusion that the ASCE/SEI 41-06 underestimates the values for the equivalent properties of the diagonal strut. On the contrary, the Canadian code (NBCC) gives realistic results.

“Infill-frames have demonstrated good earthquakes-resistant behavior, at least for serviceability level earthquakes in which the masonry infill can provide enhanced stiffness and strength”. “In several moderate earthquakes, such buildings have shown excellent performance during earthquake” (Alguhane et al. 2015).

Several researchers studied the effect of infill walls in reinforced concrete frame on the performance of structures against earthquakes. Many of those researchers developed empirical formula for computing strut widths.

Experimental work of researchers showed that performance of infill walls varied with levels of applied lateral loads, as an example, for low lateral loads the contact between infill wall and reinforced concrete frames remain the same before application of load, thus lateral stiffness of structure becomes much higher if compared to bare frame case. On the other hand, and as a result of increasing lateral forces infill walls tend to crack and a separation takes place between the frame and the infill panel in the tension zone, while in the compression zone the contact still exists. (Maidiawati, 2013).

The most important properties of infill panels are both the compressive and tensile strength, where these properties affect the structural performance. Since infill panels are with no reinforcing it is suspected that the compression capacity is much higher if compared to tension capacity.

Literature review shows that it is agreed that the role of infill walls is vital and must be considered in studying structures against lateral loads. “Frames under seismic loads should be modeled to consider the effect of the infill walls on the seismic performance of the structure. The gaps occurred between the frame elements (beam or columns) and the walls and the cracks on the walls are the most important parameters for structural design if infill walls are considered as structural members.” (Ugur Albayarak, 2017).

According to research, infill non reinforced walls are suspected to behave as shear walls in the case of minor seismic actions. Figure 2-2 shows the infill wall-reinforced concrete frame element interaction against lateral movement. (Ugur Albayarak, 2017). Joints 2 and 4 are in tension state, no resistance. Unlike joints 1 and 3 are in compression state, lateral resistance (strut action).

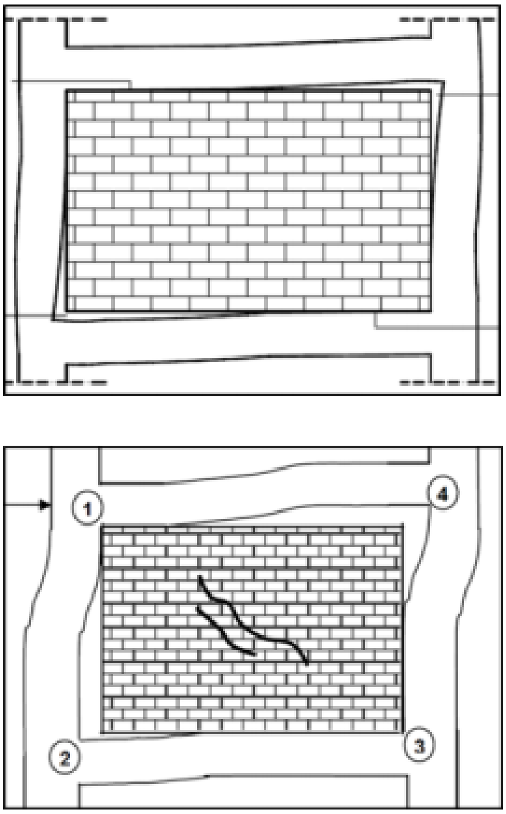

Figure 2-2: Suspected behavior of frames with non-reinforced infill walls in frame structures (Ugur Albayarak, 2017)**.**

2.6.1 Infill Walls Modeling Techniques

Micro Modeling and Macro Modelling are the two main known approaches of infill walls simulation. In Micro Modeling the reinforced concrete frame, the masonry panel, and connection between masonry elements (in case of bricks) are being modeled through finite element. For Macro Modeling the method of “equivalent strut” is popular and being used (Alguhane et al. 2015a).

Equivalent strut as shown in figure 2-3 is a method that focuses on computing a basic parameter of equivalent width which affects both strength and stiffness. In other words, equivalent strut method computes the width of a structural element that replaces the infill panel which is supposed to truly model the actual behavior of such infill panels (K.H. Abdelkareem et. al, 2013).

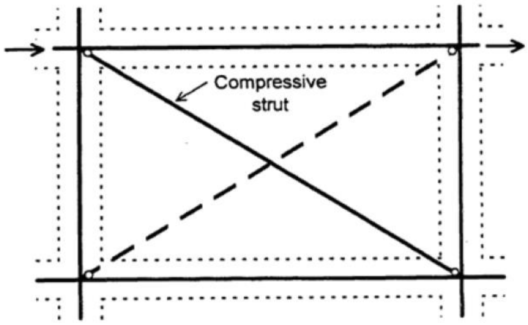

Figure 2-3: Compressive diagonal strut model representing infill panel in a frame (K.H. Abdelkareem et. al, 2013)**.**

One single strut was the first approach developed by Holmes; the method replaces infill panel with equivalent structural compressive pinned jointed element. Later on, studies performed by researchers showed that more complex models of two, three or multiple diagonal (figure 2-4) struts are more reasonable due to lack of accuracy in the case of single strut (Alguhane et. al,2015).

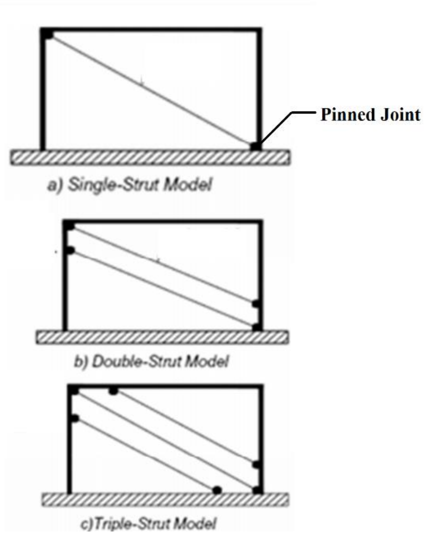

Figure 2-4: a) single strut b) Double strut c) Triple Strut (Alguhane et. al,2015)

According to FEMA infill walls may be either masonry infill, or concrete infill.

2.6.2 Equivalent Strut Formulas

Formulas for computing equivalent compression strut have been developed since 1961. In this section many of those formulas will presented including what some codes suggest.

Holmes Equivalent Strut Formula (1961)

Holmes in 1961 suggested replacing infill walls by equivalent pin-jointed diagonal strut composed of the same material of the original infill wall, with a thickness exactly the same to the infill, and using a width of one-third the diagonal distance between the two compressed corners. Holmes approach of determining strut width may be expressed as below (Equation 2-9):

$$w = \frac{1}{3} d_{inf} \quad \text{[Equation 2-9]}$$

Mainstone Formula (1971)

In 1971 Mainstone proposed a formula for the equivalent strut based on performed tests on brick infills (Mainstone 1971):

$$w = 0.16 d_{inf} (\lambda_h h_{inf})^{-0.3} \quad \text{[Equation 2-10]}$$

Mainstone and Weeks Formula (1974)

In 1974 Mainstone and Weeks proposed a formula based on test results:

$$w = 0.175 d_{inf} (\lambda_h h_{inf})^{-0.4} \quad \text{[Equation 2-11]}$$

Bazan and Meli Formula (1980)

In 1980 Bazan and Meli on the basis of parametric finite-element studies for one-bay, one-story, infilled frames, produced an empirical expression (Equation 2-12) to calculate the equivalent width for infilled frame.

$$w = (0.35 + 0.22\beta) h \quad \text{[Equation 2-12]}$$

Where:

$$\beta = \frac{E_c A_c}{G_{inf} A_{inf}} \quad \text{[Equation 2-13]}$$

β is a dimensionless parameter, Ac is the gross area of the column, Area of infill is the product of infill length by strut thickness, and finally G_{inf} is the shear modulus of the infill.

Paulay and Preistely Formula (1992)

In 1992 Paulay and Preistely stated that higher width of strut will increase structure stiffness and therefore it is response to earthquakes (Paulay and Priestley 1992), thus and to be conservative they recommended the following conservative formula (Equation 2-14) for design purposes:

$$w = \frac{1}{4} d_{inf} \quad \text{[Equation 2-14]}$$

Durrani and Luo Formula (1994)

In 1994 Durrani and Luo proposed an equation (Equation 2-15) for the effective width of the diagonal strut:

$$w = \gamma\sqrt{L^2 + h^2}\sin 2\theta \quad \text{[Equation 2-15]}$$

Where:

$$\gamma = 0.32\sqrt{\sin 2\theta}\left[\frac{H^4 E_{inf} t}{m E_c I_c h_{inf}}\right]^{-0.1} \text{[Equation 2-16]}$$

$$m = 6\left[1 + \frac{6 E_c I_b h}{\pi E_c I_c L}\right] \quad \text{[Equation 2-17]}$$

Hendry Formula (1998)

In 1998 Hendry suggested a formula for computing the equivalent strut width (Equation 2-18), the width is supposed to truly contribute in resisting the lateral force in the composite structure.

$$w = 0.5\sqrt{{\alpha_h}^2 + {\alpha_L}^2} \quad \text{[Equation 2-18]}$$

$$\alpha_h = \frac{\pi}{2}\left[\frac{4 E_c I_c h_{inf}}{E_{inf} t \sin 2\theta}\right]^{\frac{1}{4}} \quad \text{[Equation 2-19]}$$

$$\alpha_L = \frac{\pi}{2}\left[\frac{4 E_c I_b L_{inf}}{E_{inf} t \sin 2\theta}\right]^{1/4} \text{[Equation 2-20]}$$

Papia Formula (2008)

In 2008 Papia and others developed an empirical formula (Equation 2-21) for calculating the effective width of the diagonal strut:

$$w = \frac{c}{z}\frac{1}{\lambda^*} d_{inf} \quad \text{[Equation 2-21]}$$

Where:

$$c = 0.249 - 0.0116 v_{inf} + 0.567 {v_{inf}}^2 \quad \text{[Equation 2-22]}$$

$$\beta = 0.146 + 0.0073 v_{inf} + 0.126 {v_{inf}}^2 \text{[Equation 2-23]}$$

$$\lambda^* = \frac{E_{inf} t h_{inf}}{E_C A_C}\left[\frac{{h_{inf}}^2}{{L_{inf}}^2} + \frac{A_C L_{inf}}{4 A_b h_{inf}}\right]$$ [Equation 2-24]

$$z = 1\ if\ \frac{L_{inf}}{h_{inf}} = 1, z = 1.125\ if\ \frac{L_{inf}}{h_{inf}} \geq 1.5$$

Computation of Equivalent Strut – FEMA356-2000

Based on FEMA356-2000 the ASCE/SEI 41-06 suggests a formula that computes the equivalent width of strut (Equation 2-25).

for the computation of the parameter (a_1), which is the width of the equivalent compression strut, that simulate the in-plane stiffness of a solid un-reinforced masonry infill panel before cracking.

$$w = 0.175(\lambda_1 h)^{-0.4} d_{inf}$$ [Equation 2-25]

Where the expression λ_1 can be computed using the following formula:

$$\lambda_1 = \left[\frac{E_{inf} t \sin 2\theta}{4 E_C I_C h_{inf}}\right]^{\frac{1}{4}}$$ [Equation 2-26]

Figure 2-5 illustrates the geometrical parameters in the formula of the equivalent strut of ASCE/SEI 41-06.

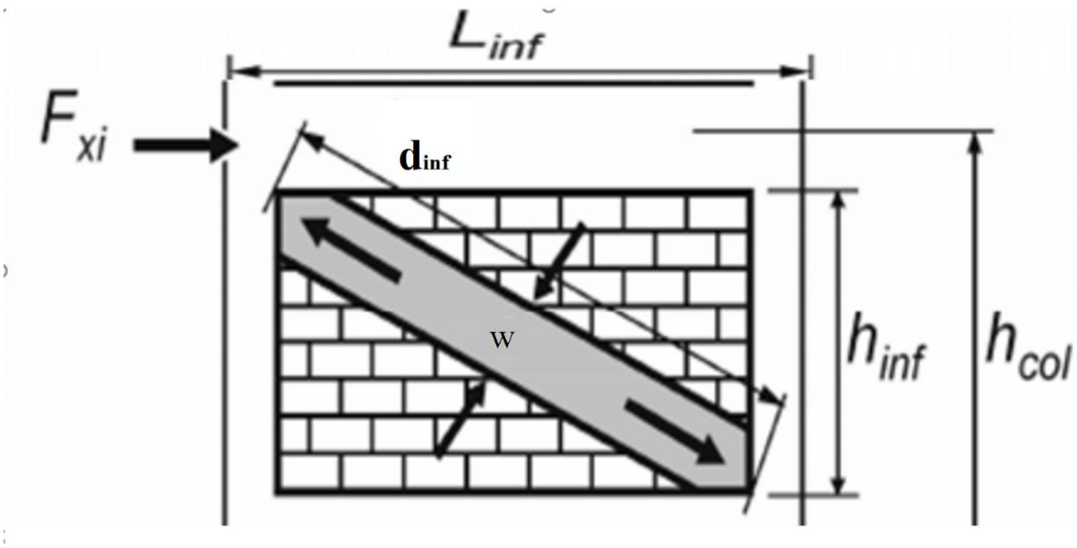

Figure 2-5: Illustrations of geometric parameters, ASCE/SEI 41-06

Computation of Equivalent Strut – NBCC 2005

The width of the equivalent compression strut is calculated using the equation 2-27 as suggested by the NBCC 2005 code:

$$w = \sqrt{{\alpha_h}^2 + {\alpha_L}^2} \quad \text{[Equation 2-27]}$$

Where,

$$\alpha_h = \frac{\pi}{2}\left[\frac{4E_c I_c h_{inf}}{E_m t_e \sin 2\theta}\right]^{\frac{1}{4}} \quad \text{[Equation 2-28]}$$

$$\alpha_L = \frac{\pi}{2}\left[\frac{4E_c I_b L}{E_{inf} t_e \sin 2\theta}\right]^{\frac{1}{4}} \text{ [[Equation 2-29]}$$

w_e is the effective diagonal strut width, and shall be calculated according to these conditions:

$$w_e \leq \frac{w}{2} \ or \ \leq \frac{l_s}{4} \ (smaller\ control)$$

Figure 2-6 shows the illustration of geometric parameters in the NBCC formula:

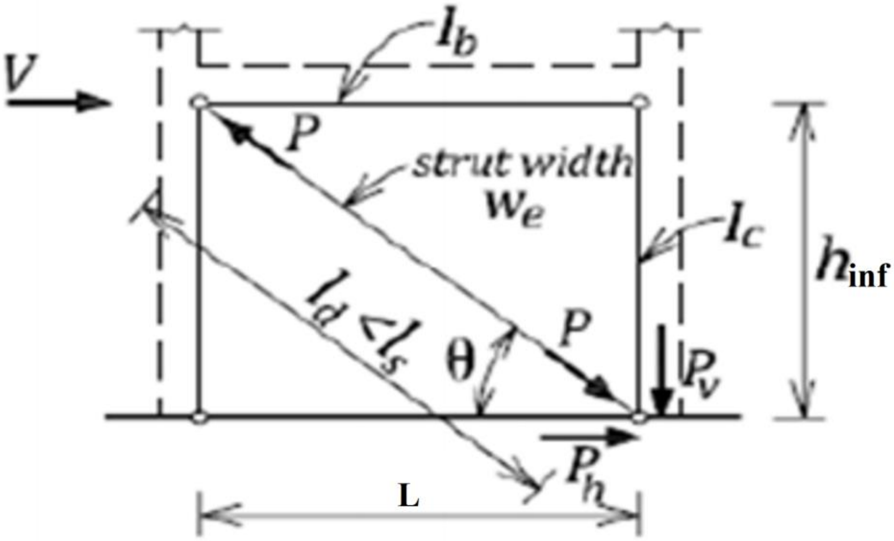

Figure 2-6: Diagonal strut model in the NBCC code

2.6.3 Modeling of Openings in Infill Walls

It is obvious from different local buildings facades in figures 2-7, and 2-8 that openings are forming a considerable percentage if compared to infill wall area; thus, infill walls contribution in lateral stiffness may be reduced considerably.

Figure 2-7: Residential building-Palestine

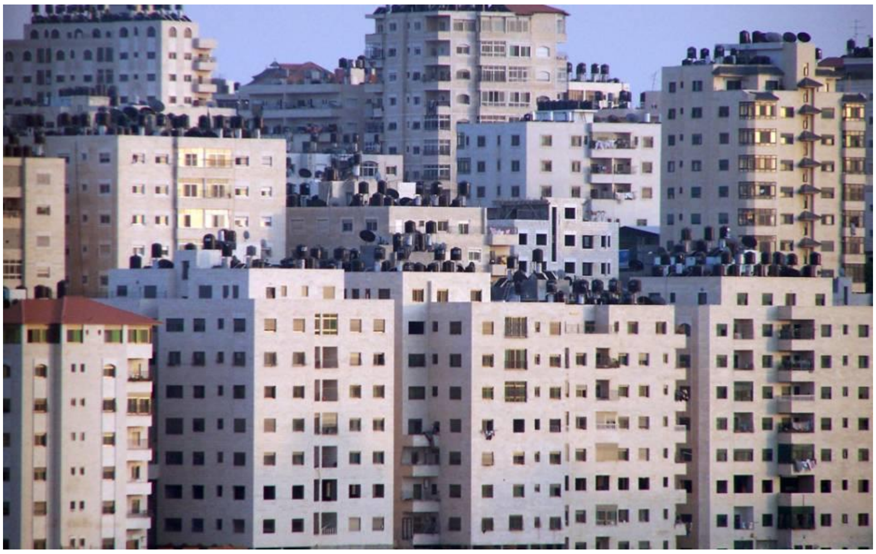

Figure 2-8: General view for residential buildings-Palestine

Although the common case of having oversized openings in the infill walls, most of available researches have focused on the simple case of solid infill walls. Actually, available research on infill walls with openings is limited to specific cases with specific materials and limited opening sizes. Thus, no unified approach is adopted in dealing with openings in infill walls. (Asteris et. al, 2012).

Stiffness and strength of the infilled frames with openings are not considered by most of the codes that deal with infill walls modeling. Indeed, most current publications like FEMA deals with calculations of stiffness for solid infilled frames without having clear approach of impact of openings on the effective strut width (Mondal et. al, 2008).

In 1971 a study developed by Mallick and Grag about openings effect on the behavior of infill walls, the study concluded that for small central opening the effect can be ignored, but on the contrary considerable decrease was recorded where openings are positioned close to the loaded ends of the compressed diagonal of the infill panel (Mallick et. al,1971, Devi et. al, 2012).

In 1994 Choubey.U.B and Sinha used an experimental program that examine frame with masonry infill performance against cyclic loading, and a conclusion was carried out that infilled frames with central openings have more stiffness within a range of 4 to 6.35 if compared to the bare frame et. al, 2017).

In a study published in 2014 by Bhagyalaxmi Sindagi and others an analytical investigation using Finite Element Method was performed. The study included using different opening sizes and impact of such openings were tested (Sindagi et al. 2015).

Observations of study confirmed that the presence of opening significantly reduces the initial lateral stiffness of the infilled frame. The study states that for area opening 15% of the infill panel, the lateral stiffness is reduced by 20-32%. Moreover, the study stated that the reduction in lateral stiffness is a function of infill modulus of elasticity, as an example when reducing modulus of elasticity from 2750 MPa to 1000 MPa the reduction of lateral stiffness is in the range of 52-53% (Popescu et al. 2015).

Other studies suggest using formulas to compute reduction factors, where these reduction factors can be multiplied by the strut width for solid infill panels, and the final result will be a modified strut with less width value that takes in consideration role of opening in decreasing the lateral stiffness of the system.

It is agreed that existence of openings will reduce the contribution infill panels have in the total performance of the infill frames, and to take this reduction in the analysis of equivalent strut a reduction factor may be suggested to reduce the width of the strut to increase the accuracy of modeling of infill panels.

Asteris developed a formula for computation of λ factor (Equation 2-30) which indicates the infill stiffness reduction factor, the formula is as following:

$$\lambda = 1 - 2{\alpha_w}^{0.54} + {\alpha_w}^{1.14} \quad \text{[Equation 2-30]}$$

Figure 2-9 shows the variation of λ with respect to change in the opening percentage. It can be concluded that for opening percentage exceeding 50%, the reduction factor is near to zero.

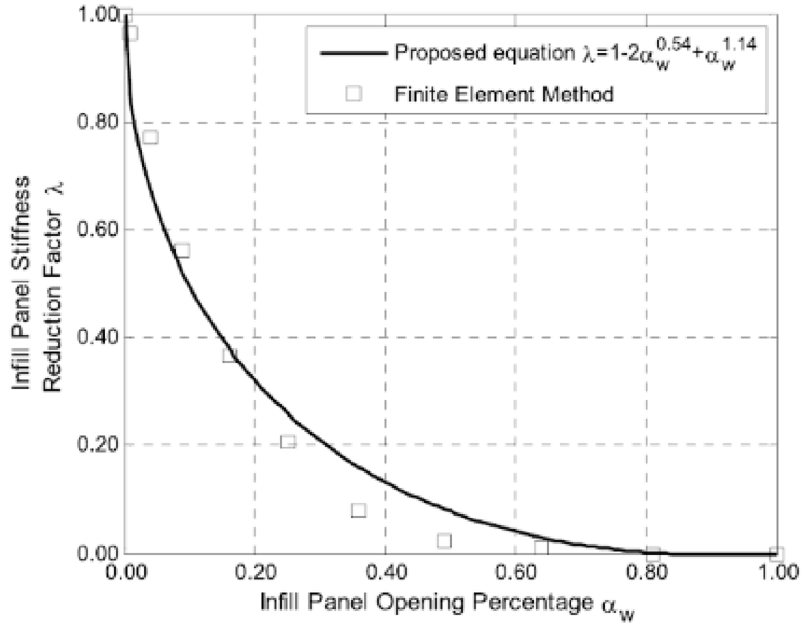

Figure 2-9: Infill panel stiffness reduction factor Vs. Infill panel opening percentage (Mallick and Garg)**.**

Based on experimental and analytical research, it was found that an opening at either end of the loaded diagonal reduces the stiffness of infilled frame by about 85%–90% in comparison with infilled frame without opening (Mallick et. al, 1971).

The effective width of diagonal strut for infilled frame without opening may be reduced by a reduction factor to simulate the presence of openings of various aspect ratios in the infilled frame (Durrani and Luo 1994, Al-Chaar, Lamb, and Abrams 2003).

A study developed by Goutam Mondal and Sudhi K. Jain in 2008 focused on the computation of a reduction factor for the purpose of finding the effective width of diagonal strut for infill walls with central opening of a window et. al, 2006). Goutam study is based on a load level which is taken at 10% of the lateral strength of infilled frames.

In Goutam study many openings with different sizes were tested in order to develop a general formula that represent a logical reduction factor. However, the proposed reduction factor does not depend upon the height to width ratio of opening.

Equation 2-31 represents the proposed formula by Goutam for the reduction factors of equivalent strut:

$$\rho_w = 1 - 2.6\alpha_{co} \quad \text{[Equation 2-31]}$$

According to study equation 2-31 is regardless of the number of stories. Figure 2-10 shows the relation between the opening area ratio and the strut width reduction factor as provided in Goutam study.

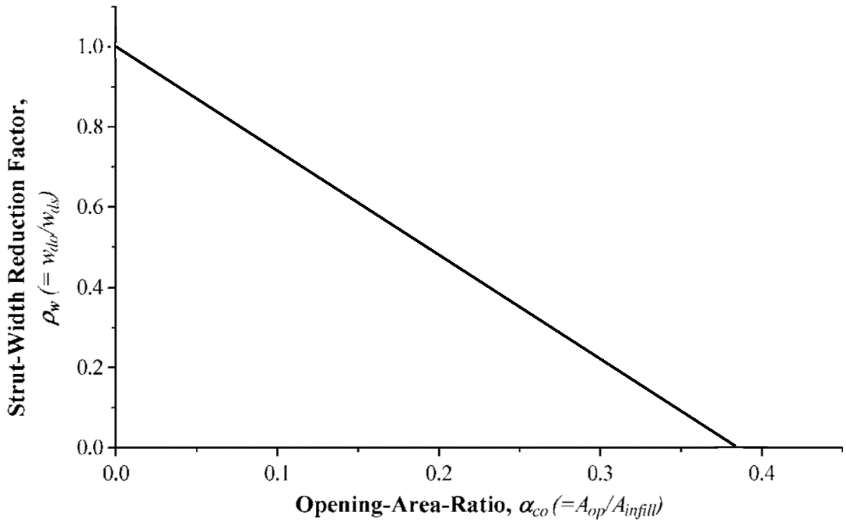

Figure 2-10: Strut width reduction factor Vs. Opening area ratio (Goutam et. al, 2008).

It can be concluded from figure 2-10 that stiffness contribution can be ignored when opening area is greater than 40% of infill area, and on the contrary openings with ratio smaller than 5% will not make considerable reduction in the stiffness and therefore it is impact can be neglected.

In Goutam study the cracking in both infill and frame is not considered as the study focuses on load level corresponding to 10% of the strength of the infill frame. Thus, failure mode and material properties are not considered important parameters on the initial lateral stiffness of the lateral frame.

Chapter Three

Methods of Stone Cladding Construction in Palestine

3.1 Introduction

Method of construction of stone cladding is an important factor that need to be considered before studying the contribution of infill walls in the lateral response of the structural system to any lateral force such as earthquakes. Applied construction methods change the components of the infill wall, with wide variation in used material that affect the physical properties of such walls, and therefore affect it is performance in responding to suspected motional loads. Moreover, studying the methods of construction will provide vital information about the role stone itself has in the suspected behavior.

This chapter aims to present the most applicable methods of construction for cladding stones in Palestine. Methods of construction in this thesis are classified into three types: *Method One*, *Two*, and *Three*. Each method is explained with illustrative figures.

3.2 Method One: Traditional Method

Method one -as will be described through this chapter- is considered to be the oldest method of cladding walls construction applications in Palestine. The method is still used in many residential and commercial buildings; and this justify the need of including it in any related study.

3.2.1 Procedures of Method One

The application of method one may be implemented through two procedures. The two procedures will be discussed in details through the following sections.

3.2.1.1 Method One – Procedure A

Procedure A indicates the first method of construction of stone cladding walls (for method one) as being practiced in Palestine. This procedure still preserve it is popularity in many residential and commercial buildings. In this procedure the construction of infill walls precedes the construction of flooring system.

In this procedure workers arrange stones in rows as shown in figure 3-1 (usually three rows). Stone layers (different rows) are attached together using a thin layer of mortar, while adjacent stones are connected through mortar layer and a special adhesive material. Also, wood stone wedges are being installed from both faces to stabilize the stone piece before concrete casting.

Figure 3-1: Method one, procedure A: arranging stone in layers.

The next stage after constructing the layers of stones will be making shutters in order to start pouring concrete behind the stone. Figure 3-2 shows a shutter that will support the casted concrete to the level of the constructed stones.

Figure 3-2: Using shutters to support poured concrete to the level of constructed stones**.**

Another way of supporting the poured concrete behind the stone is by using bricks of 10 cm thickness, those bricks will be used as internal surface that will be treated by plastering and painting later on it finishing works. Figure 3-3 illustrates using bricks as permanent shutters.

Figure 3-3: Using 10 cm hollow bricks as permanent shutters to support poured concrete behind stone.

The nature of concrete beyond stone layer plays a main role in defining the lateral stiffness of the infill wall. It is clear in this method that concrete in the façade is being poured in different stages, and necessarily in different days. Moreover, the quality of the poured concrete is questionable, as in most cases, the concrete will be pumped outside walls (as shown in figure 3-2), kept for many hours on ground, with addition of water in trying to keep the mix workable as much as possible. Figure 3-4 shows how concrete looks after removing shutters.

Figure 3-4: Plain concrete after removing shutters - method one-procedure A**.**

Figure 3-5 shows components of stone cladding infill walls of method one-type A procedure. As can be seen in figure 3-5 two types of cross section can be found; option 1 in figure 3-5 includes a space created either by using special isolation material (applicable for a case as shown in figure 3-3), or through leaving a space before constructing brick layer (case of constructing brick in different stage applicable for a situation as shown in figure 3-2). On the other hand, option 2 in figure 3-5 represents the case where brick layer is directly adjacent to concrete layer.

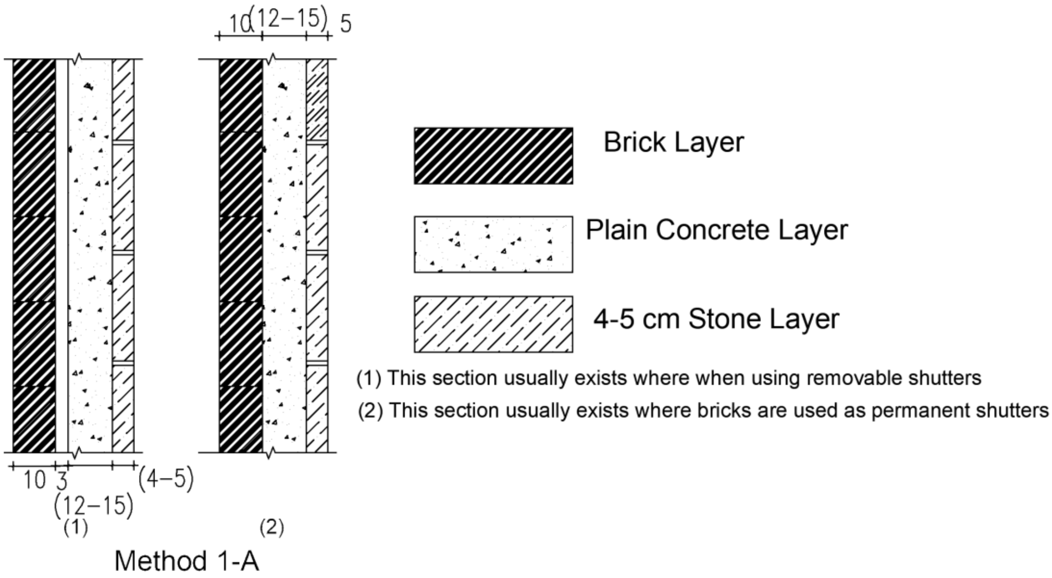

Figure 3-5: Method one-procedure A cross sections.

3.2.1.2 Method One – Procedure B

In this method the whole stone façade is constructed at the first stage, then a ready-mix concrete is directly casted using pump. This procedure needs special attention to keep stone façade stable during casting process. Figure 3-6 shows stone façade supporting system from front to avoid suspected failure due pouring concrete using pressurized pump.

Figure 3-6: Method one-procedure B: stone façade casted once using ready mix concrete poured through pump**.**

Figure 3-7 shows how concrete looks after removing the shutters.

Figure 3-7: Plain concrete appearance after removing shutters, method one- procedure B – constructing stone cladding façade as one unit.

Figure 3-8 shows components of stone cladding infill walls of *Method One-Type B* procedures, where the section clearly contains three layers of brick, plain concrete and 4-5 cm stone layer, besides an isolation layer (void) of 3 cm as can be seen in figure 3-8.

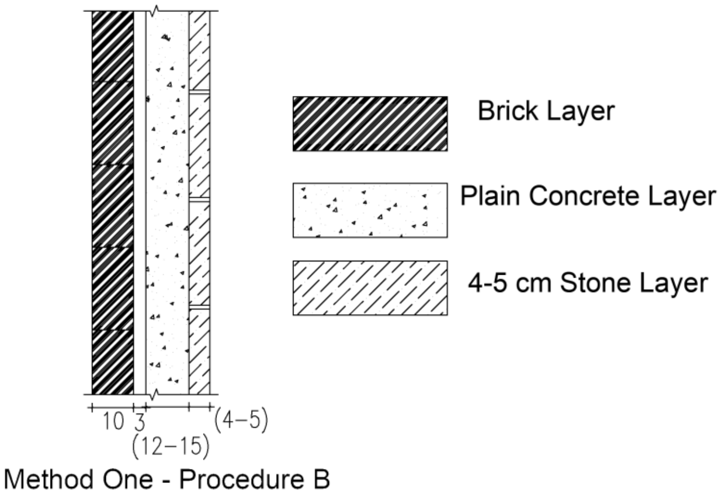

Figure 3-8: Method one-procedure B cross section.

3.3 Method Two: Attaching Stone Layer to A Brick Infill Wall

Method two of construction is another way of constructing stone facades, where in this type of construction the façade consists mainly of brick layer that exists within the frame. In addition to brick layer, another layer of plain concrete (not within the frame) is used to attach stone to brick layer. Following steps are the details of application of method two.

1- A brick façade of 10-20 cm thickness is constructed.
2- A layer of cement base is painted to coat the surface of brick.
3- A steel mesh of usually 6 mm bars diameters spaced each 20 cm in both directions is being attached to brick face using steel anchors of 8 mm bars.
4- Stone layers are installed in two to three layers.
5- Steel wires are being attached to stones and connected with the steel mesh.
6- An in situ concrete mix is poured to fill a void of 6-10 cm between stone and brick face.

Figure 3-9 shows an application of construction using method two.

Figure 3-9: Construction of stone façade using method two**.**

In this type of construction, concrete beyond stone must be followable to ease work in site. Moreover, the concrete is being mixed on site with usually no guaranty on concrete's compressive strength quality.

Figure 3-10 shows the components of Method Two section.

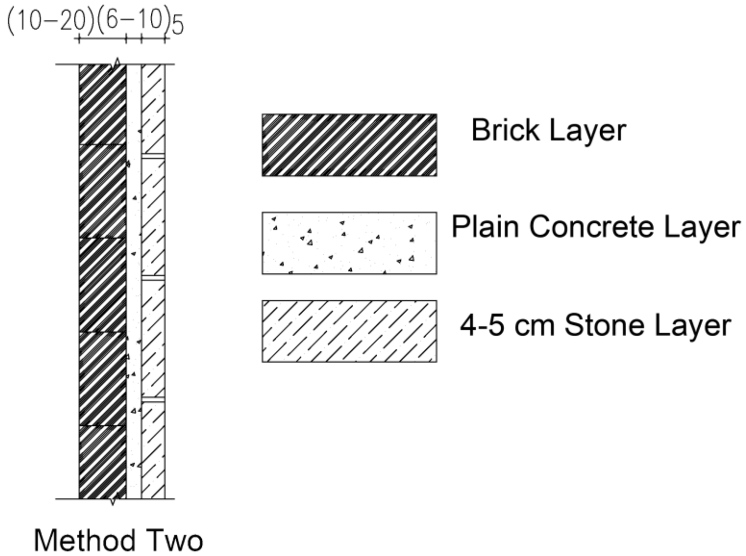

Figure 3-10: Method two cross section**.**

3.4 Method Three

As mentioned previously through chapter two, definition of infill wall is limited to either masonry brick walls or plain concrete walls. For method three the case is totally different, as the infill layer is usually a concrete layer with two steel layers. Therefore, method three is presented just to fully cover methods of stone façade construction.

Due to high cost, application of method three is limited to special type of projects. In this method, the procedure starts by constructing reinforced walls on the outer boundary of the building (where stone cladding exists).

Cladding procedure starts usually after finishing all construction works. The procedure is similar to method two, where steel meshes of 6 mm diameter bars are attached to the reinforced wall, and a layer of 6-10 cm concrete is poured to connect stone layers to existing walls.

Figure 3-11 shows application of Method Three in an under construction building in Palestine.

Figure 3-11: Cladding on 20 cm reinforced wall using a 6 mm steel mesh and a layer of 6-10 cm concrete.

Figure 3-12 shows components of Method Three cross section.

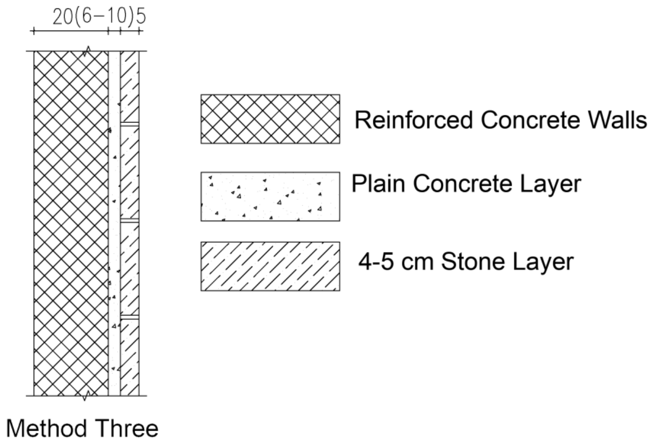

Figure 3-12: Method three cross section**.**

3.5 Effective Cross Sections of the Three Methods

3.5.1 Summary of Methods

Methods of construction of infill walls varies in a wide range. This variation necessarily affects infill walls contribution in the performance of structures when structures are subjected to motional loads like earthquakes. Figure 3-13 is an illustrative chart that summarize the discussed methods of construction of stone cladding in Palestine.

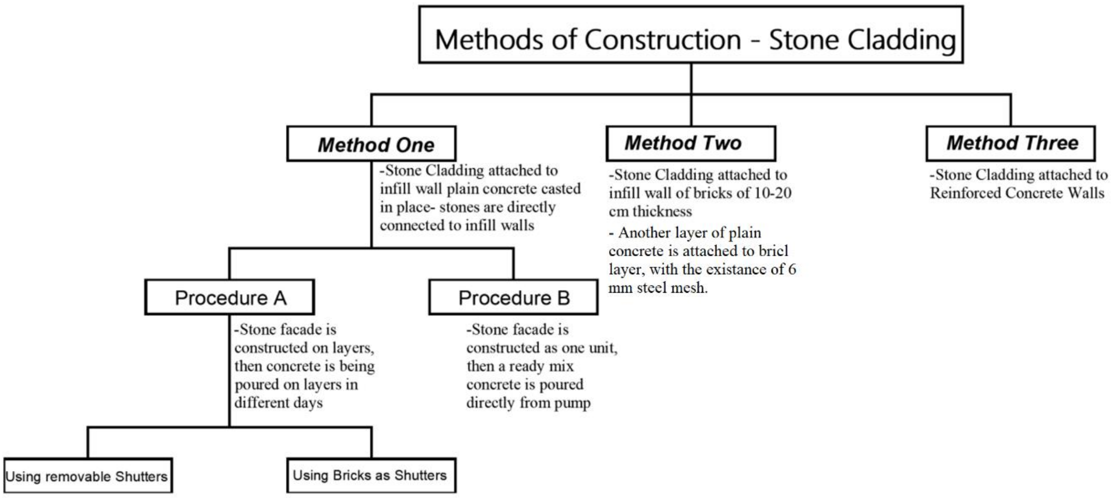

Figure 3-13: Tree chart shows methods of stone cladding construction in Palestine**.**

It is agreed that the existence of infill walls will change the lateral stiffness of the system, but the challenge is how to include these complicated infill walls in analysis in a conservative way.

3.5.2 Challenges in Modeling Infill Walls in the Three Methods

Modeling of materials that can sustain both actions of tension and compression is a clear direct approach, while it is somehow challengeable to model materials that are supposed to fail in tension as plain concrete, and brick.

Therefore, and due to the existence of reinforced walls, modeling of Method Three is the easiest if compared to the other two approaches. For the other two methods a procedure of Macro Modeling is a common approach that will be used in this thesis.

Following points may explain why modeling of infill walls in both Approaches one and two is considered complex and challengeable:

1- Complexity of pouring in situ concrete on layers in different days using different mixes.
2- Lack of reinforcement – Method One.
3- The low reliability in determining concrete compressive strength for the concrete behind stone.

Figure 3-14 shows the three methods cross sections, and as mentioned previously, only method three cross section can be modeled smoothly using available models of tension-compression walls.

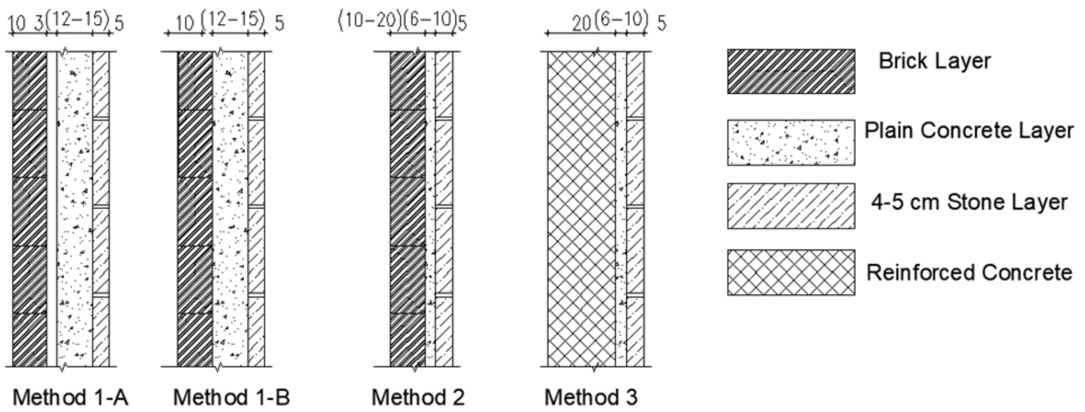

Figure 3-14: Cross sections for the three methods of construction of cladding facades**.**

3.5.3 Determination of the Effective Infill Walls Cross Section Components

One of the main questions that needs an answer is what parts of cross sections need to be considered in the modeling of infill walls. In the following section each component will be discussed before having the final conclusion of what to consider and what to neglect.

3.5.3.1 Stone Layer

In the three methods there is a common feature that stone layer does not lay within the frame, as in all cases stone layer is supposed to cover the face of column (cladding of column surface-see figure 3-15).

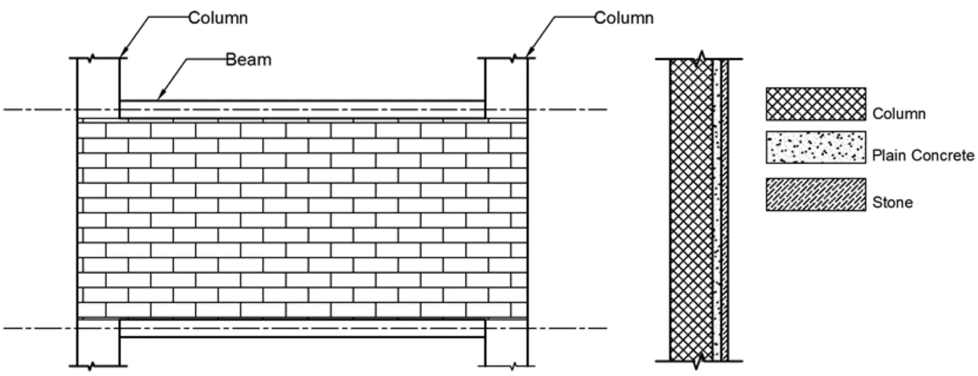

Figure 3-15: Layer of stone cladding location regarding frame system- same in all three methods

Components not within the frame will not be included in the effective cross section of the infill wall; this assumption of removing elements that lay out of the frame can be supported by definition of infill wall as provided by FEMA356-2000; where according to FEMA infill walls need to be constructed in a way that permits interaction between concrete frame and components of infill walls; and since elements out of the frame is not directly connected to concrete frame, then an assumption of neglecting such elements will be adopted through this study. Another point that may support the assumption of not include elements out of the frame is that it is suspected at the first stage under any lateral load that those components will be separated from other components within the frame, and therefore not contributing in the lateral stiffness.

Figure 3-16 shows an evident that may support the claim that elements not within the frame can be neglected from modeling. The figure shows part of façade in a commercial building in Palestine where some stones of the façade were separated under gravity load. Such failure may provide an indication that the connection between stone layer and plain concrete is not strong enough to contribute in defining the lateral stiffness of the composite façade that is composed of interaction between frame and infill wall.

Figure 3-16: 10 stone rows separated in a stone façade under gravity load

It is important to keep in mind that assumption of removing layers out of the frame is one of the limitations of this study, and for future studies it is recommended to investigate such an assumption to increase reliability about defining structural components of infill walls.

Figures 3-17, and 3-18 shows an application of what is known as "Mechanical Fixation" in constructing stone cladding that is not adopted yet in Palestine. Application of such method may open the discussion of including stone layer in the modeling of the infill wall.

Figure 3-17: Application of mechanical fixation -1 (source: Jerusalem gardens company brochure)

Figure 3-18: Application of mechanical fixation -2 (source: Jerusalem gardens company brochure)

3.5.3.2 Plain Concrete Layer

Another important point that needs attention other than stone layer is the layer of plain concrete. In Method One the plain concrete is supposed to lay within the frame, while in the two other methods (Method Two and Three) plain concrete lays out of the frame. It is important to note that the fact of constructing infill wall before slab will probably subject infill wall to act as bearing wall.

Figure 3-19 shows how layer of plain concrete (6-10 cm) in both methods two and three doesn’t lay within the frame. Figures 3-2,3-3, and 3-4 illustrates how plain concrete lays within the frame in Method One.

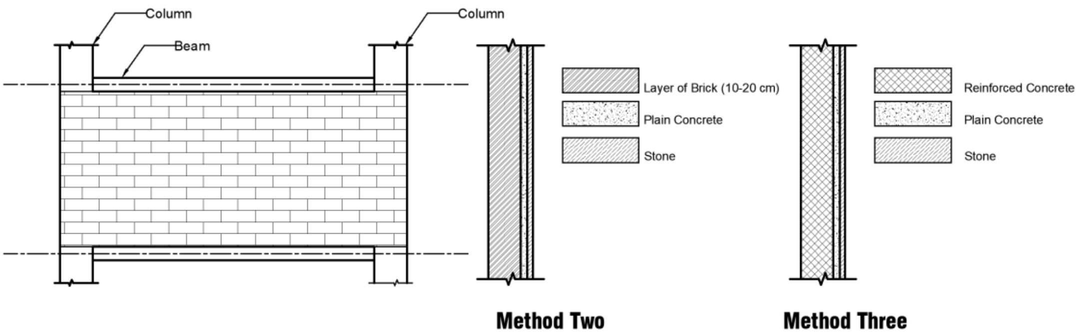

Figure 3-19: Layer of stone cladding location regarding frame system

Table 3-1 shows thickness of plain concrete of each method, and status of the existence of the infill wall within the structural frame system.

Table 3-1: Plain concrete thicknesses in the three methods, and concrete location status (within or not within the frame)

	Method One	Method Two	Method Three
Plain Concrete Thickness	12-15 cm	6-10 cm	6-10 cm
Plain Concrete of Infill wall within the frame	Yes	No	No

Table 3-2 shows which components are within the frame, and which components are out of the frame, for the three methods.

Table 3-2: Cladding components location regarding frame

	Method One	Method Two	Method Three
Stone Layer	Not within the frame	Not within the frame	Not within the frame
Plain Concrete layer	Within the frame	Not within the frame	Not within the frame
Bricks	Within the frame	Within the frame	No Bricks
Reinforced Concrete	No Reinforcement	No Reinforcement	Reinforced Section

3.5.3.3 Brick Layer

As mentioned previously, brick layer only exists in methods one and two, and as shown bricks layer is always within the frame, and so brick component will be considered in the effective cross section of the infill wall.

3.5.3.4 Summary of Components Within the Frame

The components that are included in the stiffness may be as provided in table 3-3.

Table 3-3: Components of infill walls for each method of construction

Method One	Method Two	Method Three
Brick layer of 10 cm	Brick layer of 10-20 cm	No Brick
Plain concrete of 12-15 cm	No Plain concrete layer	No Plain concrete; just reinforced concrete

Figure 3-20 shows the components that may be included in the infill wall analysis. Elements included in the infill walls are the only members within the frame.

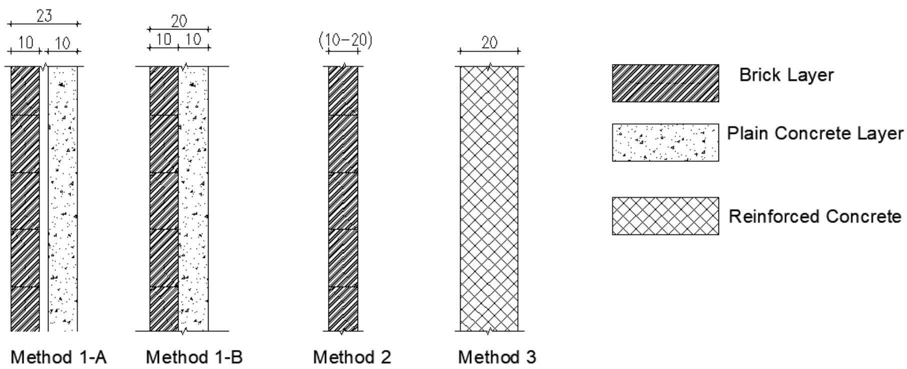

Figure 3-20: Structural components of infill walls that will be included in the analysis

3.5.3.5 Structural Properties of Local Bricks

Dealing with plain concrete as a structural component is not a debatable topic, while it is not the same case when talking about used bricks. Figure 3-21 shows a sample of the mostly used brick in the construction in

Palestine. It is obvious that the brick is voided and this may weaken its strength.

Figure 3-21: 10 cm brick sample

A master thesis issued in 2018 in Al-Najah University concluded that local used bricks in Palestine have a modulus of elasticity of around 260 MPa according to laboratory tests. This is around 1% of the modulus of elasticity of concrete. Thesis states that such low value can be justified for existence of voids, and weakness of material used in forming bricks (Qarout, 2018).

Table 3-4 shows comparison between modulus of elasticity of most common used concrete in engineering practice in Palestine, and for local bricks.

Table 3-4: Comparison of "E" value between concrete of fc'=24 MPa and local bricks in Palestine

Concrete Modulus of Elasticity (fc'=24 MPa) (1)	Brick Modulus of Elasticity (2)	Ratio (2/1)
23025	260	1.12%

Based on test results, and due to low value of structural parameter of modulus of elasticity for bricks; layer of brick will be excluded from the effective cross section of infill wall section that need to be modeled for method one only. Indeed, for method two where the effective section of the infill wall consists of only layer of bricks, bricks need to be modeled to check it is role on the total behavior of the structural system.

Table 3-5 shows the status of including bricks in the modeling of the infill walls regarding the three methods.

Table 3-5: Bricks modeling status in the three construction methods

Method One	Method Two	Method Three
Bricks will be excluded from the effective section	Bricks will be included in the effective section	No Bricks- so no concerns regarding bricks modeling

3.5.3.6 Components of Effective Infill Wall Cross Section

Figure 3-22 finalize the effective section of each method, therefore, modeling will deal with these components as structural elements, while other components will be included only on the weight of the infill wall, but structurally their contribution will be neglected.

The decision of neglecting some components of infill walls is an important assumption that is one of the limitations of this study, and it is important to emphasize that future studies need to focus on role of components out of the frame on the definition of lateral stiffness of infill walls.

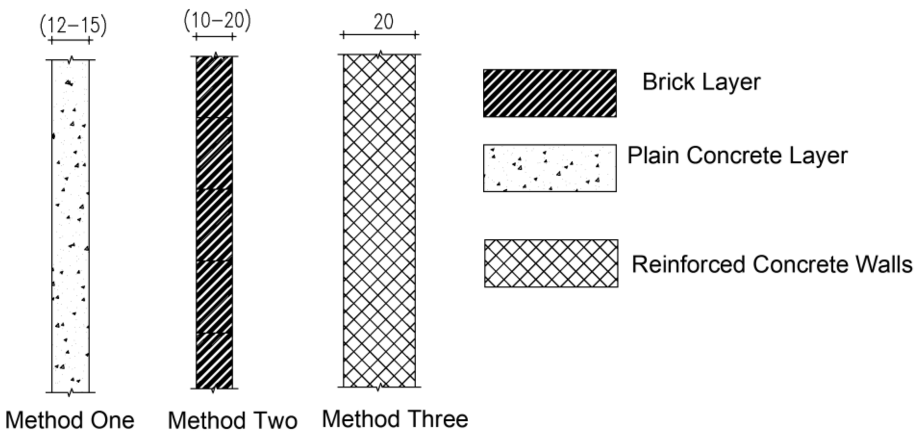

Figure 3-22: Effective section for the three models

For this study, effective sections with the shown dimensions in Figure 3-23 will be used in the analysis.

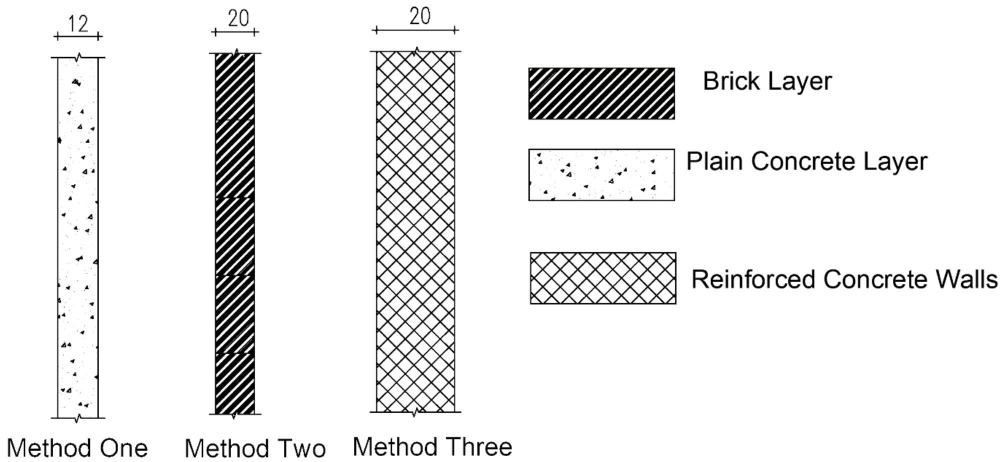

Figure 3-23: Effective section dimensions as will be used through this study

3.6 Weight of Each Method Cross Section

3.6.1 Components Unit Weights

It is obvious that the self-weight of each method varies based on the variation of components and dimensions. Table 3-6 shows the unit weight of infill walls components.

Table 3-6: Unit weights for infill wall components (stone, plain concrete, and brick)

Component	Unit Weight (kN/m^3)
Stone Layer	27
Plain Concrete	23
Reinforced Concrete	25
Brick	12

3.6.2 Height of Cross Section

Height of wall will be 312 cm for all analyzed infill walls (see figure 3-24).

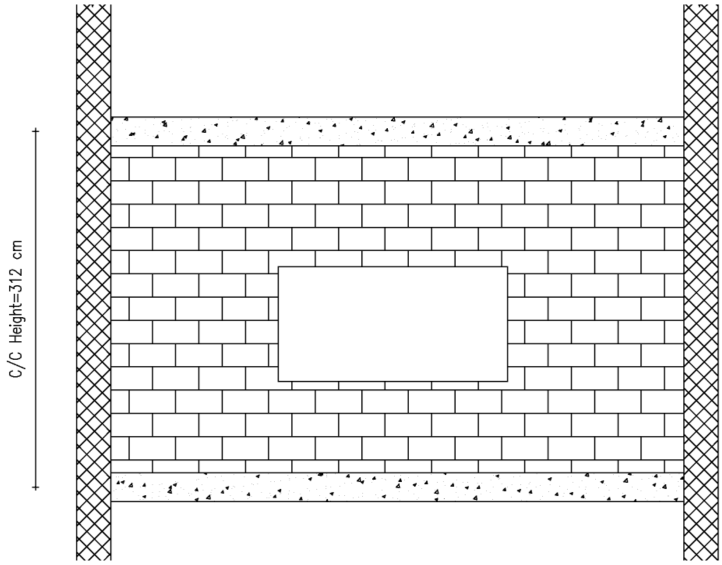

Figure 3-24: Height of infill wall – for all cases in this study

3.6.3 Openings in Infill Wall

Weight calculation must consider the existence of windows openings. Figure 3-25 shows suggested window opening in an infill wall, this pattern will be used in computation the ratio of opening to the area of the infill wall to estimate final value for line loads.

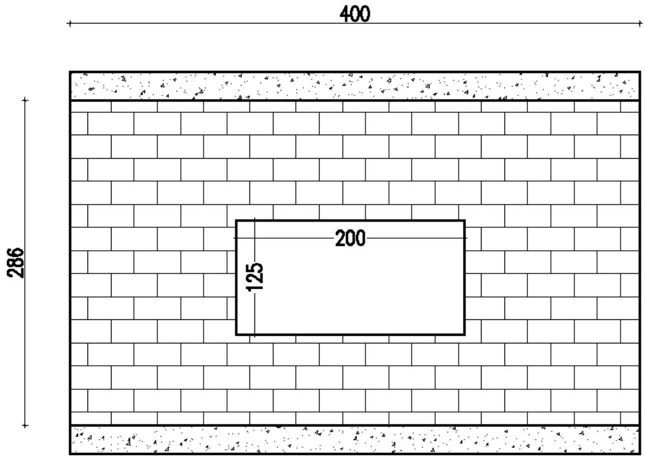

Figure 3-25: Suggested window dimensions in the infill wall

Table 3-7 shows the ratio of window opening to infill wall, for line weight modifications purposes.

Table 3-7: Ratio of area opening to infill wall area

Area of infill wall (m^2)	Area of Opening (m^2)	Opening area/Infill wall area
11.44	2.5	0.22

A deduction of 20% will be applied on the value of line load based on value computed in table 3-7.

3.6.4 Weight of Method One Section

Method One cross section that will be analyzed in this study is shown in figure 3-26.

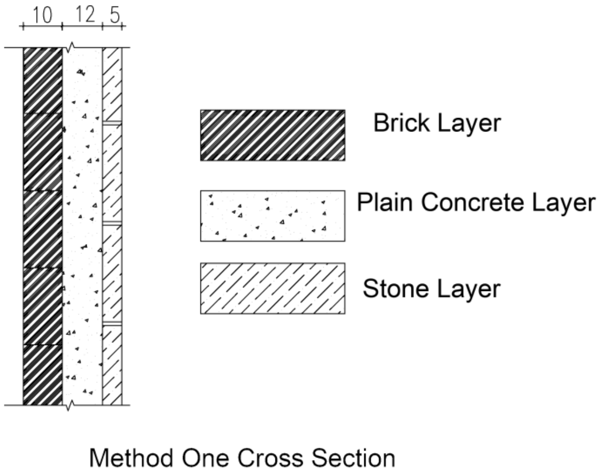

Figure 3-26: Dimensions of method one cross section that will be used in this study

Table 3-8 shows calculations of wall weight assuming a center to center wall height of 312 cm.

Table 3-8: Weight of cladding wall calculations for 1 meter length and 3.12 meter height (Method One)

Component	**Width (cm)**	**Unit Weight (kN/m^3)**	**1 meter length x 3.12 m height Weight (kN)**
Stone layer	5	27	4.21
Plain concrete	12	22	8.24
Brick	10	12	3.74
Sum			16.2

Table 3-9 shows the final line load value after applying the deduction due to the existence of windows openings. Why not as SDL applied to wall as load/area).

Table 3-9: Final line load of infill wall cladding after deducting of openings-method one section

Final line load value of infill wall cladding	13 kN/m

3.6.5 Weight of Method Two Section

Method Two cross section that will be analyzed in this study is shown in figure 3-27.

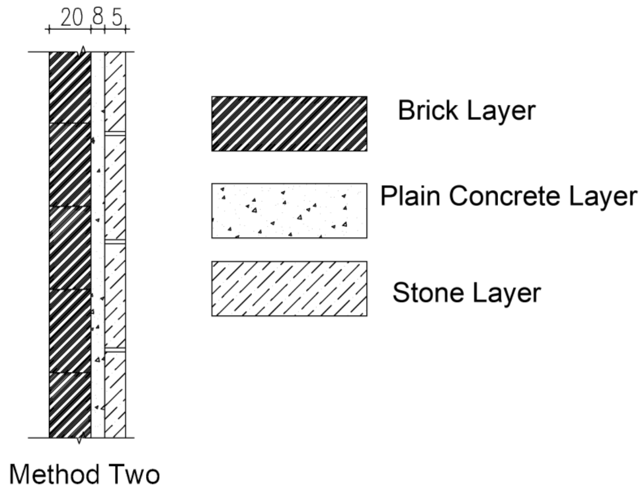

Figure 3-27: Dimensions of Method Two cross section that will be used in this study

Table 3-10 shows calculations of wall weight assuming a center to center wall height of 312 cm.

Table 3-10: Weight of cladding wall calculations for 1-meter length and 3.12-meter height (Method Two)

Component	**Width (cm)**	**Unit Weight (kN/m^3)**	**1-meter length x 3.12 m height Weight (kN)**
Stone layer	5	27	4.21
Plain concrete	8	22	5.49
Brick	20	12	7.48
Sum			17.18

Table 3-11 shows the final line load value after applying the deduction due to the existence of windows openings.

Table 3-11: Final line load of infill wall cladding after deducting of openings-method one section

Final line load value of infill wall cladding	13.74 kN/m

3.6.6 Weight of Method Three Section

Method Three cross section that will be analyzed in this study is shown in figure 3-28.

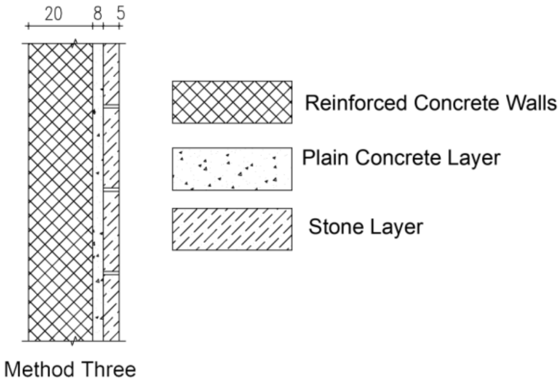

Figure 3-28: Dimensions of method three cross section that will be used in this study

Table 3-12 shows calculations of wall weight assuming a center to center wall height of 312 cm.

Table 3-12: Weight of cladding wall calculations for 1-meter length and 3.12-meter height (Method Two)

Component	Width (cm)	Unit Weight (kN/m^3)	1-meter length x 3.12 m height Weight (kN)
Stone layer	5	27	4.21
Reinforced concrete	20	24	14.98
Plain concrete	8	22	5.49
Sum			24.68

Table 3-13 shows the final line load value after applying the deduction due to the existence of windows openings.

Table 3-13: Final line load of infill wall cladding after deducting of openings-method one section

Final line load value of infill wall cladding	19.74 kN/m

3.6.7 Weight of Sections' Methods (Summary)

Table 13-4 summarize the net line weight the represents each method cross section as will be analyzed through this thesis. It must be noted that values are modified to be with no frictions.

Table 3-14: Weight of cladding wall calculations for 1-meter length and 3.12-meter height (method two)

Cross Section	1-meter length x 3.12 m height Weight (kN/m)
Method One	13
Method Two	14.0
Method Three	20.0

Chapter Four

Modeling of Infill Walls

4.1 Introduction

Modeling of infill walls is an interest of many researchers due to their contribution in the behavior of structures specially in resisting lateral forces. The main challenge facing structural engineers is the accurate modeling of these walls.

Two methods of modeling of infill walls have been developed since the start of the research efforts; the first method of Macro Modeling is based on the equivalent strut method, while the second approach “Micro Modeling” is based on finite element method. The fact that macro-modeling technique is easier and simpler, and the possibility of using the structural mechanical properties from related tests justifies the common use of equivalent strut method (Abdelkareem et al. 2013).

Reinforced concrete frames with masonry infilled walls can be modeled by replacing the infill wall by an equivalent diagonal strut. The diagonal strut is mainly defined by an equivalent width that will affect the lateral stiffness and strength of frames (K.H. Abdelkareem et. al, 2013).

The flexibility and availability of 3D Analysis software enhanced the ability of creating complex numerical models for construction projects worldwide. Therefore, the use of complex modeling techniques has become the most practical tool for structural analysis purposes, and finite element method almost replaced the use of conventional mathematical procedures in the structural analysis.

One of the main challenges in adopting 3D analysis results is the assumptions analyzer have in the model itself. The degree of accuracy depends mainly on how much these assumptions reflect what will be built in reality. Incorrect model assumptions and input could lead to a situation where expectations may greatly differ from what the real behavior is.

Structural modeling assumptions include the establishment of three mathematical models. The first model is general representation of structural members including connections between different elements, and the boundary conditions like the foundation system. The second model is for the material, while the final model is for the load (bridge design practice, 2015).

The two modeling techniques of macro and micro modeling are both important for analysis purposes; as the adaptation of macro modeling techniques must come after verification with both experimental and comparison with micro modeling results. In other words, for engineering practices and due to the fact that macro modeling is simpler than micro modeling, both methods need to be understood for the sake of easing and increasing reliability of infill walls modeling.

Method of construction regarding cladding facades may have important influence on the modeling of infill walls. In Chapter Three in this thesis three methods of construction are presented and discussed in details.

4.2 Common Practiced Modeling Techniques

Common practiced modeling techniques in Palestine usually ignores modeling of infill walls as structural elements. This ignorance can be justified by assuming that infill walls have no capacity of tension due to weakness of bricks (for Method two), and the nature of poured concrete without much quality control (for Method One), besides the assumption of only defining the structural system that is responsible of supporting the gravity loads. In other words, modeling consists of load carrying elements, where infill walls are not supposed to share in the gravity load system.

The sequence of construction may contradict with the assumption of not participating in the gravity loads system; as the common practice to construct infill wall facades, then to cast the slab, and this means that slab when deflected will transfer loads to infill walls, and this make these walls bearing walls.

Therefore, one of the assumptions that need to be adopted through this study is that infill walls are assumed to be only part of the lateral system, where for gravity loads, the system will be limited to concrete frame system.

Figure 4-1 shows a multistory building in Ramallah city in Palestine and its structural model.

Figure 4-1: 3D analytical model and photo taken during construction for a building -Palestine

As shown in figure 4-1 the analytical model is considering only slabs, reinforced walls, and columns. The existence of infill walls is neglected. Indeed, the only considered contribution of such walls are by modeling their weight as line load as shown in figure 4-2.

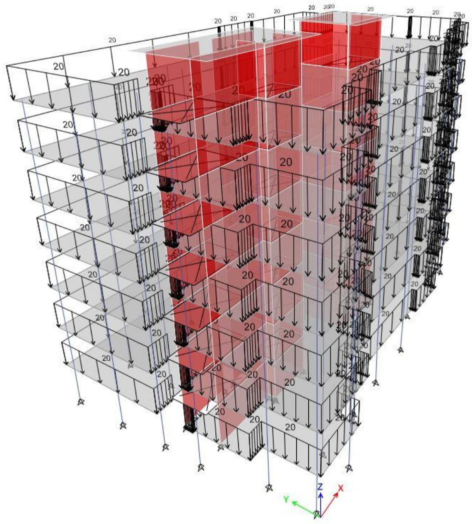

Figure 4-2: Common practice of representing infill walls as line load

4.3 Definition of Concrete Frame with Infills in FEMA356-2000

According to FEMA356-2000 “the concrete frames with infills are elements with complete gravity-load-carrying concrete frames infilled with masonry or concrete, constructed in such a way that the infill and the concrete frame interact when subjected to vertical and lateral loads” (FEMA356-2000).

FEMA states that isolated infill walls with gaps that separate infill from concrete frame can be neglected in the analysis. The minimum gap requirements are specified in section 7.5.1 in FEMA.

Infill panels are considered isolated from the surrounding frame when having gaps at both top and sides to accommodate maximum expected lateral frame deflections. Isolated panels shall be restrained in the transverse direction to ensure stability under normal forces. Panels in full contact with the frame elements on all four sides are termed “shear infill panels”.

The nature of infill panel depends on the method of construction. In Chapter Three two types of infill panels are defined: a plain concrete infill panel, and a brick infill panel.

According to FEMA panels may be masonry (section 6.7.1.2-FEMA356-2000) or concrete infill (section 6.7.1.3-FEMA 356-2000). For both cases

FEMA states that such infills must comply with provisions of section 6.7 in FEMA.

For concrete infills FEMA mentions that the infill panels of concrete are constructed to fill the space within the bay of a complete gravity frame without special provision for continuity from story to story.

4.4 Modeling of Infill Walls

4.4.1.1 General Considerations for Concrete Frames with Masonry Infills

According to FEMA (section 6.7.2.1) “the analytical model for a concrete frame with masonry infills shall represent strength, stiffness, and deformation capacity of beams, slabs, columns, beam column joints, masonry infills, and all connections and components of the element”. Moreover, any potential failure in flexure, shear, anchorage, reinforcement development, or crushing at any section shall be considered, besides the interaction with other nonstructural elements and components shall be included.

Modeling of infill masonry walls using a linear static model shall be permitted if the infill wall will not crack when subjected to design lateral forces. If this happens then modeling the assemblage of frame and infill as a homogeneous medium shall be permitted.

“For a concrete frame with masonry infills that will crack when subjected to design lateral forces, modeling of the response using a diagonally braced frame model, in which the columns act as vertical chords, the beams act as horizontal ties, and the infill acts as an equivalent compression strut, shall be permitted. Requirements for the equivalent compression strut analogy shall be as specified in Chapter 7." (FEMA356-2000).

4.4.1.2 General Considerations for Concrete Frames with Masonry Infills

Besides representing strength, stiffness, deformation capacity of columns, slabs, and beams, and modeling all connections and components of elements, the analytical model shall take in consideration both of the relative stiffness and strength of the frame and the infill, as well as the level of deformations and associated damage.

FEMA states that for the case of low deformation levels, and where the frame is relatively flexible, the infilled frame shall be permitted to be modeled as a shear wall, but taking in consideration locations of openings for accurate modeling. However, in other cases of higher level of deformations, the frame-infill system shall be modeled using a braced-frame analogy similar to that described for concrete frames with masonry infills.

4.5 Comparative Study for Equivalent Strut Widths Calculations

In this section a comparative study will be performed for a specific single bay single frame model for both infill panels for Method One and Method

Two (plain concrete, and brick layer of thickness 20 cm). Figure 4-3 shows the frame dimensions.

Output of different approaches will be compared to check range of strut width, and obtained results are supposed to help in determining which method to adopt for later on calculations that will be applied in Chapter Five in the analytical part.

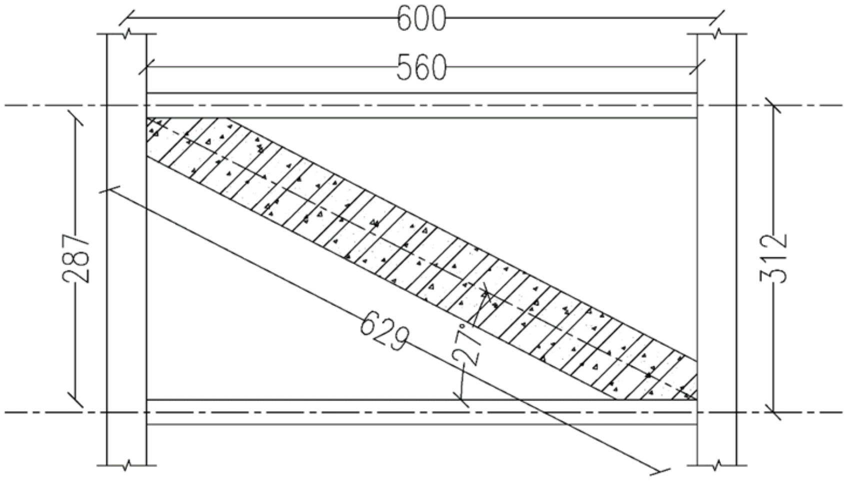

Figure 4-3: The infill wall that will be replaced by the shown diagonal strut

4.5.1 Equivalent Strut Width for Method One (Plain Concrete Infill Wall)

Figure 4-4 shows the section that will be converted to an equivalent compression strut.

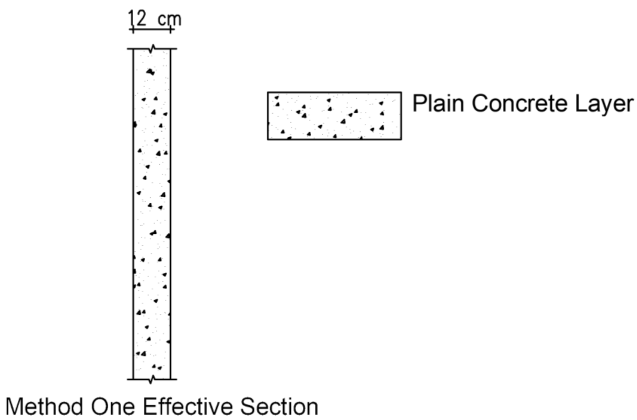

Figure 4-4: Method one effective section

Table 4-1 shows data of single bay single story frame with plain concrete infill.

Table 4-1: Data for the single bay single frame with plain concrete infill panel

Column's dimensions (mm)	400x400
Beam's dimensions (mm) (WidthxDepth)	400x250
f_c' of frame elements (MPa)	24
t (mm): thickness of infill wall	120
f_c' of infill wall (MPa)	24
θ : angle between diagonal and the length of infill wall (degree)	27
E_c: Modulus of elasticity of frame element (MPa)	$2.3\text{x}10^5$
E_f: Modulus of elasticity of infill wall (MPa)	$2.3\text{x}10^5$
h_{inf}: Height of infill wall (m)	2.86
H_{column}: Height of column (m)	3.12
d_{inf} (m)	6.29
I_c: Moment of Inertia of the column of the frame (m^4)	$2.13\text{x}10^{-3}$
I_b: Moment of Inertia of the beam of the frame (m^4)	$5.21\text{x}10^{-4}$

4.5.1.1 Equivalent Strut Width Using Holmes Formula

Strut width is computed using equation 2-9 as following:

$$w = \frac{1}{3} d_{inf} = \frac{1}{3}(629) = 209.67\ cm$$

Table 4-2 shows strut width value using Holmes formula:

Table 4-2: Equivalent strut width-Holmes formula

Holmes Formula	
Strut Width	209.67 cm

4.5.1.2 Equivalent Strut Width Using Mainstone and Weeks Formula

Since formula of Mainstone and Weeks is a development of Mainstone formula that was published in 1971, the equivalent strut will be computed only by the developed formula (Equation 2-11) as following:

$$w = 0.175 d_{inf} (\lambda_h h_{inf})^{-0.4} = 0.175 \times 6.26 \times (1.41 \times 2.87)^{-0.4} = 0.627\, m$$

Table 4-3 shows strut width value using Mainstone and Weeks formula:

Table 4-3: Equivalent strut width- Mainstone and Weeks formula

Mainstone and Weeks formula	
Strut Width	62.7 cm

4.5.1.3 Equivalent Strut Width Using Bazan and Meli Formula

Following are calculations related to Bazan and Meli formula:

$$A_c = 0.4 \times 0.4 = 0.16\, m^2$$

$$G_{inf} = \frac{E_c}{2(1+v)} = \frac{23025000}{2(1+0.15)} = 10010869.57$$

$$A_{inf} = L_{inf} \times t_{inf} = 5.6 \times 0.12 = 0.672$$

Table 4-4 shows parameters required in computing β value:

Table 4-4: Parameters for β calculations

A_c (m^2)	0.16
G_{inf}	$10x10^6$
A_{inf} (m^2)	0.672

$$\beta = \frac{E_c A_c}{G_{inf} A_{inf}} = \frac{23025000 \times 0.16}{10 \times 10^6 \times 0.672} = 0.548$$

$$w = (0.35 + 0.22 \times 0.548) \times 3.12 = \ 1.47\ m$$

Table 4-5 shows strut width value using Bazan and Meli formula:

Table 4-5: Equivalent strut width- Bazan and Meli formula

Bazan and Meli formula	
Strut Width	147 cm

4.5.1.4 Equivalent Strut Width Using Paulay and Preistely Formula

According to Paulay and Preistely width of the equivalent strut is one fourth the diagonal length of the infill wall (equation 2-14).

$$w = \frac{1}{4} d_{inf} = \frac{1}{4} \times 6.29 = 1.57 \text{ m}$$

Table 4-7 shows strut width value using Paulay and Preistely formula:

Table 4-6: Equivalent strut width Paulay and Preistely formula

Paulay and Preistely fromula	
Strut Width	157 cm

4.5.1.5 Equivalent Strut Width Using Durrani and Luo Formula

Following are the calculations of strut width using Durrani and Luo formula (equation 2-15):

$$m = 6\left[1 + \frac{6E_c I_b h}{\pi E_c I_c l}\right] = 6\left[1 + \frac{6 \times 23025000 \times 0.00052 \times 3.12}{\pi \times 23025000 \times 0.00213 \times 6}\right] = 6.15$$

$$\gamma = 0.32\sqrt{sin2\theta}\left[\frac{h^4 E_{inf} t}{mE_c I_c h_{inf}}\right]^{-0.1}$$

$$= 0.32\sqrt{\sin(2 \times 27)}\left[\frac{3.12^4 \times 23025000 \times 0.12}{7.45 \times 23025000 \times 0.00213 \times 2.87}\right]^{-0.1}$$

$$= 0.166$$

$$w = \gamma\sqrt{L^2 + h^2} sin2\theta = 0.166 \times \sqrt{6^2 + 3.12^2}\ \ sin54 = 0.91\,\text{m}$$

Table 4-7 shows strut width value using Durrani and Luo formula:

Table 4-7: Equivalent strut width- Durrani and Luo formula

Durrani and Luo formula	
Strut Width	91 cm

4.5.1.6 Equivalent Strut Width Using Hendry Formula

Following are the calculations of strut width using Hendry formula (equation 2-18):

$$\alpha_h = \frac{\pi}{2}\left[\frac{4E_c I_c H_{inf}}{E_{inf} t sin2\theta}\right]^{\frac{1}{4}} = \frac{\pi}{2}\left[\frac{4 \times 23025000 \times 0.00213 \times 2.87}{23025000 \times 0.12 \times \sin 54}\right]^{\frac{1}{4}} = 1.11$$

$$\alpha_L = \frac{\pi}{2}\left[\frac{4E_b I_b L_{inf}}{E_{inf} t sin2\theta}\right]^{1/4} = \frac{\pi}{2}\left[\frac{4 \times 23025000 \times 0.00052 \times 6}{23025000 \times 0.12 \times \sin 54}\right]^{\frac{1}{4}} = 0.94$$

$$w = 0.5\sqrt{{\alpha_h}^2 + {\alpha_L}^2} = 0.5\sqrt{1.11^2 + 0.94^2} = 0.727\ m$$

Table 4-8 shows strut width value using Hendry formula:

Table 4-8: Equivalent strut width- Hendry formula

Hendry formula	
Strut Width	72.7 cm

4.5.1.7 Equivalent Strut Width Using Papia

Following are the calculations of strut width using Papia formula (equation 2-21):

$$c = 0.249 - 0.0116v_{inf} + 0.567{v_{inf}}^2$$
$$= 0.249 - 0.0116 \times 0.15 + 0.567(0.15)^2 = 0.26$$

$$\beta = 0.146 + 0.0073v_{inf} + 0.126{v_{inf}}^2$$
$$= 0.146 + 0.0073 \times 0.15 + 0.126 \times 0.15^2 = 0.15$$

$$\lambda^* = \frac{E_{inf}th_{inf}}{E_cA_c}\left[\frac{{h_{inf}}^2}{{l_{inf}}^2} + \frac{A_cl_{inf}}{4A_bh_{inf}}\right]$$

$$\lambda^* = \frac{23025000 \times 0.12 \times 2.87}{23025000 \times 0.16}\left[\frac{2.87^2}{5.60^2} + \frac{0.16 \times 5.60}{4 \times 0.1 \times 2.87}\right] = 2.25$$

$$z = 1.125 \; since \; \frac{l_{inf}}{h_{inf}} > 1.5$$

$$w = \frac{c}{z}\frac{1}{\lambda^*}d_{inf} = \frac{0.26}{1.125} \times \frac{1}{2.25} \times 6.29 = 0.646 \text{ m}$$

Table 4-9 shows strut width value using Papia formula:

Table 4-9: Equivalent strut width- Papia formula

Papia formula	
Strut Width	64.6 cm

4.5.1.8 Equivalent Strut Width Using FEMA356-2000 Formula

Following are the calculations of strut width using FEMA356-2000 formula (equation 2-25):

$$\lambda_1 = \left[\frac{E_{inf} t \sin 2\theta}{4E_c I_c h_{inf}}\right]^{\frac{1}{4}} = \left[\frac{23025000 \times 0.12 \times \sin 54}{4 \times 23025000 \times 0.00213 \times 2.87}\right]^{\frac{1}{4}} = 1.41$$

$$w = 0.175(\lambda_1 h_{col})^{-0.4} d_{inf} = \ 0.175(1.41 \times 3.12)^{-0.4} \times 6.29 = 0.608\, m$$

Table 4-10 shows strut width value using FEMA356-2000 formula:

Table 4-10: Equivalent strut width- FEMA356-2000 formula

FEMA356-2000 formula	
Strut Width	60.8 cm

4.5.1.9 Equivalent Strut Width Using NBCC 2005

NBCC formulas are same to those suggested by Hendry. Calculations using NBCC 2005 are as following:

$$\alpha_h = \frac{\pi}{2}\left[\frac{4E_c I_c h}{E_m t_e \sin 2\theta}\right]^{\frac{1}{4}} = 1.11$$

$$\alpha_L = \frac{\pi}{2}\left[\frac{4E_c I_b L}{E_m t_e \sin 2\theta}\right]^{\frac{1}{4}} = 0.94$$

$$w = \sqrt{{\alpha_h}^2 + {\alpha_L}^2} = 1.45\, m$$

Calculation of equivalent strut continues as the effective width of strut is calculated as following:

w_e is the effective diagonal strut width, and shall be calculated according to these conditions:

$$w_e \leq \frac{w}{2} \rightarrow w_e \leq \frac{1.45}{2}\ (0.725\, m) or\ \leq \frac{l_s}{4} \rightarrow \frac{6.29}{4}\ (1.573\, m)(smaller\ control)$$

Therefore,

$$w_e = 0.725\ m$$

Table 4-11 shows strut width value using NBCC-2005 formula:

Table 4-11: Equivalent strut width- NBCC 2005 formula

NBCC 2005 formula	
Strut Width	72.5 cm

4.5.1.10 Comparison Between Equivalent Strut Width Calculation Approaches

For the same single bay single story concrete frame with infill of plain concrete of 12 cm thickness different approaches yielded values in a wide range. Figure 4-16 shows graph of different approaches regarding the value of equivalent strut.

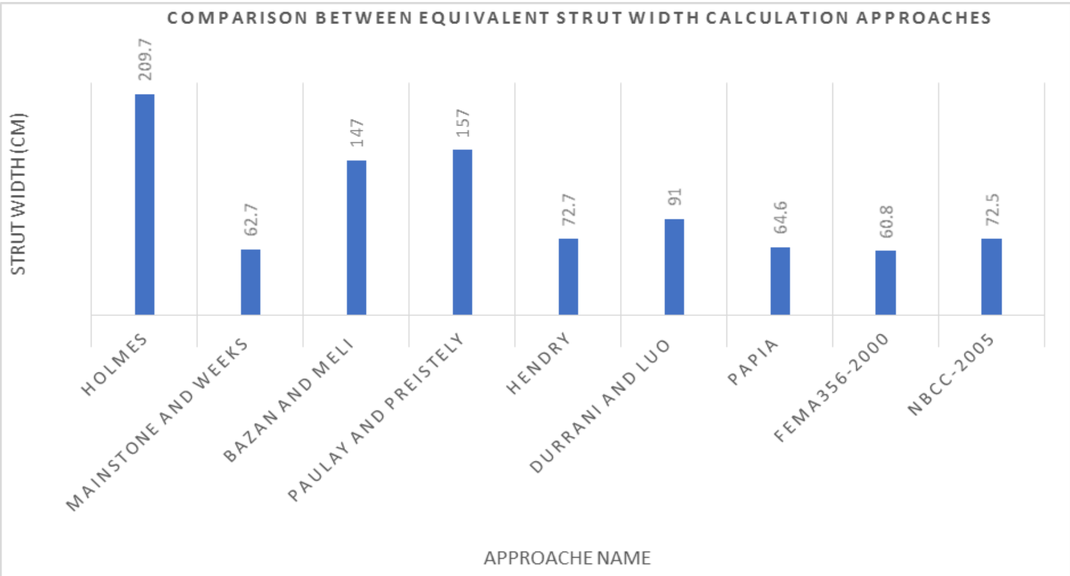

Figure 4-5: Strut width as suggested by each approach

Results shown in figure 4-5 shows wide difference between the different approaches. It can also be noted that the values between 60-70’s cm are most repeated (5 results of 9 lays within this range).

4.5.1.11 Calculating Equivalent Strut Using 2D Model Through ETABS Software

In this section a single bay single story frame with infill panel will be modeled in ETABS 2016 software. A point lateral force will be assigned to the frame, then the frame will be analyzed and tension areas in the infill panel will be determined and removed, based on the assumption that infill wall with plain concrete has no tension capacity.

After determining the tension areas, those areas will be removed and the lateral stiffness of the concrete frame with the remaining areas that are subjected to compression will be determined. Based on this value of lateral stiffness the equivalent strut will be determined and compared to different approaches.

4.5.1.11.1 Single Bay Single Story Frame with Solid Infill Wall Panel

Figure 4-6 shows the model of the single bay single frame that will be used in determining the equivalent strut width.

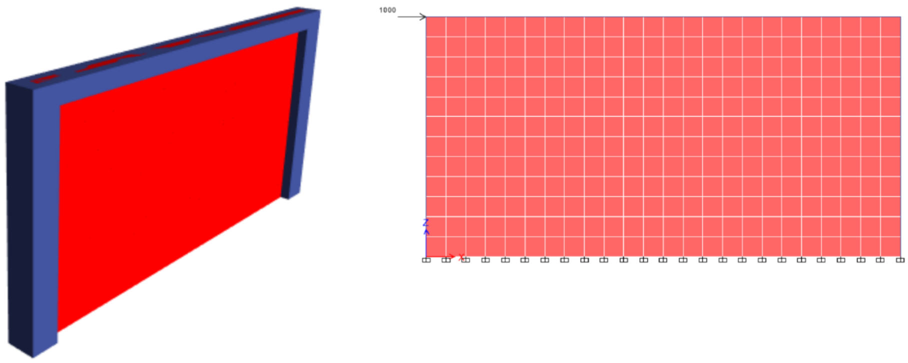

Figure 4-6: 2D model of concrete frame with plain concrete infill wall

Table 4-12 shows the data of the 2D model.

Table 4-12: Data of the 2D model that is used for equivalent strut calculations

2D Model Data	
Columns' dimensions (mm)	400x400
Beam's dimension (mm)	400x250 (width x depth)
Infill wall thickness (mm)	120 mm
Frame, and infill material concrete Ec (MPa)	$2.3x10^5$
Mesh dimension (mm)	Squares of 125x125
Lateral Load value (kN)	1000
Frame Height (mm)	2860
Frame Width (mm)	6000
Posion's Ratio	0.15

4.5.1.11.2 Computation of Reduction Factor for Accurate 2D Model

An important point that need to be mentioned here that the fact that the frame is being modeled with height of 2.86 meters instead of 3.12 m will increase the stiffness of the frame itself as the stiffness of the frame will increase when column height is reduced. Below equation illustrates this issue.

$$K = \frac{24EI_c}{h^3{}_{c/c}} \frac{(12\rho+1)}{(12\rho+4)} \rightarrow$$

$$as\ h\ decreased\ to\ 2.86\ instead\ of\ 3.12\ meters\ K\ will\ increase$$

To avoid this issue the moment of inertia of the column will be modified so that the final value of stiffness is same as if it modeled with 3.12 meters. Calculations of reduction factor I shown below.

$$Reduction\ Factor = \frac{K\ (with\ column\ 3.12)}{K\ (with\ column\ 2.86)} = \frac{\frac{24EI_c}{h^3{}_{3.12}} \frac{(12\rho+1)}{(12\rho+4)}}{\frac{24EI_c}{h^3{}_{2.87}} \frac{(12\rho+1)}{(12\rho+4)}} = \frac{h^3{}_{2.86}}{h^3{}_{3.12}}$$

$$= 0.77$$

In order to verify that such reduction will accurately model the contribution of column with center to center height of 3.12 meter in a model with actual height of 2.86 m, two models with single bay single frame will be modeled with modification in the model of 2.86 by applying the reduction factor on the moment of inertia value.

Figure 4-7 shows the two models as built on ETABS.

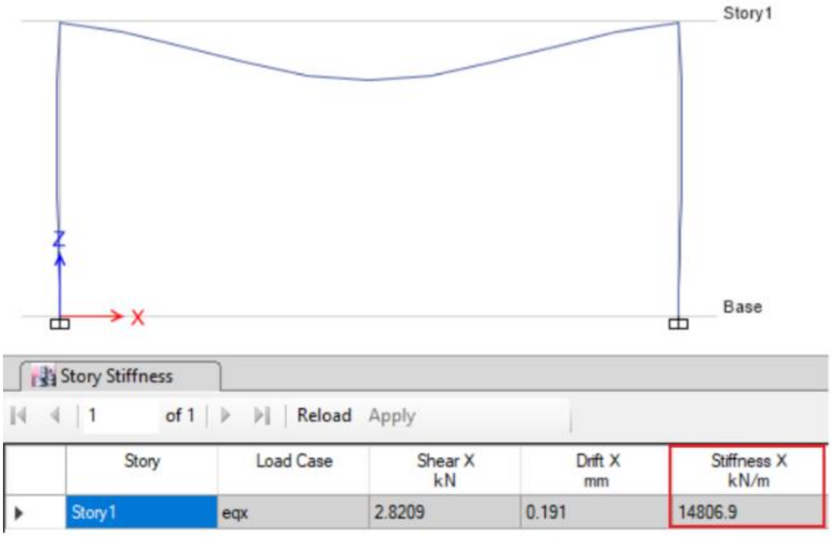

	Story	Load Case	Shear X kN	Drift X mm	Stiffness X kN/m
▸	Story1	eqx	2.8209	0.191	14806.9

Model with Column's Height=2.86 m

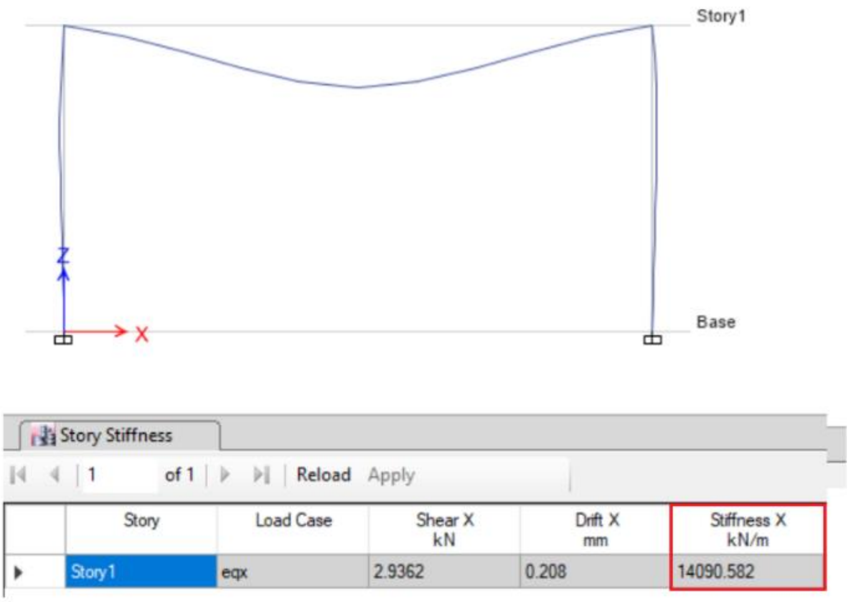

	Story	Load Case	Shear X kN	Drift X mm	Stiffness X kN/m
▸	Story1	eqx	2.9362	0.208	14090.582

Model with Column's Height=3.12 m

Figure 4-7: Models of 2.86, 3.12 meters height lateral stiffness output

Table 4-13 shows comparison between the two models with an acceptable difference of 5.4%.

Table 4-13: 2D Frame models Lateral Stiffness Outputs (2.86 and 3.12 m Heights) (kN/m)

2D Frame Models Lateral Stiffness Outputs (2.86 and 3.12 m Heights) (kN/m)		
2D Model With 2.87 m height	2D Model With 3.12 m height	Difference (%)
14806.9	14090.582	5.4%

Based on previous verification, a model with height of 2.86 meters will be built for a concrete frame with infill panel, taking in consideration reduction of column's moment of inertia by almost 23% to truly model columns' height and their contribution in the overall stiffness.

4.5.1.11.3 Determining Tension Areas in The Infill Panel Due to Applied Lateral Load

Before discussing output of the model, the local axis must be determined. Figure 4-8 shows the local axis as assigned automatically by the software (Computer & Structures Inc. 2016).

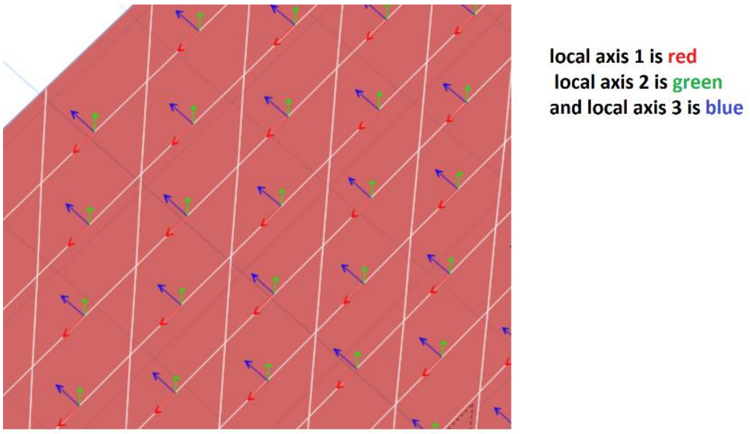

Figure 4-8: Direction of local axis in the model, and color keys: red=1, green=2, and blue=3

Figure 4-9 shows the resultant force in the infill walls due to the application of the lateral load in the direction of local axis 1 (red local axis as shown in figure 4-8).

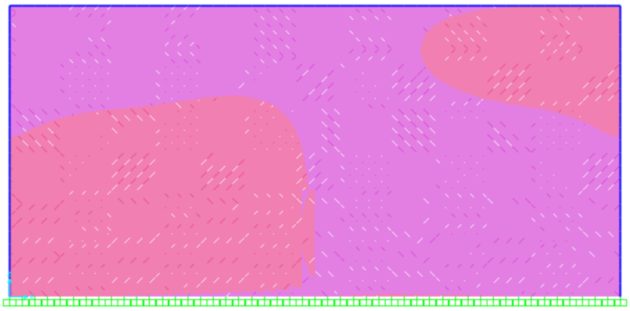

Figure 4-9: Purple area=under compression, Red area=under tension

Figure 4-10 shows the frame after removing areas under tension.

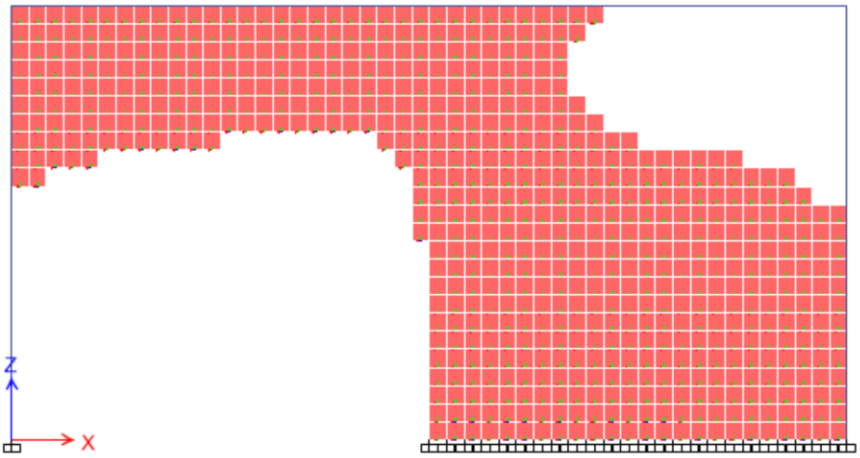

Figure 4-10: Frame after removing areas under tension of the infill panel

4.5.1.11.4 Determining Strut Width Using Output of the 2D Model

The lateral stiffness of a single-story single bay frame with diagonal strut can be computed as provided by the following formula:

$$Lateral\ stiffness\ (infilled\ frame) = Frame\ Lateral\ Stiffness + Diagonal\ Axial\ Stiffness$$

$$K = \frac{24EI_c}{h^3}\frac{(12\rho+1)}{(12\rho+4)} + \frac{w \times E_{inf} \times t_{inf}}{d_{inf}} \times cos^2\theta$$

Where,

$$\rho = (\frac{EI_b}{L}) \div (\frac{2EI_c}{h})$$

Following are the detailed calculations of lateral stiffness:

$$\rho = \frac{I_b h}{2LI_c} = \frac{3.12 \times 0.00052}{2 \times 6 \times 0.0023} = 0.059$$

Value of lateral stiffness of the concrete frame with the infill with removed areas under tension can be taken from ETABS model. Figure 4-11 shows the lateral stiffness of the model.

	Story	Stiffness X kN/m
	Story1	525892.945

Figure 4-11: Lateral stiffness of the modified frame (frame with removed tension areas from infill panel)

$$545180.4 = \frac{24 \times 23025000 \times 0.00213}{3.12^3} \frac{(12 \times 0.059 + 1)}{(12 \times 0.059 + 4)} + \frac{w \times 23025000 \times 0.12}{6.29} \times cos^2 27$$

$$\boxed{545180.4 = 14059.77 + 348732.2w \rightarrow w = 1.52\, m}$$

4.5.1.11.5 Comparison Between 2D Model Results and Used Formulas

Table 4-14 shows the width of equivalent strut for the single bay single story frame as concluded from the 2D model analysis with removing tension areas.

Table 4-14: Computation of Equivalent Strut Width using 2D Model

Computation of Equivalent Strut Width using 2D Model	
Equivalent Strut Width (cm)	152 cm

Table 4-15 shows only the close results of the used formulas compared to value concluded from the 2D model.

Table 4-15: Comparison Between Equivalent Strut Width Calculation Approaches in cm units

2D model results with the closet formula results (strut width in cm)		
2D analysis equivalent strut	**Bazan and Meli Formula**	**Paulay and Preistely Formula**
152	147	157

It is important to mention that the NBCC code compute two values of the strut width, the first is general, and the second is called effective width, and as shown in table 4-16 the general width is very similar to that gained from 2D analysis.

Table 4-16: 2D model results compared to NBCC formula

2D model results compared to NBCC formula		
2D analysis equivalent strut	**NBCC Strut Width (cm) (w)**	**NBCC Equivalent Strut Width**
152	145	72.5

4.5.2 Equivalent Strut Width for Method Two (Brick Infill Wall)

Method Two as presented in Chapter Three is an infill wall with 20 cm voided brick layer. Structural property that need to be determined for such brick is the modulus of elasticity. In Master's Thesis issued in 2018 in Al-

Najah University it was found that the modulus of elasticity for used bricks in Palestine is around 260 MPa. This value will be used in the coming procedures of determining the equivalent strut width.

Table 4-17 shows the value of modulus of elasticity of brick that will be used through the coming sections, while the properties for the model is the same as provided previously in this chapter.

Table 4-17: Modulus of Elasticity of used bricks in construction in Palestine

Modulus of Elasticity of used bricks in construction in Palestine	
E (MPa)	260

For equivalent strut for brick some methods will not be used; as results of equivalent strut for plain concrete showed that methods such as Stafford Smith and Carter formula and Holmes formula gives values that may not be logical. Moreover, formulas of Bazan and Meli, and Papia will not be used as the shear modulus parameter, and the poisson's ratio is not available for the used brick in Palestine.

4.5.2.1 Equivalent Strut Width Using Mainstone and Weeks Formula

Calculations of equivalent strut for bricks are as following:

$$\lambda_h = \sqrt[4]{\frac{E_{inf} t \sin 2\theta}{4 E_c I_c h_{inf}}} = \sqrt[4]{\frac{260 \times 0.2 \times \sin(2 \times 27)}{4 \times 23025 \times 0.00213 \times 2.87}} = 0.523$$

$$\mathrm{w} = 0.175 \mathrm{d_{inf}} (\lambda_h \mathrm{H_{inf}})^{-0.4} = 0.175 \times 6.29 \times (0.523 \times 2.87)^{-0.4} = 0.937m$$

Table 4-18 shows strut width value using Mainstone and Weeks formula:

Table 4-18: Equivalent strut width- Mainstone and Weeks formula

Mainstone and Weeks formula	
Strut Width	93.7 cm

4.5.2.2 Equivalent Strut Width Using Paulay and Preistely Formula

Strut width for brick is the same as for the plain concrete, as the formula suggests a width that is one fourth the diagonal length despite the nature of forming material for the infill wall. Table 4-19 shows the suggested width of the equivalent strut based on Paulay and Preistely suggestion.

Table 4-19: Equivalent strut width Paulay and Preistely formula

Paulay and Preistely formula	
Strut Width	157 cm

4.5.2.3 Equivalent Strut Width Using Durrani and Luo Formula

Following are the calculations of strut width using Durrani and Luo formula:

$$m = 6\left[1 + \frac{6E_{inf}I_b h}{\pi E_c I_c L}\right] = 6\left[1 + \frac{6 \times 260000 \times 0.00052 \times 3.12}{\pi \times 23025000 \times 0.00213 \times 6}\right] = 6.1$$

$$\gamma = 0.32\sqrt{sin2\theta}\left[\frac{h^4 E_{inf} t}{mE_c I_c h_{inf}}\right]^{-0.1} = 0.32\sqrt{\sin(2 \times 27)}\left[\frac{3.12^4 \times 260000 \times 0.20}{7.45 \times 23025000 \times 0.00213 \times 2.87}\right]^{-0.1} = 0.24$$

$$w = \gamma\sqrt{L^2 + h^2}sin2\theta = 0.24 \times \sqrt{6^2 + 3.12^2}\ sin54 = 1.32 \text{ m}$$

Table 4-20 shows strut width value using Durrani and Luo formula:

Table 4-20: Equivalent strut width- Durrani and Luo formula

Durrani and Luo formula	
Strut Width	132 cm

4.5.2.4 Equivalent Strut Width Using Hendry Formula

Following are the calculations of strut width using Hendry formula:

$$\alpha_h = \frac{\pi}{2}\left[\frac{4E_cI_ch_{inf}}{E_{inf}tsin2\theta}\right]^{\frac{1}{4}} = \frac{\pi}{2}\left[\frac{4\times 23025000\times 0.00213\times 2.87}{260000\times 0.2\times \sin 54}\right]^{\frac{1}{4}} = 3.0$$

$$\alpha_L = \frac{\pi}{2}\left[\frac{4E_bI_bL_{inf}}{E_{inf}tsin2\theta}\right]^{1/4} = \frac{\pi}{2}\left[\frac{4\times 23025000\times 0.00052\times 6}{260000\times 0.2\times \sin 54}\right]^{\frac{1}{4}} = 2.54$$

$$w = 0.5\sqrt{\alpha_h{}^2 + \alpha_L{}^2} = 0.5\sqrt{3^2 + 2.54^2} = 1.96\ m$$

Table 4-21 shows strut width value using Hendry formula:

Table 4-21: Equivalent strut width- Hendry formula

Hendry formula	
Strut Width	196 cm

4.5.2.5 Equivalent Strut Width Using FEMA356-2000 Formula

Following are the calculations of strut width using FEMA356-2000 formula:

$$\lambda_1 = \left[\frac{E_{me}tsin\theta}{4E_cI_ch_{inf}}\right]^{\frac{1}{4}} = \left[\frac{260000\times 0.2\times sin54}{4\times 23025000\times 0.00213\times 2.87}\right]^{\frac{1}{4}} = 0.523$$

$$a_1 = 0.175(\lambda_1 h_{col})^{-0.4} d_{inf} = 0.175(1.41\times 3.12)^{-0.4}\times 6.29 = 0.903\ m$$

Table 4-22 shows strut width value using FEMA356-2000 formula:

Table 4-22: Equivalent strut width- FEMA356-2000 formula

FEMA356-2000 formula	
Strut Width	90.3 cm

4.5.2.6 Equivalent Strut Width Using NBCC 2005

NBCC formulas are same to those suggested by Hendry. Calculations using NBCC 2005 are as following:

$$\alpha_h = \frac{\pi}{2}\left[\frac{4E_c I_c h}{E_m t_e sin2\theta}\right]^{\frac{1}{4}} = 3.0$$

$$\alpha_L = \frac{\pi}{2}\left[\frac{4E_c I_c h}{E_m t_e sin2\theta}\right]^{\frac{1}{4}} = 2.53$$

$$w = \sqrt{{\alpha_h}^2 + {\alpha_L}^2} = 3.92\,m$$

Calculation of equivalent strut continues as the effective width of strut is calculated as following:

w_e is the effective diagonal strut width, and shall be calculated according to these conditions:

$$w_e \leq \frac{w}{2} \rightarrow w_e \leq \frac{3.92}{2}\ (1.96\ m) or\ \leq \frac{l_s}{4} \rightarrow \frac{6.29}{4}\ (1.573\ m)(smaller\ control)$$

Therefore,

$$w_e = 1.573\ m$$

Table 4-23 shows strut width value using NBCC-2005 formula:

Table 4-23: Equivalent strut width- NBCC 2005 formula

NBCC 2005 formula	
Strut Width	157.3 cm

4.5.2.7 Comparison Between Equivalent Strut Width Calculation Approaches

For the same single bay single story concrete frame with infill of voided brick of 20 cm thickness, different approaches yielded values in a wide range.

Figure 4-12 shows graph of different approaches regarding the value of equivalent strut.

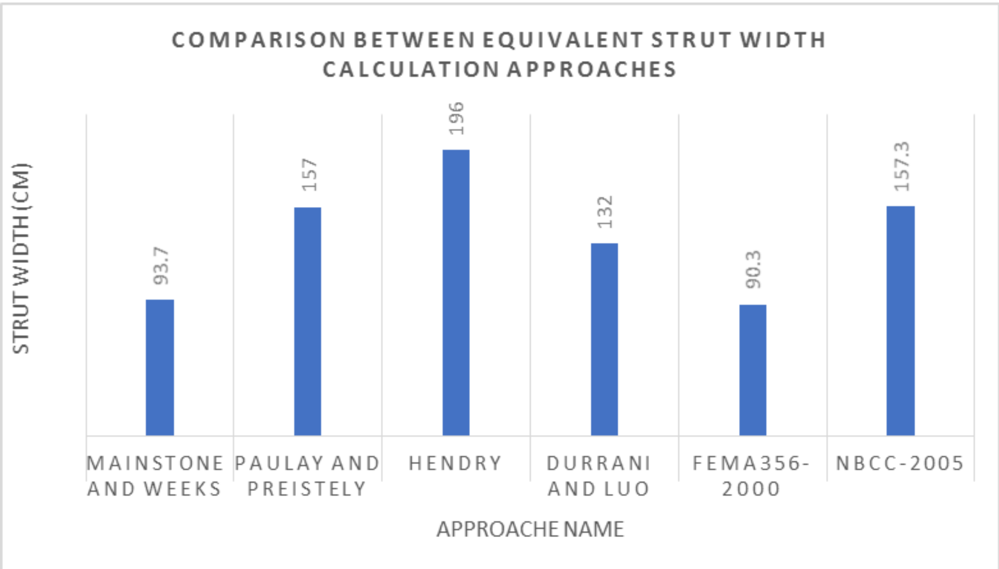

Figure 4-12: Strut width as suggested by each approach (Brick infill wall)

Results shown in figure 4-12 shows wide difference between the different approaches. It can be noted that NBCC formula matches with Paulay and Preistely formula, while FEMA formula matches with Mainstone and Weeks formula.

4.6 Determination of Equivalent Strut Width for Modeling Purposes

In previous section values computed using different approaches show a large difference making it hard to determine which value to use. However, equivalent strut width as computed using the 2D frame supported two formulas of Bazan and Meli, and Paulay an Preistely. Moreover, NBCC formula also presented a near value if the value of effective width is neglected at this stage; as the effective width is assumed to consider openings within the infill wall.

Impact of openings on the equivalent strut width will play main role in determining which formula to use, as formulas of Bazan and Meli, and Paulay and Preistely suggests strut width only for solid infills.

4.6.1 Accuracy of Equivalent Strut Different Formulas

A unique approach will be used through the coming chapter in the analytical study of this thesis, and in order to choose this unique approach a literature review was performed to investigate which formula may be more accurate in modeling the equivalent strut.

A study conducted by Tarek M. Alguhane and others in 2015 states that the formula suggested by FEMA 356-2000 and adopted in the ASCE/SEI 41-06 code underestimates the values of the equivalent properties of the diagonal strut. Thus, a significant reduce of infill wall contribution is suspected. Moreover, the study states that deformation limits provided by the ASCE/SEI 41-06 are overly conservative.

According to study the Canadian code (NBCC 2005) gives realistic values for the equivalent properties of the diagonal strut when compared to fields measurements. The study compares between many analytical approaches of modeling versus experimental results.

In conclusion it was found through the study that ASCE/SEI 41-06 equation underestimates properties of the equivalent strut. On the other hand, the NBCC formula gives realistic values for the properties of equivalent strut and this justify the use of NBCC formula in determining equivalent strut width in the coming chapter.

Another point that will support the use of the NBCC code is that the code deals with openings by reducing the computed width to either half the calculated value using the suggested formula, or by taking quarter diagonal length (smaller controls).

Chapter Five

Numerical Study

5.1 Introduction

Modeling is a vital step in the procedure of analysis and design for any structural system. In this chapter a pattern of common practice building will be evaluated using different modeling techniques.

As mentioned previously in Chapter Four, and as can be found in the literature review the common practice of modeling regarding systems having infill walls is to ignore those walls as structural elements. Therefore, modeling frame system with no attention to structural properties of such walls need to be evaluated to investigate impact of such assumption on the suspected behavior of system under application of lateral load.

Another modeling technique that will be investigated is the modeling using the equivalent strut method. In this method a compression strut will replace the infill wall using the same depth of the infill wall, while the width is computed using formula of the NBCC 2005 code. As discussed in Chapter Four the NBCC formula reduces the obtained width in order to include existence of openings; as openings are supposed to reduce the contribution infill walls have in defining the lateral stiffness of the infilled frames.

Chapter Four shows that equivalent strut width computational procedures vary widely between different methods. Experimental study supported that using NBCC formula is supposed to provide results close to those obtained through experimental study.

Another modeling technique that will be discussed through this chapter is that suitable for Method Three. In Method Three the cross section of wall is composed of two layers of reinforced concrete, where such a wall is supposed to have a tension capacity that will ease the modeling using available software.

Figure 5-1 shows two modeling techniques that defines the two extreme boundaries where the real behavior is, i.e. the real performance of the infilled frames systems must lay within the defined area between techniques one and three. Equivalent strut approach must lay within these boundaries with no specification of location (not necessarily in the middle of the space between the two boundaries).

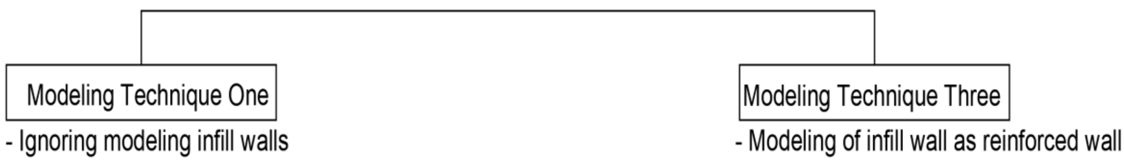

Figure 5-1: Boundaries where the real behavior is between

Location of real behavior -whether closer to technique one or three- depends on many parameters such as location and size of opening, modulus of elasticity of the infill material, and many other parameters.

Figure 5-2 shows what those boundaries really define, as the lower boundary limit defines the maximum displacement structure may face, while the upper boundary defines the maximum strength\stiffness structure may have.

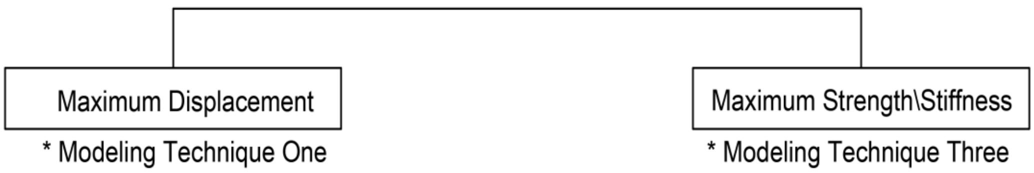

Figure 5-2: Boundaries indications: Maximum displacement, maximum strength/stiffness

Indeed, this thesis focuses of the computed base shear, therefore, focus will be on the lower limits of the fundamental period that will yield higher design forces.

The analysis through this chapter will be performed for the following cases:

1- A pattern of bare frame structure, where no shear walls, and the flooring system is solid slab with no beams. For this pattern the upper boundary of fundamental period will be computed by neglecting the contribution of infill walls. The next stage will be by defining the lower boundary of the fundamental period by assuming infill walls with tension capacity (as reinforced walls) and by considering openings through walls. It is important to mention that analysis will be performed for different assumptions regarding materials, and cracked and non-cracked sections. In the final stage an equivalent strut as suggested by the NBCC code will be modeled and results will be compared with both limits. Analysis will cover sections of both Method one and two (plain concrete section of 12 cm thickness, and a layer of 20 cm brick).

2- The second pattern that will be studied is for a structural system where a slab with no beams is supported on columns and central core shear walls. Analysis will be performed for the case of not including infill walls, then a second analysis will be by assuming infill walls as reinforced walls, and finally analysis will be performed with the existence of equivalent struts. The analysis will also be performed for both sections of methods one and two.

3- The third pattern will be for method three only, where models will be analyzed only with the existence of parameter shear walls (reinforced walls with an assumption of 20 cm reinforced walls) for both systems with and without core shear walls. The analysis will consider both cracked and non-cracked sections. For this method equivalent strut will not be used as wall section has capacity to take tension.

5.2 Limitations of Study

The higher level of complication of infill wall modeling makes the study really tough and complicated; therefore, some assumptions need to be used to simplify analysis. Indeed, some of these assumptions may be critical and it is recommended for further experimental works to test some or all of these assumptions in order to increase accuracy and reliability.

Limitations of study is as follows:

1- Infill wall center is in the same alignment of frame’s center line as can be seen in figure 5-3.

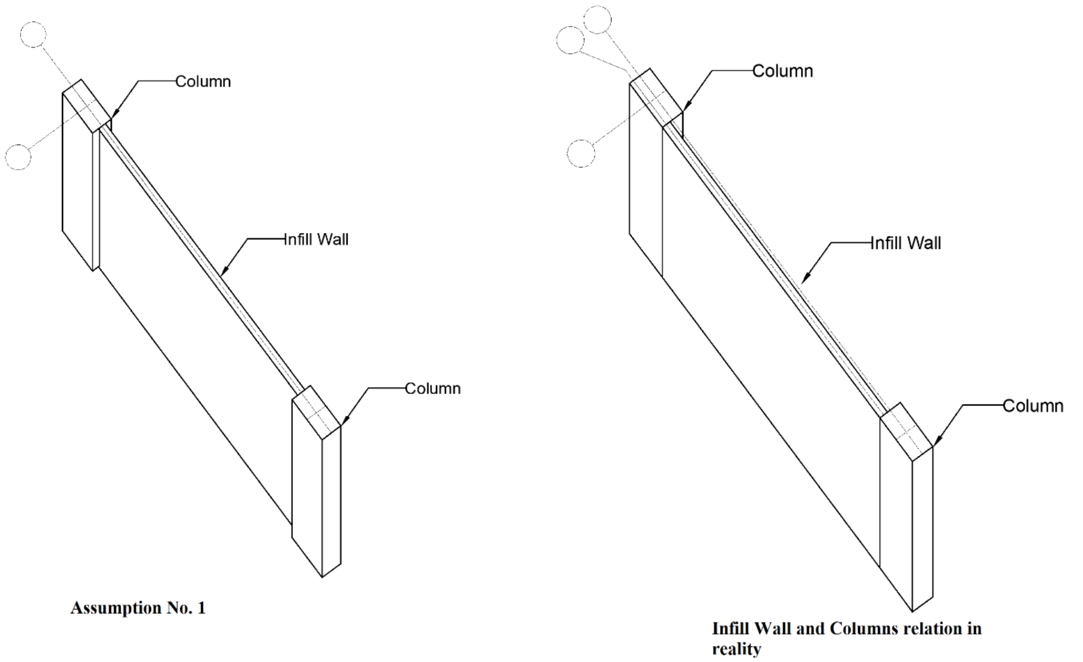

Figure 5-3: Assumption 1: Columns and infill wall is on the same center line (same alignment)

2- The concrete material of the infill wall has uniform compressive strength.

3- Infill walls are not supposed to be part of the gravity load system; therefore, the only axial load in these walls are from infill walls self-weight.

4- Elements not within the frame (stone layer as an example) are excluded from effective cross section.

5- The study is concerned with both fundamental period and stiffness, while displacement is not considered, thus, the study defines conservativity by estimating higher values of base shear (this happens for lower values of fundamental period).

5.3 Determination of Plan Geometry Properties

In this section the structure properties will be determined, and the determined geometry will be analyzed for the three methods with difference in infill walls properties of compressive strength, width, and the modulus of elasticity. Figure 5-4 shows the geometry of the system that is a square geometry with square columns. Columns dimensions are variable based on number of stories, and properties of infill wall depend on the method of construction.

Columns spacing for the shown system will be determined later on through this chapter based on the structural properties of the flooring system.

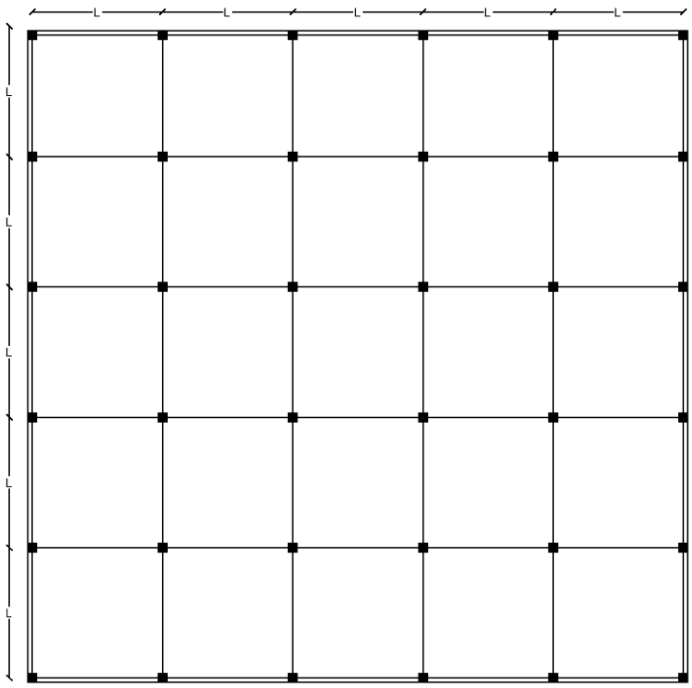

Figure 5-4: Plan of the structure that will be studied through Chapter Five

5.3.1 Determination of Columns' Spacing

One-way ribbed slab system, and flat slab with no beams are the most common practices of flooring construction in Palestine. The absence of beams in flat systems makes the simulation of such systems as frame structures questionable. Wide use of flat slab systems explains the need of focusing on earthquake response of such systems.

Derivation of fundamental period formula regarding flat slabs supported on columns is controlled by many parameters. The variety of span lengths, used material, and applied load need consideration of too many of patterns and probabilities. Therefore, this study will focus on the most common practiced type; that is used in many structural systems in both commercial and residential building.

The height of one stone cladding piece is usually 25 cm. Therefore, most slabs in Palestine comes with a depth similar to stone piece which is 25 cm depth. Thus, the analyzed flat slab thickness will be controlled by one value of 25 cm.

Using reverse method, the maximum allowable span length will be determined using Table 8.3.1.1 from ACI318-14 (ACI Committee 318 2014).

Table 5-1: Part of table 8.3.1.1 in the ACI318-14: Minimum thickness of non-prestressed two-ways slabs without interior beams

f_y MPA	Without drop panels		
	Exterior Panels		Interior panels
	Without edge beams	With edge beams	
280	$\frac{l_n}{33}$	$\frac{l_n}{36}$	$\frac{l_n}{36}$
420	$\frac{l_n}{30}$	$\frac{l_n}{33}$	$\frac{l_n}{33}$
520	$\frac{l_n}{28}$	$\frac{l_n}{33}$	$\frac{l_n}{31}$

Steel with yielding strength of 420 MPa is used for both longitudinal and shear reinforcement for construction purposes of reinforced concrete structures in Palestine. Thus, the second row in table 5-1 will control the maximum clear spans computed values.

For exterior panel, an assumption of not having edge beams will be used for determining maximum span lengths. Also, a uniform span length will be used for simplicity.

$$For\ exterior\ panel\ with\ no\ edge\ beam \rightarrow 250\ mm = \frac{l_n}{30} \rightarrow l_n = 7500\ mm$$

The value of clear span of 7500 mm is an initial value, therefore, in the coming section analysis using finite element method will be used in evaluating the adequacy of such depth regarding both serviceability and strength requirements.

Flat Slab Structural Analysis Using Finite Element Software

Previous section suggests a uniform columns' spacing of 7500 mm for a system of 25 cm slab with no beams. In this section the suggested spacing will be investigated by applying finite element analysis through the widespread software SAFE. Table 5-2 shows the properties of SAFE model.

Table 5-2: Data for analyzed slab in SAFE for the purpose of checking adequacy of slab's depth

Number of spans in each direction	5 spans
Center to Center Spacing (mm)	7900
Column dimension (mm)	400 (square)
Slab thickness (mm)	250
Self-weight Load (kN/m^2)	6.25
Super Imposed Loads (kN/m^2)	4.0
Live Load (kN/m^2)	2.0
Concrete Compressive Strength (fc') MPa	24 MPa

Figure 5-5 shows the slab layout in SAFE.

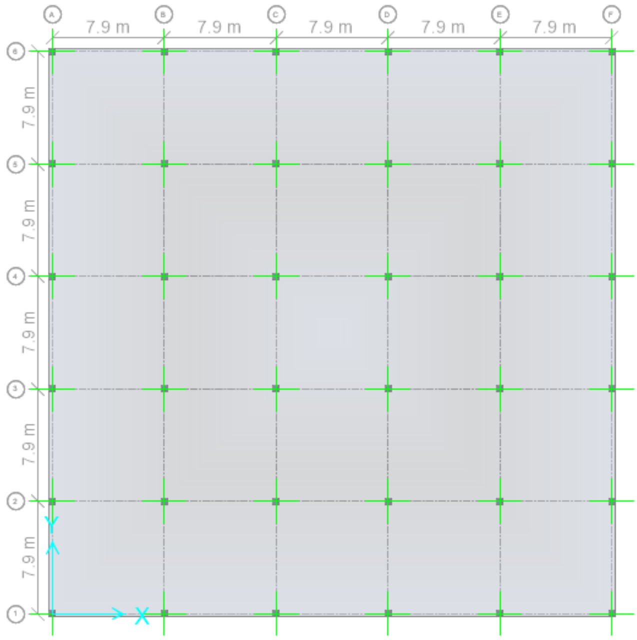

Figure 5-5: SAFE slab model for the purpose of determining suitable columns' spacing

Analysis of punching shear shows that slab depth is not adequate (Figure 5-6); values shown at each column represents the ratio between the shear ultimate value and the shear capacity of concrete thus each value larger than one indicates a punching problem.

$$Punching\ Ratio = \frac{Vu}{\emptyset V_c}$$

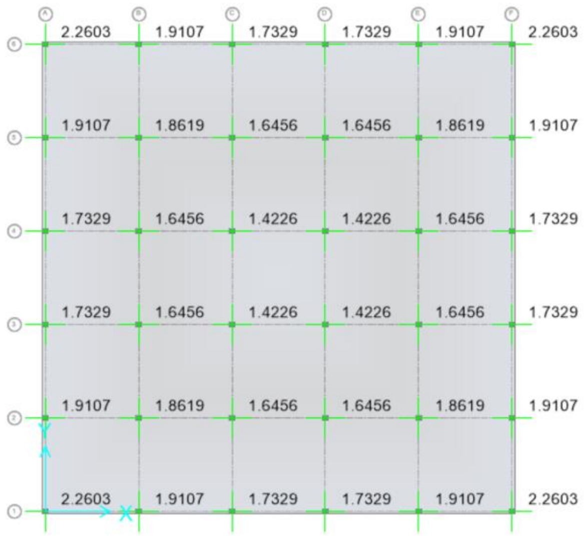

Figure 5-6: Punching ratio check as provided by SAFE

A random column will be chosen and checked to verify SAFE output; this column will be one of those having a ratio of 1.4226. Following are the manual calculations of resultant reaction on the chosen column:

$$Tributary\ area\ for\ the\ chosen\ column = 7.9 \times 7.9 = 62.41\ m^2$$

$$\begin{aligned} Ultimate\ reaction\ on\ colum &= 62.41 \times (6.25 + 4) \times 1.2 + 62.41 \times 2 \times 1.6 \\ &= 767.6 + 199.7 - [0.65 \times 0.65 \times ((6.25 + 4) \times 1.2 + 2 \times 1.6) \\ &= 967.3 - 6.54 = 960.75\ kN \end{aligned}$$

SAFE output shows a value of 898.7 kN (Figure 5-7).

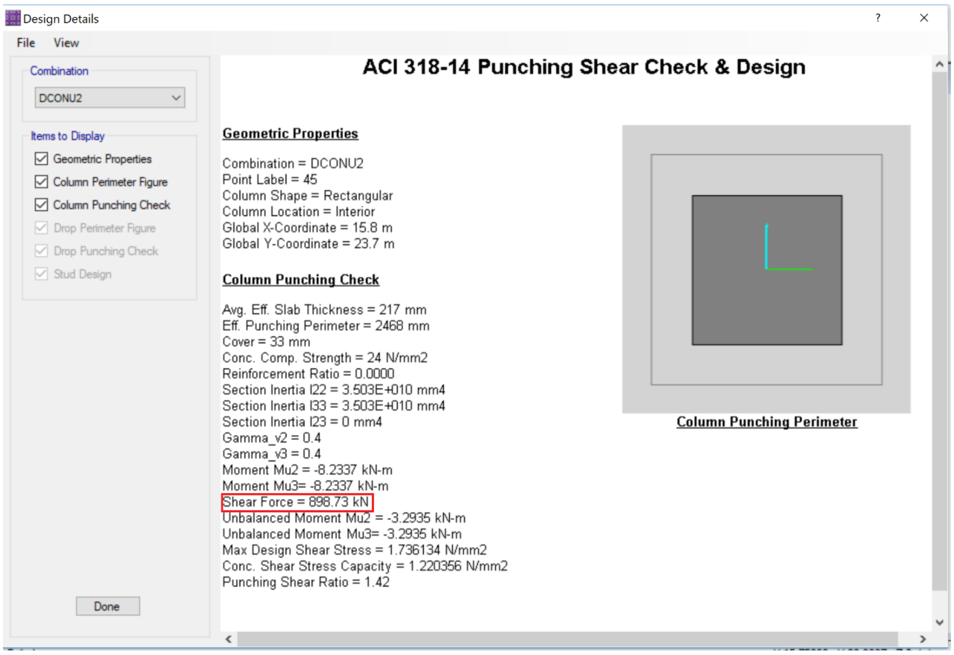

Figure 5-7: SAFE output regarding the checked column

Table 5-3 shows a comparison between manual computed value and result of SAFE.

Table 5-3: Manual Shear force Vs SAFE Shear force and difference between them

Manual Shear Force (kN)	SAFE Shear Force (kN)	Difference
960.7	898.7	6.5%

Since difference is below 10%, then analysis result of SAFE is acceptable.

Following are the manual calculations -using ACI formulas- of punching check for verification purposes. Smaller output of the three formulas will control the shear capacity of concrete.

$$V_c = \frac{1}{6}\left(1 + \frac{2}{\beta}\right)\lambda\sqrt{f'_c}\,b_0 d$$

$$V_c = \frac{1}{12}\left(\frac{\alpha_s d}{b_0} + 2\right)\lambda\sqrt{f'_c}\,b_0 d$$

$$V_c = \frac{1}{3}\lambda\sqrt{f'_c}b_0 d$$

Where,

β =Ratio of long side to short side of the rectangular column.

$\lambda = one$ for normal − weight concrete

$\alpha_s = 40$ For interior columns

For the case, value of "d" will be taken same as provided by SAFE model (Figure 5-7); which is 217 mm. Calculation of b_0 then shear capacity is as following:

$$b_0 = (400 + 217) \times 4$$
$$= 2468\, mm\ (same\ as\ provided\ by\ SAFE\ in\ Figure\ 5-7)$$

$$V_c = \frac{1}{6}\left(1 + \frac{2}{1}\right)1\sqrt{24}(2468)(217) = 1311.86\, kN$$

$$V_c = \frac{1}{12}\left(\frac{40(217)}{2468} + 2\right)1\sqrt{30}(2468)(217) = 1206.2\, kN$$

$$V_c = \frac{1}{3}1\sqrt{24}(2468)(217) = 874.57\ (controls)$$

Concrete capacity is reduced using reduction factor of 0.75, therefore concrete capacity will be as following:

$$\emptyset V_c = 0.75(847.57) = 655.93\, kN$$

The manual punching ratio will be computed manually as following:

$$Punching\ Ratio = \frac{Vu}{\emptyset V} = \frac{960.7}{655.93} = 1.46$$

Table 5-4 shows a comparison between manual computed value and result of SAFE.

Table 5-4: Manual Shear force Vs SAFE Shear force and difference between them

Manual Punching Ratio	SAFE Punching Ratio	Difference
1.46	1.42	3.1%

The matching between manual and SAFE results allows adaptation of SAFE results. Trails in SAFE demonstrate that center to center spacing of 6 meters gives a safe punching ratio (Figure 5-8).

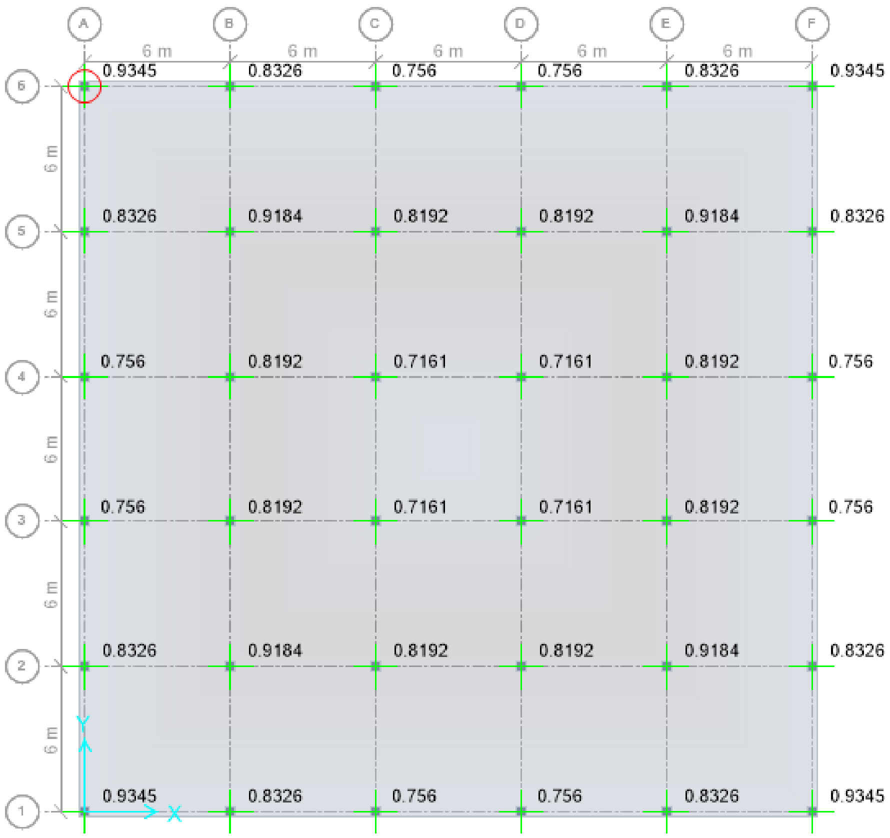

Figure 5-8: The appropriate column spacing for 25 cm square paneled flat slab

Table 5-5 shows the slab properties that will be used in the analytical study.

Table 5-5: Slab's depth that will be analyzed in the analytical study

Slab's Depth	25 cm
Center to Center Spacing (between columns)	600 cm

5.4 Plan Patterns

Two patterns for the plan will be analyzed as shown in figure 5-9.

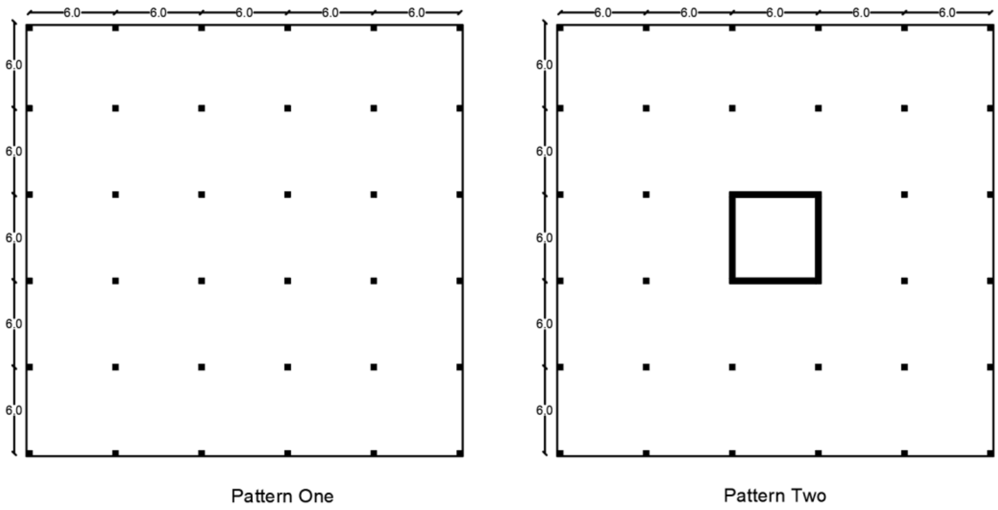

Figure 5-9: Pattern one and two, without and with core shear walls

Openings modeling impact is supposed to be with considerable change in results. Therefore, a pattern of openings will be applied on the structural models as provided in figure 5-9. Opening sizes and allocation is based on what being implemented in the common practice. It must be noted that elevation in figure 5-10 represents the four elevations of the structure.

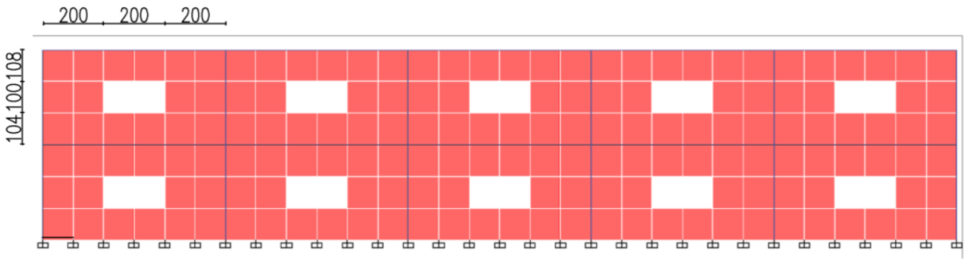

Figure 5-10: Elevation of two stories shows windows openings patterns with dimensions

5.5 Analysis of Methods One and Two-Pattern One

Method one is represented by a plain concrete layer of 12 cm, while method two is represented by a brick layer of 20 cm thickness.

Table 5-6 shows specifications of both method one and method two cross section:

Table 5-6: Illustration of method one, and method two

Method No.	Method Details
Method one	Plain concrete of 12 cm layer
Method two	Brick layer of 20 cm

5.5.1 Bare Frame System

Analysis through this section will be for a system where a slab with no beams is supported directly on a system of columns without existence of any type of walls. Analysis through this section represents both methods one and two.

5.5.1.1 Modeling Patterns

After determining the appropriate columns' spacing that fit with the 25 cm flat slab, different patterns are suggested in table 5-7, in order to conclude effect of different patterns on the fundamental period of the structure.

Table 5-7: Different Patterns that will be analyzed in the numerical study-bare frames-methods one and two

Compressive strength of column concrete fc'	24,28,32, MPa
Compressive strength of slab concrete fc'	24 MPa
Number of stories	2,4,6,8, and 10 stories
Building Length/Building width	1 pattern (5 bays in both directions)
Span lengths (c/c)	6 meters
Cracked Section	Yes/No

Line Load Values for Method One and Two

An important parameter that need to be taken in consideration is the line load of the cladding walls. In chapter three it is shown that each method has different value of line load, thus different models will be analyzed based on which method is being used in the analysis.

Table 5-8 shows the value of line load for both methods one and two.

Table 5-8: Weight of cladding wall calculations for 1-meter length and 3.12-meter height (method one and two)-with openings deductions

Cross Section	1-meter length x 3.12 m height Weight (kN/m)
Method one	14
Method two	14

5.5.1.2 Cracked Section Analysis

Another important parameter that may affect analysis results is the cracked section analysis. Data in table 5-9 is taken from table 6.6.3.1.1(a) in ACI318-14 code.

Table 5-9: Table 6.6.3.1.1 (a) in ACI318-14: Moment of inertia and cross-sectional area permitted for elastic analysis at factored load level

<table>
<tr><th colspan="2">Member and condition</th><th>Moment of inertia</th><th>Cross-sectional area</th></tr>
<tr><td colspan="2">Columns</td><td>$0.7I_g$</td><td rowspan="5">$1.0\ A_g$</td></tr>
<tr><td rowspan="2">Walls</td><td>Uncracked</td><td>$0.7I_g$</td></tr>
<tr><td>Cracked</td><td>$0.35I_g$</td></tr>
<tr><td colspan="2">Beams</td><td>$0.35I_g$</td></tr>
<tr><td colspan="2">Flat plates and flat slabs</td><td>$0.25I_g$</td></tr>
</table>

Thus, cracked models will be analyzed taken in consideration needed modifications as provided in table 5-10. On the other hand, non-cracked models will be analyzed without any change in moment of inertia.

Table 5-10: Modifiers of moment of inertia for columns and slabs-bare frame analysis- Method One-Pattern one and two

Non-Cracked Model			Cracked model		
Columns	**Slab**	**Walls**	**Columns**	**Slab**	**Walls**
$1.0\ I_g$	$1.0\ I_g$	$1.0\ I_g$	$0.7I_g$	$0.25\ I_g$	$0.35\ I_g$

5.5.1.3 Analysis of Bare Frames Systems

Bare frame system is the upper boundary of the fundamental period, as the maximum value of fundamental period is when assuming infill walls with no lateral stiffens. Indeed, applied methods of analysis in practice doesn’t consider the stiffness of the infill walls. Therefore, the suspected behavior of structure and the computed base shear used in designing structures in most applications depend on bare frame results.

Estimation of the approximate fundamental period is one of the main scopes in studying any structural system for the sake of earthquake design. Codes such as ASCE suggest formulas that usually approximate the fundamental period as a function of structures heights.

Availability and simplicity of 3D modeling software eased the computation of fundamental time period for structures.

Reliability of structural analysis software outputs must be examined before any results adaptation. Thus, before developing conclusions based on software's calculations, verifications must be performed, and assumptions being used by software must be well understood and modified if needed.

Models Properties- Method One and Two-Pattern One

Depth of slab was determined previously to be 25 cm based on gravity design and by the control of strength requirements of shear design.

Columns dimensions are variable due to number of stories; Therefore, columns dimensions depend on how many stories there is in the pattern.

Table 5-11 shows the different structures that will be analyzed.

Table 5.11: Columns size with respect to number of stories and compressive strength of columns- for both method one and two

Patterns of Bare Frame Structures					
Model Number	No. of stories	Columns size (mm)	(fc') MPa -columns		
Model 1	2	400x400	24	28	32
Model 2	4	500x500	24	28	32
Model 3	6	600x600	24	28	32
Model 4	8	700x700	24	28	32
Model 5	10	800x800	24	28	32

As shown in table 5-11 each pattern of the same number of stories has different compressive strength for columns elements; these different values will illustrate the effect of increasing compressive strength on the computed fundamental period for the structure.

Analysis results for Column's Concrete Compressive of 24 MPa-Bare Frame (Method One and Two -Pattern One)

Table 5-12 shows the results of fundamental period for bare frames using constant compressive strength of 24 MPa for columns.

Table 5.12: Fundamental Period: ASCE Formula, Cracked and Non-Cracked Models for Bare Frames with Columns of 24 MPa Compressive Strength-Method one and two-Pattern one

No. of Stories	Compressive Strength for columns concrete (fc') MPa	Elevation	Fundamental Period (seconds)				
			ASCE7-10 Formula			Non-Cracked model	Cracked Model
			Lower	Upper	Average		
2	24	6.24	0.339	0.411	0.375	0.616	0.934
4	24	12.48	0.63	0.768	0.699	1.037	1.698
6	24	18.60	0.896	1.088	0.992	1.46	2.450
8	24	24.96	1.176	1.428	1.302	1.89	3.20
10	24	31.2	1.442	1.751	1.597	2.324	3.94

Figure 5-11 shows the relation between story height and fundamental period for the three cases of: Average value of ASCE formula, cracked and non-cracked model for columns with compressive strength of 24 MPa (results for method one and two-pattern one).

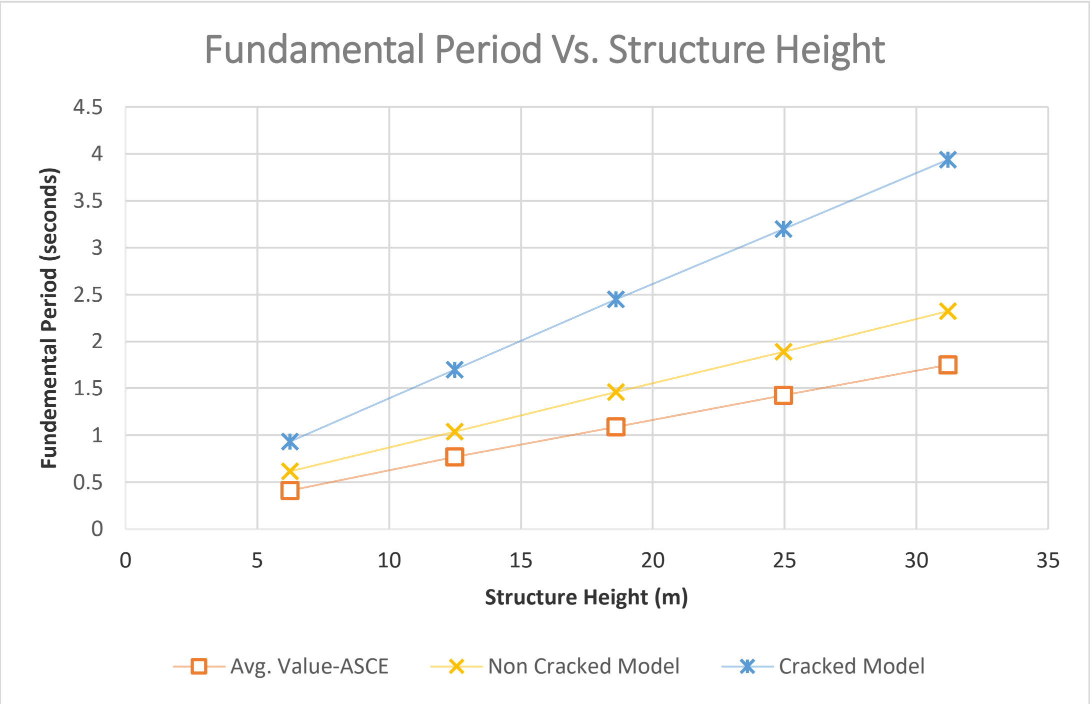

Figure 5-11: Fundamental period Vs. height-columns of fc'=24 MPa-analysis of bare structures-method one and two -pattern one

Table 5-13 shows the results of fundamental period for bare frames using constant compressive strength of 28 MPa for columns of pattern one for method one and method two.

Table 5-13: Fundamental period: ASCE formula, cracked and non-cracked models for bare frames with columns of 28 MPa compressive strength

No. of Stories	Compressive Strength for columns concrete (fc') MPa	Elevation	Fundamental Period (seconds)				
			ASCE7-10 Formula			Non-Cracked model	Cracked Model
			Lower	Upper	Average		
2	28	6.24	0.339	0.411	0.375	0.59	0.889
4	28	12.48	0.63	0.768	0.699	0.994	1.63
6	28	18.60	0.896	1.088	0.992	1.41	2.36
8	28	24.96	1.176	1.428	1.302	1.82	3.08
10	28	31.2	1.442	1.751	1.597	2.24	3.79

Figure 5-12 shows the relation between story height and fundamental period for the three cases of: average value of ASCE formula, cracked and non-cracked model for columns with compressive strength of 28 MPa (results for method one and two-pattern one-pattern one).

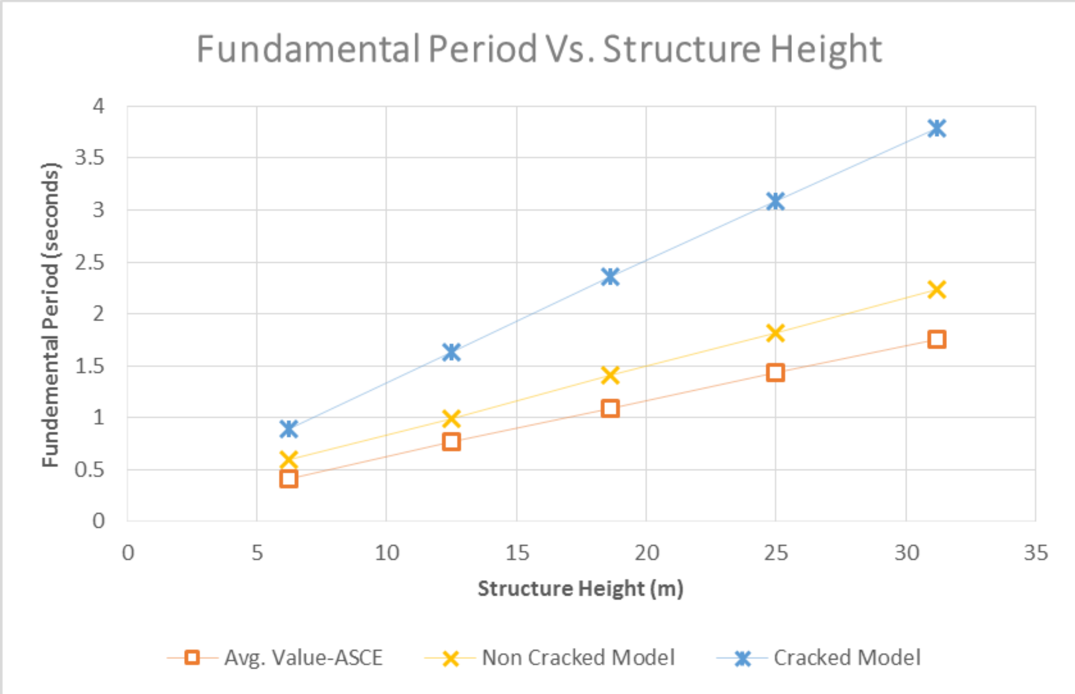

Figure 5-12: Fundamental period vs. height-columns of fc'=28 MPa-analysis of bare structures-method one and two-pattern one

Table 5-14 shows results of fundamental period for bare frames using constant compressive strength of 32 MPa for columns.

Table 5-14: Fundamental Period: ASCE formula, cracked and non-cracked models for bare frames with columns of 32 MPa compressive strength

No. of Stories	Compressive Strength for columns concrete (fc') MPa	Elevation	Fundamental Period (seconds)				
			ASCE7-10 Formula			Non-Cracked model	Cracked Model
			Lower	Upper	Average		
2	32	6.24	0.339	0.411	0.375	0.57	0.86
4	32	12.48	0.63	0.768	0.699	0.96	1.575
6	32	18.60	0.896	1.088	0.992	1.36	2.28
8	32	24.96	1.176	1.428	1.302	1.76	2.98
10	32	31.2	1.442	1.751	1.597	2.17	3.67

Figure 5-13 shows the relation between story height and fundamental period for the three cases of: Average value of ASCE formula, cracked and non-cracked model for columns with compressive strength of 32 MPa (results for method one and two-pattern one).

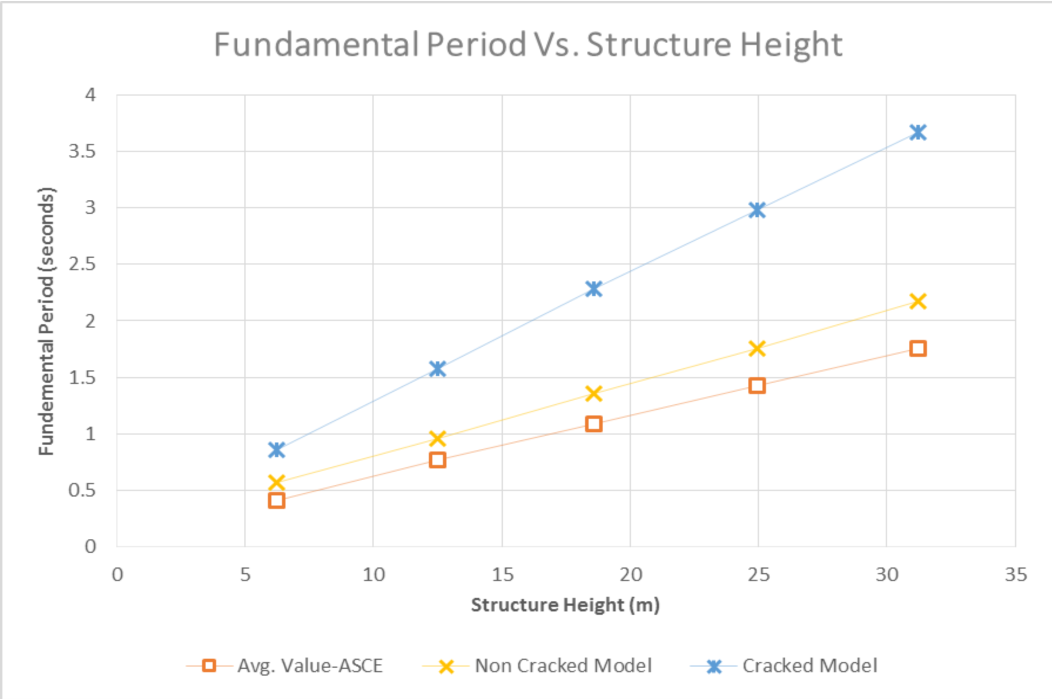

Figure 5-13: Fundamental period Vs. height-columns of fc'=32 MPa-analysis of bare structures-method one and two-pattern one

Results for different columns' compressive strengths can be compared as shown in tables 5-15. ASCE7-10 code formula only depends on structural height; therefore, results will not change whatever columns' compressive strength is.

Table 5-15: Impact of increasing fc' of columns on the fundamental period (for cracked and non-cracked model)- method one and two-Pattern one

No. of Stories	Elevation	Fundamental Period (seconds)/ Non-Cracked		
		fc'=24 MPa	fc'=28 MPa	fc'=32 Mpa
2	6.24	0.616	0.59	0.57
4	12.48	1.037	0.994	0.96
6	18.6	1.46	1.41	1.36
8	24.96	1.89	1.82	1.76
10	31.2	2.324	2.24	2.17
No. of Stories	**Elevation**	**Fundamental Period (seconds)/ Cracked**		
		fc'=24 MPa	**fc'=28 MPa**	**fc'=32 Mpa**
2	6.24	0.934	0.889	0.86
4	12.48	1.698	1.63	1.575
6	18.6	2.45	2.36	2.28
8	24.96	3.20	3.10	2.98
10	31.2	3.94	3.79	3.67

Figure 5-14 and 5-15 shows the relation between story height and fundamental period for different compressive strengths columns for both cracked and non-cracked sections.

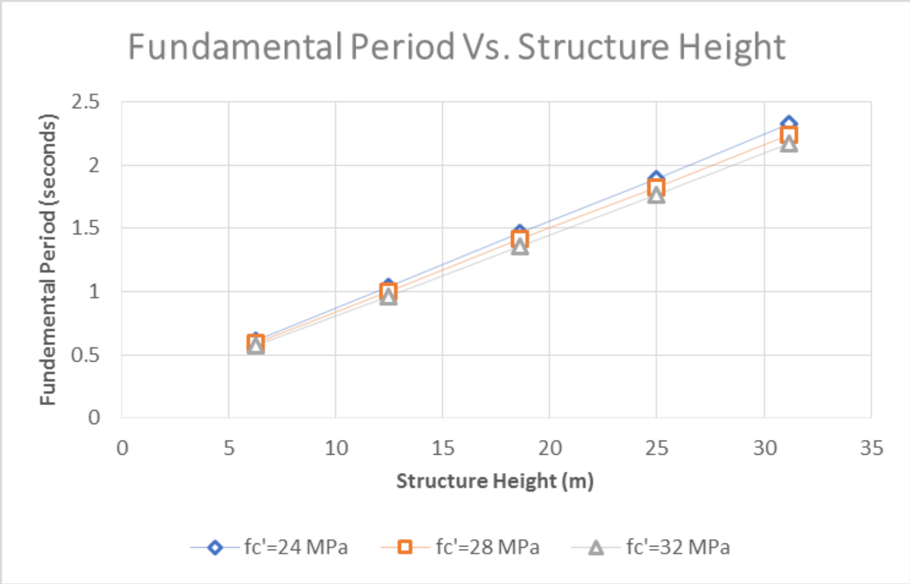

Figure 5-14: Fundamental period Vs. structure height-non-cracked model for different compressive strength (columns)-method one and two- pattern one

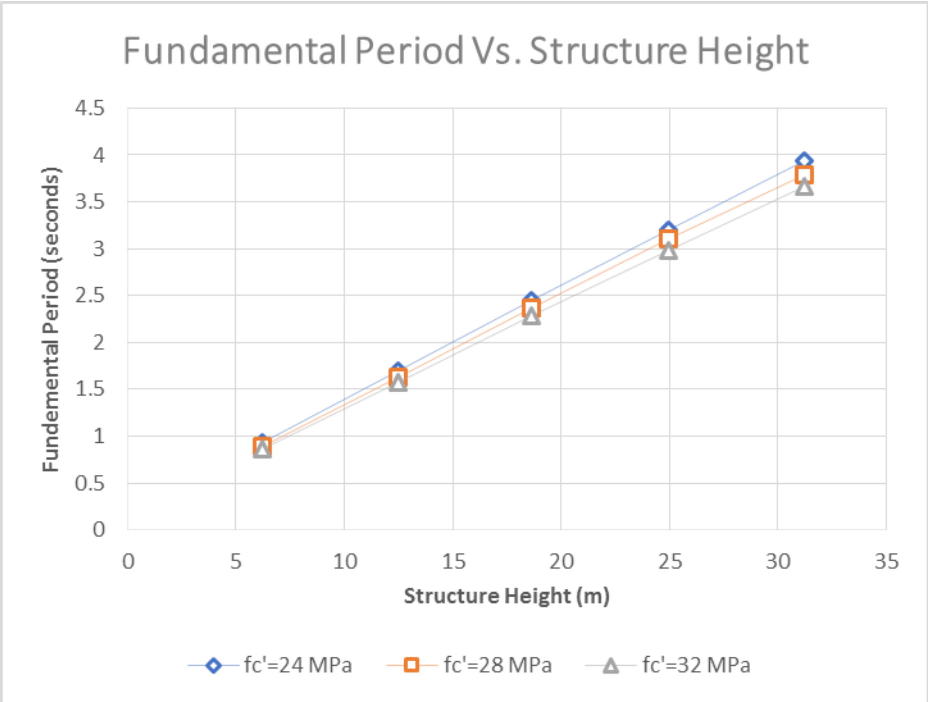

Figure 5-15: Fundamental period Vs. structure height- cracked model for different compressive strength (columns)- method one and two- pattern one

Table 5-16 shows the impact of increasing compressive strength on the fundamental period. It can be noted that increasing compressive strength by 33% only contributes in reducing the fundamental period by a maximum value of almost 8% which is not a considerable change.

Table 5-16: Impact of increasing columns' compressive strength on the fundamental period (increasing from 24 MPa to 32 MPa)- results of method one and two -pattern one

Percent of Change in Fundamental period		
Structure Height (m)	Non-Cracked Model	Cracked Model
6.24	7.5%	7.9%
12.48	7.5%	7.2%
18.60	6.8%	6.9%
24.96	6.9%	6.9%
31.2	6.6%	6.9%

Table 5-17 shows the difference between cracked and non-cracked sections analysis results for bare frames method one and two pattern one.

Table 5-17: Impact of increasing columns' compressive strength on the fundamental period (increasing from 24 MPa to 32 MPa)

Impact of Cracked Analysis of the Fundamental Period – Bare Frames-Pattern One					
fc'=24 MPa	**No. of Stories**	**Elevation**	**Cracked**	**Non-Cracked**	**Difference**
	2	6.24	0.934	0.616	51.6%
	4	12.48	1.698	1.037	63.7%
	6	18.6	2.45	1.46	67.8%
	8	24.96	3.20	1.89	69.3%
	10	31.2	3.94	2.324	69.5%
fc'=28 MPa	2	6.24	0.889	0.59	50.7%
	4	12.48	1.63	0.994	64.0%
	6	18.6	2.36	1.41	67.3%
	8	24.96	3.10	1.82	70.3%
	10	31.2	3.79	2.24	69.1%
fc'=32 MPa	2	6.24	0.86	0.57	50.9%
	4	12.48	1.575	0.96	64.0%
	6	18.6	2.28	1.36	67.6%
	8	24.96	2.98	1.76	69.3%
	10	31.2	3.67	2.17	69.1%

Since difference is in the same range for the three models with three different compressive strength value; a unique value of difference regarding compressive strength of 24 MPa will be plotted in figure 5-16.

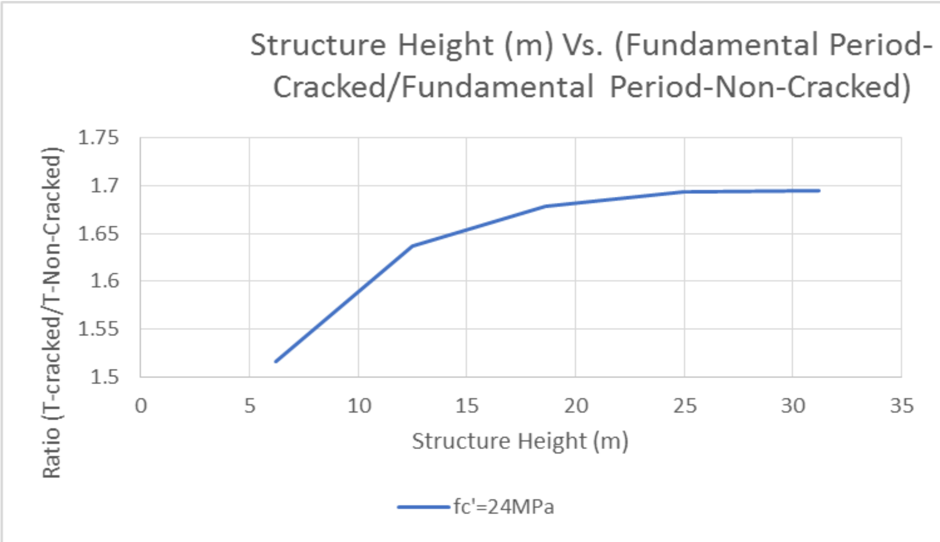

Figure 5-16: Structure height (m) Vs. $\frac{Fundamental\ Period-Cracked}{Fundamental\ Period-Non-Cracked}$ for bare frames-pattern one

Conclusions

Numerical study for bare frames for the specific pattern of having square geometry using square columns with uniform spacing shows that the suggested ASCE formula is always less with a considerable difference, thus the design base shear as suggested by the code will be conservative regarding the bare frames.

For the displacement it is clear that bare frames are suspected to go in large deformations, and this arise the need of construct ductile frames that can deform largely.

Numerical study shows that the impact of increasing compressive strength of concrete is not considerable as results are showing that an increase by almost 33% on the compressive strength of columns may decrease the fundamental only by a maximum value of almost 8%.

Results of cracked analysis shows a considerable difference of an average of 64% on the fundamental period.

5.5.2 Analysis Results for System Assuming Solid Reinforced Concrete Walls of 12 cm Thickness

After having results for the upper boundary of the fundamental period, analysis results for the lower boundary will be obtained assuming parameter walls as reinforced walls (as shown in figure 5-17) with the same thickness of infill wall. It is worth mentioning that this analysis will be limited only for method one; as method two as composed of a layer of brick and therefore it is not logical to assume the lower boundary of stiffness the same as provided by concrete.

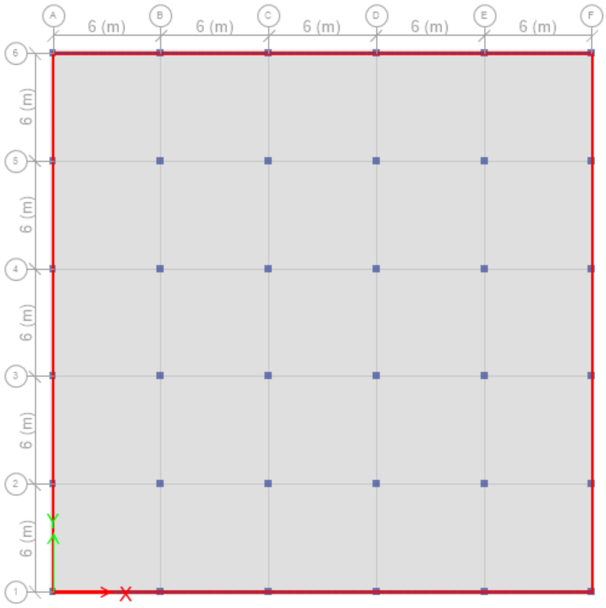

Figure 5-17: Plan layout of the analyzed structural system with parameter shear wall-Bare Frames-Pattern One

As mentioned previously, an empirical formula is suggested in section 12.8.2.1 in the ASCE7-10 code is commonly used in computing fundamental period. The formula that suggest the fundamental period is as following:

$$Ta = 0.0488 h_n^{0.75} \quad \text{[Equation 5-1]}$$

In this section a square geometry of plan (Figure 5-17) will be analyzed assuming different number of stories, and with an assumption of analyzing solid walls with no consideration of windows opening. Each model will be analyzed twice, first assuming non-cracked model, and then assuming cracked model.

An important factor that may affect the behavior of walls is the quality of concrete in the wall section. Chapter three shows that concrete quality is really questionable; as the concrete compressive strength has no much reliability due to many factors. Thus, concrete compressive strength for walls is being lowered to study impact of low compressive concrete results effects on the structure behavior. Table 5-18 shows the data of the analyzed models.

Table 5-18: Data of numerical models – models with parameter shear walls – no openings-method one-pattern one

Data of Numerical Models	
Compressive strength of column, slab concrete fc’	24 MPa
Compressive strength of structural walls fc’	12,16, and 24 MPa
Number of stories	2,4,6,8, and 10 stories
Building Length/Building width	1 pattern (5 bays in both directions)
Span lengths (c/c)	6 meters
Cracked Section	Yes/No
Reinforced Concrete Unit Weight (kN/m^3)	25
Wall thickness (cm)	12
Line Load value	14 kN/m

Analysis Results

Table 5-19 shows the data of the five analyzed models for pattern one.

Table 5-19: Columns size with respect to number of stories and compressive strength of walls-method one-pattern one

Model Number	No. of stories	Columns size (mm)	Compressive Strength for columns concrete (fc’) MPa	Compressive Strength for walls concrete (fc’) MPa		
Model 1	2	400x400	24	24	16	12
Model 2	4	500x500	24	24	16	12
Model 3	6	600x600	24	24	16	12
Model 4	8	700x700	24	24	16	12
Model 5	10	800x800	24	24	16	12

Analysis results shown in table 5-20 are for pattern one assuming a compressive strength of 24 MPa for solid infill walls.

Table 5-20: Fundamental period: ASCE formula, cracked and non-cracked models for infill solid walls of 24 mpa compressive strength

No. of Stories	Elevation	Fundamental Period (seconds)				
		ASCE7-10 Formula			Non-Cracked Model	Cracked Model
		Lower	Upper	Average		
2	6.24	0.27	0.33	0.30	0.073	0.121
4	12.48	0.45	0.55	0.50	0.139	0.223
6	18.60	0.62	0.74	0.68	0.202	0.322
8	24.96	0.76	0.93	0.85	0.267	0.423
10	31.2	0.90	1.10	1.0	0.336	0.526

As can be seen in table 5-20 the estimation of ASCE7-10 is always larger than what analysis provide, and this is expected as the analyzed model is not practical since walls are solid with no openings.

Figure 5-18 shows the relation between story height and the fundamental period for structures with solid reinforced wall all around (infill wall with 24 MPa compressive strength).

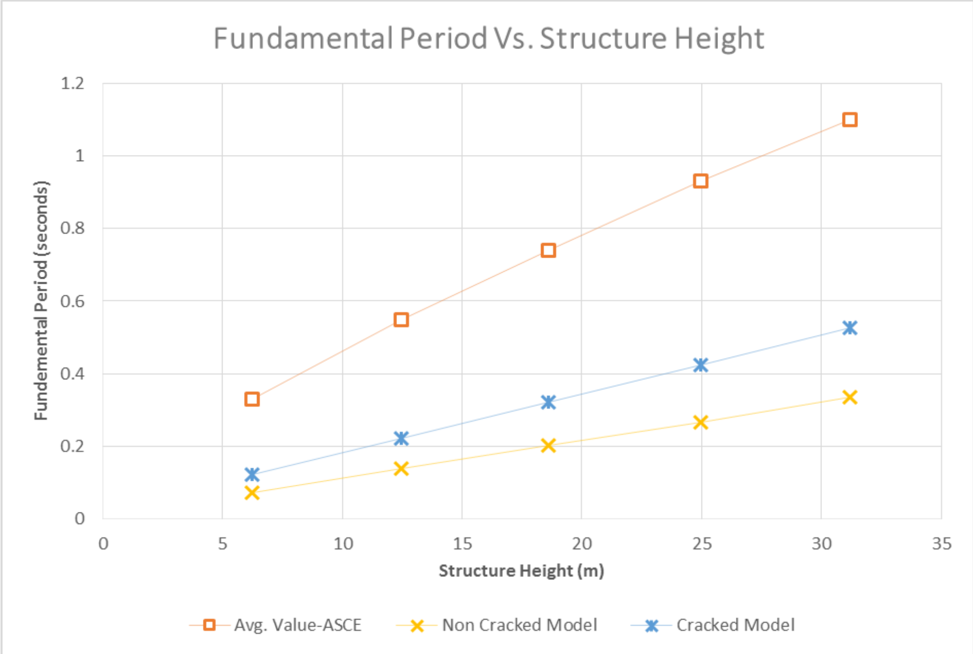

Figure 5-18: Fundamental period Vs structure height using average ASCE formula, and non-cracked models for walls with fc'=24 MPa-method one-pattern one

Table 5-21 shows the results of analysis for walls with compressive strength of 16 MPa instead of 24 MPa.

Table 5-21: Fundamental period: ASCE formula, cracked and non-cracked models for infill solid walls of 16 MPa compressive Strength

No. of Stories	Elevation	Fundamental Period (seconds)				
		ASCE7-10 Formula			Non-Cracked model	Cracked model
		Lower	Upper	Average		
2	6.24	0.27	0.33	0.30	0.08	0.134
4	12.48	0.45	0.55	0.50	0.152	0.244
6	18.60	0.62	0.74	0.68	0.226	0.352
8	24.96	0.76	0.93	0.85	0.291	0.461
10	31.2	0.90	1.10	1.0	0.365	0.572

Figure 5-19 shows the relation between story height and the fundamental period for structures with solid reinforced wall of 16 MPa compressive strength concrete.

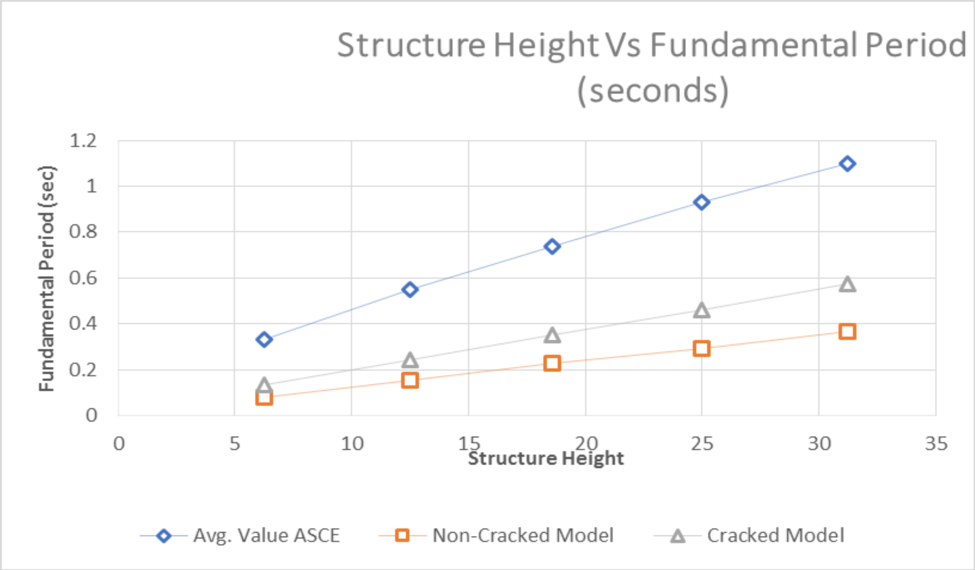

Figure 5-19: Fundamental period Vs structure height using ASCE formula, and non-cracked models for walls with fc'=16 MPa-method one-pattern one

Table 5-22 shows the results of analysis for walls with compressive strength of 12 MPa.

Table 5-22: Fundamental Period: ASCE formula, cracked and non-cracked models for infill solid walls of 24 MPa compressive strength

Fundamental Period: ASCE Formula, Cracked and Non-Cracked Models for Infill Solid Walls of 12 MPa compressive Strength						
No. of Stories	Elevation	Fundamental Period (seconds)				
		ASCE7-10 Formula			Non-Cracked model	Cracked model
		Lower	Upper	Average		
2	6.24	0.27	0.33	0.30	0.086	0.143
4	12.48	0.45	0.55	0.50	0.162	0.26
6	18.60	0.62	0.74	0.68	0.234	0.374
8	24.96	0.76	0.93	0.85	0.309	0.489
10	31.2	0.90	1.10	1.0	0.388	0.607

Figure 5-20 shows the relation between story height and the fundamental period for structures with solid reinforced wall of 12 MPa compressive strength concrete.

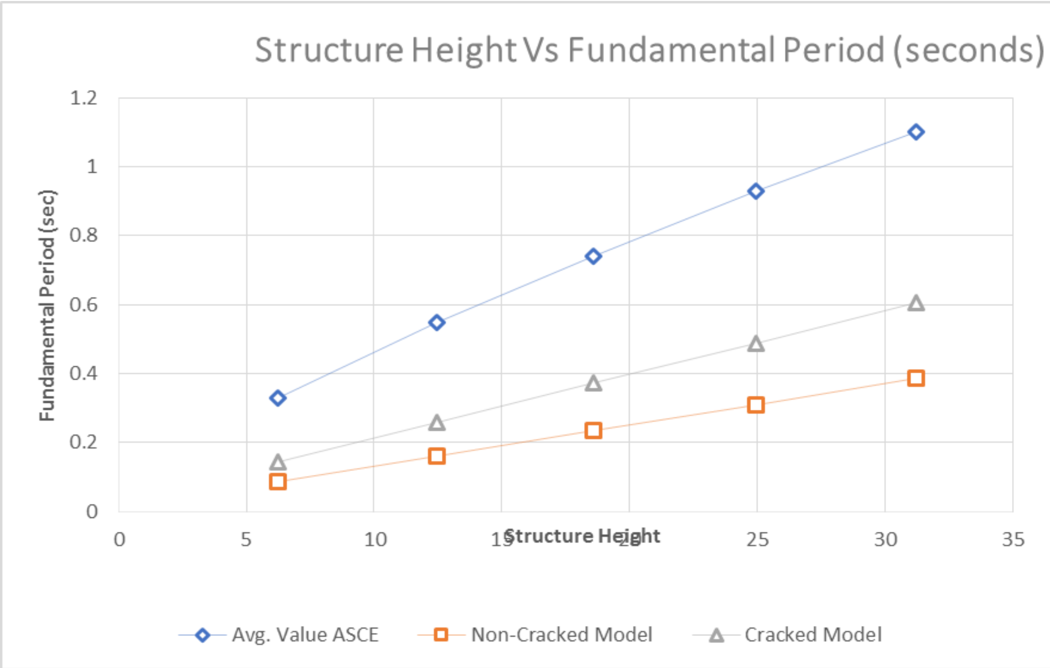

Figure 5-20: Fundamental period Vs structure height using ASCE formula, and non-cracked models for walls with fc'=12 MPa-method one-pattern one

Table 5-23 shows the relation of walls' compressive strength with respect to structure height for method one-pattern one.

Table 5-23: Fundamental period of different walls' compressive strength

No. of Stories	**Elevation**	**Fundamental Period (seconds)/ Non-Cracked**		
		fc'=12 MPa	fc'=16 MPa	fc'=24 Mpa
2	6.24	0.086	0.08	0.073
4	12.48	0.162	0.152	0.139
6	18.6	0.234	0.226	0.202
8	24.96	0.309	0.291	0.267
10	31.2	0.388	0.365	0.336
No. of Stories	**Elevation**	**Fundamental Period (seconds)/ Cracked**		
		fc'=12 MPa	**fc'=16 MPa**	**fc'=24 Mpa**
2	6.24	0.143	0.134	0.121
4	12.48	0.26	0.244	0.223
6	18.6	0.374	0.352	0.322
8	24.96	0.489	0.461	0.423
10	31.2	0.607	0.572	0.526

Figured 5-21 shows the impact of decreasing compressive strength of infill solid reinforced walls on the fundamental period for non-cracked models.

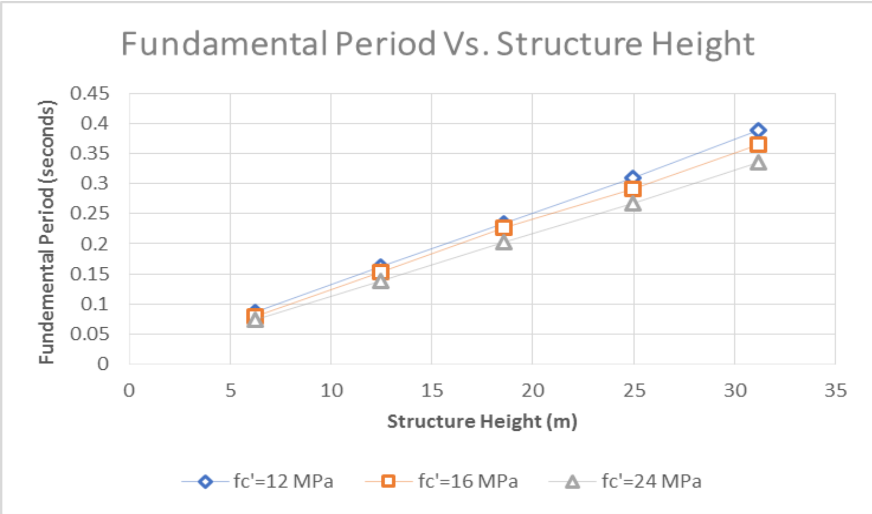

Figure 5-21: Fundamental period Vs. structure height for different compressive strength of infill solid reinforced walls-non-cracked model -method one-pattern one

Figured 5-22 shows the impact of decreasing compressive strength of infill solid reinforced walls on the fundamental period for cracked models.

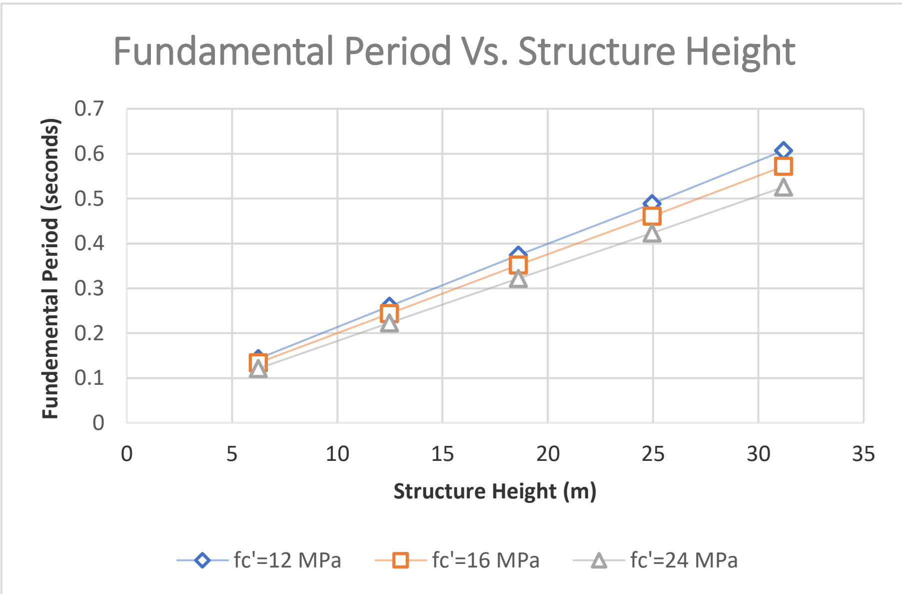

Figure 5-22: Fundamental period Vs. Structure height for different compressive strength of infill solid reinforced walls-cracked models

Table 5-24 shows the difference on the fundamental period when decreasing compressive strength to its half value (from 24 MPa to 12 MPa) for non-cracked section.

Table 5-24: Impact of decreasing compressive strength from 24MPa to 12 MPa on the fundamental period- models with parameter solid reinforced walls -method one-pattern one

No. of Stories	**Elevation**	**Fundamental Period (seconds)**		**Difference**
		fc'=12 MPa	fc'=24 Mpa	
2	6.24	0.086	0.073	17.8%
4	12.48	0.162	0.139	16.5%
6	18.6	0.234	0.202	15.8%
8	24.96	0.309	0.267	15.7%
10	31.2	0.388	0.336	15.4%

As can be noted from table 5-24 decreasing compressive strength of walls have some considerable effect on the fundamental period (average of 16.2%).

Table 5-25 shows the difference on the fundamental period between cracked and non-cracked models for the three type of compressive strength concrete.

Table 5-25: Difference between cracked and non-cracked analysis results for three values of compressive strength (12, 16, 24 MPa) – method one-pattern one

No. of Stories	**Elevation**	**Fundamental Period (seconds)/ fc'=12 MPa**		**Difference**
		Non-Cracked	Cracked	
2	6.24	0.086	0.143	66.2%
4	12.48	0.162	0.26	60.4%
6	18.6	0.234	0.374	59.8%
8	24.96	0.309	0.489	58.2%
10	31.2	0.388	0.607	56.4%
fc'=16 MPa				
2	6.24	0.08	0.134	67.5%
4	12.48	0.152	0.244	60.5%
6	18.6	0.226	0.352	55.8%
8	24.96	0.291	0.461	58.4%
10	31.2	0.365	0.572	56.7%
fc'=24 MPa				
2	6.24	0.073	0.121	65.7%
4	12.48	0.139	0.223	60.4%
6	18.6	0.202	0.322	59.4%
8	24.96	0.267	0.423	58.4%
10	31.2	0.336	0.526	56.5%

5.5.3 Analysis Results for Model with Walls with Openings-Method One-Pattern One

Analysis results that are shown in table 5-26 are for pattern assuming a compressive strength of 24 MPa for infill walls with walls of 12 cm thickness (method one) including openings.

Table 5-26: Fundamental period: ASCE formula, cracked and non-cracked models for infill walls with openings of 24 MPa compressive strength

No. of Stories	Elevation	Fundamental Period (seconds)				
		ASCE7-10 Formula			Non-Cracked model	Cracked Model
		Lower	Upper	Average		
2	6.24	0.27	0.33	0.30	0.088	0.152
4	12.48	0.45	0.55	0.50	0.169	0.274
6	18.60	0.62	0.74	0.68	0.248	0.401
8	24.96	0.76	0.93	0.85	0.331	0.535
10	31.2	0.90	1.10	1.0	0.42	0.674

Figure 5-23 shows the relation between story height and the fundamental period for structures with reinforced walls with openings of 24 MPa compressive strength concrete.

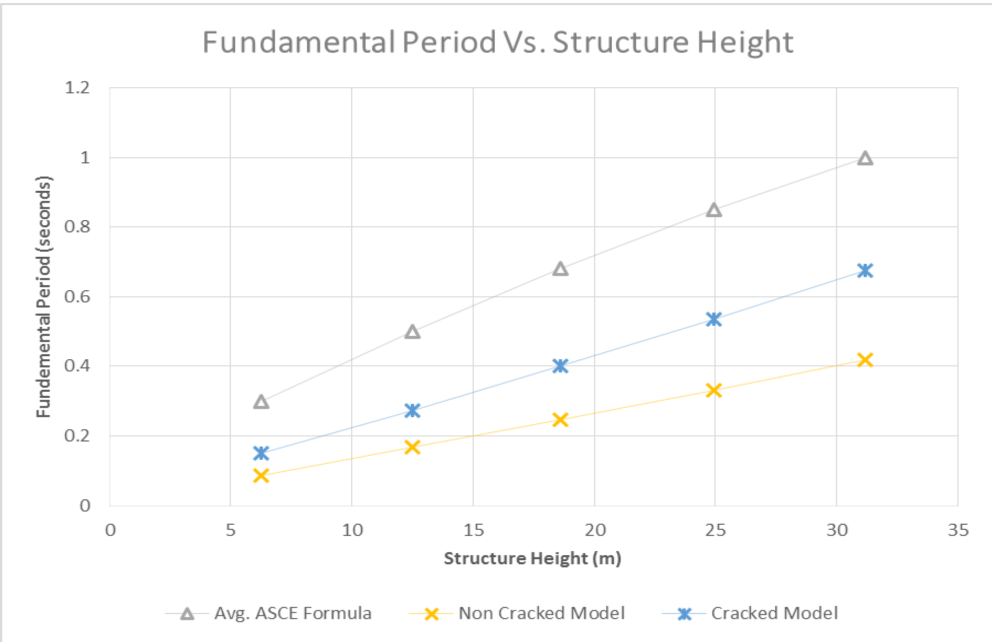

Figure 5-23: Fundamental period Vs structure height using ASCE formula, cracked and non-cracked models for walls with openings with fc'=24 MPa-method one-pattern one

Analysis results that are shown in table 5-27 are for pattern assuming a compressive strength of 16 MPa for infill walls with openings-method one pattern one.

Table 5-27: Fundamental period: ASCE formula, cracked and non-cracked models for infill walls with openings of 16 MPa compressive strength

No. of Stories	Elevation	Fundamental Period (seconds)				
		ASCE7-10 Formula			Non-Cracked model	Cracked Model
		Lower	Upper	Average		
2	6.24	0.27	0.33	0.30	0.105	0.166
4	12.48	0.45	0.55	0.50	0.185	0.30
6	18.60	0.62	0.74	0.68	0.271	0.439
8	24.96	0.76	0.93	0.85	0.362	0.585
10	31.2	0.90	1.10	1.0	0.459	0.737

Figure 5-24 shows the relation between story height and the fundamental period for structures with reinforced walls with openings of 16 MPa compressive strength concrete.

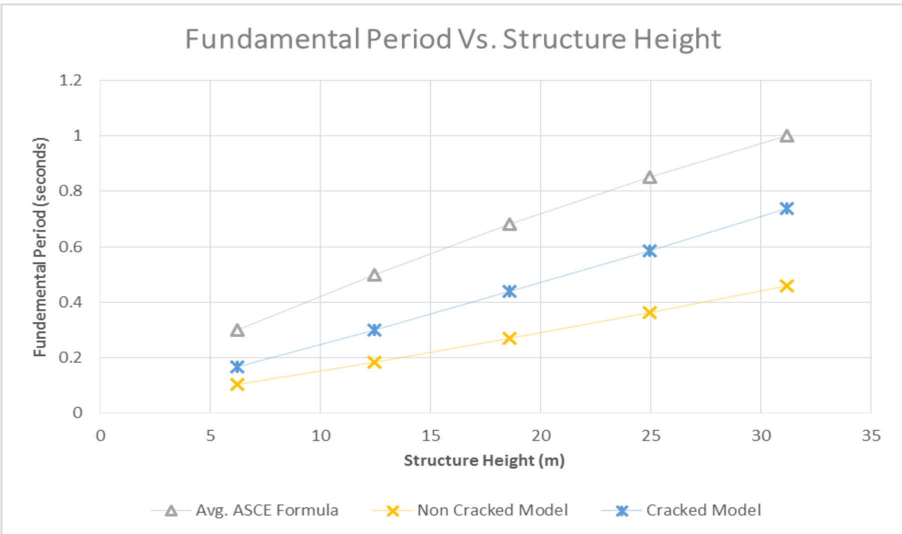

Figure 5-24: Fundamental period Vs structure height using ASCE formula, cracked and non-cracked models for walls with openings with fc’=16 MPa-method one-pattern one

Analysis results that are shown in table 5-28 are for pattern assuming a compressive strength of 12 MPa for infill walls with openings for method one-pattern one.

Table 5-28: Fundamental period: ASCE formula, cracked and non-cracked models for infill walls with openings of 12 MPa compressive strength

No. of Stories	Elevation	Fundamental Period (seconds)				
		ASCE7-10 Formula			Non-Cracked model	Cracked Model
		Lower	Upper	Average		
2	6.24	0.27	0.33	0.30	0.111	0.177
4	12.48	0.45	0.55	0.50	0.197	0.319
6	18.60	0.62	0.74	0.68	0.289	0.468
8	24.96	0.76	0.93	0.85	0.386	0.623
10	31.2	0.90	1.10	1.0	0.488	0.784

Figure 5-25 shows the relation between story height and the fundamental period for structures with reinforced walls with openings of 12 MPa compressive strength concrete.

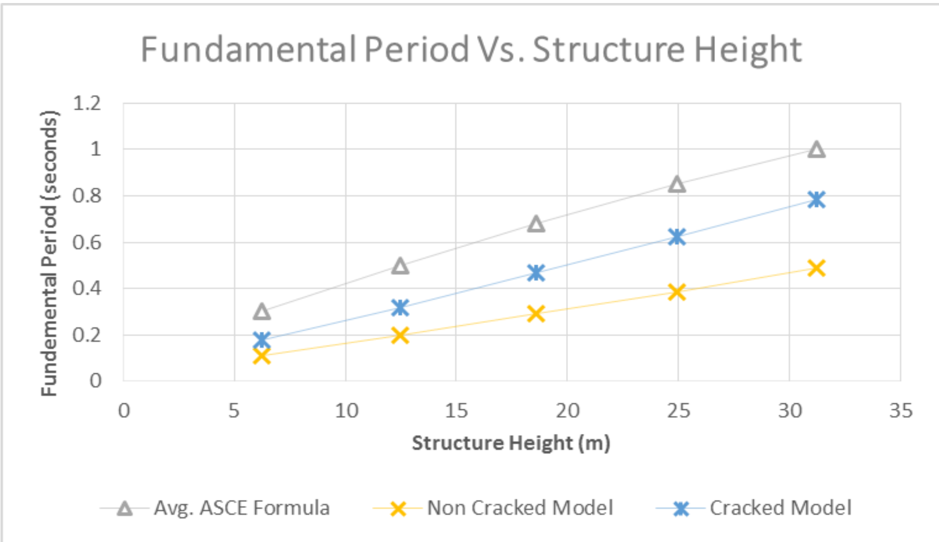

Figure 5-25: Fundamental period Vs structure height using ASCE formula, cracked and non-cracked models for walls with openings with fc’=12 MPa-method one-pattern one

Table 5-29 shows the relation of walls’ compressive strength with respect to structure height for the model with parameter walls with openings for non-cracked models for method one pattern one.

Table 5-29: Fundamental period of different walls’ compressive strength- reinforced walls with openings for non-cracked models-method one-pattern one

No. of Stories	Elevation	Fundamental Period (seconds)		
		fc'=12 MPa	fc'=16 MPa	fc'=24 Mpa
2	6.24	0.111	0.105	0.088
4	12.48	0.197	0.185	0.169
6	18.6	0.289	0.271	0.248
8	24.96	0.386	0.362	0.331
10	31.2	0.488	0.459	0.42

Figure 5-26 shows the impact of decreasing compressive strength of infill reinforced walls with openings on the fundamental period.

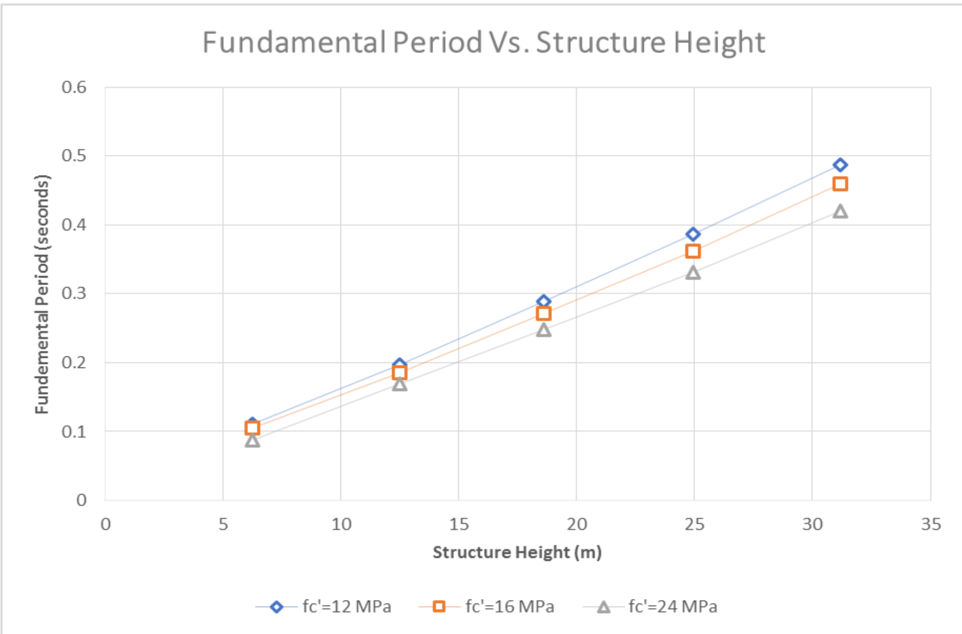

Figure 5-26: Fundamental period Vs. structure height for different compressive strength of infill reinforced walls with openings-non-cracked models-method one- pattern one

Table 5-30 shows the relation of walls' compressive strength with respect to structure height for the model with parameter walls with openings for cracked models.

Table 5-30: Fundamental period of different walls' compressive strength- reinforced walls with openings for cracked models -method one-pattern one

Cracked Models				
No. of Stories	Elevation	Fundamental Period (seconds)		
		fc'=12 MPa	fc'=16 MPa	fc'=24 Mpa
2	6.24	0.177	0.166	0.152
4	12.48	0.319	0.30	0.274
6	18.6	0.468	0.439	0.401
8	24.96	0.623	0.585	0.535
10	31.2	0.784	0.737	0.674

Figure 5-27 shows the impact of decreasing compressive strength of infill cracked reinforced walls with openings on the fundamental period.

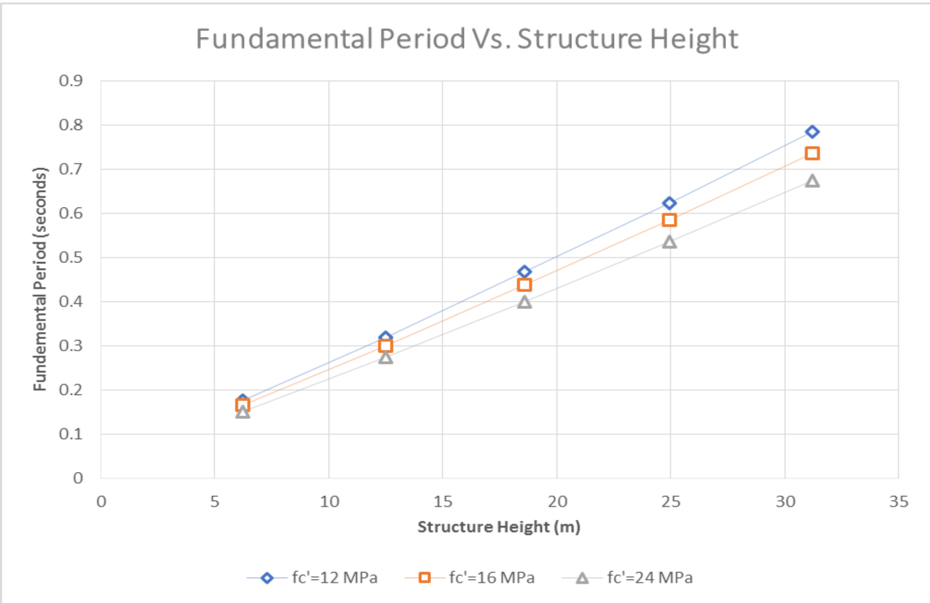

Figure 5-27: Fundamental period Vs. structure height for different compressive strength of infill reinforced walls with openings cracked models-method one-pattern one

Table 5-31 shows the difference on the fundamental period when decreasing compressive strength to its half value (from 24 MPa to 12 MPa) for non-cracked models for walls with openings for method one pattern one.

Table 3-31: Impact of decreasing compressive strength from 24MPa to 12 MPa on the fundamental period- models with parameter reinforced walls with openings-cracked models-method one-pattern one

Non-Cracked Models				
No. of Stories	**Elevation**	**Fundamental Period (seconds)**		**Difference**
		fc'=12 MPa	fc'=24 Mpa	
2	6.24	0.111	0.088	26.3%
4	12.48	0.197	0.169	16.6%
6	18.6	0.289	0.248	16.8%
8	24.96	0.386	0.331	16.6%
10	31.2	0.488	0.42	16.2%

As can be noted from table 5-31 decreasing compressive strength of walls have some considerable effect on the fundamental period (average of 16%). Table 5-32 shows the difference on the fundamental period when decreasing compressive strength to its half value (from 24 MPa to 12 MPa) for cracked models.

Table 3-32: Impact of decreasing compressive strength from 24MPa to 12 MPa on the fundamental period- models with parameter reinforced walls with openings-cracked models-method one-pattern one

Cracked Models				
No. of Stories	**Elevation**	**Fundamental Period (seconds)**		**Difference**
		fc'=12 MPa	fc'=24 Mpa	
2	6.24	0.177	0.152	16.4%
4	12.48	0.319	0.274	16.4%
6	18.6	0.468	0.401	16.7%
8	24.96	0.623	0.535	16.4%
10	31.2	0.784	0.674	16.3%

5.5.4 Analysis Using Equivalent Strut Method

The behavior of infill walls for both methods one and two is not the same as method three due to lack of tension capacity. In this section modeling of infill walls for both methods will be applied using the formula of NBCC code.

Determination of Equivalent Strut Width

Determination of width of the equivalent strut will be carried using NBCC code formula. The NBCC formula depends on columns, beams, and the infill material it-self.

Since no beams are used in flat system slab an imaginary beam is logically assumed with a width equal to column dimensions, and with a depth similar to the slab. Indeed, width of strut is limited to minimum value of wither half what the formula provides, or quarter the diagonal length of the strut, i.e. however assumption of beam width value of equivalent strut at specific point will not increase due to limitation of formula. Following is formula of NBCC code.

The NBCC formula is provided in Chapter 4 in Equation 4-21. Following is the formula of the NBCC code:

$$w = \sqrt{{\alpha_h}^2 + {\alpha_L}^2}$$

Where the width of the strut depends on the following two parameters:

$$\alpha_h = \frac{\pi}{2}\left[\frac{4E_b I_b L}{E_{inf} t_e \sin 2\theta}\right]^{\frac{1}{4}}$$

$$\alpha_L = \frac{\pi}{2}\left[\frac{4E_cI_ch}{E_{inf}t_e sin2\theta}\right]^{\frac{1}{4}}$$

Where the two parameters are the contact length between the strut and beam, and between the column and the strut.

The value of the effective width of the strut is the smaller of either half what NBCC formula suggests, or one fourth the length of the strut. Since columns dimensions are not constant and change based on number of stories in the studied models, then each pattern will have a unique value of width regarding the strut width.

Figure 5-28 shows an illustrative figure for the varying dimensions in the frame.

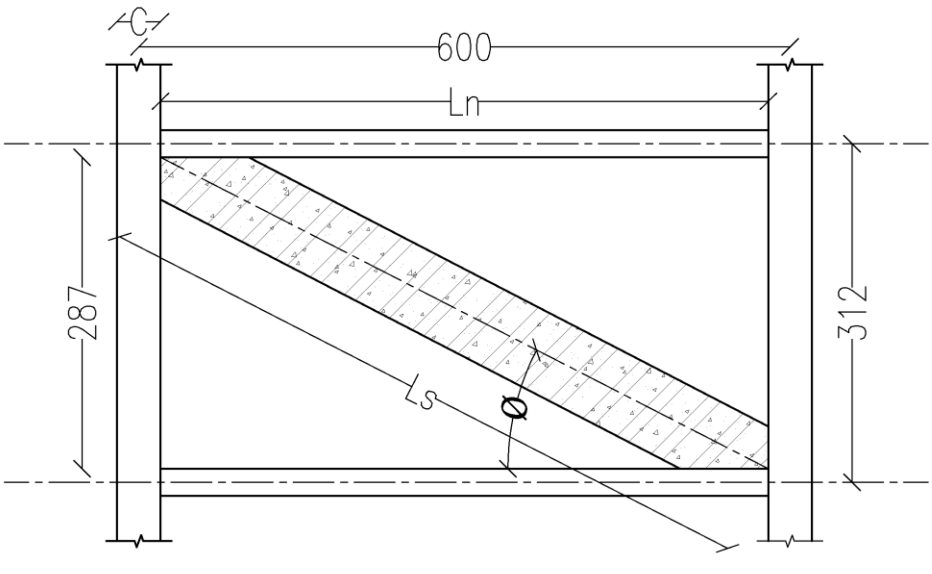

Figure 5-28: Equivalent strut illustrative figure

Table 5-33 shows values of variables shown in figure 5-28 for models with different stories height.

Table 5-33: Values of variable parameters- equivalent strut calculations

No. of stories	Columns' dimensions (m)	L_s (m)	L_n (m)	θ (degrees)
2	0.4x0.4	6.29	5.60	27
4	0.5x0.5	6.20	5.50	28
6	0.6x0.5	6.11	5.40	28
8	0.7x0.5	6.03	5.30	28
10	0.8x0.5	5.94	5.20	29

Value of effective width is controlled based by the following rule:

$$w_e \leq \frac{w}{2} \ or \ \leq \frac{l_s}{4} \ (smaller\ control)$$

Determination of Equivalent Strut Width for Infill Walls with Different Values of Compressive Strength

Table 5-34 shows the value of equivalent strut regarding different models with variable number of stories for models with infill walls with constant columns' compressive strength of 24 MPa.

Table 5-34: parameters of: diagonal length, clear length, angle between diagonal and the horizontal projection, for equivalent strut calculations

No. of stories	Columns' dimensions (m)	L_s (m)	L_n (m)	θ (degrees)
2	0.4x0.4	6.29	5.60	27
4	0.5x0.5	6.20	5.50	28
6	0.6x0.5	6.11	5.40	28
8	0.7x0.5	6.03	5.30	28
10	0.8x0.5	5.94	5.20	29

Table 5-35 shows dimensions of columns and beams that will be used in the computation of strut width.

Table 5-35: Columns, and beams dimensions that will be used in the computation of equivalent strut width for plain concrete infill walls

No. of Stories	Columns' dimensions (cm)	Beams' Dimensions (cm)
2	40x40	40x25
4	50x50	50x25
6	60x60	60x25
8	70x70	70x25
10	80x80	80x25

5.5.4.1 Analysis Results of Method One

Table 5-36 shows strut width values regarding number of stories and the variation of compressive strength of the infill wall itself.

Table 5-36: Strut widths (cm)- for infill walls with different compressive strength values-method one

No. of stories	fc'=24 MPa	fc'=16 MPa	fc'=12 MPa
2	73	77	79
4	85	89	93
6	98	103	107
8	111	116	121
10	124	130	135

Table 5-37 shows analysis results for non-cracked bare frames models with constant compressive strength for columns (fc'=24 MPa) and variable compressive strength of struts. It is important to note that according to table 5-37 that changing of compressive strength of the infill wall change the width of the equivalent strut.

Table 5-37: Fundamental Period for different strut compressive strength values-non cracked model-method one-pattern one

No. of Stories	fc'=24 MPa	fc'=16 MPa	fc'=12 MPa
1	0.223	0.237	0.248
2	0.337	0.4	0.416
3	0.522	0.553	0.576
4	0.664	0.704	0.731
5	0.804	0.85	0.883

5.5.4.2 Analysis Results of Method Two

In method two a case of having 20 cm of bricks of 260 MPa modulus of elasticity in addition to columns with 24 MPa compressive strength will be analyzed to check the impact of such walls in the performance of structures against lateral loads. In this case a constant strut width will be used for all the five models as the strut width is controlled by the minimum of quarter diagonal length.

Table 5-38 shows the constant value of the strut width that represent the 20 cm brick wall.

Table 5-38: Properties of the strut in bare frame models with brick infill walls

Strut Width (cm)	157
Strut Modulus of Elasticity (MPa)	260
Strut Depth (cm)	20

Table 5-39 shows analysis results of bare frames with brick of 20 cm.

Table 5-39: Fundamental period for brick infill wall- non-cracked model-method two-pattern one

No. of Stories	Fundamental Period (seconds)
1	0.537
2	0.92
3	1.30
4	1.691
5	2.087

Table 5-40 compares analysis results of bare frames with and without considering the strut width.

Table 5-40: Results of models with and without struts- brick infill walls

Results of Models with and without Struts- Brick Infill Walls			
No. of Stories	**No Strut Model**	**Strut Model**	**Difference (%)**
2	0.616	0.537	12.8%
4	1.037	0.92	12.7%
6	1.46	1.30	10.9%
8	1.89	1.691	10.5%
10	2.324	2.087	10.2%

As can be noted in table 5-40 the impact of modeling brick walls using equivalent strut method is around 11.4% on average, therefore, contribution of infill walls composed of bricks on the lateral stiffness of a system may not cause a dramatic change in the behavior of structural system.

5.5.4.3 Comparative Study for the Numerical results

A pattern of construction that consists of slab with no beams supported on columns with the existence of parameter infill walls was analyzed using three different levels of analysis; the first level is the common practice of neglecting those walls in the analysis, the next level is by analyzing walls assuming capacity tension (as reinforced walls with openings), and finally modeling using equivalent strut method using NBCC code formula.

5.5.4.3.1 Method One Models

Model with Columns and Walls of 24 MPa Compressive Strength

Table 5-41 shows analysis results for the three types of analysis for a system where columns and infill walls are with a constant compressive strength of 24 MPa.

Table 5-41: Comparison between different analysis approaches- for columns/ infill walls with compressive strength of 24 MPa-method one pattern one

No. of Stories	Bare Frame Analysis Results		Model with Parameter reinforced walls with openings		Equivalent Strut Model
	Non-cracked model	Cracked model	Non-cracked model	Cracked model	
2	0.616	0.934	0.088	0.152	0.223
4	1.037	1.698	0.169	0.274	0.337
6	1.46	2.450	0.248	0.401	0.522
8	1.89	3.20	0.331	0.535	0.664
10	2.324	3.94	0.42	0.674	0.804

Figure 5-29 shows the numerical results for non-cracked model results for the approaches.

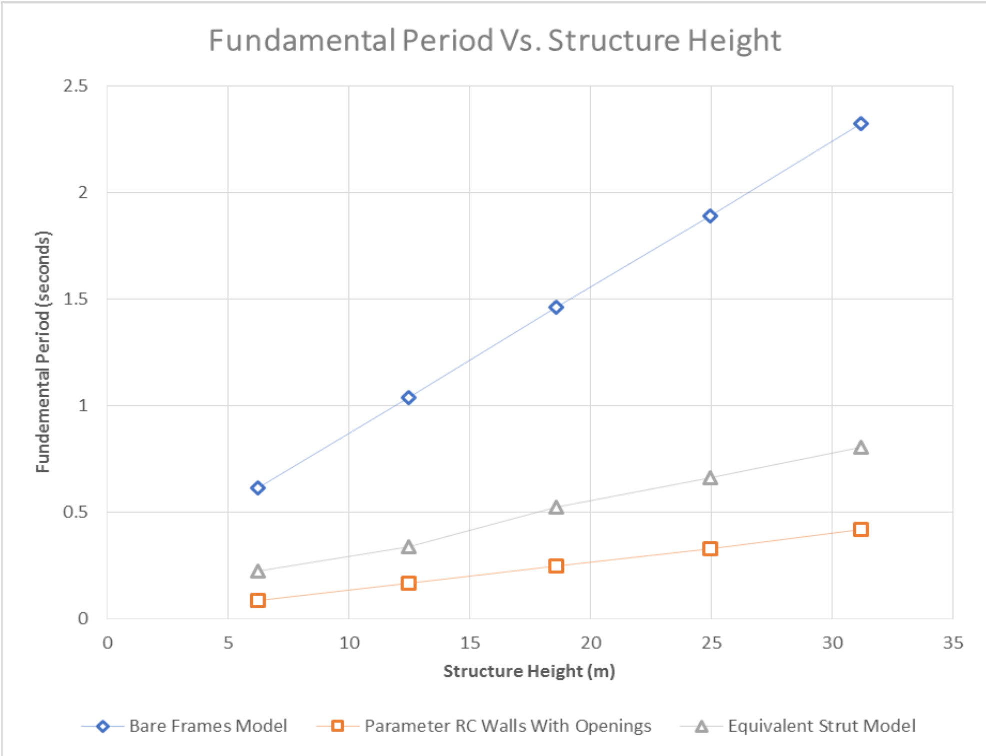

Figure 5-29: Bare frames model, parameter RC walls with openings, equivalent strut model, for a system of slab with no beams supported on columns with infill walls of plain concrete, columns' concrete of 24 MPa compressive strength-method one pattern one

As can be noted from figure 5-29 the analysis results of bare frames with neglecting infill walls overestimated the fundamental period in an unacceptable range. Moreover, results of infill walls of plain concrete are somehow close to results of reinforced walls, and this emphasize the need of considering such walls in analysis to increase accuracy of modeling and calculated base shear value.

Table 5-42 compares what ASCE code formula suggest and what equivalent strut for non-cracked models provide.

Table 5-42: ASCE formula results Vs. equivalent strut model – method one- columns and walls with compressive strength of 24 MPa- pattern one

No. of Stories	ASCE formula Value – without multiplying by the factor Cu	ASCE formula -Lower boundary (Cu=1.4)	ASCE formula -Upper Boundary (Cu=1.7)	Equivalent Strut Model
2	0.242	0.339	0.411	0.223
4	0.45	0.63	0.768	0.337
6	0.64	0.896	1.088	0.522
8	0.84	1.176	1.428	0.664
10	1.03	1.442	1.751	0.804

Figure 5-30 shows comparison between equivalent strut model results and ASCE-7-10 code formula.

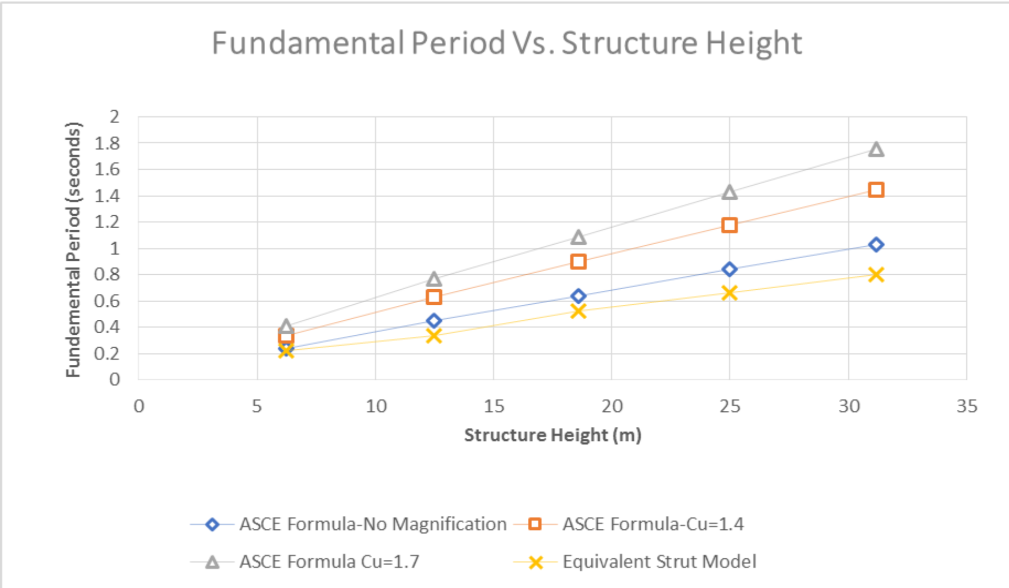

Figure 5-30: Results of ASCE Formula without magnification, with Cu=1.4, Cu=1.7, and equivalent strut model- method one-columns and walls with compressive strength of 24 MPa

As can be noted from figure 5-30 the ASCE formula over estimates the value of the fundamental period even when not multiplying with the magnification factor; this can be explained by the fact that the used factors in the formula is based on the assumption of moment resisting frame, while in this case infill walls will change the define of the system and therefore values of factors may be as shown in table 5-43.

Table 5-43: Part of 12.8-2 table that includes concrete moment resisting frames in metric units

Structure Type	C_t (metric units)	X (metric units)
Other systems than moment resisting frames	0.0488	0.75

Therefore, ASCE code formulas for reinforced concrete moment frames can be written as following.

$$Ta = 0.0488 h_n^{0.75} \quad \text{[Equation 5-2]}$$

Table 5-44 shows the modified values of suggested values by ASCE formula (equation 5-2).

Table 5-44: ASCE formula results Vs. equivalent strut model – method one- pattern one-columns and walls with compressive strength of 24 MPa-assuming formula of $Ta = 0.0488 h_n^{0.75}$

No. of Stories	ASCE formula Value – without multiplying by the factor Cu	ASCE formula -Lower boundary (Cu=1.4)	ASCE formula -Upper Boundary (Cu=1.7)	Equivalent Strut Model
2	0.193	0.27	0.328	0.223
4	0.261	0.365	0.444	0.337
6	0.44	0.616	0.748	0.522
8	0.545	0.763	0.927	0.664
10	0.644	0.91	1.09	0.804

Figure 5-31 shows comparison between equivalent strut model results and ASCE-7-10 code formula after adopting equation 5-2.

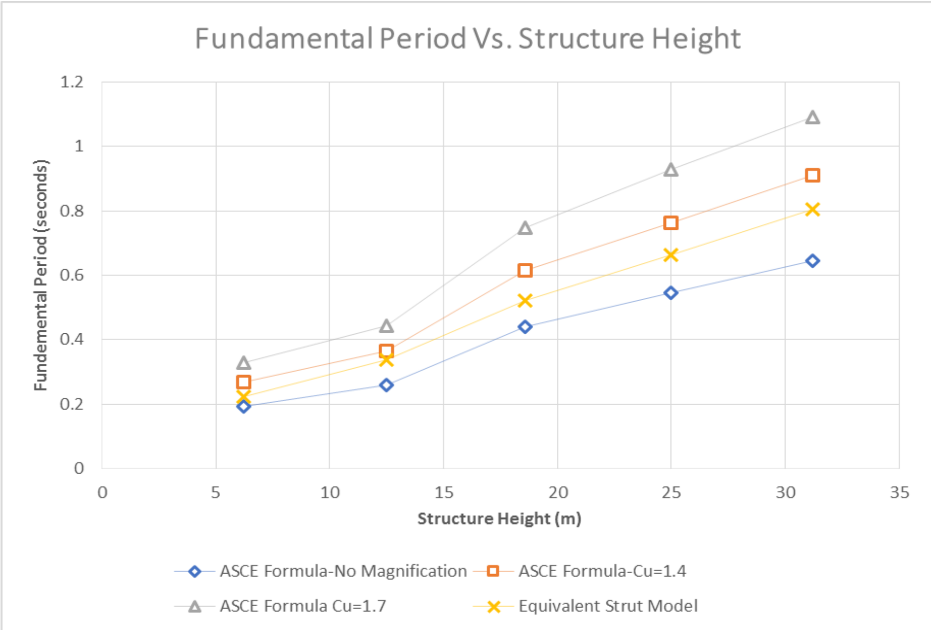

Figure 5-31: Results of ASCE Formula without magnification, with Cu=1.4, Cu=1.7, and equivalent strut model- method one-pattern one-columns and walls with compressive strength of 24 MPa- formula of $Ta = 0.0488h_n{}^{0.75}$

As can be noted from figure 5-31 ASCE formula without magnification is the only conservative formula; as the other formulas over estimated the value of the fundamental period.

Model with Columns of 24 MPa and Walls of 16 MPa Compressive Strength

Table 5-45 shows analysis results for the three types of analysis for a system of columns of 24 MPa compressive strength and 16 MPa for infill walls.

Table 5-45: Comparison between different analysis approaches- for columns of compressive strength of 24 MPa and infill walls of compressive strength of 16 MPa-method one-pattern one

No. of Stories	Bare Frame Analysis Results		Model with Parameter reinforced walls with openings		Equivalent Strut Model
	Non-cracked model	Cracked model	Non-cracked model	Cracked model	
2	0.616	0.934	0.105	0.166	0.237
4	1.037	1.698	0.185	0.30	0.4
6	1.46	2.450	0.271	0.439	0.553
8	1.89	3.20	0.362	0.585	0.704
10	2.324	3.94	0.459	0.737	0.85

Figure 5-32 shows the numerical results for non-cracked model results for the three approaches for the system with columns' compressive strength of 24 MPa, and infill walls of compressive strength of 16 MPa.

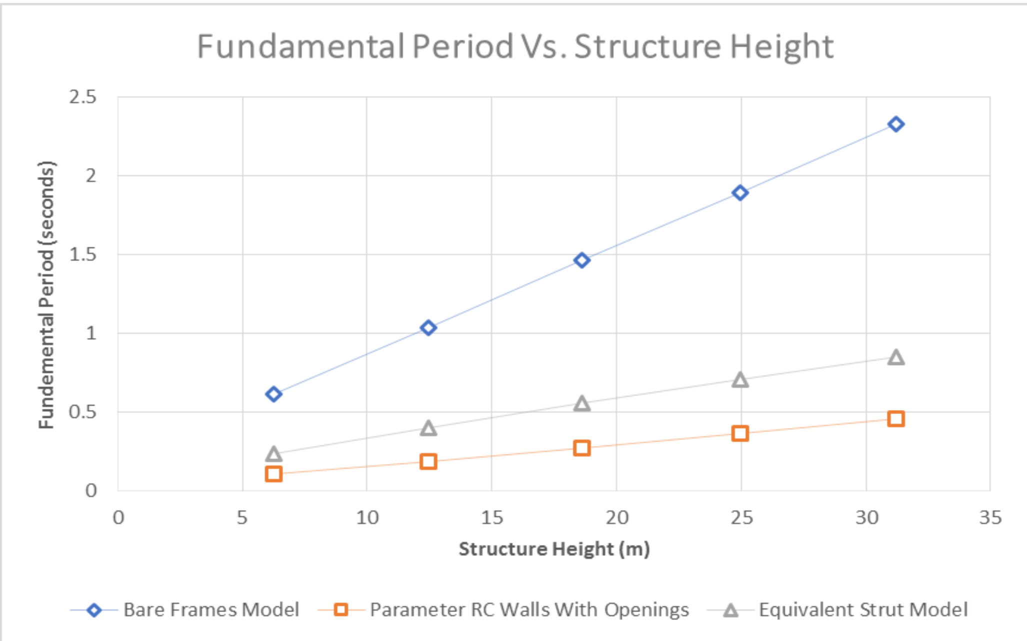

Figure 5-32: Bare frames model, parameter RC walls with openings, equivalent strut model, for a system of slab with no beams supported on columns with infill walls of plain concrete of 16 MPa compressive strength, columns' concrete of 24 MPa compressive strength-method one-pattern one

Table 5-46 shows the modified values of suggested values by ASCE formula.

Table 5-46: ASCE formula results Vs. equivalent strut model – method one-pattern one columns of 24 MPA compressive strength and walls with compressive strength of 16 MPa-assuming formula of $Ta = 0.0488 h_n{}^{0.75}$

No. of Stories	ASCE formula Value – without multiplying by the factor Cu	ASCE formula - Lower boundary (Cu=1.4)	ASCE formula - Upper Boundary (Cu=1.7)	Equivalent Strut Model
2	0.193	0.27	0.328	0.237
4	0.261	0.365	0.444	0.4
6	0.44	0.616	0.748	0.553
8	0.545	0.763	0.927	0.704
10	0.644	0.91	1.09	0.85

Figure 5-33 shows comparison between equivalent strut model results and ASCE-7-10 code formula after adopting equation 5-2.

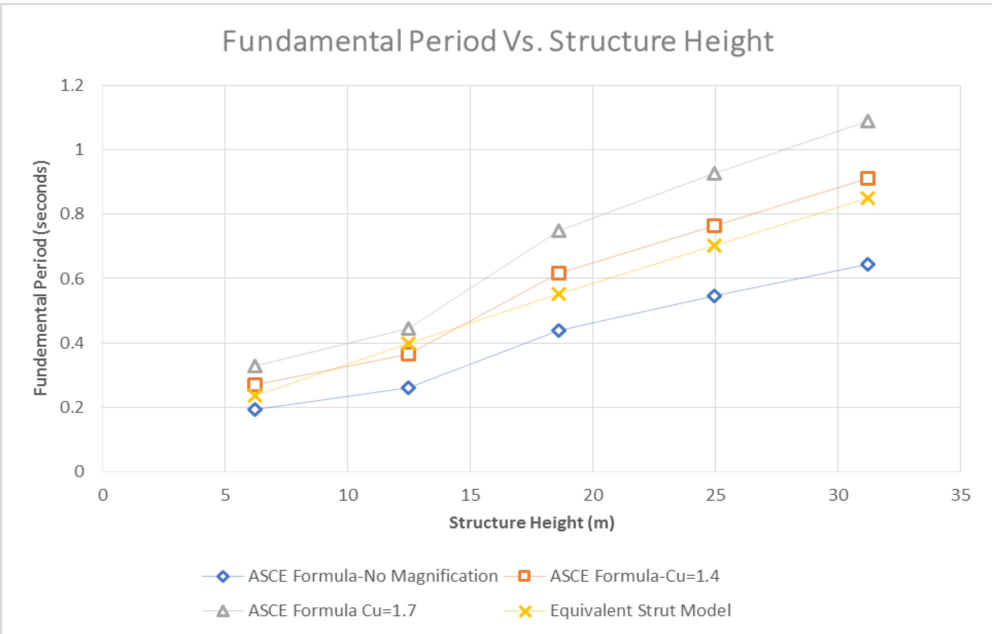

Figure 5-33: Results of ASCE formula without magnification, with Cu=1.4,Cu=1.7, and equivalent strut model- method one-pattern one columns with compressive strength of 24 MPa, and walls of compressive strength of 16 MPa- formula of $Ta = 0.0488 h_n{}^{0.75}$

As can be noted from figure 5-33 ASCE formula with magnification of 1.4 is close to equivalent strut analysis results. However, ASCE formula is still the only conservative formula for infill walls with compressive strength of 16 MPa.

Model with Columns of 24 MPa and Walls of 12 MPa Compressive Strength

Table 5-47 shows the modified values of suggested values by ASCE formula.

Table 5-47: ASCE formula results Vs. equivalent strut model – method one- columns of 24 MPA compressive strength and walls with compressive strength of 12 MPa-assuming formula of $Ta = 0.0488{h_n}^{0.75}$

No. of Stories	ASCE formula Value – without multiplying by the factor Cu	ASCE formula - Lower boundary (Cu=1.4)	ASCE formula - Upper Boundary (Cu=1.7)	Equivalent Strut Model
2	0.193	0.27	0.328	0.248
4	0.261	0.365	0.444	0.416
6	0.44	0.616	0.748	0.576
8	0.545	0.763	0.927	0.731
10	0.644	0.91	1.09	0.883

Figure 5-34 shows the numerical results for non-cracked model results for the three approaches for the system with columns' compressive strength of 24 MPa, and infill walls of compressive strength of 12 MPa.

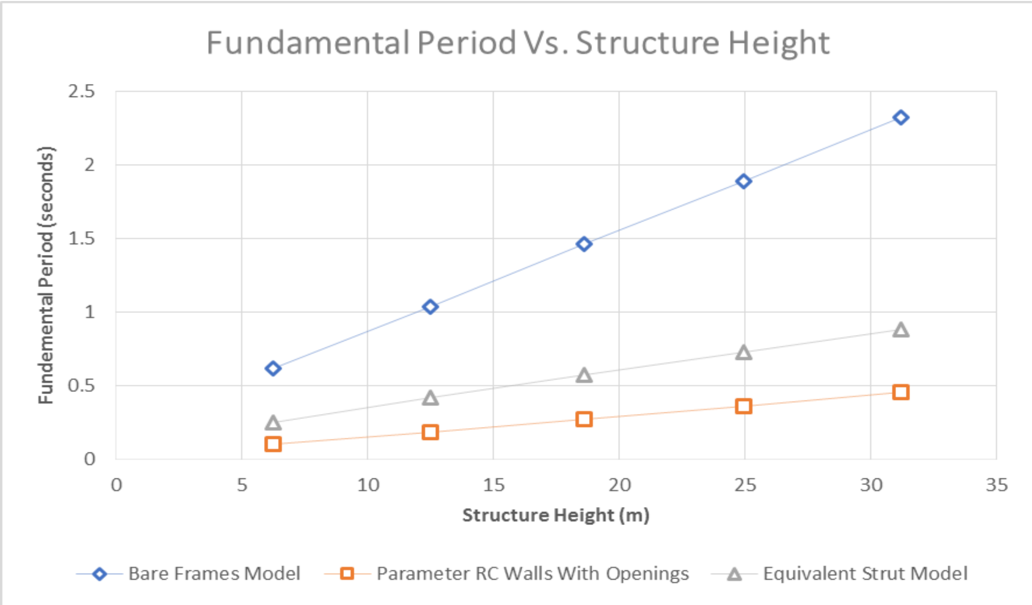

Figure 5-34: Bare Frames Model, Parameter RC walls with openings, equivalent strut model, for a system of slab with no beams supported on columns with infill walls of plain concrete of 12 MPa compressive strength, columns' concrete of 24 MPa compressive strength-method one-pattern one

Figure 5-35 shows comparison between equivalent strut model results and ASCE-7-10 code formula after adopting equation 5-2.

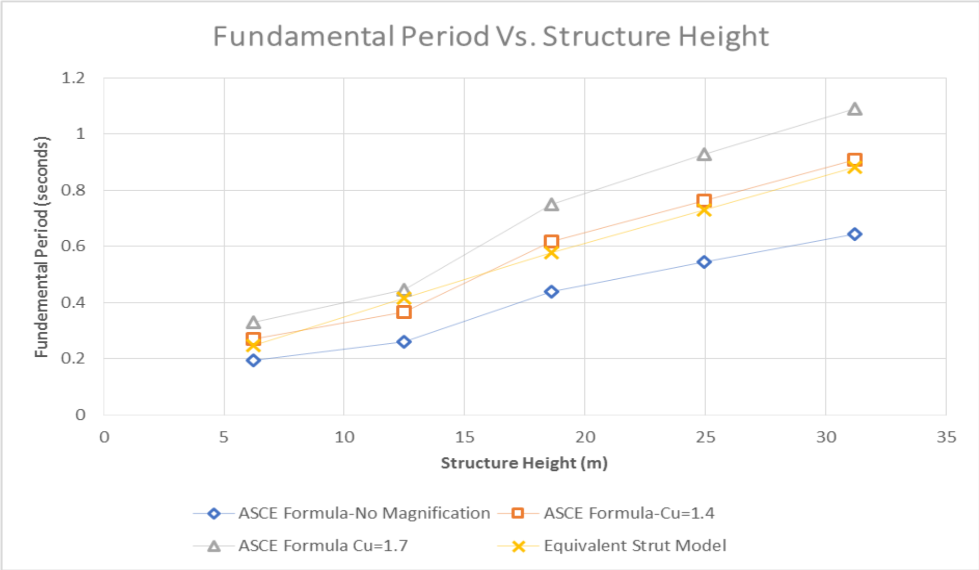

Figure 5-35: Results of ASCE Formula without magnification, with Cu=1.4,Cu=1.7, and equivalent strut model- method one-pattern one-columns with compressive strength of 24 MPa, and walls of compressive strength of 12 MPa- formula of $Ta = 0.0488h_n{}^{0.75}$

As can be noted from figure 5-35 ASCE formula with magnification of 1.4 is close to equivalent strut analysis results. However, ASCE formula without magnification is still the only conservative formula for infill walls with compressive strength of 12 MPa.

5.5.4.3.2 Method Two Models

In method two there is only a unique case where models are analyzed for columns of 24 MPa compressive strength and a constant width and depth of strut.

Table 5-48 shows results of model with and without equivalent strut.

Table 5-48: Results of models with and without struts- brick infill walls-method two-pattern one

No. of Stories	No Strut Model	Strut Model	Difference (%)
2	0.616	0.537	12.8%
4	1.037	0.92	12.7%
6	1.46	1.30	10.9%
8	1.89	1.691	10.5%
10	2.324	2.087	10.2%

Table 5-49 shows the modified values of suggested values by ASCE formula for moment resisting frames.

Table 5-49: ASCE formula results Vs. equivalent strut model – method two- pattern one columns of 24 MPA compressive and equivalent strut

No. of Stories	ASCE formula Value – without multiplying by the factor Cu	ASCE formula - Lower boundary (Cu=1.4)	ASCE formula - Upper Boundary (Cu=1.7)	Equivalent Strut Model
2	0.242	0.339	0.411	0.537
4	0.45	0.63	0.768	0.92
6	0.64	0.896	1.088	1.30
8	0.84	1.176	1.428	1.691
10	1.03	1.442	1.751	2.087

Figure 5-36 shows the equivalent strut fundamental period as compared to ASCE formula with and without magnifications.

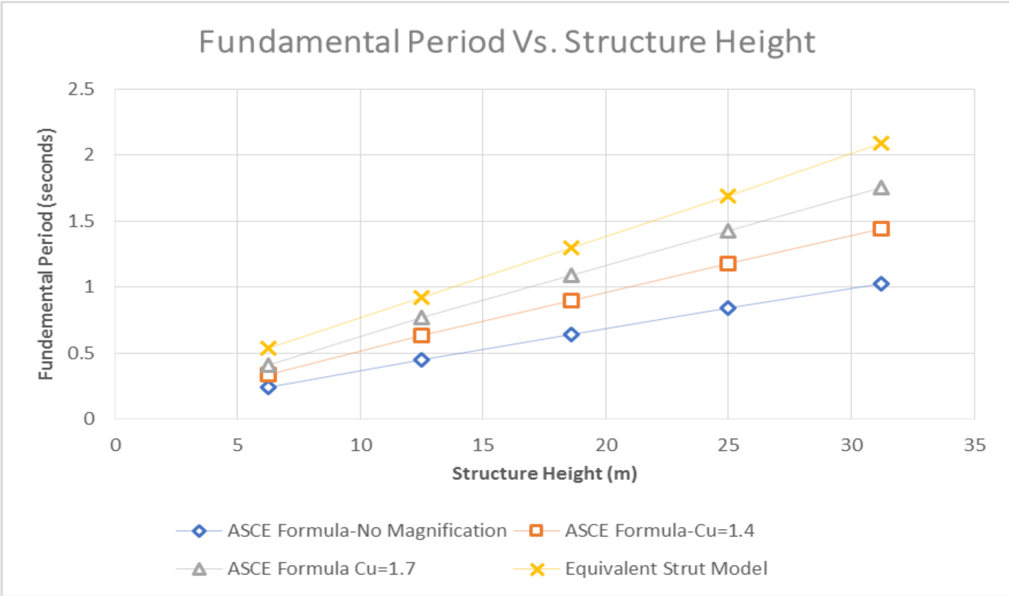

Figure 5-36: Results of ASCE Formula without magnification, with Cu=1.4,Cu=1.7, and equivalent strut model- method two-pattern one columns with compressive strength of 24 MPa

It can be concluded that effect of brick infill wall can be neglected as there is no major change on the fundamental period value. Moreover, ASCE code formula is conservative as estimated value of fundamental period is below modal analysis results.

5.6 Analysis of Method One and Two-Pattern Two

In the local practice in Palestine the construction of bare frames is not common, as the majority of structures have shear walls that surround the stair case. Figure 5-37 shows the plan layout of the structural system that will be analyzed in this section.

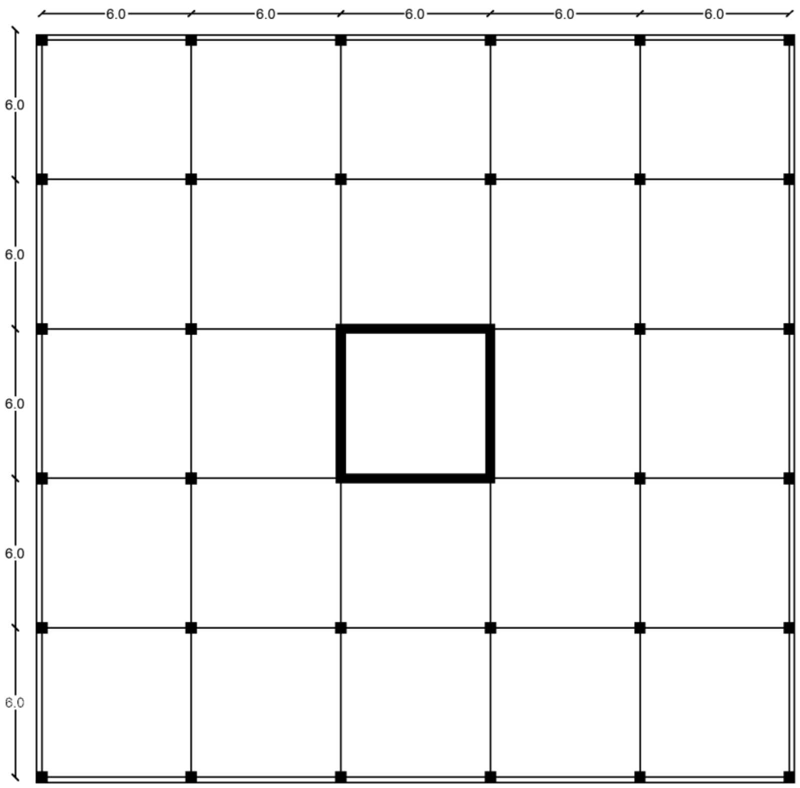

Figure 5-37: Plan layout for flat slab system supported on columns and a core shear wall system that surrounds stair case

The properties of this pattern are the same for the bare frame model. In other words, the only change that is made to this pattern is removing four columns at the center and adding a core shear wall as shown in figure 5-37.

Patterns of Analyzed Structures/ Frames with Core Walls

Patterns of analyzed structure will be limited to a unique value of concrete compressive strength (only 24 MPa) for columns; as results previously showed that impact of increasing columns' compressive strength on the fundamental period may be negligible. Indeed, effect of changing columns' compressive strength with the existence of core shear wall will be less compared to bare frames.

On the other hand, infill walls will be analyzed for two values of 24, and 12 MPa for all the cases.

Table 5-50 shows the different columns' sizing that will be used in the analysis of pattern two.

Table 5-50: Columns' sizing for all models-pattern two

Patterns of Bare Frame with Core Walls Structures/fc'=24 MPa		
Model Number	No. of stories	Columns size (mm)
Model 1	2	400x400
Model 2	4	500x500
Model 3	6	600x600
Model 4	8	700x700
Model 5	10	800x800

Analysis will be performed for both cases of cracked and non-cracked structural elements. Cracked sections will be modified according to ACI-314 suggestion, taking in consideration that for cracked wall it is suggested that cracked section is with 0.35 modifier factor.

5.6.1 Analysis Results for Frames with Core Walls Structures

Table 5-51 shows the results of fundamental period for pattern two using constant compressive strength of 24 MPa for columns without considering infill walls in analysis.

Table 5-51: Fundamental period: ASCE Formula, cracked and non-cracked models for pattern two with compressive strength of 24 MPa

No. of Stories	Elevation	Fundamental Period (seconds)				
		ASCE7-10 Formula			Non-Cracked model	Cracked Model
		Lower	Upper	Average		
2	6.24	0.27	0.33	0.30	0.30	0.48
4	12.48	0.45	0.55	0.50	0.54	0.86
6	18.60	0.62	0.74	0.68	0.77	1.24
8	24.96	0.76	0.93	0.85	0.99	1.62
10	31.2	0.90	1.10	1.0	1.23	2.0

Figure 5-38 shows the relation between story height and fundamental period as provided in table 5-51.

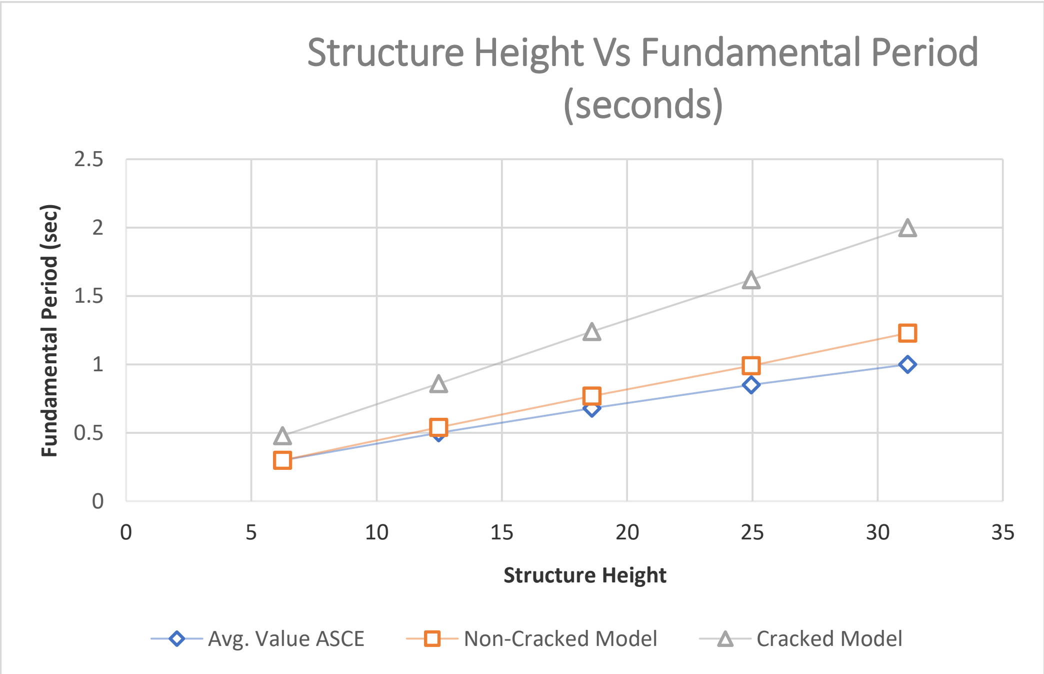

Figure 5-38: Fundamental period Vs. height analysis of bare structures with central core walls-no infill walls-columns and walls of 24 MPa compressive strength

As can be noted form figure 5-38 ASCE formula under estimate the value of fundamental period for the system when neglecting core shear walls.

5.6.2 Analysis Results for Pattern Two with Existence of Parameter Reinforced Walls with Openings

In this section analysis results for the assumption of modeling infill walls as reinforced walls with openings will be introduced for two values of compressive strength for the infill walls (24, and 12 MPa) for Method One (wall thickness of 12 cm).

Analysis Results

Analysis results that are shown in table 5-52 are for pattern assuming a compressive strength of 24 MPa for infill walls with openings and core shear walls.

Table 5-52: ASCE formula, cracked and non-cracked models for frames with core shear walls with compressive strength of 24 MPa and parameter walls with openings of compressive strength of 24 MPa

No. of Stories	Elevation	Fundamental Period (seconds)				
		ASCE7-10 Formula			Non-Cracked model	Cracked Model
		Lower	Upper	Average		
2	6.24	0.27	0.33	0.30	0.067	0.121
4	12.48	0.45	0.55	0.50	0.130	0.235
6	18.60	0.62	0.74	0.68	0.191	0.355
8	24.96	0.76	0.93	0.85	0.255	0.481
10	31.2	0.90	1.10	1.0	0.323	0.613

Figure 5-39 shows the relation between story height and the fundamental period for structures with reinforced walls with openings of 24 MPa compressive strength concrete.

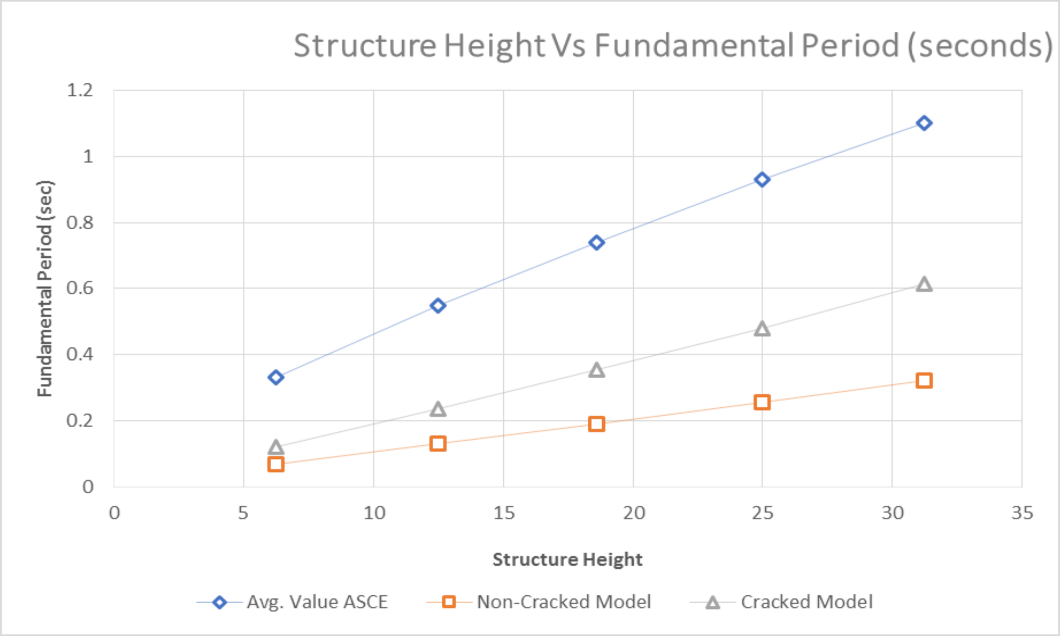

Figure 5-39: Fundamental period Vs. height analysis of pattern two- infill walls-columns and walls of 24 MPa compressive strength-assumptions of reinforced walls with openings

Figure 5-39 shows that ASCE formula over estimated the value of fundamental period even for case of analysis for cracked sections.

Analysis results that are shown in table 5-53 are for pattern assuming a compressive strength of 24 MPa for columns and core shear walls. On the other hand, the value of compressive strength for infill walls is 12 MPa.

Table 5-53: Fundamental period: ASCE formula, cracked and non-cracked models for frames with core shear walls with compressive strength of 24 MPa and parameter walls with openings of compressive strength of 12 MPa

No. of Stories	Elevation	Fundamental Period (seconds)				
		ASCE7-10 Formula			Non-Cracked model	Cracked Model
		Lower	Upper	Average		
2	6.24	0.27	0.33	0.30	0.081	0.135
4	12.48	0.45	0.55	0.50	0.162	0.261
6	18.60	0.62	0.74	0.68	0.249	0.402
8	24.96	0.76	0.93	0.85	0.341	0.54
10	31.2	0.90	1.10	1.0	0.439	0.69

Figure 5-40 shows the relation between story height and the fundamental period for structures with reinforced walls with openings of 24 MPa compressive strength concrete for columns and core shear walls, and for infill walls with compressive strength of 12 MPa.

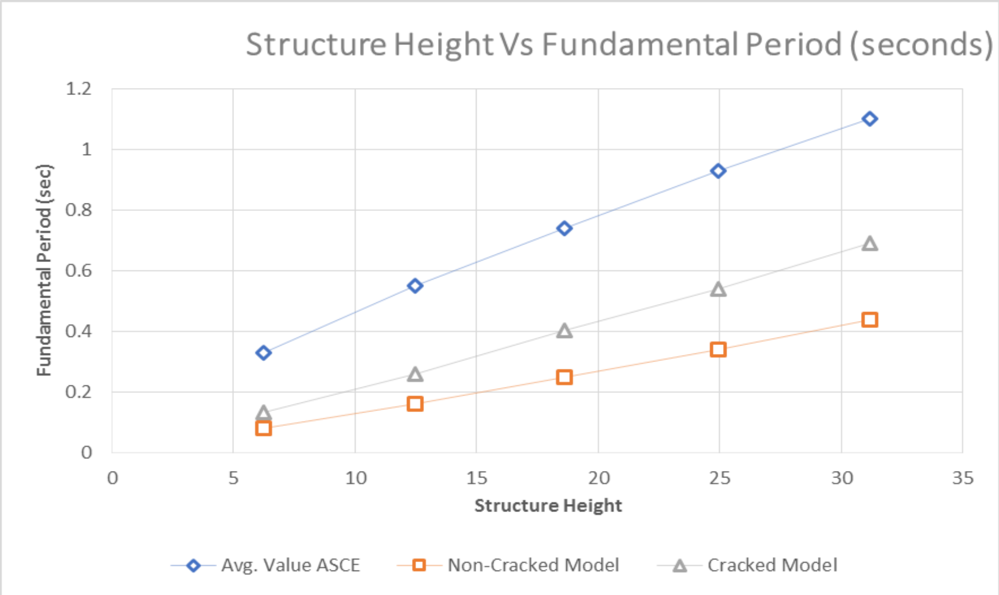

Figure 5-40: Fundamental period Vs. height analysis of pattern two- columns and core walls of 24 MPa compressive strength, and infill walls with 12 MPa compressive strength-assumption of reinforced walls with openings

Figure 5-40 shows that for parameter reinforced walls of 12 cm ASCE formula over estimates the fundamental period even for the cracked model.

5.6.3 Modeling with Equivalent Strut

In this section analysis results for the assumption of modeling infill walls as equivalent compression strut for two values of compressive strength for the infill wall (24, and 12 MPa) for pattern two.

Method One – Pattern Two - Analysis Results

Table 5-54 shows analysis results for frames with constant compressive strength for columns (fc'=24 MPa) and variable compressive strength of struts.

Table 5-54: Fundamental period for different strut compressive strength values-non cracked model-system with core shear walls - method one-patter two

Non-cracked Models		
No. of Stories	fc'=24 MPa	fc'=12 MPa
1	0.132	0.146
2	0.228	0.246
3	0.357	0.373
4	0.498	0.516
5	0.625	0.661

Table 5-55 compares analysis results of frames with and without considering the strut width for non-cracked models.

Table 5-55: results of models with and without struts- core shear wall system-fc'=24 MPa for the strut-method one-pattern two

Results of Models with and without Struts- Core Shear Wall System-fc'=24 MPa for the Strut – Non-Cracked Models			
No. of Stories	**No Strut Model**	**Strut Model**	**Difference (%)**
2	0.30	0.132	56%
4	0.54	0.228	57.8%
6	0.77	0.357	53.6%
8	0.99	0.498	49.7%
10	1.23	0.625	49.2%

Table 5-56 shows analysis results for the three types of analysis for a system of columns of 24 MPa compressive strength and 24 MPa for infill walls.

Table 5-56: Comparison between different analysis approaches- for columns of compressive strength of 24 MPa and infill walls of compressive strength of 24 MPa-method one-pattern two

No. of Stories	Pattern two- neglecting infill walls		Model with Parameter reinforced walls with openings		Equivalent Strut Model (non-cracked)
	Non-cracked model	Cracked model	Non-cracked model	Cracked model	
2	0.30	0.48	0.081	0.135	0.132
4	0.54	0.86	0.162	0.261	0.228
6	0.77	1.24	0.249	0.402	0.357
8	0.99	1.62	0.341	0.54	0.498
10	1.23	2.0	0.439	0.69	0.625

Figure 5-41 shows the relation between story height and the fundamental period for the non-cracked analysis for the three cases of first ignoring modeling of infill wall, second by considering those walls as reinforced with openings, and finally using the equivalent strut method.

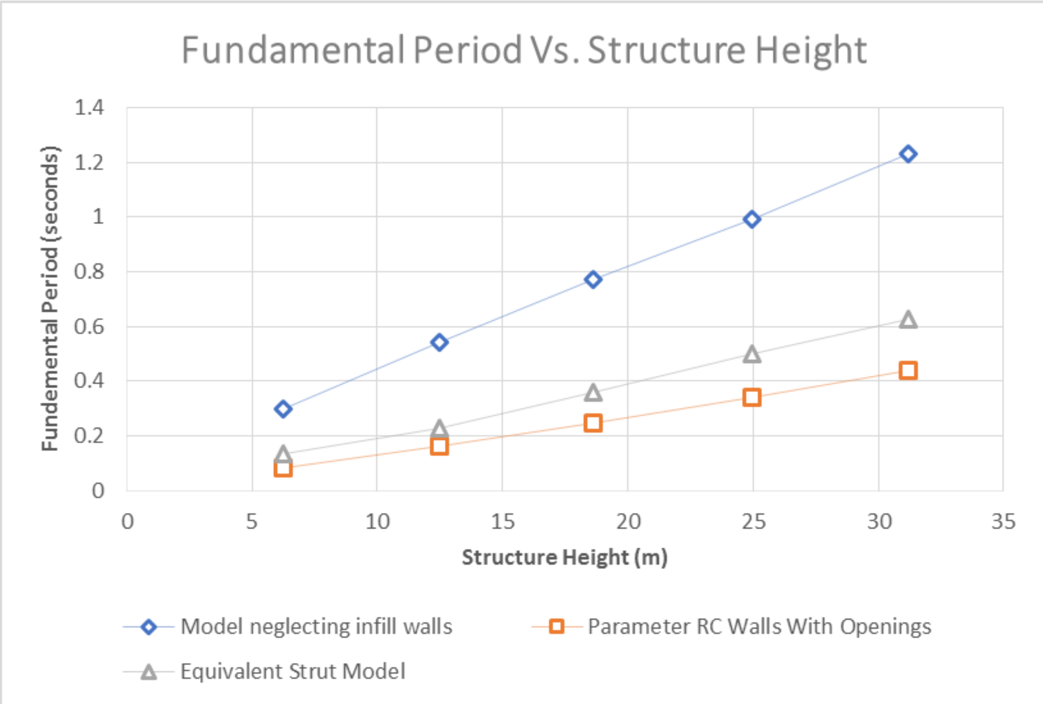

Figure 5-41: Ignoring infill walls, Parameter RC walls with openings, equivalent strut model, for a system of slab with no beams supported on columns with infill walls of plain concrete of 24 MPa compressive strength, columns' concrete of 24 MPa compressive strength-method one-pattern two

Table 5-57 shows the modified values of suggested values by ASCE formula (equation 5-2).

Table 5-57: ASCE formula results Vs. equivalent strut model – method one-pattern two columns and walls with compressive strength of 24 MPa-assuming formula of $Ta = 0.0488{h_n}^{0.75}$

No. of Stories	ASCE formula Value – without multiplying by the factor Cu	ASCE formula - Lower boundary (Cu=1.4)	ASCE formula - Upper Boundary (Cu=1.7)	Equivalent Strut Model
2	0.193	0.27	0.328	0.132
4	0.261	0.365	0.444	0.228
6	0.44	0.616	0.748	0.357
8	0.545	0.763	0.927	0.498
10	0.644	0.91	1.09	0.625

Figure 5-42 shows comparison between equivalent strut model results and ASCE-7-10 code formula (equation 5-2).

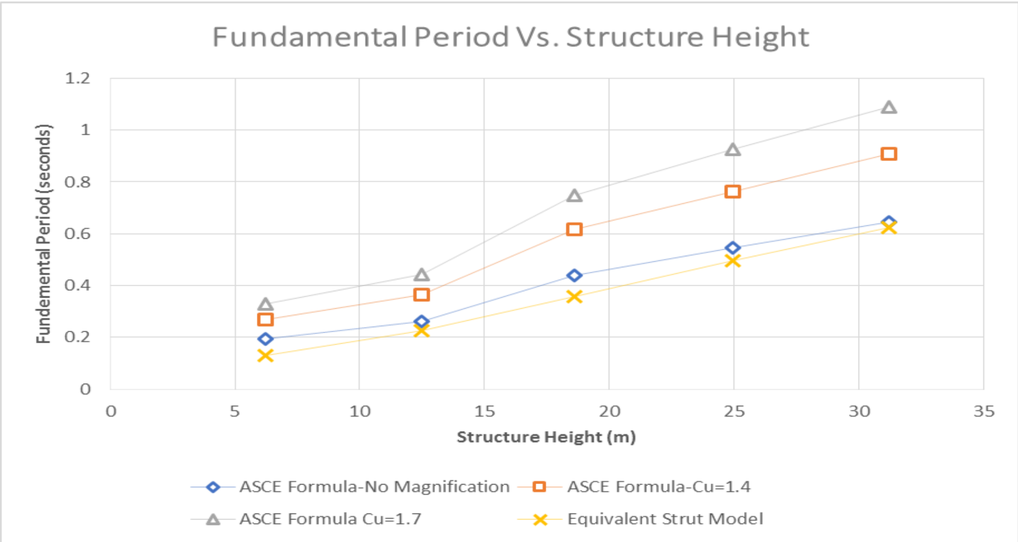

Figure 5-42: Results of ASCE Formula without magnification, with Cu=1.4,Cu=1.7, and equivalent strut model- method one-pattern two-columns with compressive strength of 24 MPa, and walls of compressive strength of 24 MPa- formula of $Ta = 0.0488{h_n}^{0.75}$

As can be noted from figure 5-42 ASCE formula without magnification factor is close to equivalent strut model results. However, results of equivalent strut are still lower than what is suggested by the ASCE formula.

Table 5-58 shows the modified values of suggested values by ASCE formula (equation 5-2).

Table 5-58: ASCE formula results vs. equivalent strut model – method one- pattern two columns and walls with compressive strength of 12 MPa-assuming formula of $Ta = 0.0488{h_n}^{0.75}$

No. of Stories	ASCE formula Value – without multiplying by the factor Cu	ASCE formula - Lower boundary (Cu=1.4)	ASCE formula - Upper Boundary (Cu=1.7)	Equivalent Strut Model
2	0.193	0.27	0.328	0.146
4	0.261	0.365	0.444	0.246
6	0.44	0.616	0.748	0.373
8	0.545	0.763	0.927	0.516
10	0.644	0.91	1.09	0.661

Figure 5-43 shows comparison between equivalent strut model results and ASCE-7-10 code formula (equation 5-2).

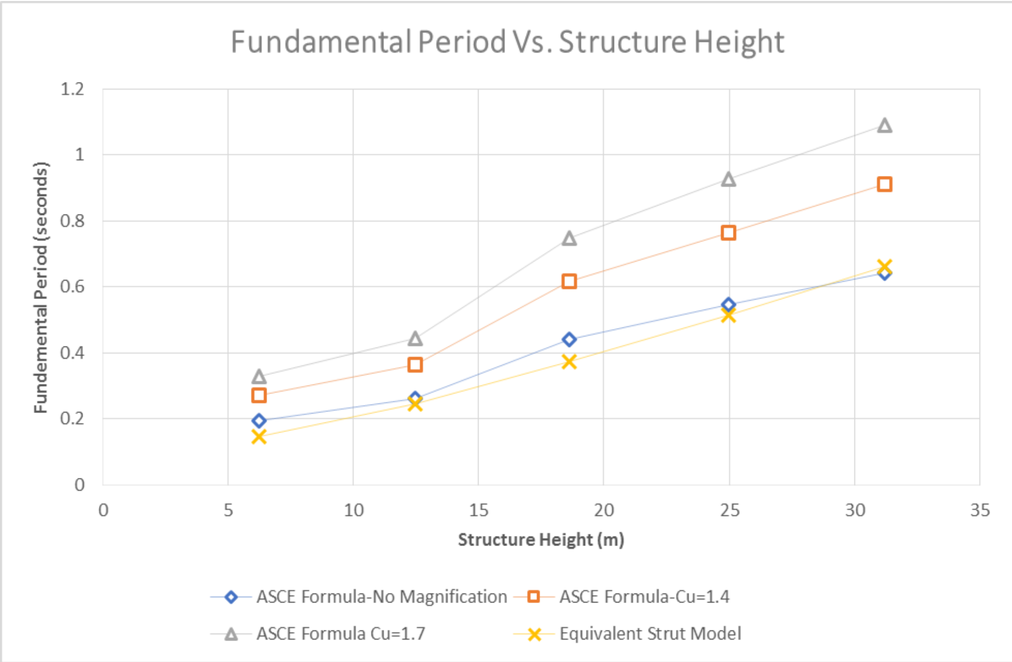

Figure 5-43: Results of ASCE formula without magnification, with Cu=1.4, Cu=1.7, and equivalent strut model- method one-pattern two columns with compressive strength of 12 MPa, and walls of compressive strength of 24 MPa- formula of $Ta = 0.0488 {h_n}^{0.75}$

As can be noted from figure 5-43 ASCE formula without magnification factor is close to equivalent strut model results for strut with assumption of 12 MPa compressive strength.

Method Two-Pattern Two

Analysis with strut for bare frames for 20 cm thickness bricks shows that impact of including infill walls by strut modeling is limited to a change of an average of 10%. Therefore, the change of results for system with core shear wall is expected to be negligible.

The case that will be tested is for system with core shear walls, where models are non-cracked and equivalent strut widths are according to table 5-40.

Table 5-59 shows analysis output for the case of system with core shear walls with and without considering brick infill walls.

Table 5-59: Method two, pattern two, with equivalent strut for a brick layer of 20 cm with E=260 MPa, for non-cracked analysis

No. of Stories	Elevation	Fundamental Period (seconds)		Difference (%)
		Non-Cracked model	Model with Strut	
2	6.24	0.30	0.284	5.3%
4	12.48	0.54	0.493	8.7%
6	18.60	0.77	0.704	8.6%
8	24.96	0.99	0.918	7.2%
10	31.2	1.23	1.135	7.7%

5.7 Method Three

5.7.1 Analysis for Method Three

In method three walls are constructed reinforced with usually two steel layers. In this section analysis of structures with parameter walls with and without opening will be performed to study effect of using such walls on the behavior of structures. The layout of the structure will be same to previously studied layouts for both systems with and without core shear walls. Figure 5-44 shows the two layouts that will be analyzed.

It is important to note that method three wall section is not part of what is defined as infill walls, and the only purpose of analyzing method three system is to create the upper boundary of stiffness.

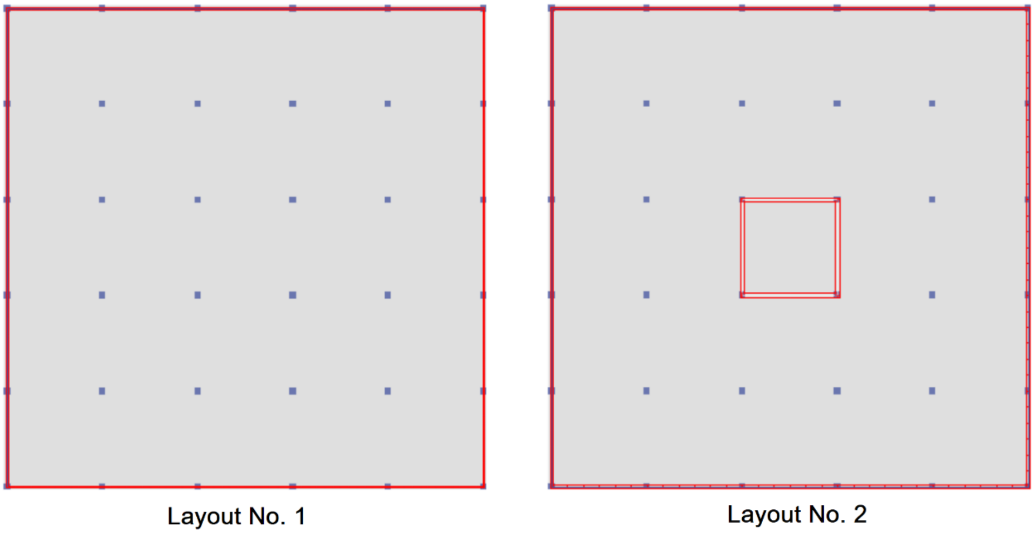

Figure 5-44: Structural layout of the two models-method three

Table 5-60 shows the data of the models, taking in consideration that compressive strength of concrete will be taken only as a unique value of 24 MPa as a result of controlling concrete quality in such walls.

Table 5-60: Data of analytical models – models with parameter shear walls -Method Three

Compressive strength of column, slab concrete fc'	24 MPa
Compressive strength of structural walls fc'	24 MPa
Number of stories	2,4,6,8, and 10 stories
Building Length/Building width	1 pattern (5 bays in both directions)
Span lengths (c/c)	6 meters
Cracked Section	Yes/No
Concrete Unit Weight (kN/m^3)	25
Wall thickness (cm)	20
Line Load value	20 kN/m

Table 5-61 shows columns' dimensions for each model for both structural layouts.

Table 5-61: Columns size with respect to number of stories and compressive strength of walls

Pattern one		
Model Number	No. of stories	Columns size (mm)
Model 1	2	400x400
Model 2	4	500x500
Model 3	6	600x600
Model 4	8	700x700
Model 5	10	800x800

5.7.1.1 Analysis Results for Layout No. 1 -Walls with No Openings

Analysis results that are shown in table 5-62 are for pattern assuming a compressive strength of 24 MPa for infill walls.

Table 5-62: Fundamental period: ASCE Formula, cracked and non-cracked models for method three with parameter walls with no openings-walls of compressive strength of 24 MPa-method three

No. of Stories	**Elevation**	**Fundamental Period (seconds)**				
		ASCE7-10 Formula			**Non-Cracked model**	**Cracked model**
		Lower	**Upper**	**Average**		
2	6.24	0.27	0.33	0.30	0.057	0.098
4	12.48	0.45	0.55	0.50	0.115	0.183
6	18.60	0.62	0.74	0.68	0.166	0.265
8	24.96	0.76	0.93	0.85	0.22	0.35
10	31.2	0.90	1.10	1.0	0.278	0.438

Figure 5-45 shows the relation between story height and the fundamental period for structures with solid reinforced wall all around (infill wall with 20 cm thickness 24 MPa compressive strength).

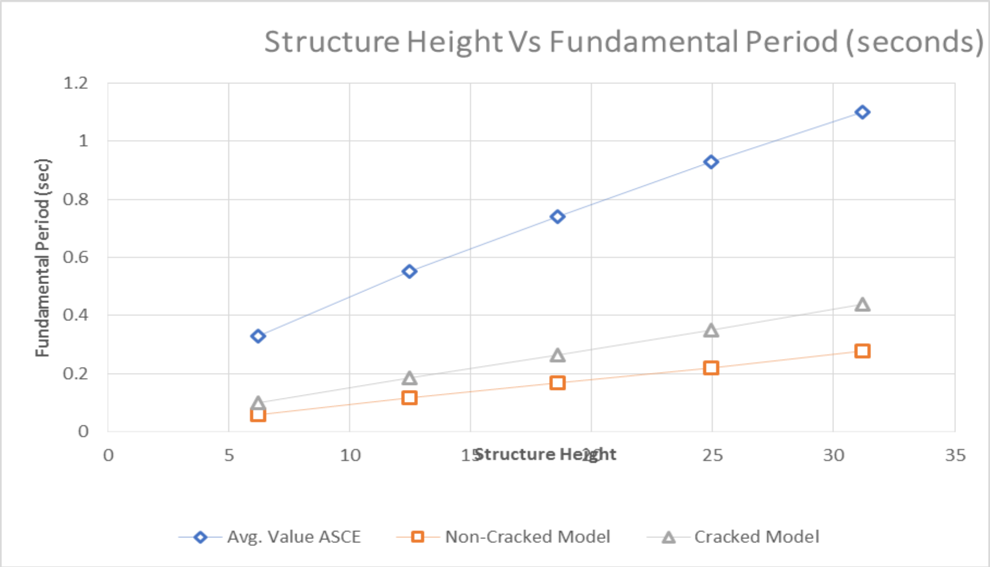

Figure 5-45: Fundamental period Vs structure height using ASCE formula, and non-cracked models for walls with fc'=24 MPa

5.7.1.2 Analysis Results for Layout-1 Walls with Openings

Analysis results that are shown in table 5-63 are for pattern assuming a compressive strength of 24 MPa for infill walls with openings assuming both non-cracked and cracked sections.

Table 5-63: Fundamental period: ASCE Formula, cracked and non-cracked models for method three-layout No. 1 with parameter walls with openings-walls of compressive strength of 24 MPa

No. of Stories	Elevation	Fundamental Period (seconds)				
		ASCE7-10 Formula			Non-Cracked model	Cracked Model
		Lower	Upper	Average		
2	6.24	0.27	0.33	0.30	0.069	0.115
4	12.48	0.45	0.55	0.50	0.135	0.216
6	18.60	0.62	0.74	0.68	0.197	0.318
8	24.96	0.76	0.93	0.85	0.265	0.426
10	31.2	0.90	1.10	1.0	0.336	0.538

Figure 5-46 shows the relation between story height and the fundamental period for structures with reinforced walls with openings of 24 MPa compressive strength concrete.

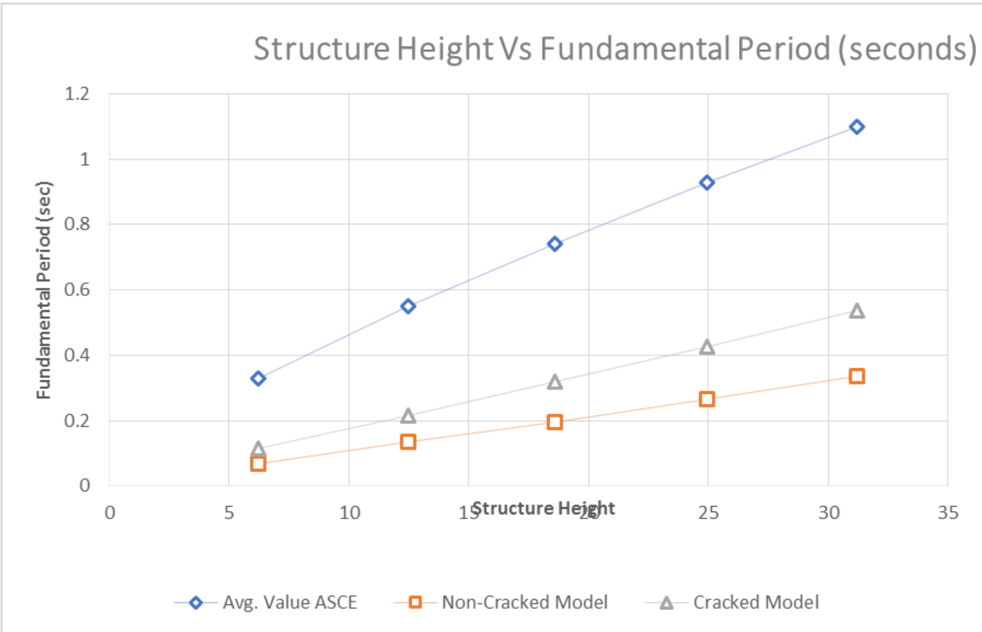

Figure 5-46: Fundamental period Vs structure height using ASCE formula, cracked and non-cracked models for walls with openings with fc'=24 MPa

5.7.1.3 Analysis Results for Layout No. 2 -Walls with No Openings

Analysis results that are shown in table 5-64 are for pattern assuming a compressive strength of 24 MPa for infill walls.

Table 5-64: Fundamental period: ASCE formula, cracked and non-cracked models for method three-layout No. 2 with parameter walls with no openings-walls of compressive strength of 24 MPa

No. of Stories	Elevation	Fundamental Period (seconds)				
		ASCE7-10 Formula			Non-Cracked model	Cracked Model
		Lower	Upper	Average		
2	6.24	0.27	0.33	0.30	0.052	0.088
4	12.48	0.45	0.55	0.50	0.105	0.166
6	18.60	0.62	0.74	0.68	0.153	0.243
8	24.96	0.76	0.93	0.85	0.205	0.324
10	31.2	0.90	1.10	1.0	0.261	0.408

Figure 5-47 shows the relation between story height and the fundamental period for structures with reinforced walls without openings of 24 MPa compressive strength concrete.

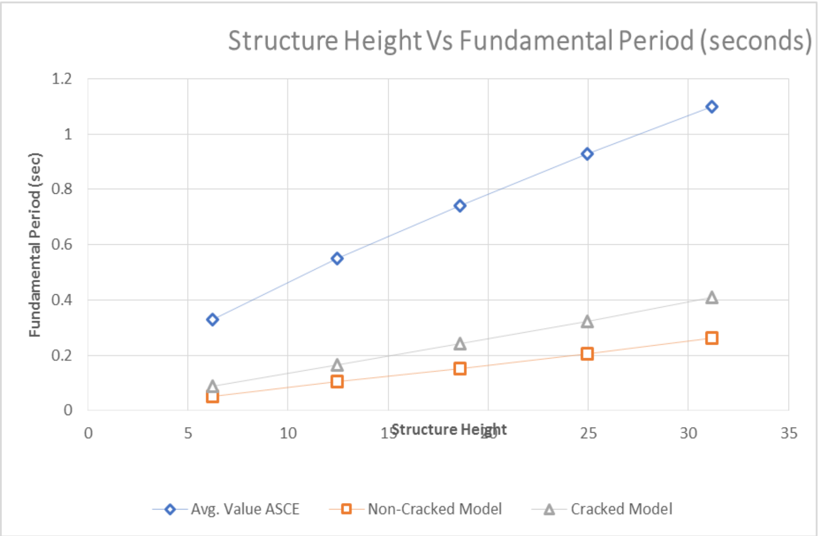

Figure 5-47: Fundamental period Vs structure height using ASCE formula, and non-cracked models for walls with fc’=24 MPa

5.7.1.4 Analysis Results for Layout No. 2 -Walls with Openings

Analysis results that are shown in table 5-65 are for pattern assuming a compressive strength of 24 MPa for infill walls.

Table 5-65: Fundamental period: ASCE, non-cracked and cracked model without walls of fc’=24 MPa

No. of Stories	Elevation	Fundamental Period (seconds)				
		ASCE7-10 Formula			Non-Cracked model	Cracked Model
		Lower	Upper	Average		
2	6.24	0.27	0.33	0.30	0.061	0.086
4	12.48	0.45	0.55	0.50	0.122	0.173
6	18.60	0.62	0.74	0.68	0.184	0.267
8	24.96	0.76	0.93	0.85	0.25	0.369
10	31.2	0.90	1.10	1.0	0.32	0.476

Figure 5-48 shows the relation between story height and the fundamental period for structures with reinforced walls with openings of 24 MPa compressive strength concrete.

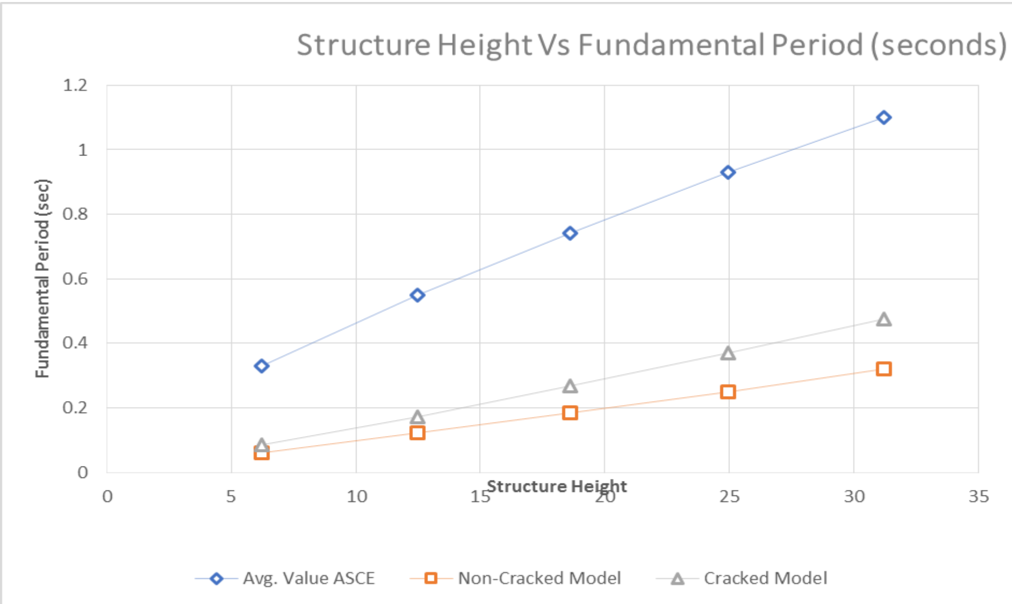

Figure 5-48: Fundamental period Vs structure height using ASCE formula, cracked and non-cracked models for walls with openings with fc’=24 MPa

5.7.1.5 Model Analysis Results Compared to ASCE Formula

Estimation of fundamental period based on ASCE formula need to be checked against models results. It is expected that models' results are much less than those suggested by formula as the suggested system can be rarely found in reality. Indeed, such systems may be limited to special systems with special needs (shelters, hospitals, schools, … etc.).

Results of Layout No. 1

Table 5-66 compares analysis results of the first layout for models with openings with what formula suggests.

Table 5-66: ASCE formula results Vs. equivalent strut model – method three- layout No. 1 – columns and walls of 24 MPa compressive strength

No. of Stories	ASCE formula Value – without multiplying by the factor Cu	ASCE formula - Lower boundary (Cu=1.4)	ASCE formula - Upper Boundary (Cu=1.7)	Non-Cracked Model	Cracked Model
2	0.27	0.33	0.30	0.069	0.115
4	0.45	0.55	0.50	0.135	0.216
6	0.62	0.74	0.68	0.197	0.318
8	0.76	0.93	0.85	0.265	0.426
10	0.90	1.10	1.0	0.336	0.538

Tabulated results show that ASCE code overestimated the period value for both cracked and cracked structural systems.

Figure 5-49 shows comparison between equivalent strut model results and ASCE-7-10 code formula.

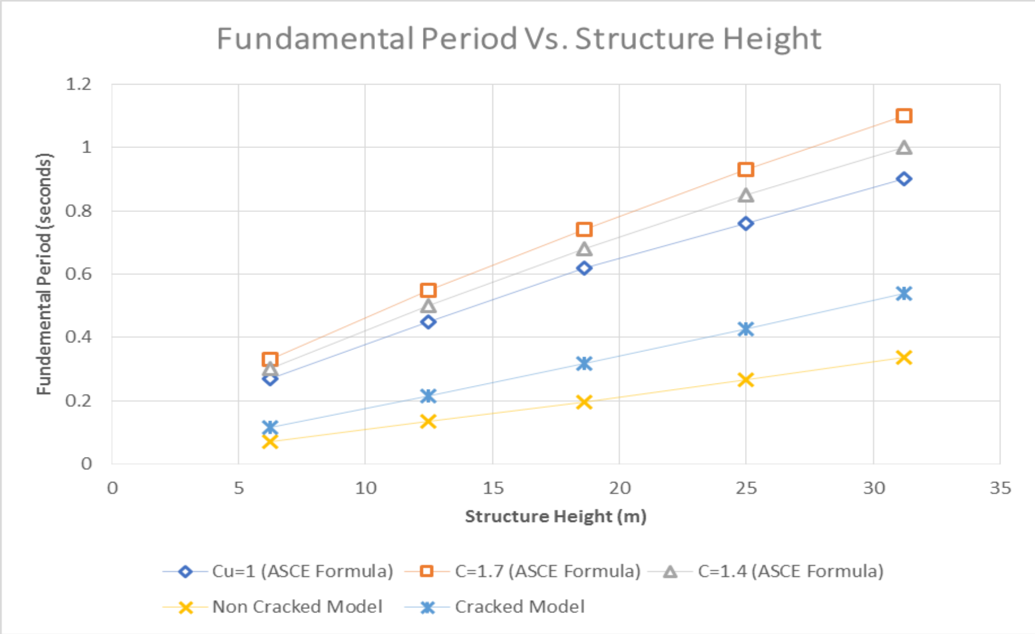

Figure 5-49: Results of ASCE Formula without magnification, with Cu=1.4, Cu=1.7, and equivalent strut model- method three-columns with compressive strength of 24 MPa, and walls of compressive strength of 24 MPa- formula of $Ta = 0.0488 h_n^{0.75}$

Results of Layout No. 2

Table 5-67 compares analysis results of the second layout for models with openings with what formula suggests.

Table 5-67: ASCE formula results Vs. equivalent strut model – method three- layout No. 2 – columns and walls of 24 MPa compressive strength

No. of Stories	ASCE formula Value – without multiplying by the factor Cu	ASCE formula - Lower boundary (Cu=1.4)	ASCE formula - Upper Boundary (Cu=1.7)	Non-Cracked Model	Cracked Model
2	0.27	0.33	0.30	0.061	0.086
4	0.45	0.55	0.50	0.122	0.173
6	0.62	0.74	0.68	0.184	0.267
8	0.76	0.93	0.85	0.25	0.369
10	0.90	1.10	1.0	0.32	0.476

Tabulated results show that ASCE code overestimated the period value for both cracked and cracked structural systems.

Figure 5-50 shows comparison between equivalent strut model results and ASCE-7-10 code formula.

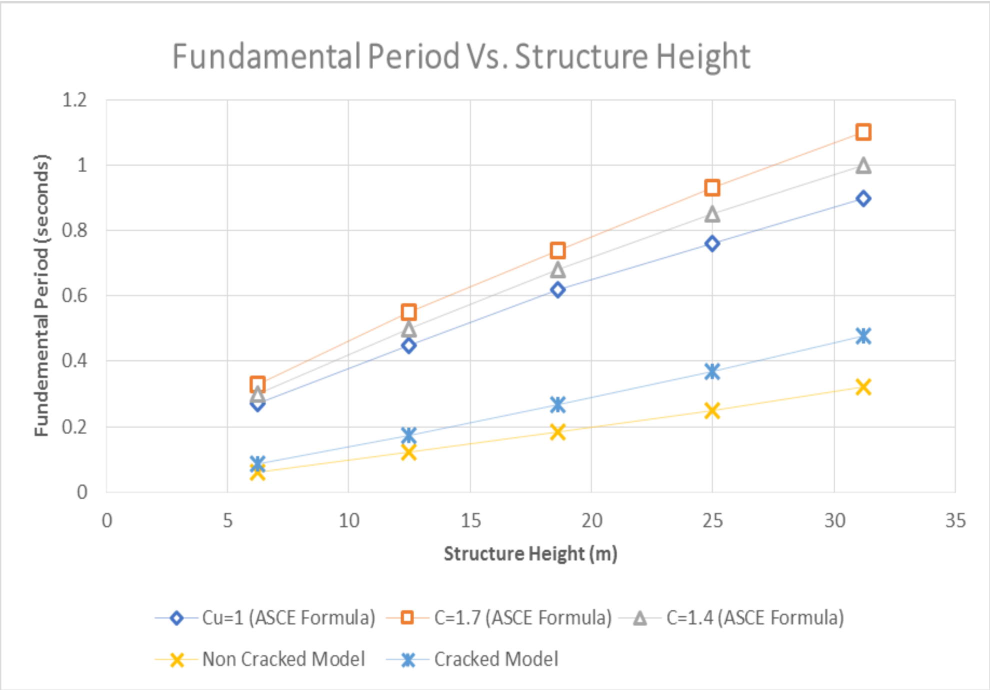

Figure 5-50: Results of ASCE Formula without magnification, with Cu=1.4, Cu=1.7, and equivalent strut model- method three-columns with compressive strength of 24 MPa, and walls of compressive strength of 24 MPa- formula of $Ta = 0.0488 h_n{}^{0.75}$

5.8 Impact of Infill Walls on the Base Shear

According to ASCE code, base shear in a given direction shall be determined in accordance with the following equation:

$$V = C_s W \quad \text{[Equation 5-3]}$$

Calculation of the seismic response coefficient is calculated using the following formula:

$$C_s = \frac{S_{DS}}{\left(\frac{R}{I_e}\right)} \quad \text{[Equation 5-4]}$$

Value computed equation 5-4 must not exceed the following:

$$C_s = \frac{S_{D1}}{T\left(\frac{R}{I_e}\right)} \ for\ T \leq T_L \quad \text{[Equation 5-5]}$$

$$C_s = \frac{S_{D1} T_L}{T\left(\frac{R}{I_e}\right)} \ for\ T \geq T_L \quad \text{[Equation 5-6]}$$

The minimum value of C_s shall not be less than:

$$C_s = 0.44 S_{DS} I_e \geq 0.01 \quad \text{[Equation 5-7]}$$

As can be noted in equation 5-5 and 5-6 the value of the factor C_s is inversely proportional to the fundamental period, thus, when the fundamental period of the structural system is less than approximate value, the base shear needs to be calculated based on modal analysis. This leads to a clear conclusion that modeling neglecting infill walls will yield a fundamental period higher than what code formula suggests, then value of base shear will be computed based on the approximate period suggested by code's formula. Indeed, existence of infill walls may decrease the fundamental period to values less than approximate, and that means that the computed base shear value is inaccurate and less conservative.

5.8.1 Method One-Pattern One (No Core Walls)

Table 5-68 compares between ASCE formula value of fundamental period and results of equivalent strut for non-cracked models for infill walls with assumption of 12 cm plain concrete with the lowest value of compressive strength of concrete of 12 MPa.

Table 5-68: Ratio between model fundamental period for equivalent strut and approximated period as suggested by ASCE formula- for infill walls of 12 MPa compressive Strength

Structure Height (m)	C_uT_a (C_u=1.4)	Model of Equivalent Strut – T (seconds)	$\frac{\text{Model T}}{\text{CuTa}}$	Conservative: Yes/No
6.24	0.27	0.237	0.88	No
12.48	0.365	0.4	1.10	Yes
18.72	0.616	0.553	0.90	No
24.96	0.763	0.704	0.922	No
31.2	0.91	0.85	0.934	No

Table 5-69 compares between ASCE formula value of fundamental period and results of equivalent strut for non-cracked models for infill walls with assumption of 12 cm plain concrete of 24 MPa compressive strength.

Table 5-69: Ratio between model fundamental period for equivalent strut and approximated period as suggested by ASCE formula- for infill walls of 24 MPa compressive Strength

Structure Height (m)	C_uT_a (C_u=1.4)	Model of Equivalent Strut – T (seconds)	$\frac{\text{Model T}}{\text{CuTa}}$	Conservative: Yes/No
6.24	0.27	0.223	0.83	No
12.48	0.365	0.337	0.923	No
18.72	0.616	0.522	0.85	No
24.96	0.763	0.664	0.87	No
31.2	0.91	0.804	0.884	No

5.8.2 Method One-Pattern Two (Core Shear Walls)

Table 5-70 shows results of pattern two with core shear walls as compared with the lower boundary of ASCE formula.

Table 5-70; ratio between model fundamental period for equivalent strut and approximated period as suggested by ASCE formula- for infill walls of 24 and 12 MPa compressive strength-method one-pattern two

Fc'=24 MPa				
Structure Height (m)	**C_uT_a (C_u=1.4)**	**Model of Equivalent Strut – T (seconds)**	$\frac{\text{Model T}}{\text{CuTa}}$	**Conservative: Yes/No**
6.24	0.27	0.132	0.49	No
12.48	0.365	0.228	0.62	No
18.72	0.616	0.357	0.58	No
24.96	0.763	0.498	0.65	No
31.2	0.91	0.625	0.69	No
Fc'=12 MPa				
6.24	0.27	0.146	0.54	No
12.48	0.365	0.246	0.67	No
18.72	0.616	0.373	0.61	No
24.96	0.763	0.516	0.68	No
31.2	0.91	0.661	0.73	No

5.9 Impact of Infill Walls on the Lateral Stiffness

Impact of infill walls is not limited to base shear value, as the lateral stiffness is another important factor that affect behavior of structures against lateral forces. Existence of infill walls will increase the lateral stiffness of the structural system, and this increase may need attention when infill walls are not distributed uniformly. Moreover, in some cases infill walls are removed from the lowest level for the purpose of providing parking. Figure 5-51 shows three buildings in Ramallah-Palestine where infill walls are removed only in the lowest level.

Figure 5-51: Photo captured in Ramallah-Palestine showing a common type of construction where first level is with no infill walls

In this section the lateral stiffness for models with and without equivalent strut will be compared, and an example of multi-story building will be investigated by assuming no infill walls in the lowest level.

5.9.1 Impact of Equivalent Strut Modeling on the Lateral Stiffness-Method One-Pattern One (No Core Shear Wall)

For 10 story building the output of lateral stiffness for model with and without equivalent strut will be compared to see the effect of infill walls on story stiffnesses. Table 5-71 shows the output of lateral stiffness as provided by ETABS for system with and without equivalent strut for infill walls with compressive strength of 24 MPa.

Table 5-71: Lateral stiffness of bare frames Vs. lateral stiffness of equivalent strut model

Lateral Stiffness of Bare Frames Vs. Lateral Stiffness of Equivalent Strut Model-Infill walls with assumption of 24 MPa Compressive Strength			
Story Elevation (m)	**Bare Frames Model (kN/m)**	**Equivalent Strut Model (kN/m)**	$\frac{\textbf{Equivalent Strut Model}}{\textbf{Bare Farmes Model}}$
3.12	12.4×10^5	64.0×10^5	5.16
6.24	5.28×10^5	38.7×10^5	7.32
9.36	4.0×10^5	36.5×10^5	9.13
12.48	3.53×10^5	34.9×10^5	9.88
15.6	3.31×10^5	33.9×10^5	10.24
18.72	3.18×10^5	33.1×10^5	10.41
21.84	3.08×10^5	32.30×10^5	10.48
24.96	2.92×10^5	30.91×10^5	10.58
28.08	2.54×10^5	28.8×10^5	11.34
31.2	1.64×10^5	20.07×10^5	12.20

Table 5-72 shows the output of lateral stiffness as provided by ETABS for system with and without equivalent strut for infill walls with compressive strength of 12 MPa.

Table 5-72: lateral stiffness of bare frames VS. lateral stiffness of equivalent strut model-infill walls with assumption of 12MPa compressive strength

Lateral Stiffness of Bare Frames Vs. Lateral Stiffness of Equivalent Strut Model-Infill walls with assumption of 12MPa Compressive Strength			
Story Elevation (m)	Bare Frames Model (kN/m)	Equivalent Strut Model (kN/m)	$\frac{\text{Equivalent Strut Model}}{\text{Bare Farmes Model}}$
3.12	$12.4\text{x}10^5$	$54.20\text{x}10^5$	4.37
6.24	$5.28\text{x}10^5$	$31.9\text{x}10^5$	6.04
9.36	$4.0\text{x}10^5$	$29.70\text{x}10^5$	7.43
12.48	$3.53\text{x}10^5$	$28.60\text{x}10^5$	8.10
15.6	$3.31\text{x}10^5$	$27.90\text{x}10^5$	8.42
18.72	$3.18\text{x}10^5$	$27.40\text{x}10^5$	8.70
21.84	$3.08\text{x}10^5$	$26.80\text{x}10^5$	8.70
24.96	$2.92\text{x}10^5$	$25.80\text{x}10^5$	8.84
28.08	$2.54\text{x}10^5$	$23.8\text{x}10^5$	9.37
31.2	$1.64\text{x}10^5$	$17.1\text{x}10^5$	10.43

5.9.2 Impact of Equivalent Strut Modeling on the Lateral Stiffness-Method One-Pattern Two (with Core Shear Wall)

Table 5-73 shows values of lateral stiffness for models of core shear walls with and without equivalent strut for infill walls with infill walls of 24 MPa.

Table 5-73: Lateral stiffness of bare frames Vs. lateral stiffness of equivalent strut model

Lateral Stiffness of Bare Frames Vs. Lateral Stiffness of Equivalent Strut Model-Infill walls with assumption of 24 MPa Compressive Strength			
Story Elevation (m)	**Bare Frames Model (kN/m)**	**Equivalent Strut Model (kN/m)**	$\frac{\textbf{Equivalent Strut Model}}{\textbf{Bare Farmes Model}}$
3.12	$64x10^5$	$133.1x10^5$	2.08
6.24	$31.03x10^5$	$77.42x10^5$	2.50
9.36	$22.4x10^5$	$68x10^5$	3.03
12.48	$17.94x10^5$	$59.7x10^5$	3.32
15.6	$15.03x10^5$	$53.20x10^5$	3.53
18.72	$12.78x10^5$	$47.9x10^5$	3.75
21.84	$10.74x10^5$	$42.50x10^5$	3.96
24.96	$8.65x10^5$	$36.5x10^5$	4.21
28.08	$6.26x10^5$	$29.2x10^5$	4.64
31.2	$3.4x10^5$	$17.35x10^5$	5.10

Table 5-74 shows values of lateral stiffness for models of core shear walls with and without equivalent strut for infill walls with infill walls of 12 MPa.

Table 5-74: Lateral stiffness of bare frames Vs. lateral stiffness of equivalent strut model

Lateral Stiffness of Bare Frames Vs. Lateral Stiffness of Equivalent Strut Model-Infill walls with assumption of 12 MPa Compressive Strength			
Story Elevation (m)	**Bare Frames Model (kN/m)**	**Equivalent Strut Model (kN/m)**	$\frac{\textbf{Equivalent Strut Model}}{\textbf{Bare Farmes Model}}$
3.12	$64x10^5$	$122.9x10^5$	1.92
6.24	$31.03x10^5$	$70.46x10^5$	2.27
9.36	$22.4x10^5$	$60.8x10^5$	2.71
12.48	$17.94x10^5$	$53.1x10^5$	2.96
15.6	$15.03x10^5$	$47.1x10^5$	3.13
18.72	$12.78x10^5$	$42x10^5$	3.29
21.84	$10.74x10^5$	$37.12x10^5$	3.48
24.96	$8.65x10^5$	$31.6x10^5$	3.65
28.08	$6.26x10^5$	$24.99x10^5$	3.99
31.2	$3.4x10^5$	$14.8x10^5$	4.35

Figure 5-52 shows the relation between story height and the ratio of model with strut to model without strut for infill walls with compressive strength of 24 MPa.

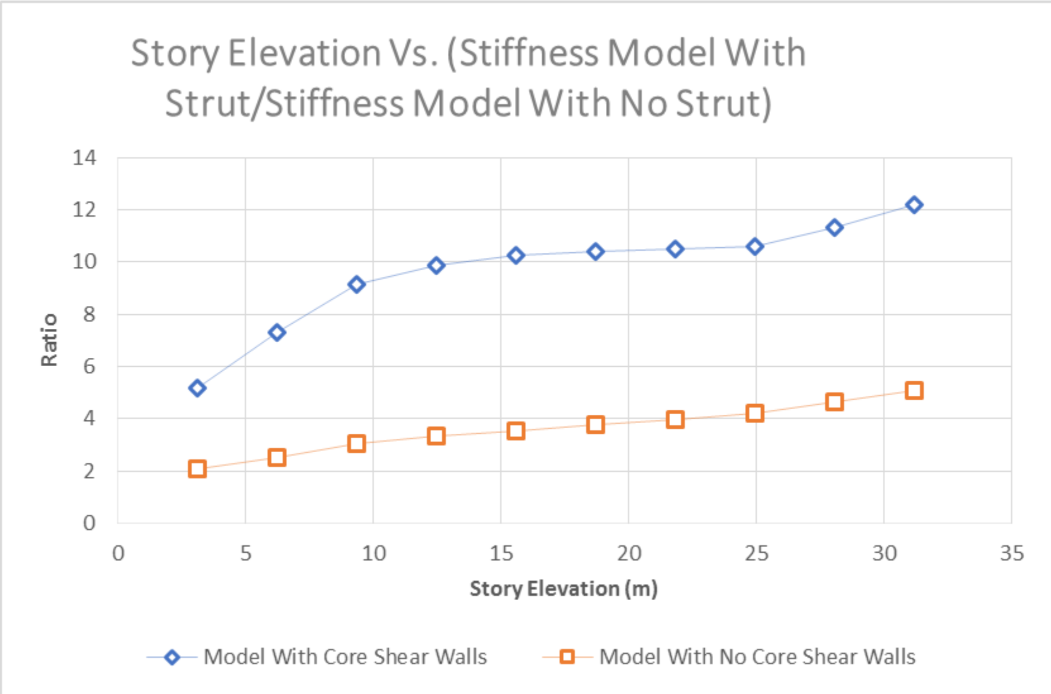

Figure 5-52: Story Elevation Vs. Ratio of: [Stiffness model with strut/Stiffness model with no strut], infill walls with 24 MPa compressive strength

Figure 5-53 shows the relation between story height and the ratio of model with strut to model without strut for infill walls with compressive strength of 12 MPa.

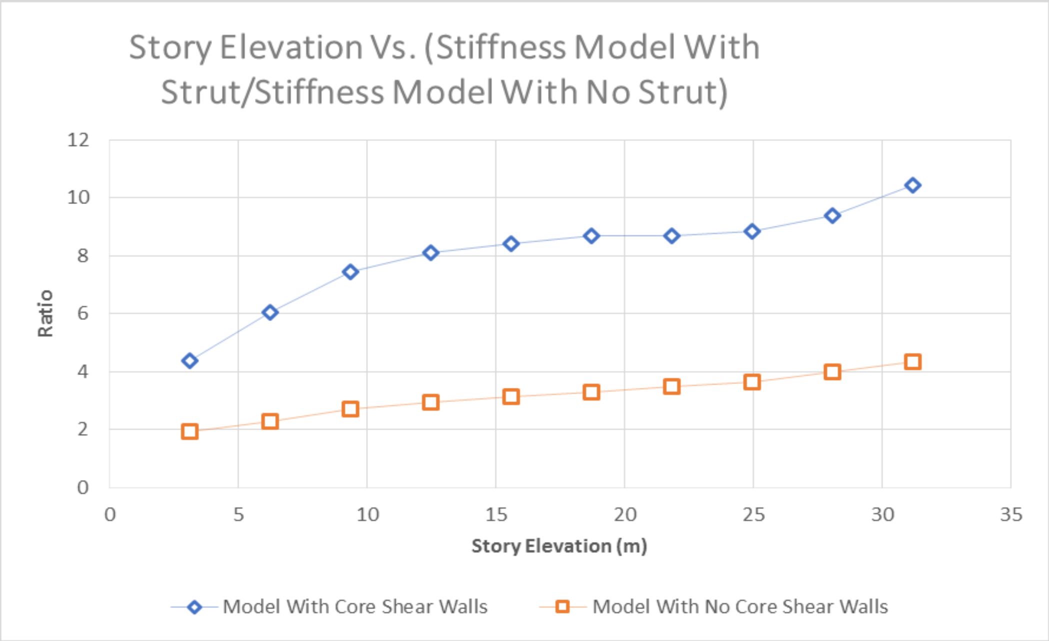

Figure 5-53: Story Elevation Vs. Ratio of: [Stiffness model with strut/Stiffness model with no strut], infill walls with 12 MPa compressive strength

5.9.3 Impact of Equivalent Strut Modeling on the Lateral Stiffness-Method Two-Pattern One (No Core Shear Wall)

Table 5-75 shows values of lateral stiffness for models with no core shear walls with and without equivalent strut for infill walls of bricks of 20 cm thickness.

Table 5-75: Lateral stiffness of bare frames Vs. lateral stiffness of equivalent strut model

Lateral Stiffness of Bare Frames Vs. Lateral Stiffness of Equivalent Strut Model-Infill Brick of 20 cm Thickness			
Story Elevation (m)	**Bare Frames Model (kN/m)**	**Equivalent Strut Model (kN/m)**	$\frac{\textbf{Equivalent Strut Model}}{\textbf{Bare Farmes Model}}$
3.12	12.4×10^5	14.47×10^5	1.17
6.24	5.28×10^5	6.35×10^5	1.20
9.36	4.0×10^5	4.93×10^5	1.23
12.48	3.53×10^5	4.43×10^5	1.25
15.6	3.31×10^5	4.2×10^5	1.27
18.72	3.18×10^5	4.1×10^5	1.29
21.84	3.08×10^5	4.0×10^5	1.30
24.96	2.92×10^5	3.84×10^5	1.32
28.08	2.54×10^5	3.41×10^5	1.34
31.2	1.64×10^5	2.25×10^5	1.37

Figure 5-54 shows the relation between story height and the ratio of model with strut to model without strut for infill walls with 20 cm bricks.

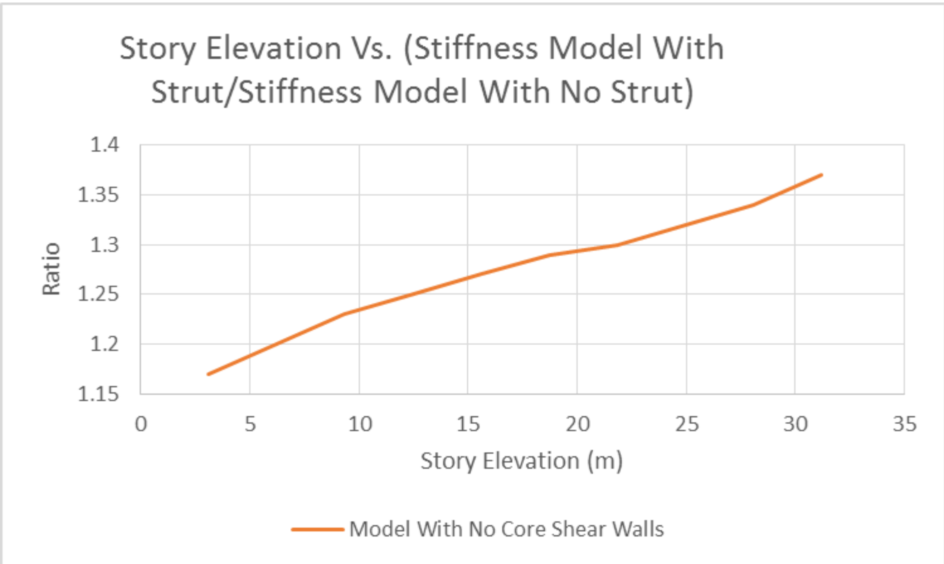

Figure 5-54: Story elevation Vs. ratio of Story Elevation Vs. Ratio of: [Stiffness model with strut/Stiffness model with no strut], infill walls with 20 cm block

5.10 Infill Walls Share of Story Forces (for Strut Model)

As can be concluded from previous results, existence of infill walls will increase the base shear value, and this means that the story forces will increase.

In this section reactions on columns (shear force) from a specific lateral load case will be compared for two type of models; the first type is for bare frames without struts for non-cracked analysis, while the second type is for non-cracked frames with struts. Table 5-76 shows the data models that will be tested.

Table 5-76: Data of model that will be tested to check frame forces after including the infill wall

No. of Stories (5 models)	2,4,6,8, and 10
Frames' compressive strength (fc') (MPa)	24
Infill Walls' compressive strength (fc') (MPa)	12
Type of model	Non-Cracked

Figure 5-55 shows the lateral load case that is defined in ETABS in the x direction (UBC97).

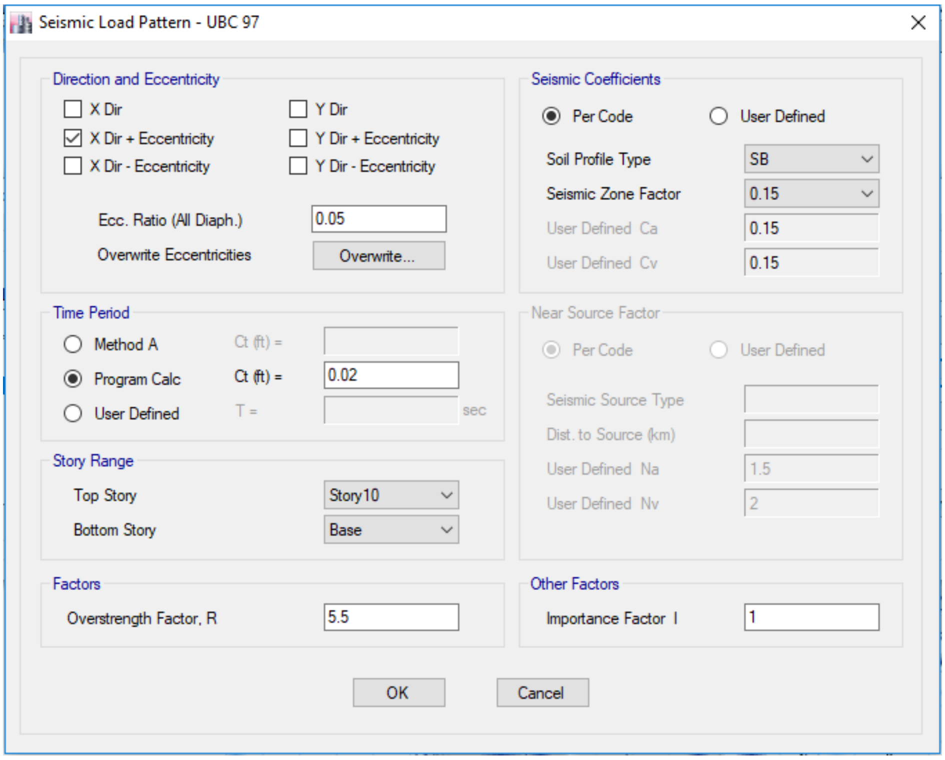

Figure 5-55: Lateral load case-ETABS

Table 5-77 shows the base shear value for the two type of models (each type has 5 models).

Table 5-77: Model one and model two base shear results as provided by ETABS

Model Type One (With Strut)	
No. of Stories	**Base Shear (kN)**
2	1599
4	3175
6	3547
8	3854
10	4132
Model Type Two (Without Strut)	
No. of Stories	**Base Shear (kN)**
2	1017
4	1425
6	2194
8	3012
10	3892

Figure 5-56 shows relation between number of stories (total height of structure) with the base shear value based on assumptions mentioned previously through this section.

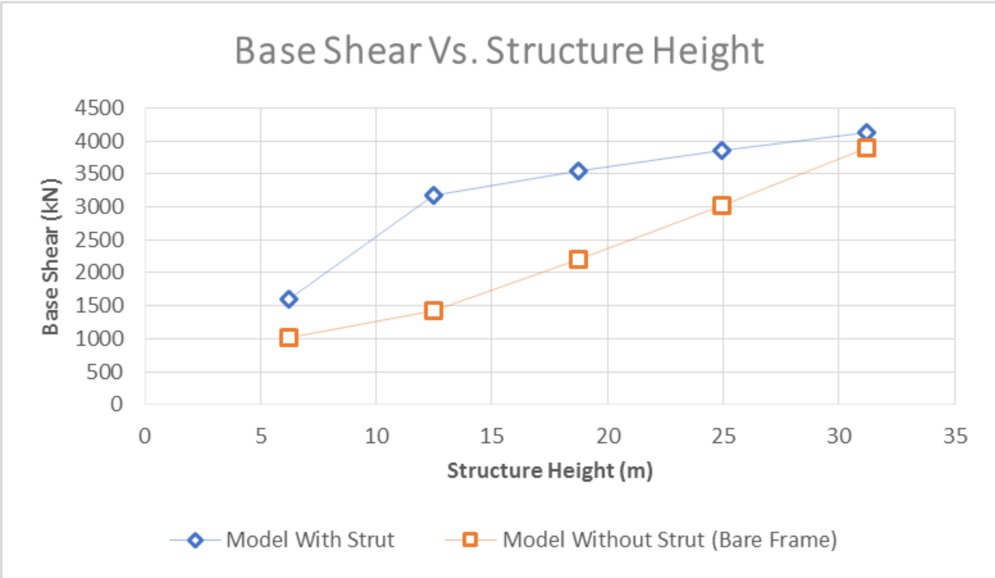

Figure 5-56: Base shear Vs structure height for models with and without strut

Table 5-78 shows columns share of base shear reaction at the lowest level.

Table 5-78: Shear force in columns- Models one and two (with and without strut)

Shear Force in Columns (kN)		
No. of Stories	**Model Type One**	**Model Type Two**
2 Stories	300.3	1017
4 Stories	815.49	1425
6 Stories	1156.8	2194
8 Stories	1507.1	3012
10 Stories	1860.7	3892

Figure 5-57 sows the relation between story height and the shear force in columns due to lateral force for the two types of models.

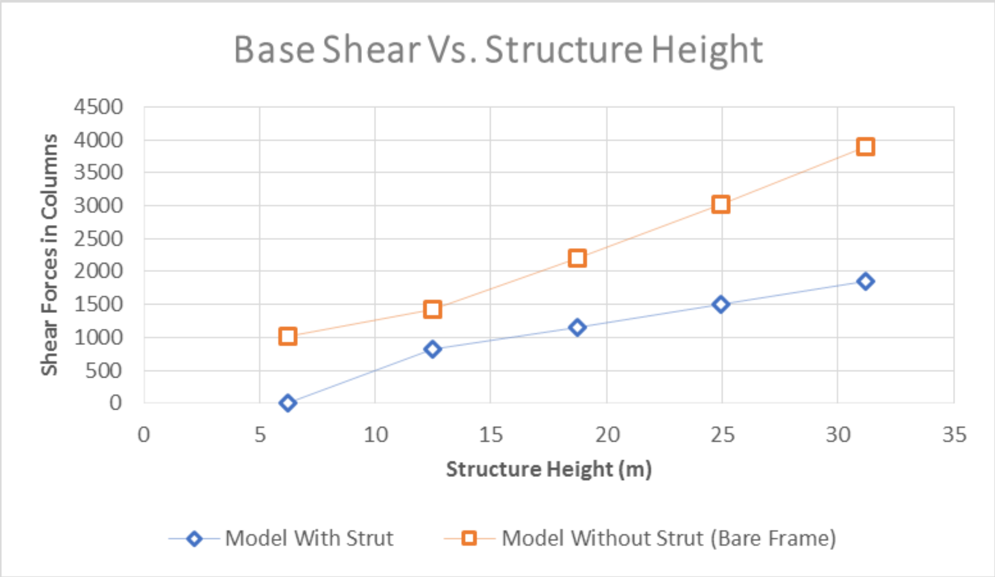

Figure 5-57: Base shear Vs. structure height for models one and two

Although base shear value increases when analyzing models including strut, shear forces in columns decrease considerably, and this may explain why structures with infill walls don’t collapse under earthquakes. Figure 5-58 shows structure with infill walls after earthquake. As can be seen columns managed to survive while infill walls suffered major failure.

Figure 5-58: Collapse of infill walls after occurrence of an earthquake, (Furtado et. al, 2019)

Chapter Six
Conclusions and Recommendations

6.1 Introduction

This study shows that analysis of infill walls is not a straight forward procedure; as there is many complications and assumptions that may change our understand to the contribution of infill walls in the lateral stiffness.

It is agreed in research that infill wall has a significant role in earthquakes, and accurate analysis require including infill walls in modeling.

6.2 Study Assumptions

Level of complexity of infill walls topic makes analysis procedure challengeable. In this thesis many assumptions are used to simplify the problem, therefore, the complicated cross section of infill wall is reduced to only a one layer.

In future studies it is recommended to check how much used assumptions can be logical. Decreasing assumptions will increase reliability.

6.3 Calculations of Equivalent Strut

Calculations of equivalent strut using variable methods show a wide range of variability. Therefore, it can be concluded that any used method will not be much reliable unless supported with experimental results (or post-earthquakes observations).

In this thesis the NBCC formula is adopted based on experimental results obtained in a research performed in Saudi Arabia.

The wide range of variation in computed strut width emphasizes the need of more deep research in such a topic, especially for infill panel cross section with similar properties and method of construction as applied in Palestine.

For the sake of conservative force-based design, the recommendation would be to use the NBCC code formula instead of ASCE formula; as the Canadian formula suggests higher values of strut width, which increase the computed base shear.

Another important point in analysis is to model the structure as non-cracked for the same reason of increasing computed value of base shear.

6.4 Results Summary

Study results are restricted to structural geometry and assumptions. Following sections introduce different systems.

6.4.1 Frame System with and without Core Shear Wall

Frame system in this thesis is a system where slabs are directly supported on columns, with no existence of any reinforced walls at specific pattern (pattern one), and with core shear walls for the other pattern (pattern two).

Through this thesis two types of plans are studied (pattern one and two, see section 5.4 for details).

6.4.1.1 Results for Pattern One

Results of pattern one as will be shown in this section is applicable for both method one and method two, as each of the two methods consists of non-reinforced infill walls, and neglecting infill walls in both two methods will give exactly the same model.

Table 6-1 shows summary of all results related to bare frame systems including the estimated value as computed by ASCE formula.

Table 6-1: Bare frame analysis results for both cracked and non-cracked sections, with different columns compressive strength (24,28, and 32 MPa)

Structure Height (m)	**Non-Cracked**			**Cracked**			**Avg. Value / ASCE Formula**
	fc'=24 MPa	fc'=28 MPa	fc'=32 Mpa	fc'=24 MPa	fc'=28 MPa	fc'=32 Mpa	
6.24	0.616	0.59	0.57	0.934	0.889	0.86	0.375
12.48	1.037	0.994	0.96	1.698	1.63	1.575	0.699
18.6	1.46	1.41	1.36	2.45	2.36	2.28	0.992
24.96	1.89	1.82	1.76	3.2	3.1	2.98	1.302
31.2	2.324	2.24	2.17	3.94	3.79	3.67	1.597

Results provided in table 6-1 is plotted in figure 6-1.

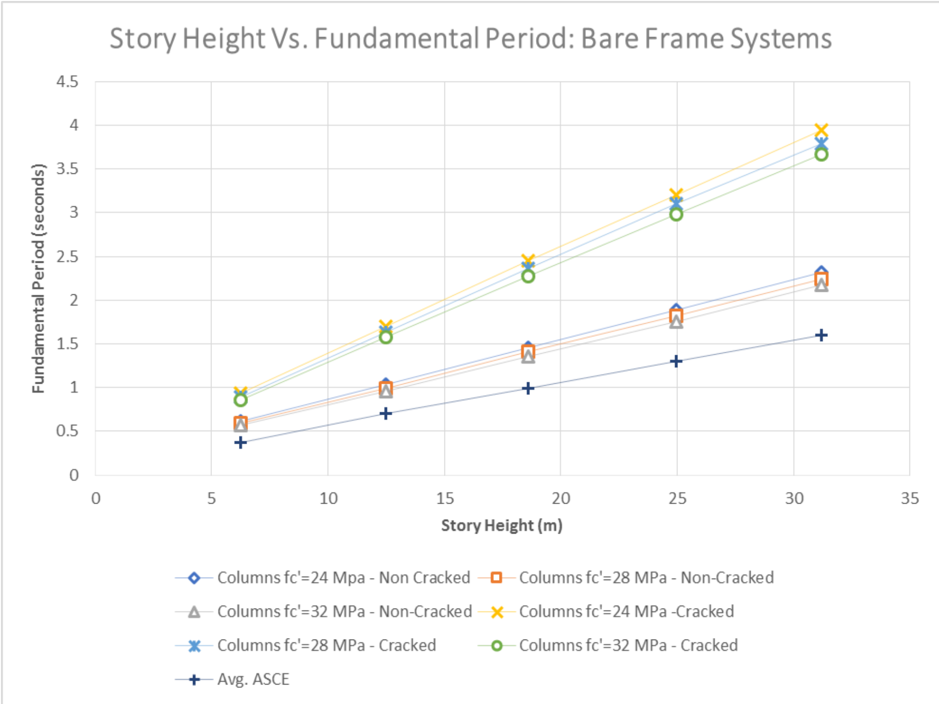

Figure 6-1: plot of tabulated results (table 6-1): Story height Vs. Fundamental period, for: cracked and cracked analysis with variable columns compressive strength, and the average value of ASCE estimation

As can be seen in figure 6-1 ASCE formula always underestimates the value of fundamental period which is considered conservative.

Also figure shows that changing columns' compressive strength by almost 33% does not make a dramatic change in results.

6.4.1.2 Results of Pattern Two

In pattern two analysis is reduced to only cracked and non-cracked section with uniform compressive strength of 24 MPa for both columns and core walls. Table 6-2 shows comparison between what ASCE formula suggests and what analysis provides (when neglecting modeling of infill walls).

Table 6-2: Summary of results- fundamental period- pattern two (slab on columns with core shear wall)-no consideration for infill walls

Fundamental Period (seconds) – Pattern Two			
Structure Height (m)	**Avg. ASCE**	**Non-Cracked**	**Cracked**
6.24	0.3	0.3	0.48
12.48	0.5	0.54	0.86
18.6	0.68	0.77	1.24
24.96	0.85	0.99	1.62
31.2	1	1.23	2

As can be noted from table 6-2 average value of ASCE is conservative.

6.4.1.3 Conclusion

Analysis neglecting modeling of infill walls shows that ASCE formula for estimating approximate fundamental period is conservative; as code's formula always underestimate the value of fundamental period.

6.4.2 Models with Equivalent Strut: Frame System Modeling with and without Core Shear Walls

6.4.2.1 Results of Pattern One

Table 6-3 shows results of pattern one for both methods one and two for a specific case of 12 cm plain concrete layer of 12 MPa compressive strength. Moreover, an average value of ASCE formula and the lower boundary is provided.

Table 6-3: Fundamental period, method one and two, pattern one (no core shear walls)

Fundamental Period (seconds)					
Structure Height (m)	**fc'=12 MPa**	**Infill Wall=20 cm Bricks**	**Avg. ASCE**	**Lower Boundary (ASCE)**	**ASCE Formula without Cu factor**
6.24	0.248	0.537	0.3	0.27	0.19
12.48	0.416	0.92	0.5	0.45	0.32
18.6	0.576	1.3	0.68	0.61	0.44
24.96	0.731	1.691	0.85	0.77	0.55
31.2	0.883	2.087	1	0.90	0.64

Figure 6-2 shows plot of tabulated results (table 6-3).

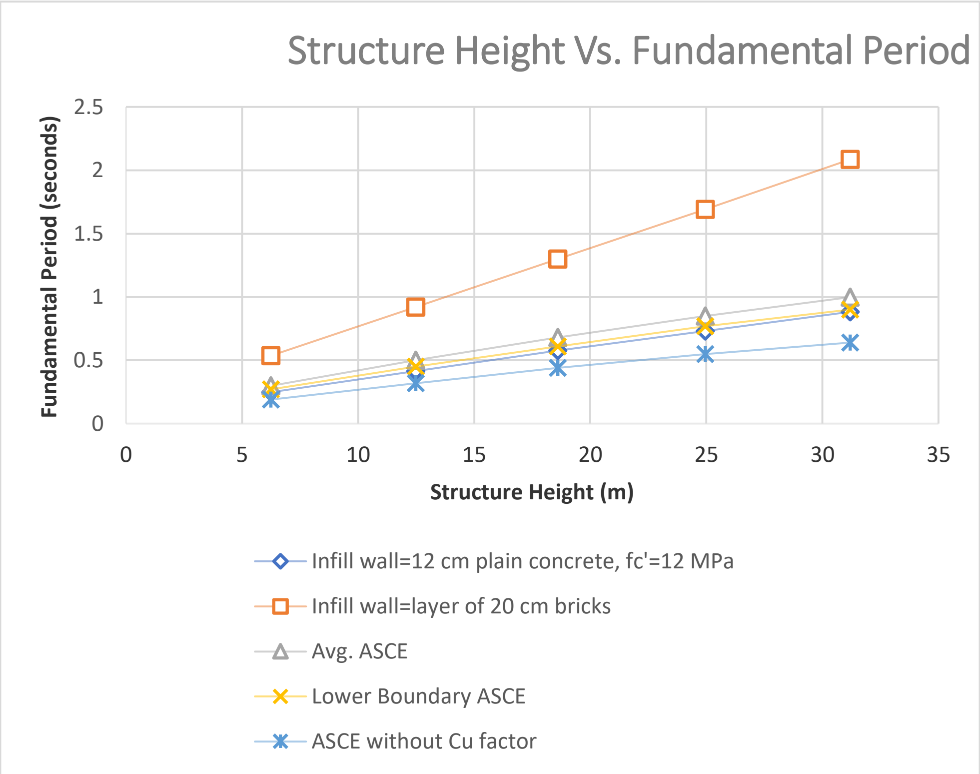

Figure 6-2: Method one and two, structure height Vs. fundamental period for method one (12 cm infill will with fc'= 12 MPa), and method two (layer of 20 cm brick)

As can be seen in figure 6-2 impact of infill walls of plain concrete is much higher than layer of 20 cm brick; and this can be justified by the low value of bricks' modulus of elasticity.

Figure 6-2 shows that lower boundary of ASCE formula (with Cu=1.4) is somehow not conservative while the formula without magnification is conservative.

6.4.3 Analysis Results of Pattern Two

6.4.3.1 Method One

Pattern two is considered more practical pattern if compared to pattern one. In this pattern a core shear is constructed besides columns.

Table 6-4 shows comparison between ASCE estimated values and the equivalent strut for specific case of 12 cm infill wall with 12 MPa compressive concrete.

Table 6-4: Fundamental period output for pattern two, method one, infill walls of 12 cm thickness and 12 MPa compressive strength, and columns of 24 MPa

Height of structure (m)	ASCE formula Value – without multiplying by the factor Cu	ASCE formula - Lower boundary (Cu=1.4)	ASCE formula - Upper Boundary (Cu=1.7)	Equivalent Strut Model
6.24	0.193	0.27	0.328	0.146
12.48	0.261	0.365	0.444	0.246
18.6	0.44	0.616	0.748	0.373
24.96	0.545	0.763	0.927	0.516
31.2	0.644	0.91	1.09	0.661

Figure 6-3 shows the relation between structure height and the fundamental period.

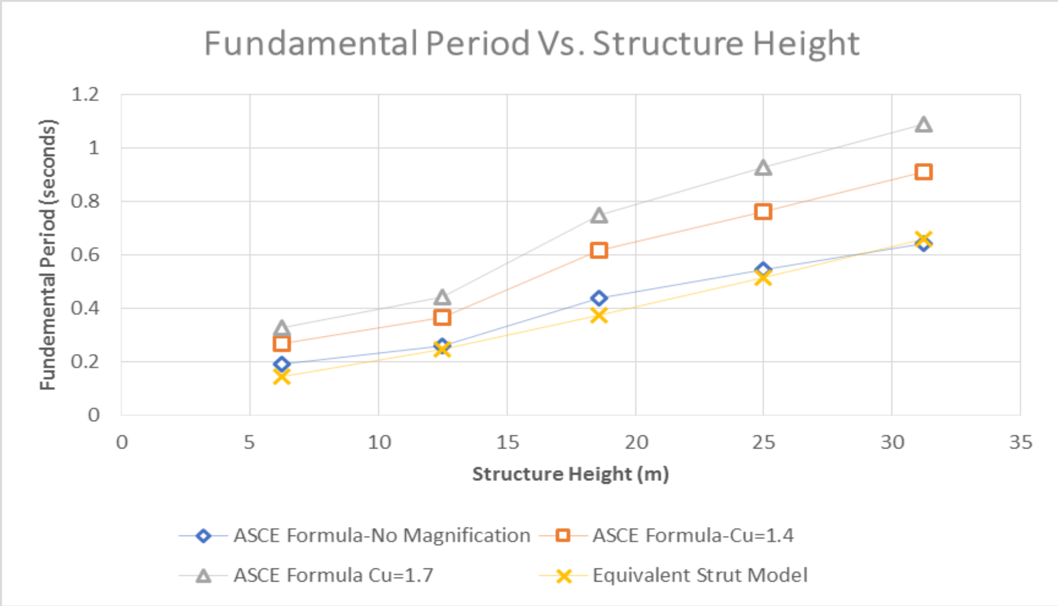

Figure 6-3: Fundamental period Vs. structure height, method one, pattern two, columns of compressive strength 24 MPa and infill walls of 12 cm thickness and 12 MPa compressive strength

6.4.3.2 Method Two

For pattern two it is found that modeling bricks has no much impact on the fundamental period. Figure 6-4 support this claim.

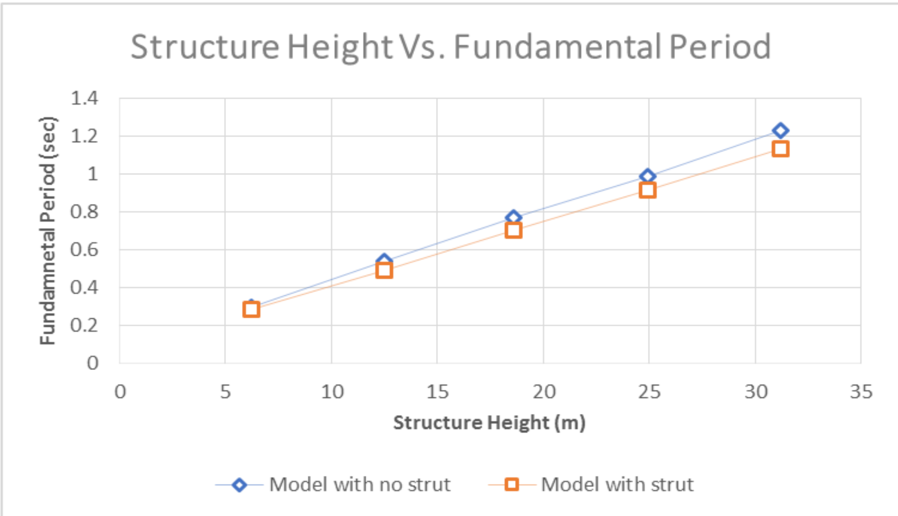

Figure 6-4: Structure height Vs. fundamental period, method two, pattern two

6.5 Impact of Infill Material on the Role of Infill Wall

In this study modulus of elasticity for plain concrete is easily determined based on assumption of having variable concrete compressive strength. On the other hand, value of modulus of elasticity for brick is used based on experimental study performed in An-Najah university laboratories.

Study shows that for plain concrete infill walls the contribution of such walls is considerable and need to be taken on consideration, as results of model with strut shows considerable change in the fundamental period value.

On the other hand, infill walls composed of brick layer instead of concrete showed a change within almost 11.0% which makes ignoring of such walls in analysis possible. This point of view is much supported for structures that consists of both frames and shear walls system.

Moreover, study shows that impact of plain concrete infill walls on lateral stiffness is considerable, and stiffness of plain concrete infill walls need to be investigated against irregularities limitations when needed.

For the case of brick results show that impact of brick infill panel does not change the stiffness in a considerable way. However, it is recommended to evaluate structures behavior using equivalent strut with brick structural properties.

Figure 6-1 shows how equivalent strut changes the behavior of structure based on the fundamental period. Results are specifically for system of bare frame with columns of 24 MPa compressive strength, and infill walls with 12 cm thickness with 12 MPa compressive strength.

6.6 Analysis of Systems with Infill Walls

Analysis with involvement of infill walls is suspected to change dramatically. For any structural system with infill panel of plain concrete with openings, it is highly recommended to evaluate the structures using 3D model with existence of equivalent strut for base shear computational procedures. It is also recommended to use formulas of NBCC code in the computational procedure.

6.7 Selection of Infill Wall Cross Section

As shown in this research method of construction and components of infill wall effectively changes the behavior of structures. It can be concluded that the best system that is expected to perform in a good manner through earthquakes is the system with infill reinforced walls with walls distributed uniformly in both vertical and horizontal layouts.

Using infill panels with reinforcement will increase reliability and will enhance accuracy of behavior estimation.

For section built using plain concrete layer it is recommended to pay attention to the quality of poured concrete, and it is recommended to increase the thickness of infill wall to increase it is contribution in the stability of structures against lateral loads.

For cases of non-uniformity of infill walls distribution that may affect structural irregularities it is recommended to use brick walls instead of plain concrete to minimize infill walls contribution in the lateral stiffness, which may be beneficial in avoiding failures such as soft story for structures as shown in figure 5-51.

6.8 Future Studies

Although literature reviews show a lot of references regarding the topic of modeling of infill walls, there still a need for more investigations especially for the methods of construction applied in Palestine.

Future studies may focus on impact of infill walls on structural irregularities, and the impact of non-uniform distribution of infill walls on suspected failure modes for structures.

Experimental studies will be beneficial in predicating behavior of such walls, where experiments may answer the question of the role of components of the cross section that exist out of the frame; as in this study elements out of the frame are neglected.

References

1. Abdelkareem, K H, F K Abdel Sayed, M H Ahmed, and N Al-Mekhlafy. 2013. “***Equivalent Strut Width For Modeling R.C. Infilled Frames.”*** **Journal of Engineering Sciences, Assiut University, Faculty of Engineering** 41(3).

2. Furtado, André, and Nelson Vila-Pouca, Humberto Varum and António Arêde.2019. "S**tudy of the Seismic Response on the Infill Masonry Walls of a 15-Storey Reinforced Concrete Structure in Nepal"**. mdpi journal, volume 9,

3. ACI Committee 318. 2014. Aci 318-14 Building Code Requirements for Structural Concrete (ACI 318-14) and Commentary (ACI 318R-14).

4. Al-Chaar, Ghassan, Gregory E. Lamb, and Daniel P. Abrams. 2003. **“Effect of Openings on Structural Performance of Unreinforced Masonry Infilled Frames.”** Special Publication - Council for Agricultural Science and Technology 211: 247–62.

5. Al-Dabbeek, Jalal, and Radwan El-kilani. 2008. “***Rapid Assessment of Seismic Vulnerability in Palestinian Refugee Camps.”*** **Journal of Applied Sciences** 8: 1371–82.

6. Albayrak, Uğur, Eşref Ünlüoğl, and Mizam Doğan. 2017. “***An Overview of the Modelling of Infill Walls in Framed Structures.”*** **International Journal of Structural and Civil Engineering Research** 6(1).

7. Alguhane, Tarek M, Ayman H Khalil, M N Fayed, and Ayman M Ismail. 2015a. "***Modeling of Masonry In-Filled R / C Frame to Evaluate Seismic Performance of Existing Building."*** **International Journal of Civil, Environmental, Structural, Construction and Architectural Engineering** 9(10).

8. Alguhane, Tarek M, Ayman H Khalil, M N Fayed, and Ayman M Ismail. 2015b. "**Seismic Assessment of Old Existing RC Buildings on Madinah with Masonry Infilled Using Ambient Vibration Measurements."** 9(1): 43–51.

9. Amato, G, L Cavaleri, M Fossetti, and M. Papia. 2008. **"Infilled Frames: Influence of Vertical Loads on the Equivalent Diagonal Strut Model."** Proc. of 14th WCEE.

10. American Society of Civil Engineers. 2010. "**Minimum Design Loads for Buildings and Other Structures, ASCE Standard,."** *ASCE standard*.

11. Asteris, Panagiotis G et al. 2016. "***Prediction of the Fundamental Period of Infilled RC Frame Structures Using Artificial Neural Networks."*** **Computational Intelligence and Neuroscience** 2016. https://www.researchgate.net/publication/283121511_Prediction_of_the_Fundamental_Period_of_Infilled_RC_Frame_Structures_Using_Artificial_Neural_Networks.

12. Bertero, Vitelmo, and Steven Brokken. 1983. “***Infills in Seismic Resistant Building.”*** **Journal of Structural Engineering** 109(6).

13. Chopra, Anil K. 1995. **Dynamics of Structures Dynamics of Structures - Theory and Applications to Earthquake Engineering.** Prentice Hall.

14. Chopra, Anil K., and Rakesh K. Goel. 2000. “**Building Period Formulas for Estimating Seismic Displacements.”** Earthquake Spectra.

15. Computer & Structures Inc. 2016. **“ETABS 2016 User’s Guide.”** https://www.csiamerica.com/products/etabs.

16. Devi, Renuka M. V., and Syed Farooquddin. 2012. “**Effect of Modulus of Masonry on the Lateral Stiffness of Infilled Frame with Openings.”** National Conference on Thrust Areas in Engineering (NCTAE-2012).

17. Dongre, Archana, and Pradeep Kumar Ramancharla. 2017. *“**Effect of Openings and Aspect Ratio on Overall Performance of Rc Framed Brick Infilled Building.”*** **Proceedings of the 16th World Conference on Earthquake.**

18. Durrani, A. J., and Y. H. Luo. 1994. “***Seismic Retrofit of Flat-Slab Buildings with Masonry Infills.”*** **In Technical Report. National Center for Earthquake Engineering Research:** 1–8.

19. Eleftheriadou, a K, a I Karabinis, and a D Baltzopoulou. 2011. **"Fundamental Period versus Seismic Damage for Reinforced Concrete Buildings It Is Important to Clarify That the Structural Types of RC Buildings in Southern Europe Differ."** Proceedings of the 15th WCEE.

20. FEMA. 2000. "**Prestandard and Commentary for the Seismic Rehabilitation of Buildings."** Rehabilitation Requirements.

21. Maidiawati. 2013. **"Modeling of Brick Masonry Infill for Seismic Performance Evaluation of RC Frame Buildings."** Toyohashi University of Technology.

22. Mainstone, R. J. 1971. "***On the Stiffness and Strengths of Infilled Frames."*** **Proceedings Institution of Civil Engineers** Supplement: 57–90.

23. Mallick, D. V.\, and R. P Garg. 1971. "***Effect of Openings on the Lateral Stiffness of Infilled Frames."*** **Proceedings of the Institution of Civil Engineers** 49(2): 193–209.

24. Mondal, Goutam, and S K Jain. 2006. "***Lateral Stiffness of Unreinforced Brick Infilled RC Frames with Central Openings."*** **8th US National Conference on Earthquake Engineering 2006 7**: 4163–71.

25. Mondal, Goutam, and Sudhir K. Jain. 2008. "L**ateral Stiffness of Masonry Infilled Reinforced Concrete (RC) Frames with Central Opening."** Earthquake Spectra 24(3): 701–23.

26. Murthy, C. V. R., Goswami; Rupen, A. R. Vijayanarayanan, and Vipul V. Mehta. 2012. "***Some Concepts in Earthquake Behavior of Buildings."*** **IITK-GSDMA Project on Review of Seismic Codes, & Preparation of Commentary and Handbooks.**

27. Paulay, T., and M. N. Priestley. 1992. **Seismic Design of Reinforced Concrete and Masonry Buildings.** New York: John Wiley & Sons.

28. Popescu, Cosmin, Gabriel Sas, Thomas Blanksvärd, and Björn Täljsten. 2015. **"Concrete Walls Weakened by Openings as Compression Members: A Review."** Engineering Structures: 172–90.

29. Qarout, Ola. 2018. "**The Effect of Various Patterns of Internal Partitions on the Fundamental Period of Reinforced Concrete Framed Buildings - Experimental and FE Modelling Study."** An-Najah National University.

30. Sindagi, Bhagyalaxmi, Anusha P. Gowda, Harshitha R. Kumar, and M. V. Renukadevi. 2015. "***Effect of Modulus of Masonry on Initial Lateral Stiffness of Infilled Frames With Openings."*** **International Journal of Research in Engineering and Technology** 03(18): 218–24.

31. Swarnkar, Shriyanshu, and Debarati Datta. 2015. "**Analysis of Building with Infill Walls.**" 2(9): 71–76. http:// www. krishisanskriti. org/ jceet. html.

APPINDEX A

A Appendix A: Verifications

A.1 Introduction

In this part of thesis verifications for the following points will be performed in order to justify adaptation of analysis results from ETABS software.

1- Lateral stiffness calculations for 2D frames.
2- Lateral stiffness calculations for multi-story buildings.

A.2 Verification of Lateral Stiffness for 2D Frames

A.2.1 Approximating Lateral Stiffness of Single Bay Single Story 2D Frame

Computation of lateral stiffness of frame structures depend on many parameters such as column and beam stiffness, relative stiffness between column and beam, and the boundary conditions of the base support.

Equation A-1 can be used in computing the lateral stiffness of single bay single story 2D frame structure. It is worth mentioning that formula assumes having both axially and flexurally rigid beams:

$$K = 2 \times \frac{(B)EI_c}{h^3},\ where \begin{cases} B = 3, for\ pin\ support \\ B = 12, for\ fix\ support \end{cases} \qquad \text{[Equation A-1]}$$

Where,

K: Lateral stiffness of the frame

E: Modulus of elasticity of column's material

I_c Moment of inertia of the column in plane direction

h: Column's height to the center of the beam

Due to the fact of rarely have the two assumptions of having both axially and flexurally rigid beam satisfied, Chopra in his book of "Dynamics of Structures, Theory and Applications to Earthquake Engineering" suggests the following formula to encounter the relative stiffness between columns and beam (Chopra 1995).

$$K = \frac{24EI_c}{h^3}\frac{(12\rho+1)}{(12\rho+4)} \qquad \text{[Equation A-2]}$$

Where

$$\rho = (\frac{EI_b}{L}) \div (\frac{2EI_c}{h})$$

In 1959 Benjamin suggests a formula to compute the lateral stiffness of frames to include the relative flexural stiffness between beams and columns. The formula is evaluated and found to be applicable only for uniform frames with girders that flexurally stiffer than columns. (Arturo E. Schultz).

The formula is expressed as:

$$K_s = \frac{\left(\frac{48n^2}{h^2}\right)}{[\Sigma\left(\frac{1}{K_{ec}}\right)+\Sigma\left(\frac{1}{K_{ic}}\right)+\Sigma\left(\frac{1}{K_{ga}}\right)+\Sigma(\frac{1}{K_{gb}})]} \qquad \text{[Equation A-3]}$$

$K_s = Apparent\ stiffness\ of\ the\ story$

$n = number\ of\ panels$

$k_{ec} = external\ column\ lateral\ stiffness = \frac{EI_c}{h}$

$k_{ic} = Internal\ column\ lateral\ stiffness = \frac{EI_c}{h}$

$k_{ga} = girder\ above\ lateral\ stiffness = \frac{EI_b}{h}$

$k_{gb} = girder\ bottom\ lateral\ stiffness = \frac{EI_b}{h}$

A.2.2 Manual Computation of Lateral Stiffness of Single Bay Single Story Frame

A sample for a 2D single bay single story will be solved three times using each of previously mentioned three equations. Table A-1 illustrates the properties and the dimensions of the frame shown in figure A-1.

Table A-1:Geometric properties of 2D verification frame

Geometric Properties of 2D Verification Frame	
Column's Section (cm)	C50x50
Beam's Section (cm)	B50x50
Column's Height (h)(cm)	312
Beam's Length (L) (cm)	450
E_c (GPa)	23
I_{column} (m^4)	5.2×10^{-3}
I_{beam} (m^4)	5.2×10^{-3}
$E_c\ I_{column}$ ($kN.m^2$)	1.2×10^{5}
$E_c\ I_{beam}$ ($kN.m^2$)	1.2×10^{5}

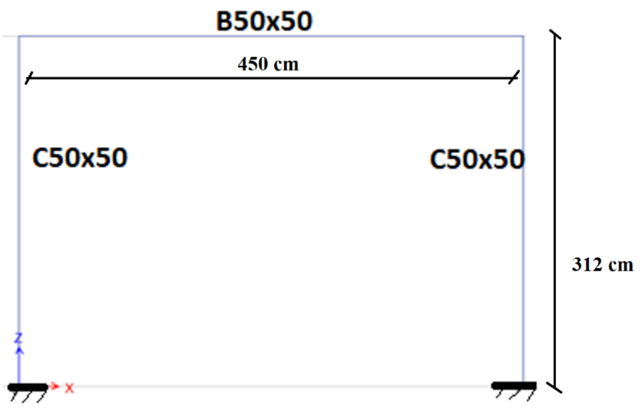

Figure A-1: 2D verification Frame

"K" symbol is for lateral stiffness value of frames. K1, K2, and K3 will be computed respectively using the three equations.

$$K1 = 2 \times \frac{(B)EI_c}{h^3} 2 \times \frac{12(1.2 \times 10^5)}{3.12^3} = 95 \times 10^3 \frac{kN}{m} \qquad (Equation\ A-1)$$

$$K2 = \frac{24EI_c}{h^3} \frac{(12\rho + 1)}{(12\rho + 4)} \ ; \rho = \left(\frac{EI_b}{L}\right) \div \left(\frac{2EI_c}{h}\right) (Equation\ A-2)$$

$$\rho = \left(\frac{EI_b}{L}\right) \div \left(\frac{2EI_c}{h}\right); E\ is\ equal\ for\ columns\ and\ beams, I_c = I_b$$

$$\rho = \frac{h}{2L} = \frac{3.12}{2 \times 4.5} = 0.3467$$

$$K2 = \frac{24 \times 23025000 \times 0.005208}{3.12^3} \frac{(12 \times 0.3467 + 1)}{(12 \times 0.3467 + 4)} = 60 \times 10^3 \frac{kN}{m}$$

Table A-2 shows the data needed for apparent stiffness calculations using Benjamin formula (Equation A-3) for the 2D frame:

Table A-2: Parameters for Benjamin Formula (Equation A-3)

Parameters for Benjamin Formula (Equation A-3)	
$E_c\ I_{column}$ (kN.m^2)	$1.2\text{x}10^5$
$E_c\ I_{beam}$ (kN.m^2)	$1.2\text{x}10^5$
n	1
Interior columns	Does not exist
Girder below	Does not exist
K_{ec}	$\frac{EI_c}{h} = \frac{1.2 \times 10^5}{3.12} = 38436.5$
K_{ga}	$\frac{EI_b}{L} = \frac{1.2 \times 10^5}{4.5} = 26649.3$

$$K3 = \frac{\left(\frac{48(1)^2}{(3.12)^2}\right)}{2\left(\frac{1}{38436.5}\right) + \left(\frac{1}{26649.3}\right)} = 55 \times 10^3\ kN/m$$

Table A-3 compares between the three formula (equations A-1, A-2, and A-3) regarding the analyzed frame.

Table A-3: Equations 1,2, and 3 lateral stiffness results-2D verification frame

	Equation A-1	**Equation A-2**	**Equation A-3**
Lateral Stiffness (kN/m)	$95\text{x}10^3$	$60\text{x}10^3$	$55\text{x}10^3$

Results provided in Table A-3 shows that Equation A-1 output is with inacceptable difference. This inacceptable range of difference prove that the use of 1st equation must be avoided, unless conditions of having flexurally and axially rigid beams are satisfied. It is clear that Equation A-1 is a special case of Equation A-2, and this case happens once the following condition is satisfied:

$$\frac{(12\rho + 1)}{(12\rho + 4)} \approx 1$$

To support this conclusion, the frame will be modified by only increasing beam's depth to four times it is original depth. Table A-4 summarize the properties of the new frame.

Table A-4: Geometric properties of modified 2D verification frame (with flexurally rigid beam)

Geometric Properties of Modified 2D Verification Frame (with Flexurally Rigid Beam)	
Column's Section (cm)	C50x50
Beam's Section (cm)	B50x200
Column's Height (h)(cm)	312 cm
Beam's Length (L) (cm)	450 cm
E_c (GPa)	23 GPa
I_{column} (m^4)	$5.2x10^{-3}$ m^4
I_{beam} (m^4)	$333.3x10^{-3}$ m^4
E_c I_{column} (kN.m^2)	$1.2x10^5$ kN.m^2
E_c I_{beam} (kN.m^2)	$76.7x10^5$ kN.m^2

Equation A-1 computation procedure will be the same as the formula doesn't include any parameter that consider any contribution of beam's stiffness. On the other hand, Equation A-2 will yield another value as the relative stiffness between beam and column is included. Following are the detailed calculations of K value using Equation A-2:

$$\rho = \left(\frac{EI_b}{L}\right) \div \left(\frac{2EI_c}{h}\right) = \left(\frac{7674232.5}{4.5}\right) \div \left(2 \times \frac{1.2\text{x}10^5}{3.12}\right) = 22.18$$

$$\frac{(12\rho + 1)}{(12\rho + 4)} = \frac{(12 \times 22.18 + 1)}{(12 \times 22.18 + 4)} = 0.99$$

$$K = \frac{24EI_c}{h^3}\frac{(12\rho + 1)}{(12\rho + 4)} = 94764.54 \times 0.99 = 94 \times 10^3\ kN/m$$

Equation A-3 includes the relative stiffness between column and beam. Therefore, computation procedure is repeated as will be shown in this section. In Table A-5 parameters needed for Benjamin formula (Equation 3) are provided.

Table A-5: Parameters for Benjamin Formula (Equation A-3)- Modified 2D Verification Frame (with Flexurally Rigid Beam)

Parameters for Benjamin Formula (Equation A-3)- Modified 2D Verification Frame (with Flexurally Rigid Beam)	
$E_c\ I_{column}$ (kN.m^2)	$1.2x10^5$
$E_c\ I_{beam}$ (kN.m^2)	7.7×10^6
n	1
Interior columns	Does not exist
Girder below	Does not exist
$\mathbf{K_{ec}}$	$\frac{EI_c}{h} = \frac{1.2x105}{3.12} = 38436.5$
$\mathbf{K_{ga}}$	$\frac{EI_b}{L} = \frac{7.7 \times 10^6}{4.5} = 1705385$

$$K3 = \frac{\left(\frac{48(1)^2}{(3.12)^2}\right)}{2\left(\frac{1}{38436.5}\right) + \left(\frac{1}{1705385}\right)} = 93.8 \times 10^3\ kN/m$$

Table A-6 compares between the three equations regarding the analyzed frame after modifying beam by increasing it is depth four times the original case.

Table A-6: Equations A-1, A-2, and A-3 lateral stiffness results

	Formula 1	**Formula 2**	**Formula 3**
Lateral Stiffness (kN/m)	$95x10^3$	$94x10^3$	$93.8x10^3$

It can be concluded that Equation A-1 is only limited to a special case of having considerably stiffer flexurally beam than supporting column. Both Equations A-2 and A-3 results are found to be close to each other within an acceptable range of less than 10% difference. However, both equations also assume special conditions; and this may limit their accuracy. Equations A-1 and A-2 accuracy will be examined later on through this chapter.

A.2.3 Software Computation of Single Bay Single Story 2D Frame Lateral Stiffness

In previous section manual calculations were performed on a single bay single story 2D frame twice; once with equal dimensions of both beam and column and later on using stiffer beam with the same columns' dimensions.

In this section many 2D frames modeled through ETABS will be analyzed in order to build reliability with software's results.

A.2.4 Modeling of 2D Frames with No assumptions

2D frame in this section will be modeled without any change for any modifier in the software. Figure A-2 shows the 2D frame model.

Figure A-2: 2D frame model built using ETABS 16.2.1 (no modifications)

Tabulated results as provided by ETABS (figure A-3) shows a lateral stiffness of a value 56.4x10^3kN/m.

	Story	Stiffness X kN/m
	Story1	56414.174

Figure A-3: Lateral stiffness value as provided by Etabs model

Table A-7 shows comparison between manual calculations and ETABS results.

Table A-7:K1, K2, K3, ETABS values for the 2D original frame

	Description	**Value**
K1	Value as calculated by Equation A-1	$95 \times 10^3 \frac{kN}{m}$
K2	Value as calculated by Equation A-2	$60 \times 10^3 \frac{kN}{m}$
K3	Value as calculated by equation A-3	$55 \times 10^3 \frac{kN}{m}$
K_{ETABS}	Value as calculated by ETABS	$56.4 \times 10^3 \frac{kN}{m}$

Result of ETABS model is close if compared to both Equations A-2 and A-3, while equation's A-1 value is far if compared to both values.

A.2.5 Modeling of 2D Frames with Assumptions

It is clear that Equation A-1 is a special case of what Chopra suggest in his formula. In this section ETABS model will be modified using assumptions to satisfy assumptions of equation A-1. Following points explains the application of those assumptions through software.

1- The first modification will be through magnifying modifiers that control flexural stiffness by increasing the moment of inertia of the beam, so the beam is flexurally rigid.
2- Another important assumption that need to be reflected in the model is the assumption of joint behavior, where the joint is allowed only to translate but not to rotate.
3- The final assumption will be increasing the shear capacity of column by magnifying column's shear capacity.

Table A-8 summarize all modifications that will make the 2D frame behavior close to equation's A-1 conditions:

Table A-8:Summery of applied modifications on the 2D frame

Modification Location	Modification Description	Modifier factor
Beam	Increase moment of inertia for the beam (Ixx)	1000 – (Figure A-4)
Joint	Restrict joint from rotation	Applying restraints on rotation at both joints (Figure A-5)
Column	Increase shear capacity of column	1000 (Figure A-6)

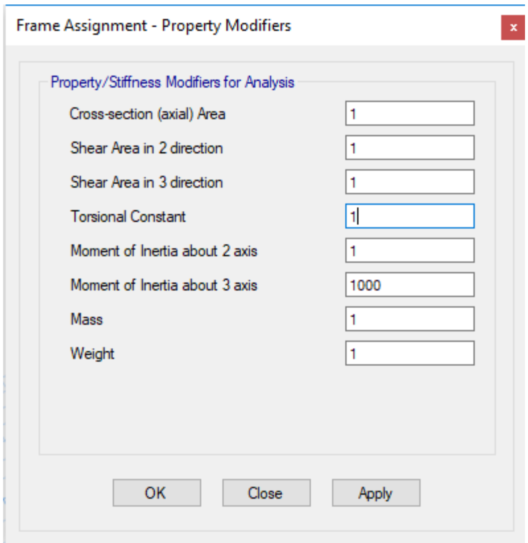

Figure A-4: Making beam flexurally rigid by increasing moment of inertia of the beam (I_{xx})

Figures A-5, A-6 show the two other modifications applied on the 2D model.

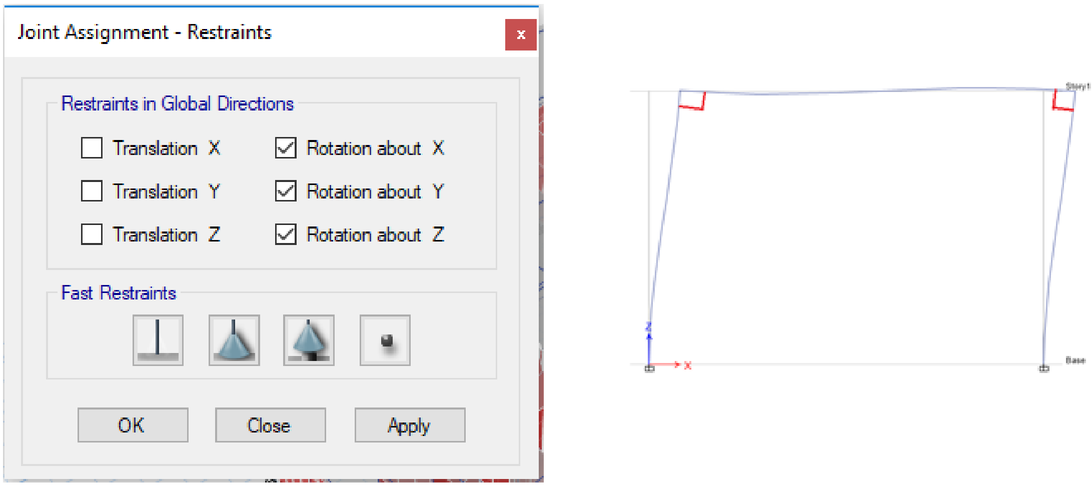

Figure A-5: Restricting joint from rotation to meet formula's 1 conditions

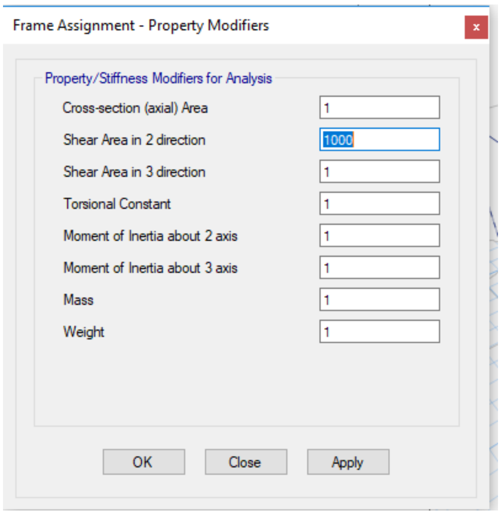

Figure A-6: Increasing shear capacity of column

Application of modifiers as provided in Table A-8 and as illustrated in figures A-4, A-5, and A-6, increase the stiffness by almost 69%. The value of lateral stiffness after the application of modifiers become 94.7×10^3 (figure A-7), which is almost 99% of the calculated value by Equation A-1.

	Story	Stiffness X kN/m
▸	Story1	94757.534

Figure A-7: Lateral stiffness as calculated by ETABS after applying the three modifications

A.2.6 Modeling of 2D Frame with Beam's size (B200x50)

Using beam with larger depth (four times the original case) will make the beam flexurally rigid. This change is assumed to increase the lateral stiffness of the frame, and moreover will utilize only assumptions in previous section.

ETABS frame is modified as shown in figure A-8 to match modifications applied previously by increasing beam's depth to 200 cm instead of 50 cm.

No assumptions are placed in the model; all modifiers are kept same as default in the software.

Figure A-8: Model of modified frame in ETABS

Tabulated results of ETABS show a value of $86x10^3$ kN/m (figure A-9).

	Story	Stiffness X kN/m
	Story1	85768.256

Figure A-9: lateral stiffness of modified frame as provided by ETABS

Table A-9 shows comparison between manual calculations and ETABS results.

Table A-9:K1, K2, K3, KETABS values for the 2D frame with beam's dimensions (50x200)

	Description	Value
K1	Value as calculated by formula 1	$95 \times 10^3 \frac{kN}{m}$
K2	Value as calculated by formula 2	$94 \times 10^3 \frac{kN}{m}$
K3	Value as calculated by formula 3	$93.7 \times 10^3 \frac{kN}{m}$
K$_{\text{ETABS}}$	Value as calculated by ETABS	$86 \times 10^3 \frac{kN}{m}$

Although results of manual computed lateral stiffness differ from ETABS result, the difference is still within 10% between software computed value and the average of three equations (94.2x10^3 kN/m).

The next step will be by applying modifications mentioned in section A.2.5 on the model. Figure A-10 shows the new computed lateral stiffness of the model after modifications.

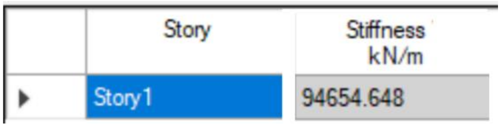

Story	Stiffness kN/m
Story1	94654.648

Figure A-10: Lateral stiffness of frame with B50x200 with application of assumptions mentioned in section 5.4.1.2.2

A.2.7 Limitations on Benjamin Formula

A paper published in 1992 by Arturo E. Schultz and others stated that Benjamin formula is accurate if beam is flexurally stiffer if compared to supporting columns. In this section the formula will be tested against Chopra's formula (Equation A-2) and ETABS results.

Table A-10 shows parameters of frame in figure A-11. Beams dimensions are reduced to be 20x20 cm, causing a dramatic drop in beams flexural stiffness.

A-10: Geometric properties of 2d verification frame-beam with less depth

Geometric Properties of 2D Verification Frame-Beam with Less Depth	
Column's Section (cm)	C50x50
Beam's Section (cm)	B20x20
Column's Height (h)(cm)	312
Beam's Length (L) (cm)	450
E_c (GPa)	23

I_{column} (m^4)	5.2×10^{-3} m^4
I_{beam} (m^4)	1.33×10^{-4} m^4
E_c I_{column} ($kN.m^2$)	1.2×10^5 $kN.m^2$
E_c I_{beam} ($kN.m^2$)	3.1×10^3 $kN.m^2$

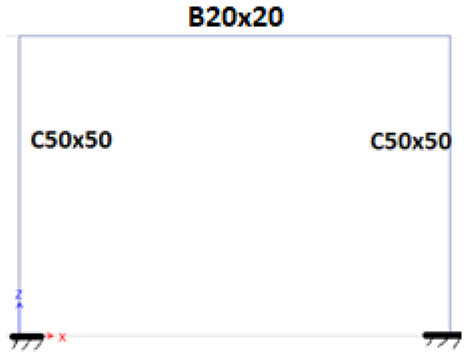

Figure A-11: 2D verification Frame- with a modification on beam's dimensions (B20x20 instead of B50x50)

Equitation A-1 output is with no change due to no involvement of relative stiffness of column and beam in the formula. Equation A-2 calculations will change as following:

$$\rho = \left(\frac{EI_b}{L}\right) \div \left(\frac{2EI_c}{h}\right) = \left(\frac{3.1\text{x}10^3}{4.5}\right) \div \left(2 \times \frac{1.2\text{x}10^5}{3.12}\right) = 8.96\text{x}10^{-3}$$

$$\frac{(12\rho + 1)}{(12\rho + 4)} = \frac{(12 \times 22.18 + 1)}{(12 \times 22.18 + 4)} = 0.27$$

$$K = \frac{24EI_c}{h^3}\frac{(12\rho + 1)}{(12\rho + 4)} = 94764.54 \times 0.27 = 25.5 \times 10^3\ kN/m$$

Equation calculations are shown below in table A-21.

Table A-11: Parameters in Benjamin Formula (Equation A-3)- Frame with beam's dimensions being decreased (B20x20)

Parameters for Benjamin Formula (Equation A-3)	
E_c I_{column}	1.2x105 $kN.m^2$
E_c I_{beam}	3.1×10^3 $kN.m^2$
n	1
Interior columns	Does not exist
Girder below	Does not exist

$\boldsymbol{K_{ec}}$	$\frac{EI_c}{h} = 38436.5$
$\boldsymbol{K_{ga}}$	$\frac{EI_b}{L} = 688.88$

$$K3 = \frac{\left(\frac{48(1)^2}{(3.12)^2}\right)}{2\left(\frac{1}{38436.5}\right) + \left(\frac{1}{688.88}\right)} = 3.28 \times 10^3\ kN/m$$

Table A-12 compares between the three equations (Equation A-1,A-2, and A-3) regarding the analyzed frame after changing beam's dimensions in a way to make column flexural stiffness much more than beam.

Table A-12: Equations A-1, A- 2, and A-3 lateral stiffness results-model with beams of dimensions of 20x20

	Equation 1	**Equation 2**	**Equation 3**
Lateral Stiffness (kN/m)	$95\text{x}10^3$	$25.5\text{x}10^3$	$3.28\text{x}10^3$

Figure A-12 shows the stiffness of 2D ETABS model.

	Story	Stiffness kN/m
▶	Story1	24997.689

Figure A-12: ETABS output: Lateral stiffness for 2D frame with B20x20

A.2.8 Conclusions

In this section manual computations for lateral stiffness of single bay single frame were compared to those obtained by ETABS software. The main aim was to verify results of software in order to adopt outputs of software regarding bare frames of single bay single frame. Following points summarize main conclusions:

1- Equation A-1 is a special case and acceptance of results obtained by this formula is limited to satisfy formula's assumptions. Application of those assumptions on 2D model will yield almost exact results.

2- Both Equations A-2 and A-3 includes the relative stiffness of columns and beam. Results of these formulas match in a good way with ETABS results when using beam with same size of columns. In this case (beam's dimension same to both columns) results are approximately the same without applying any assumption in the model. On the other hand, for the case of having stiffer beam (B50x200 instead of B50x50) results of both formulas showed a difference of about 9% without application of any assumption.

3- Equation A-3 is limited to a condition of having stiff beams. In the case of having beams with considerably less stiffness compared to columns, results of equation are with unacceptable tolerance.

4- Equation A-2 provides the most accurate results for all the cases: beam with the same size, beam with depth four times the original depth, and for the final case of having shallow beam (depth 40% of the original depth).

5- When applying assumptions mentioned in section A.2.5, results of 2D ETABS model shows an excellent agreement. Therefore, results of models with no assumptions can be adopted as the application of assumptions is supposed to be as a calibration of model to satisfy conditions of equations.

A.2.9 Approximating Lateral Stiffness of Multi Story Reinforced Concrete Frame Structure

A reinforced concrete frame structure is a structural system consists of beams supported on columns with the absence of shear walls. In this section the lateral stiffness of multistory frame structure will be computed using manual procedure and using ETABS.

Figure A-13 is showing a typical frame structure, where the lateral stiffness can be computed using either of Equation A-1 or A-3, where the calculation of lateral stiffness is carried out for each story independently.

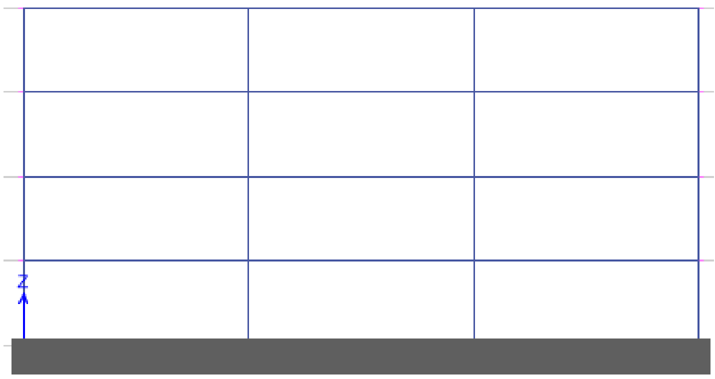

Figure A-13: Multi story frame structure-Elevation view

Equation A-1 is commonly used in manual procedures due to it is simplicity. Indeed, the use of Equation A-1 is applicable only under special circumstances that are illustrated previously in this chapter.

A.2.9.1 Calculating Lateral Stiffness of Four Stories Multi Bays Structure (Verification Example)

The following data is provided in a solved example in “The Seismic Design Handbook”, a book that was published in 1990.The lateral stiffness will be computed twice; once using manual approach of equation 1, and later on using ETABS.

Figure A-14 shows both plan and elevation view of example 3-4 in the Seismic Design Handbook, it must be noted that units in the book are in SI units, while the example is modified to metric units.

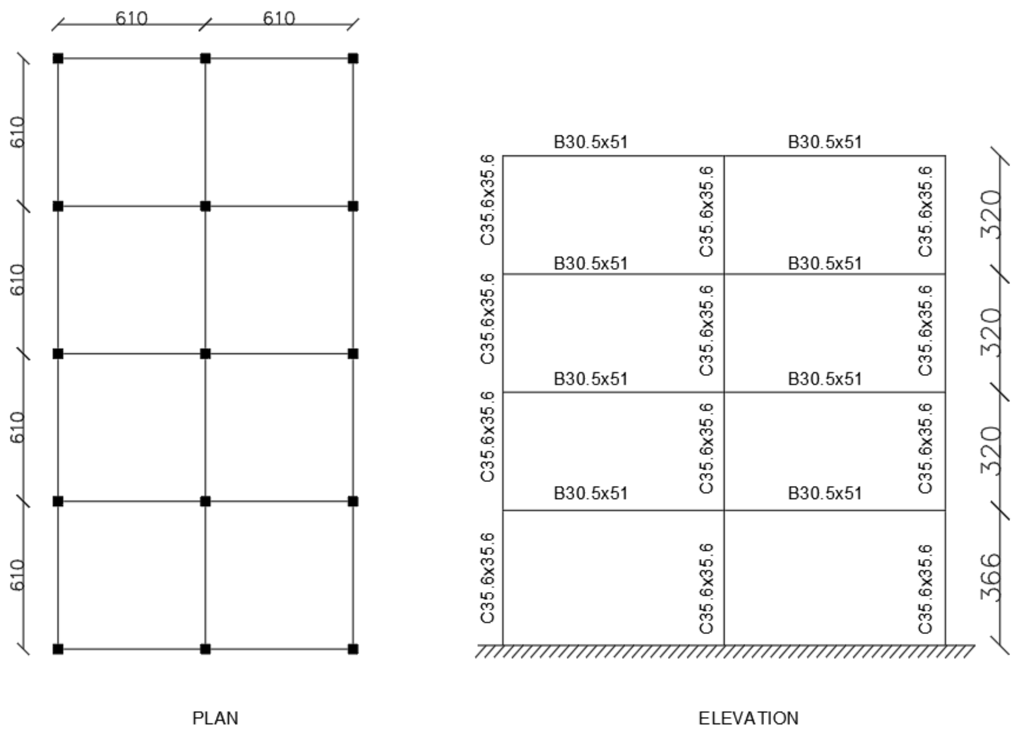

Figure A-14: Plan and Elevation View for example 3-4 in the Seismic Design Handbook

Since the base is given to be fixed support, all stories stiffness will be computed using the following formula:

$$K = 15 \times \frac{12EI_c}{h^3}$$

Where 15 is the number of columns in each story.

Table A-13 shows the parameters needed in the computational procedure of the lateral stiffness of the structure.

Table A-13:Story 1-4 stiffness-example 3-4 in the Seismic Design Handbook

	h (cm)	I_c (cm^4)	E (GPa)	K (kN/m)
Story 1	366	$3.76 x 10^3$	24.8	$12.2 x 10^4$
Story 2-4	320	$3.76 x 10^3$	24.8	$18.2 x 10^4$

As established previously through this chapter, ETABS can be calibrated to manual results of Equation A-1 by controlling some modifiers in the software. In this section ETABS model with modifiers changed to what is mentioned previously to verify the accuracy of results computed using the software. These modifiers are as following:

1- Beams are flexurally rigid.
2- There is no shear deformation in the columns.
3- Angle between columns and beams remains 90 in the deformation shape.

Table A-14 shows the tabulated results of ETABS model with the above-mentioned assumptions.

Table A-14: ETABS tabulated results for lateral stiffness-model with change in modifiers

ETABS tabulated results for lateral stiffness-model with change in modifiers		
Story	**Stiffness X**	**Stiffness Y**
	kN/m	kN/m
Story4	181868.909	181853.201
Story3	181891.896	181857.091
Story2	181894.456	181871.843
Story1	121854.103	121836.906

Table A-15 shows comparison between manual computed results and ETABS model with controlled modifiers.

Table A-15: Results of ETABS and manual calculations (Equation A-1)

	Manual (kN.m)	**ETABS (kN/m)**
Story 1	18.2×10^4	18.2×10^4
Story 2-4	12.2×10^4	12.2×10^4

ETABS model with no changes in modifiers is supposed to be better simulate real behavior. Table A-16 shows the output of lateral stiffness of non-modified ETABS model.

Table A-16: ETABS tabulated results for lateral stiffness-model with no change in modifiers

ETABS tabulated results for lateral stiffness-model with no change in modifiers		
Story	**Stiffness X**	**Stiffness Y**
	kN/m	kN/m
Story4	94912.594	101763.613
Story3	96930.702	103025.215
Story2	96904.409	102643.229
Story1	90669.299	93301

Table A-17 compares ETABS non modified model results to manual values for both directions.

Table A-17: Manual results of lateral stiffness of the multi-story frame Vs. ETABS results

	X direction			**Y direction**		
	Manual (kN.m)	ETABS (kN/m)	Difference (%)	Manual (kN.m)	ETABS (kN/m)	Difference (%)
Story 1	$18.2\text{x}10^4$	$9.1\text{x}10^4$	50%	$18.2\text{x}10^4$	$9.3\text{x}10^4$	48.9%
Story 2	$12.2\ \text{x}10^4$	$9.7\ \text{x}10^4$	20.5%	$12.2\ \text{x}10^4$	$10.3\text{x}10^4$	15.5%
Story 3	$12.2\ \text{x}10^4$	$9.7\ \text{x}10^4$	20.5%	$12.2\ \text{x}10^4$	$10.3\text{x}10^4$	15.5%
Story 4	$12.2\ \text{x}10^4$	$9.5\ \text{x}10^4$	20.5%	$12.2\ \text{x}10^4$	$10.2\text{x}10^4$	15.5%

Matching results between manual approach and ETABS model with assumption justify adopting results without modifying parameters in the software. Analysis results without applying modification to satisfy assumptions show a non-acceptable difference. This difference indicates wrong prediction of real behavior of frames systems.

A.3 Approximating Fundamental Period of Reinforced Concrete Frames

Reliable estimation of the fundamental period is essential step in predicting structures response due to earthquake forces. For design purposes codes usually suggest formulas that relate the fundamental period with structure type and height.

Fundamental time period mainly depends on both the mass and the stiffness of the structure. Equation A-4 is used in the determination of the natural period of a system of single degree of freedom.

$$T_n = 2\pi\sqrt{\frac{m}{k}} \quad \text{[Equation A-4]}$$

A.3.1 Manual Computation of Fundamental Period for Single Bay Single Story 2D Frame

For the frame shown in figure A-1 in chapter three, the fundamental period will be computed manually using the Equation A-4.

The lateral stiffness "k" was found to be $60x10^3$ using Chopra's formula (Equation A-2). Mass will be computed as following (Table A-18):

Table A-18: Mass calculation-2D frame verification

Mass Calculation-2D Frame Verification	
Concrete Unit Weight	25 kN/m^3
Beam's mass (ton)	(4.5x0.5x0.5x25)/9.81=2.867
Column's shared mass* (ton)	(0.5x0.5x3.12x25x0.5x2)=1.987
Total mass (ton)	4.85

$$T_n = 2\pi\sqrt{\frac{4.85}{60000}} = 0.0565\ seconds$$

ASCE formula estimates the fundamental period as following:

$$Ta = 0.0466(3.12)^{0.9} = 0.1297\ seconds$$

The high difference between ASCE formula output and manual calculation is due to the fact that the frame is analyzed only for self-weight, and no case of superimposed loads neither live load is assigned to the frame. Code's formula is designed for real structures which surely have other loads than the self-weight of the elements.

A.3.1.1 Computation of Fundamental Period for Single Bay Single Story 2D Frame Using ETABS

Analysis of frame shown in figure A-1 is analyzed using ETABS. Figure A-15 shows the fundamental period (mode 1).

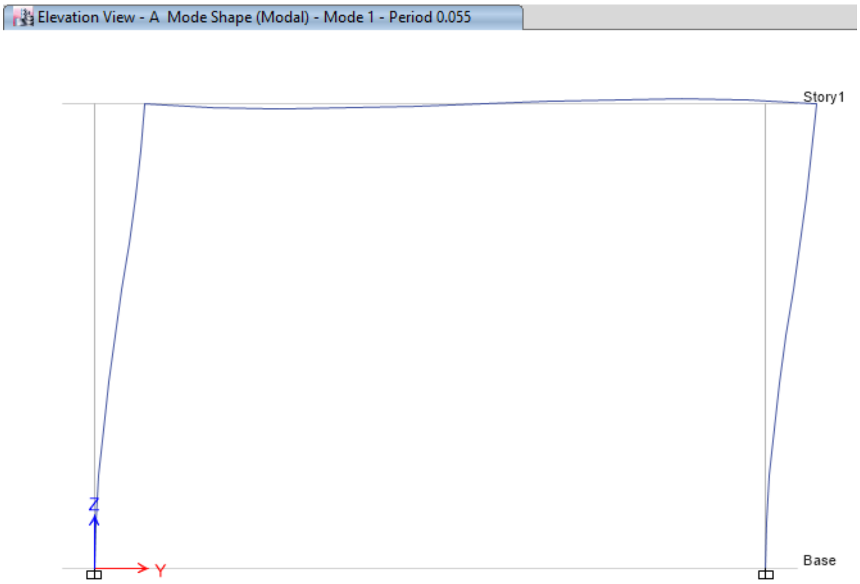

Figure A-15: First mode - deformed shape-ETABS model-Single bay single story frame

Table A-19 shows comparison between manual value, and value computed by ETABS model.

Table A-19: Manual Vs. ETABS time period values for the 2D single bay single story frame

	Manual (seconds)	**ETABS**	**Difference**
Fundamental Period	0.0565	0.055	2.6%

A.3.2 Manual Computation of Fundamental Period for Multi Story Reinforced Concrete Structure

Generalized single degree of freedom can be used in fundamental time period manual computational procedure for reinforced concrete frame structures. Shape functions and lateral stiffness are the two most important parameters that control fundamental period result.

Example 3-4 from The Seismic Design Handbook will be verified against ETABS result that will be discussed in the next section. Example 3-4 defines two shape functions, and the author chooses to use the following formula:

$$\textit{Shape Function Formula for example}\ (3-4) = \sin\frac{(\pi x)}{2L}$$

Lateral stiffness of each story is shown in chapter three, and the mass distribution in the example is as shown in figure A-16:

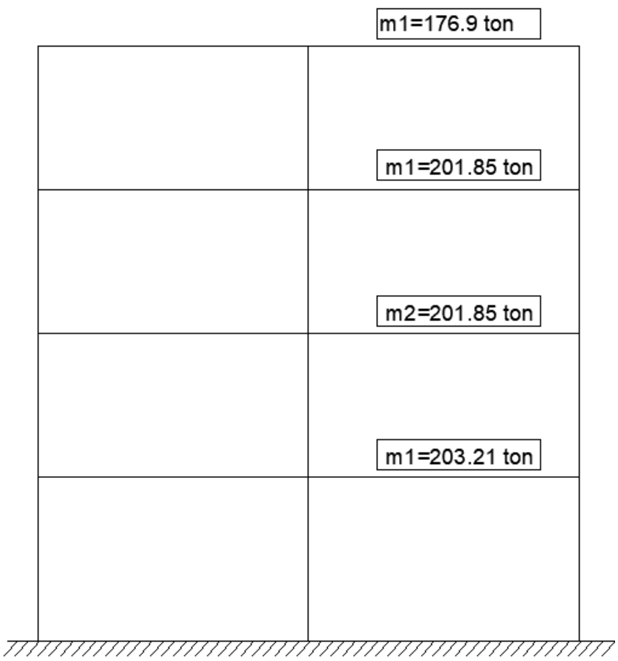

Figure A-16: mass distribution- example 3-4 from THE Seismic Design Handbook

Table A-20 summarize calculations of generalized single degree of freedom for the frame. Note that stiffness of each story as manually calculated in section A.2.9.1, and it was mentioned that these values are in accurate if compared to ETABS model with assumptions.

Table A-20: Application of Generalized Single Degree of Freedom on Example 3-4

Level	K	M	Ø	ΔØ	$M\Delta\text{Ø}^2$	$K\Delta\text{Ø}^2$
4		0.252	1		0.252	
3	18.2x10^4	0.288	0.929	0.071	0.249	1.054
2	18.2x10^4	0.288	0.726	0.203	0.152	8.613
1	18.2x10^4	0.29	0.42	0.306	0.051	19.57
	12.2x10^4			0.42		24.696
				M*	**0.704**	
					K*	**53.933**

The fundamental period of the system is calculated as following:

$$\omega = \sqrt{\frac{K^*}{m^*}} = \sqrt{\frac{53.933}{0.704}} = 8.75\frac{rad}{sec} \rightarrow Ta = \frac{2\pi}{8.75} = 0.718\, seconds$$

ASCE code estimation of the period is as following:

$$Ta = 0.0466(13.26)^{0.9} = 0.477\, seconds$$

A.3.2.1 Computation of Fundamental Period for Multi Story Reinforced Concrete Structure Using ETABS

In this section ETABS results regarding the fundamental period will be introduced. As mentioned previously in this chapter (section A.2.5 and section A.2.9.1), some modifications are applied in order to match with manual results. Therefore, the modified model results will be shown at the first stage, and in the next stage, modifiers will be changed to be as default by the software it-self, and fundamental period will be recomputed and then compared to results with modifications.

Figure A-17 shows the fundamental period of the model with modifiers changed to meet assumptions used in calculating lateral stiffness of each story. It is worth mentioning that both modes 1 and 2 are the same; and this is a result of having exactly the same stiffness for the both directions.

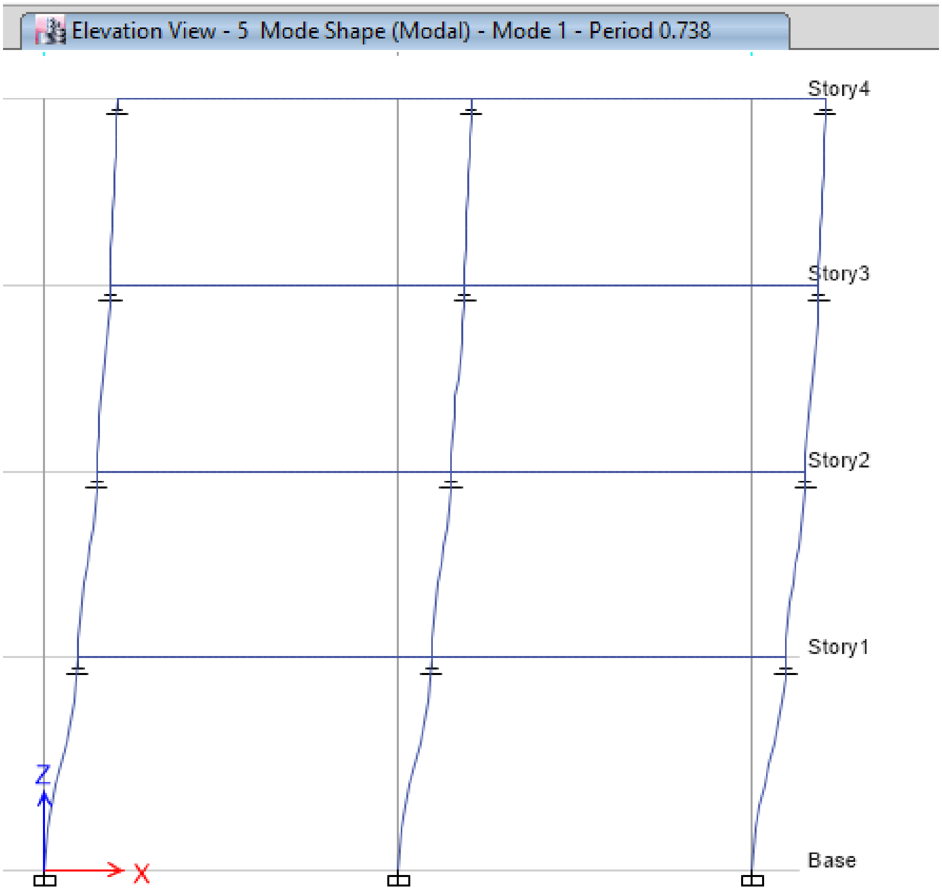

Figure A-17: Fundamental period for frame with assumption – ETABS

Table A-21shows a comparison between manual and ETABS results, with showing a difference of 2.8% which is an acceptable difference.

Table A-21: Manual Vs. ETABS modified model (fundamental period)

Manual fundamental period	ETABS fundamental period / with assumptions	Difference
0.718 seconds	0.738	2.8%

Model with no assumptions fundamental period is found to be 0.813 seconds (figure A-18), with a difference of 13.2%. Moreover, period of mode 2 is not the same (0.795 seconds) due to the fact of non-equal stiffness for the both directions.

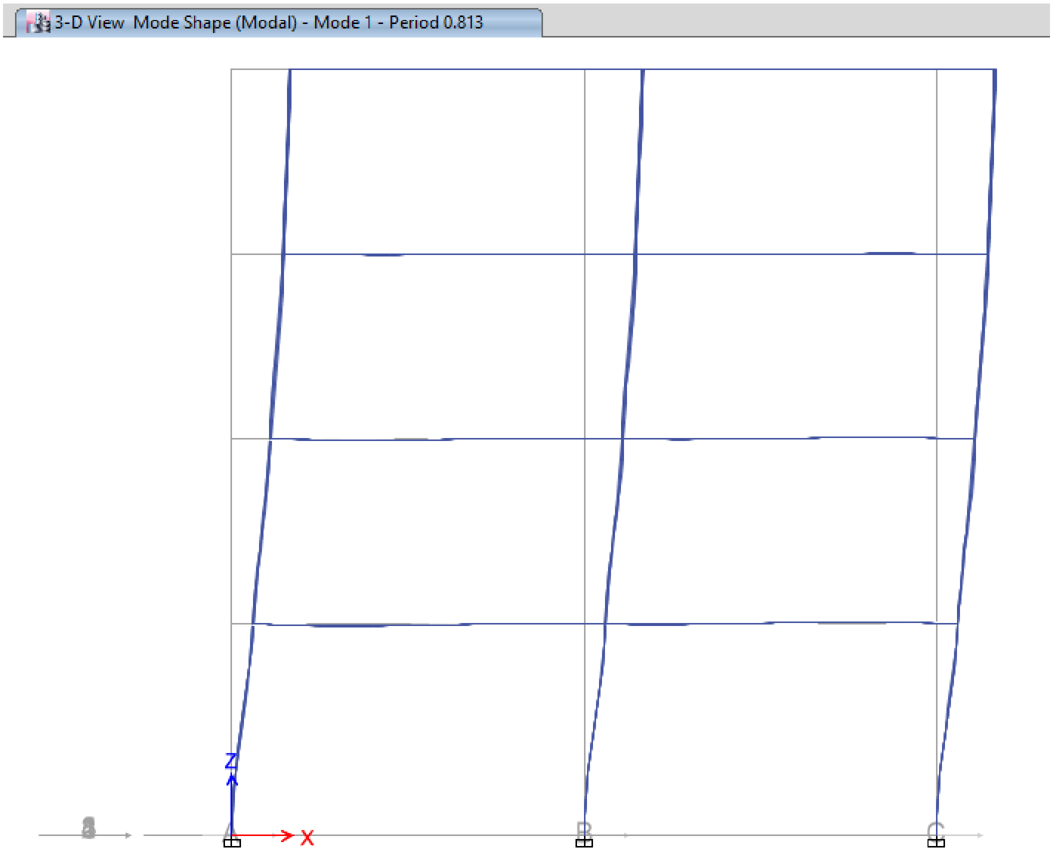

Figure A-18: Mode 1 of ETABS model with no assumptions

A.3.2.2 Conclusions

Fundamental period calculations depend on computed lateral stiffness and the suspected shape function. In this section it is proved that using assumed stiffness results of software is within an acceptable difference of 10%. If assumptions are removed from model lateral stiffness will change and the shape function may differ also.

Results of ETABS can be adopted due to the fact of matching results when applying assumptions.

A.4 Verification of Fundamental Period for Wall Structural System

Adopting software output regarding fundamental period for structures surrounded by structural walls must be after validation of software output, by comparing manual computational results with those gained by ETABS software.

A.4.1 Verification of Ten Stories Structural System

Geometry and Data of the Verification Model

Figure A-19 shows both 3D view and plan for a square two bays ten stories structure. As can be noted the structure is composed of parameter reinforced concrete walls with only a one column inside.

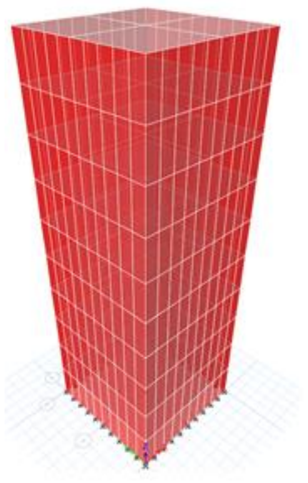

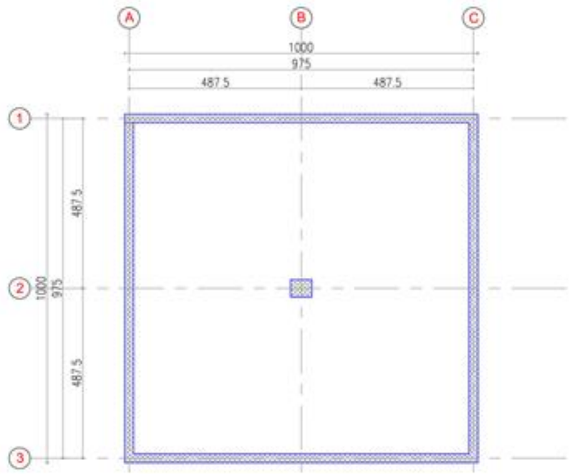

Figure A-19: Verification model, and plan view for each story

Table A-22 shows the data of the model.

Table A-22: Data for the verification model

Data for Verification model – Parameter Shear Wall	
Slab thickness	25 cm
Slab Area	100 m^2
Slab concrete Modulus of Elasticity	23025 MPa
Column Dimension	60x50 (cm)
Walls thickness	25 cm
No. of stories	10

Manual Calculations and Verification of Story Weight

Following calculations are for the mass of the structure that will be used in later on calculations.

$$\begin{aligned} &Total\ weight\ of\ the\ slab \\ &\quad = slab\ area\ x\ slab\ depth\ x\ unit\ weight\ of\ concrete \\ &\quad = 100 \times 0.25 \times 25 = 625\ kN \end{aligned}$$

$$\begin{aligned} &Total\ weight\ of\ columns\ in\ the\ floor \\ &\quad = \ columns\ weight\ x\ No.of\ columns = 0.6 \times 0.5 \times 25 \times 3 \times 1 \\ &\quad = 22.5kN \end{aligned}$$

$$Total\ mass\ of\ walls = Walls\ area\ x\ concrete\ unit\ weight$$
$$= 10 \times 0.25 \times 3 \times 4 \times 25 = 750$$

$$Total\ Weight = 1397.5\ kN$$

Figure A-20 shows the tabulated result of story mass as provided by ETABS software.

	Load Case/Combo	FZ kN
	Dead	1376.7506

Figure A-20: Tabulated result - weight of one story-ETABS

Table A-23 shows the difference between manual computed weight and the output of ETABS.

Table A-23: Manual Value Vs. ETABS – Weight of One Story

Manual Value Vs. ETABS – Weight of One Story		
Manual Calculations (kN)	**ETABS Output (kN)**	**Difference**
1397.5	1376.8	1.5%

Weight of last story will be different since only half the walls are defining the weight. Figure A-21 shows the tabulated output of ETABS regarding a one story with story height of 1.5 meters.

	Load Case/Combo	FZ kN
	Dead	1000.2506

Figure A-21: Tabulated result - weight of one story with half height (1.5 meter instead of 3 meter)-ETABS

Mass Distribution of the Verification Model

Table A-24 summarize both values of weight and mass of typical stories (9 stories) and last story.

Table A-24: Weight and Mass Values – Verification Model-10 Stories

Weight and Mass Values – Verification Model-10 Stories				
Weight of Typical Story (ETABS) (kN)	**Weight of Last Story (kN)**	**Mass of Typical Story (ton)**	**Mass of Last Story (ton)**	$\frac{\textbf{Mass of Typical Story}}{\textbf{Mass of Last Story}}$
1376.5	1000.3	140.3	102	0.73

Figure A-22 shows the distribution of masses; the mass of final story is normalized to typical story.

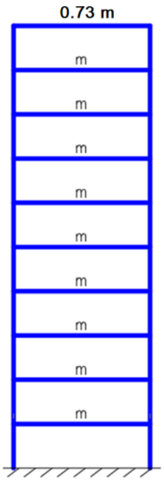

Figure A-22: Mass distribution for the verification model-parameter shear walls

Shape Function for the Verification Model

Suggested Shape Function

Determination of shape function is an essential step for accurate estimation of fundamental period computation procedure. For this structure, and due to the proportion of geometry a flexural deformation may be assumed, and therefore following formula may be used for shape function:

$$\varphi = 1 - \cos(\frac{\pi x}{2L})$$

Table A-25 shows the results of shape function for each story.

Table A-25: Shape function for the structure using the suggested formula for flexural deformation

Story Number	Story Height (m)	φ
1	3	0.012
2	6	0.049
3	9	0.109
4	12	0.191
5	15	0.293
6	18	0.412
7	21	0.546
8	24	0.691
9	27	0.844
10	30	1.000

Shape Function as Suggested by ETABS

Shape function considerably affect the final output of fundamental period; thus, the shape function output will be compared with ETABS results; in order to check the accuracy of suggested formula. Table A-26 shows shape function as provided by ETABS.

Table A-26: Shape function as computed based on ETABS output

Story	Average Displacement in mm	φ
Story1	1.085	0.04973
Story2	2.696	0.12356
Story3	4.685	0.21471
Story4	6.954	0.3187
Story5	9.406	0.43107
Story6	11.959	0.54808
Story7	14.535	0.66613
Story8	17.07	0.78231
Story9	19.509	0.89409
Story10	21.82	1

Table A-27 shows comparison between suggested shape function from formula, and the output of ETABS software.

Table A-27: Formula's output Vs. Etabs results - Shape function

Etabs Results	Manual Results
0.04973	0.012
0.12356	0.049
0.21471	0.109
0.3187	0.191
0.43107	0.293
0.54808	0.412
0.66613	0.546
0.78231	0.691
0.89409	0.844
1	1

Verification of Suggested Shape Function by ETABS Using 1D Model

As Table A-27 results are showing considerable difference between what formula suggests and what software provide, a 1D model will be used to validate accuracy of both approaches. Figure A-23 shows a cantilever model of 30-meter length, with point loads representing each story weight, and with section dimensions simulating real structure using section's thickness similar to walls thickness of 25 cm, and with width and depth similar to plan's dimensions (10 meters).

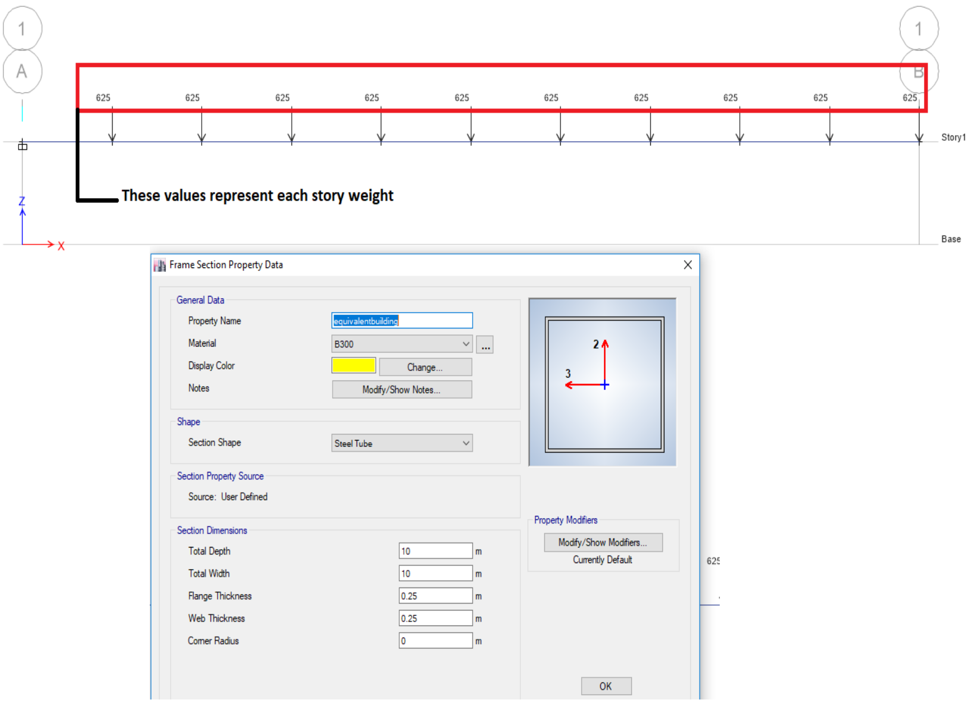

Figure A-23:1D model with geometric data for the section

Table A-28 shows the average displacement output for each story (location of point loads), and the shape function values as concluded from the 1D model.

Table A-28: Average displacement of each story (point loads locations), and the concluded shape function for the 1D model

Story	Average Displacement in mm	φ
Story1	1.085	0.05978
Story2	2.524	0.13907
Story3	4.227	0.23291
Story4	6.114	0.33688
Story5	8.116	0.44719
Story6	10.174	0.56058
Story7	12.24	0.67442
Story8	14.275	0.78655
Story9	16.25	0.89537
Story10	18.149	1

Table A-29 compares the three approaches: the suggested shape function, ETABS 3D model, and 1D model.

Table A-29: Three approaches output: manual using formula, 3D model (ETABS), 1D model (ETABS).

Manual Results	Etabs Results	1D Model
0.012	0.04973	0.05978
0.049	0.12356	0.13907
0.109	0.21471	0.23291
0.191	0.3187	0.33688
0.293	0.43107	0.44719
0.412	0.54808	0.56058
0.546	0.66613	0.67442
0.691	0.78231	0.78655
0.844	0.89409	0.89537
1	1	1

As can be concluded by table A-29 the estimated shape function is not accurate, thus value of computed fundamental period by generalized single degree freedom will not be close to what ETABS provide.

Computing Fundamental Period of the Verification Model Using the Generalized Single Degree of Freedom Approach

Stiffness of the structure using the generalized single degree of freedom will be will be computed by integration as following (Equation A-9):

$$\widetilde{K} = \int_0^L EI\emptyset''^2 dx \quad \text{[Equation A-5]}$$

The integration is done using MAPLE software of version 18. Table A-30 shows the needed data for the completing the integration.

Table A-30: Data needed in Computing Equivalent Lateral Stiffness – Verification Model

Data needed in Computing Equivalent Lateral Stiffness – Verification Model	
Ec (kN/m²)	23025000
I_{wall} (in plane) (m^4)	$\frac{1}{12} \times 10^3 \times 0.25 \times 2 = 41.67\, m^4$
I_{wall} (in the other direction) (m^4)	$\frac{1}{12} \times 0.25^3 \times 10 \times 2 = 0.026\, m^4$
Total Stiffness m^4	41.96 m^4
***EI* (kN.m²)**	9.6 x 10^8

The second derivative of the shape function is as following:

$$\emptyset'' = \frac{1}{4}\frac{\cos(\frac{\pi x}{2L})\pi^2}{L^2}$$

While the result of integration is as following:

$$\tilde{K} = EI\int_0^L (\frac{1}{4}\frac{\cos\left(\frac{\pi x}{2L}\right)\pi^2}{L^2})^2 dx = \frac{2.92\times 10^9}{L^3} = 1.08\times 10^5\ kN/m$$

Table A-31 shows the value of walls' lateral stiffness contribution.

Table A-31: Contribution of walls in the lateral stiffness

Contribution of walls in the lateral stiffness (kN/m)	$1.08x10^5$

The equivalent mass is computed using the following formula:

$$\tilde{m} = \sum_1^n m_n {\emptyset_n}^2 \quad \text{[Equation A-6]}$$

$$\tilde{m} = 140.3[0.012^2 + 0.049^2 + 0.109^2 + 0.191^2 + 0.293^2 + 0.412^2 + 0.546^2 + 0.691^2 + 0.84^2 + 0.73\times 1^2] = 391.1\ ton$$

The fundamental period using the generalized single degree of freedom is calculated as following:

$$T = 2\pi\sqrt{\frac{\tilde{m}}{\tilde{K}}} = 2\pi\sqrt{\frac{391.1}{1.08\times 10^5}} = 0.378\ seconds$$

Fundamental Period of ETABS Model

Figure A-24 shows the fundamental period value as provided by ETABS.

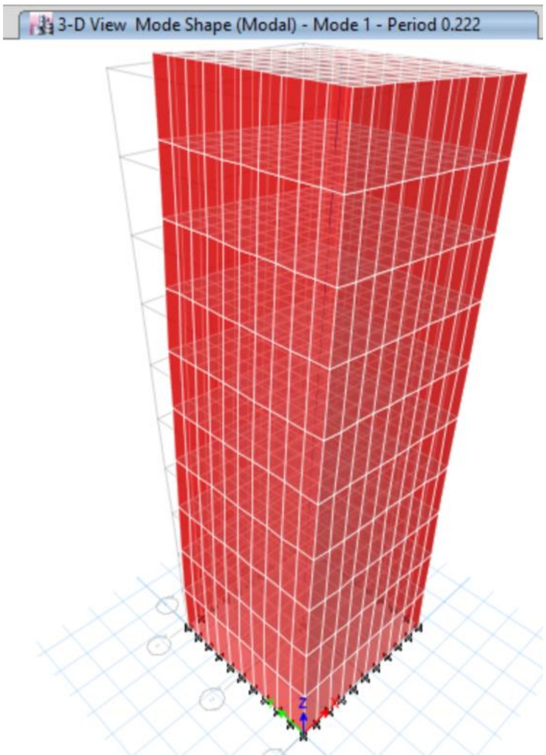

Figure A-24: Fundamental period of verification model (0.222 seconds)

Figure A-25 shows the tabulated result of the mass participation ratio as provided by ETABS.

Case	Mode	Period sec	UX	UY
Modal	1	0.222	0.7106	0
Modal	2	0.222	0	0.7106

Figure A-25: Tabulated results of mass participation ratios- mode 1 and 2 (x and y)

The value computed using the manual approach assumes full mass participation, thus, fundamental period obtained from model will be modified based on this relation:

$$Modification\ Factor - Fundemental\ Period\ from\ ETABS = \sqrt{\frac{1}{0.7106}}$$
$$= 1.19$$

Table A-32 shows the modified fundamental period of ETABS after multiplying the original value by the modification factor of 1.19.

Table A-32: Modification of fundamental value of ETABS to include the full mass of structure

Modified Fundamental Period of ETABS Model	0.263 seconds

Comparison Between Manual and ETABS Results

Table A-33 shows the comparison between ETABS output and manual calculations:

Table A-33: Manual Vs. ETABS Fundamental Period Value

Manual Vs. ETABS Fundamental Period Value		
Manual (seconds)	ETABS (seconds)	Difference
0.378	0.263	30.4%

The large difference between the two outputs can be explained by the inaccurate estimation of deformation of the system. However, in the next section another model with only three stories will be verified, and closer results are expected since the structural geometry of the system makes the use of a “sin” shape function logical.

Verification of Three Stories Structural System

Three stories structural system of 9 meters total height is supposed to deform in a pattern similar to "sin" shape function. Figure A-26 shows the model that will be verified through this section.

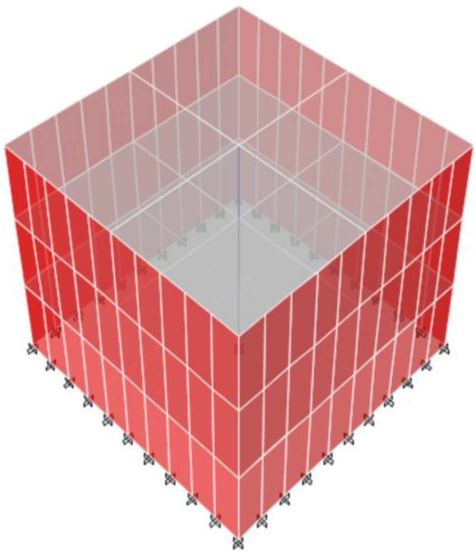

Figure A-26: Three story model for verification

The following shape function will be used in the manual procedure.

$$\varphi = sin(\frac{\pi x}{2L})$$

Table A-34 shows the results of shape function for each story.

Table A-34: Shape function for the structure using the suggested formula for shear deformation

Story Number	Story Height (m)	φ
1	3	0.5
2	6	0.866
3	9	1

Table A-35 shows the shape function as provided by ETABS model.

Table A-35: Shape function as computed based on ETABS output

Story	Average Displacement in mm	φ
Story1	0.042	0. 36
Story2	0.086	0.74
Story3	0.117	1

Table A-36 shows comparison between suggested shape function from formula, and the output of ETABS software.

Table A-36: Formula's output Vs. Etabs results - Shape function

Etabs Results	Manual Results
0.36	0.5
0.74	0.866
1	1

The second derivative of the shape function is as following:

$$\emptyset'' = -\frac{1}{4}\frac{\sin(\frac{\pi x}{2L})\pi^2}{L^2}$$

While the result of integration is as following:

$$\tilde{K} = EI\int_0^L (-\frac{1}{4}\frac{\sin\left(\frac{\pi x}{2L}\right)\pi^2}{L^2})^2 dx = \frac{2.92\times 10^9}{L^3} = 4\times 10^6\ kN/m$$

Table A-37 shows the value of walls' lateral stiffness contribution.

Table A-37: Contribution of walls in the lateral stiffness

Contribution of walls in the lateral stiffness (kN/m)	4 x10^6

The equivalent mass is computed using the following formula:

$$\tilde{m} = \sum_1^n m_n {\emptyset_n}^2 \qquad \text{[Equation A-7]}$$

$$\tilde{m} = 140.3[0.5^2 + 0.866^2 + 0.73 \times 1^2] = 242.7\ ton$$

The fundamental period using the generalized single degree of freedom is calculated as following:

$$T = 2\pi \sqrt{\frac{\tilde{m}}{\tilde{K}}} = 2\pi \sqrt{\frac{242.7}{4 \times 10^6}} = 0.0490\ seconds$$

Figure A-27 shows the fundamental period value as provided by ETABS.

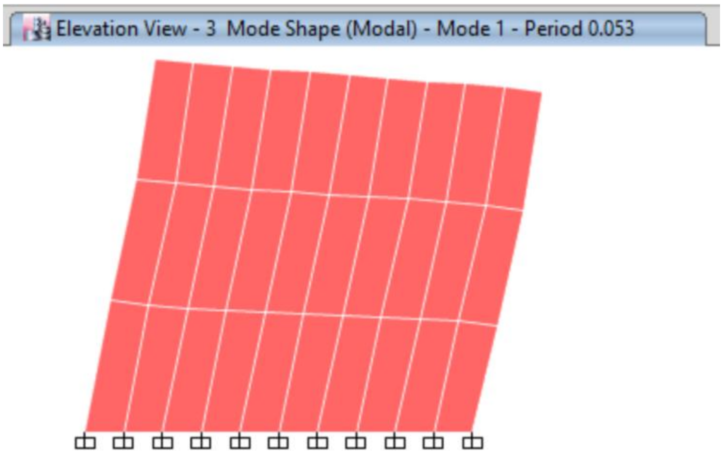

Figure A-27: Fundamental period of verification model (0.053 seconds)

Figure A-28 shows the mass participation ratio (ETABS).

Case	Mode	Period sec	UX	UY
Modal	1	0.053	0.862	0
Modal	2	0.053	0	0.8618

Figure A-28: Tabulated results of mass participation ratios- mode 1 and 2 (x and y)

$$Modification\ Factor - Fundemental\ Period\ from\ ETABS = \sqrt{\frac{1}{0.862}}$$
$$= 1.078$$

Table A-38 shows the modified fundamental period of ETABS after multiplying the original value by the modification factor of 1.078.

Table A-38: Modification of fundamental value of ETABS to include the full mass of structure

Modified Fundamental Period of ETABS Model	0.057 seconds

Table A-39 shows the comparison between ETABS output and manual calculations:

Table A-39: Manual Vs. ETABS Fundamental Period Value

Manual Vs. ETABS Fundamental Period Value		
Manual (seconds)	ETABS (seconds)	Difference
0.049	0.057	16.5%

Table A-39 shows the difference is reduced from 30% to 16.5%. In order to make results closer assumptions mentioned in section A.2.5 will be applied on the model. Figure A-29 shows the fundamental period of the model with the assumptions.

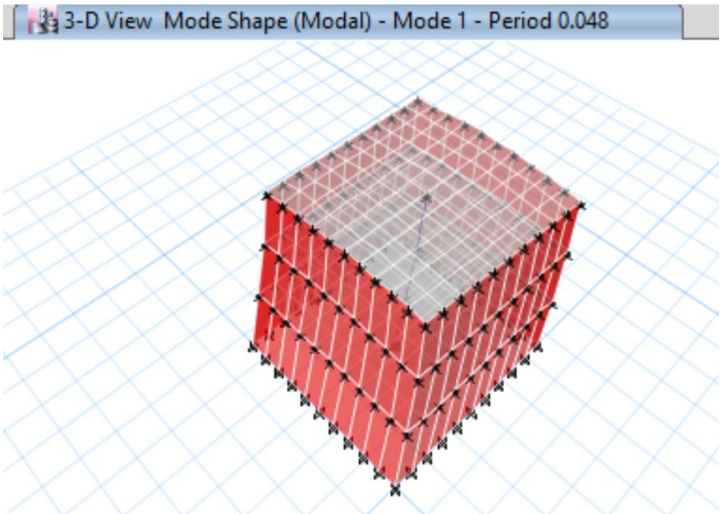

Figure A-29: Fundamental period of the verification model of three stories after applying assumptions mentioned in section A.2.5

Figure A-30 shows the tabulated result of the mass participation ratio as provided by ETABS.

	Case	Mode	Period sec	UX	UY
▸	Modal	1	0.048	0.8907	0
	Modal	2	0.048	0	0.8908

Figure A-30: Tabulated results of mass participation ratios- mode 1 and 2 (x and y)- model with assumptions

$$Modification\ Factor - Fundemental\ Period\ from\ ETABS = \sqrt{\frac{1}{0.8908}}$$
$$= 1.059$$

Table A-40 shows the modified fundamental period of ETABS after multiplying the original value by the modification factor of 1.059.

Table A-40: Modification of fundamental value of ETABS to include the full mass of structure

Modified Fundamental Period of ETABS Model	0.508 seconds

Table A-41 shows the comparison between ETABS output and manual calculations:

Table A-41: Manual Vs. ETABS Fundamental Period Value

Manual Vs. ETABS Fundamental Period Value		
Manual (seconds)	ETABS (seconds)	Difference
0.489	0.508	3.8%

Table A-41 shows that model output is reliable and therefore results of ETABS will be adopted in the coming analytical study.

A.5 Analysis Using Equivalent Strut Method

The behavior of infill walls for both methods one and two is not the same as method three due to lack of tension capacity. In this section modeling of infill walls for both methods will be applied using the formula of NBCC code.

The analysis will be performed for the following cases:

1- Bare frames models: in bare frames models equivalent strut will be modeled to represent infill walls with openings for both methods one and two. In method one the strut will replace a 12 cm plain concrete section, while in method two the strut will replace a layer of brick with 20 cm thickness.

2- For the model with core shear walls the same procedure will be applied for the both two methods.

3- The analysis will be performed for both cracked and non-cracked sections. Indeed, no change will be assumed on the modifiers of the strut itself.

Verification

In this section the time period and stiffness as computed by ETABS will be verified manually in order to adopt software output regarding fundamental period for frame structures with infill in between.

Table A-42 shows the information of the frame with the diagonal strut that will be used for verification purposes.

Table A-42: Properties of the frame with diagonal strut that will be verified

Item	Dimension
Columns Height (m)	3.12
Beams Length (m)	6.0
Beam/Column Dimension (cm)	40x40
Diagonal width ×depth (cm)	60x12

ETABS software provides an option of defining diagonal element as compression only member. This option can be applied by assigning a limit of tension for a specific member. Figure A-34 shows a value of zero as a limit for tension, that necessarily means no tension capacity.

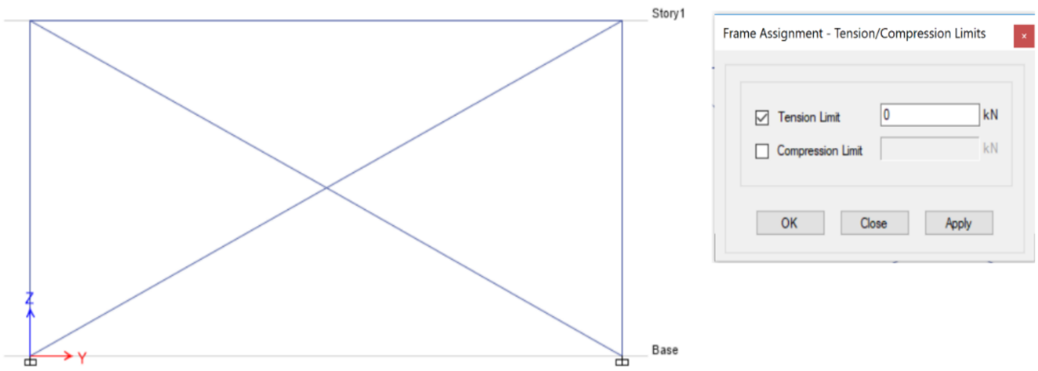

Figure A-31: Creating a compression only member on ETABS by limiting tension with a maximum value of zero

In order to test efficiency of the option of limiting tension to a maximum value of zero, a test is performed as shown in figure A-32 by applying a lateral load of 1000 kN then by viewing axial forces results in the frame and the two struts.

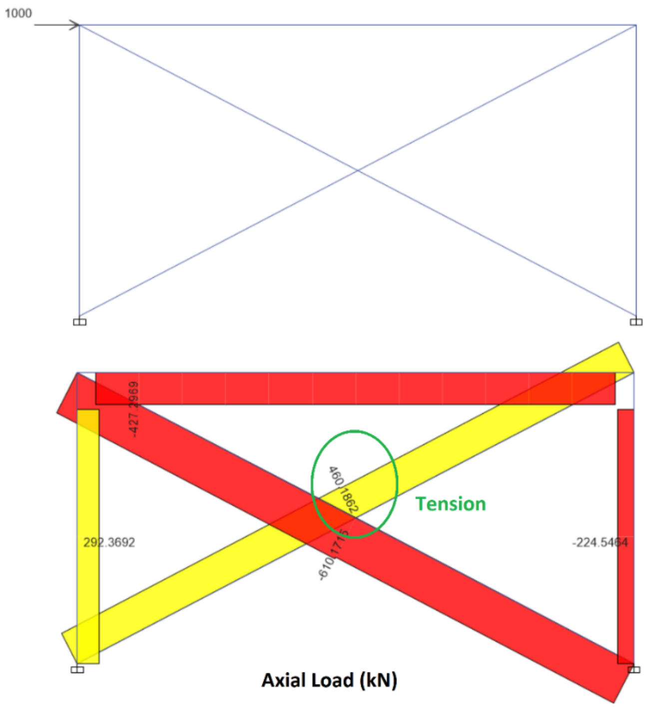

Figure A-32: Applying a point load of 1000 kN latterly to the frame and axial force results with tension values

As shown in figure A-32 the option of limiting tension is not valid yet. This is explained by the need of changing the nature of the lateral load to nonlinear instead of linear. The application of this change is shown in figure A-33. The following quote is taken from the manual of the software: “An upper limit on the amount of tension and compression force supported by a frame object can be assigned. This is used primarily to model tension-only cables and braces. The behavior modeled is nonlinear but elastic. For example, assume a compression limit of zero has been set. If the object tries to go into axial compression, it will shorten without any stiffness. If the load reverses, it will recover its shortening with no stiffness, then engage with full stiffness when it reaches its original length” (Etabs Manual).

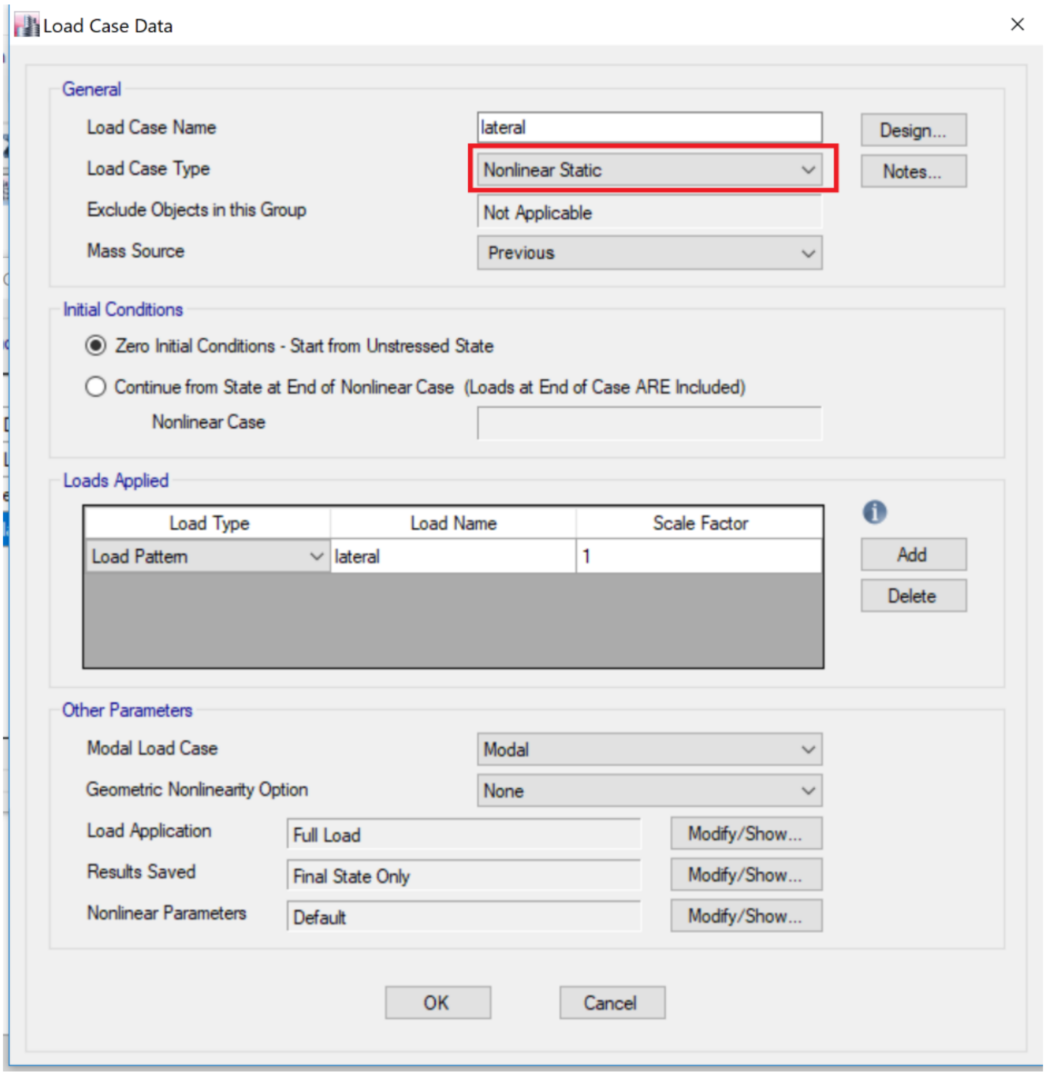

Figure A-33: Changing the lateral load case to non linear

Figure A-34 shows the axial force in the frame and the two struts with diagonal members acting as compression only members.

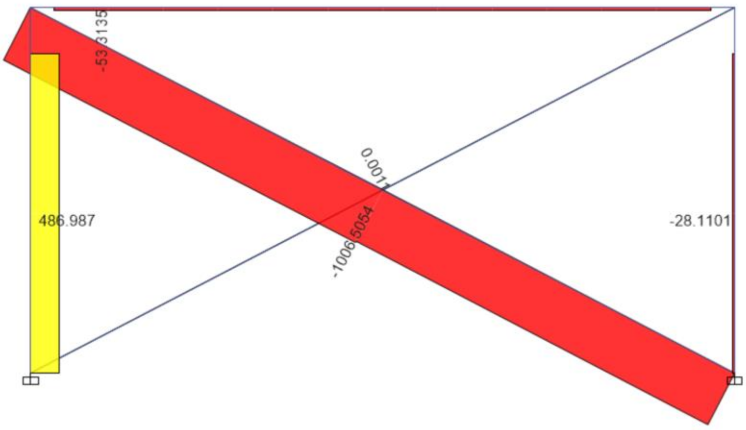

Figure A-34: Axial force results in frame elements and the two only compression struts

Model shown in figure A-34 can be remodeled as shown in figure A-35; due to the fact that other diagonal strut (the one supposed to absorb tension force) is a zero-force member.

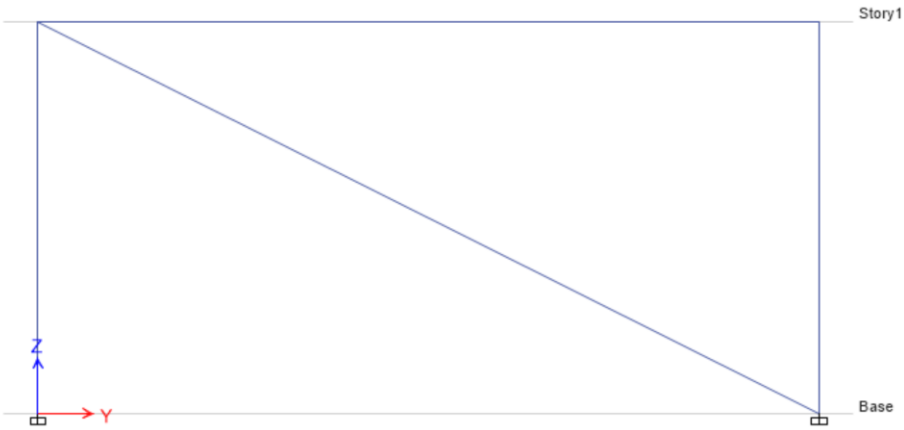

Figure A-35: Model neglecting the zero-force member – linear load case

Figure A-36 shows the axial force in the diagonal strut which is almost the same to what gained by model of x bracing with a compression only struts.

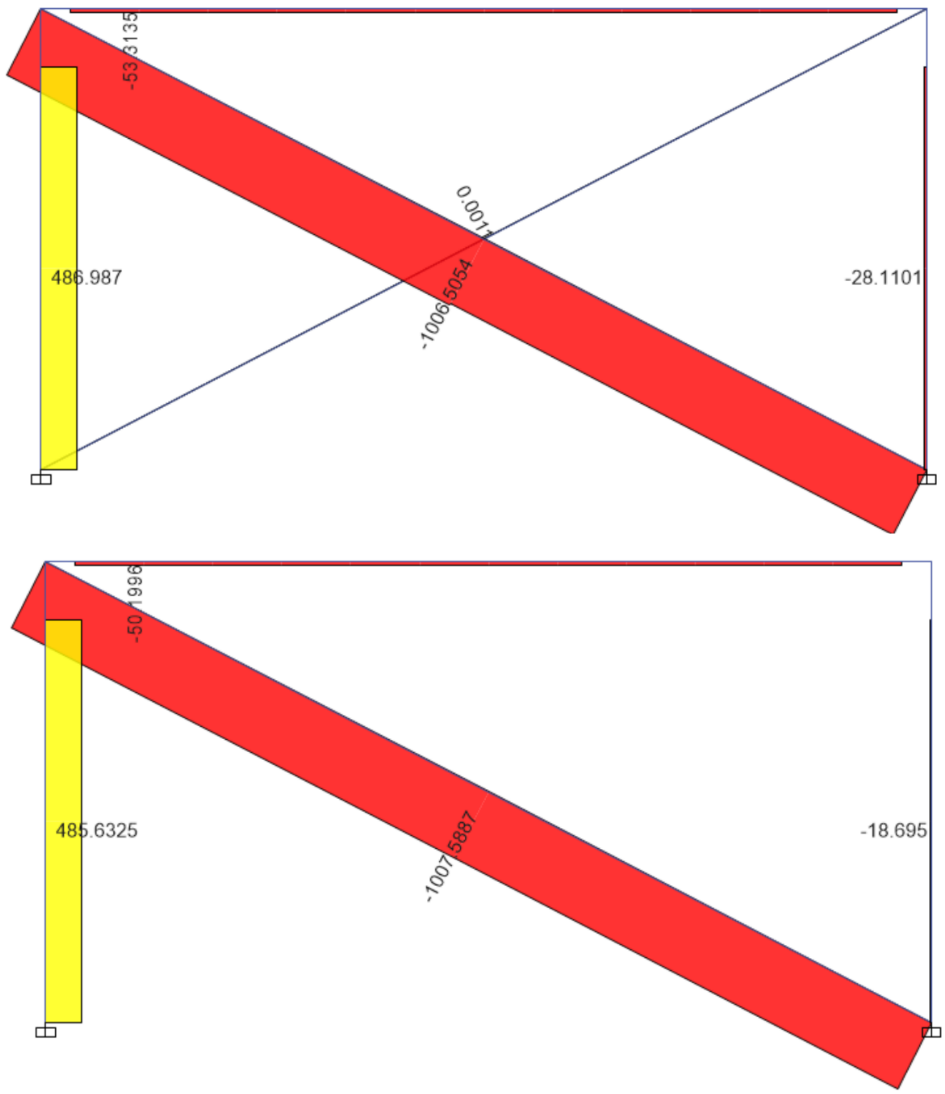

Figure A-36: Comparison between one strut model (neglecting zero force member) and the x bracing model with the nonlinear load case

After verifying force analysis for the frame with diagonal strut, the next step will be verifying the lateral stiffness of the frame with the existence of diagonal strut. The lateral stiffness of a single-story single bay frame with diagonal can be computed as provided by the following formula:

$$K = \frac{24EI_c}{h^3}\frac{(12\rho+1)}{(12\rho+4)} + \frac{w \times E_m \times t_{inf}}{r_{inf}} \times cos^2\theta$$

Where

$$\rho = (\frac{EI_b}{L}) \div (\frac{2EI_c}{h})$$

$w = \ width\ of\ equivalent\ strut$

$E_m = \ modulus\ of\ elasticity\ of\ the\ masonary\ wall$

$E_c = \ modulus\ of\ elasticity\ of\ the\ frame\ material$

$h = Height\ of\ column\ in\ the\ frame$

t_{inf}=*strut thickness*

$I_c = Moment\ of\ Intertia\ of\ the\ column$ *in the frame*

$I_b = Moment\ of\ Intertia\ of\ the\ beam$ *in the frame*

$r_{inf} = diagonal\ length\ of\ the\ infill\ panel$

Following are the detailed calculations of lateral stiffness:

$$\rho = \frac{h}{2L} = \frac{3.12}{12} = 0.26$$

$$K = \frac{24 \times 23025000 \times 0.00213}{3.12^3 \times cos^2 27} \frac{(12 \times 0.26 + 1)}{(12 \times 0.26 + 4)} + \frac{0.6 \times 23025000 \ \times 0.12}{6.76}$$

$$\boxed{K \ = 22425.59 + 193038.9 = 215464.49 \, kN/m}$$

ETABS model with single diagonal lateral stiffness is provided in figure A-37.

	Story	Stiffness Y kN/m
▸	Story1	195589.883

Figure A-37: Lateral stiffness of the frame with diagonal strut

Table A-43 shows comparison between result of manual calculations and ETABS software.

Table A-43: Comparison between Manual and ETABS lateral stiffness-Frame with diagonal

Comparison between Manual and ETABS lateral stiffness-Frame with diagonal		
Lateral stiffness (kN/m) – Manual	**Lateral stiffness (kN/m) – ETABS**	**Difference**
2.15×10^5	1.95×510^5	9.3%

A difference of almost 9.3% between manual and software results may be enhanced by controlling some assumptions in the software. A first check will be performed by comparing the frame stiffness excluding the effect of diagonal strut.

Figure A-38 shows ETABS model of the frame without the strut and its lateral stiffness value.

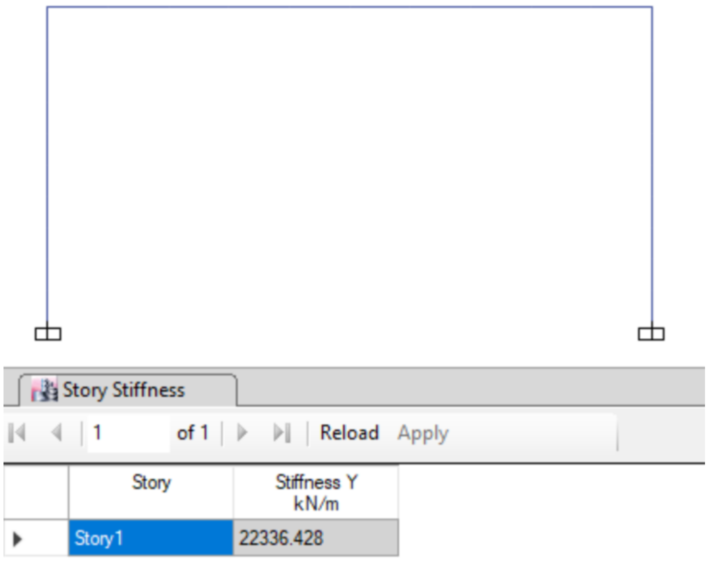

Figure A-38: ETABS model of frame with no strut and the lateral stiffness value as computed by the software

Table A-44 shows comparison between manual results and ETABS regarding the frame stiffness excluding the diagonal strut.

Table A-44: Comparison between Manual and ETABS lateral stiffness-Frame with diagonal

Comparison between Manual and ETABS lateral stiffness-Frame without diagonal		
Lateral stiffness (kN/m) – Manual	**Lateral stiffness (kN/m) – ETABS**	**Difference**
2.24×10^4	2.23×10^4	0.4%

Total lateral stiffness of frame with diagonal strut is a combination of both lateral stiffness of the frame and the diagonal strut. Therefore, the contribution of strut as suggested by ETABS can be computed as following.

$$Total\ Stiffness\ (ETABS) = Frame\ Stiffness + Strut\ Stiffness$$

$$1.95 \times 10^5 = 0.223 \times 10^5 + Strut\ Stiffess \rightarrow Strut\ stiffness = 1.73 \times 10^5$$

Table A-45 shows comparison between manual computation of strut contribution in the total stiffness of the system and strut contribution as suggested by ETABS model.

Table A-45: Comparison of diagonal contribution in the system stiffness (Manual Vs. ETABS)

Comparison of diagonal contribution in the system stiffness (Manual Vs. ETABS)		
Stiffness (kN/m) – Manual	**Stiffness (kN/m) – ETABS**	**Difference**
1.93×10^5	1.73×10^5	10.3%

As shown in table 5-96 the contribution of strut stiffness in ETABS does not comply with manual results. First step to justify this difference is to calculate the axial stiffness of the diagonal strut, this can be done using ETABS through the following formula:

$$Axial\ Stiffness = \frac{Axial\ Force\ in\ the\ diagonal\ strut}{\Delta_{axial}}$$

Figure A-39 shows the axial force in kN, and the joint displacements.

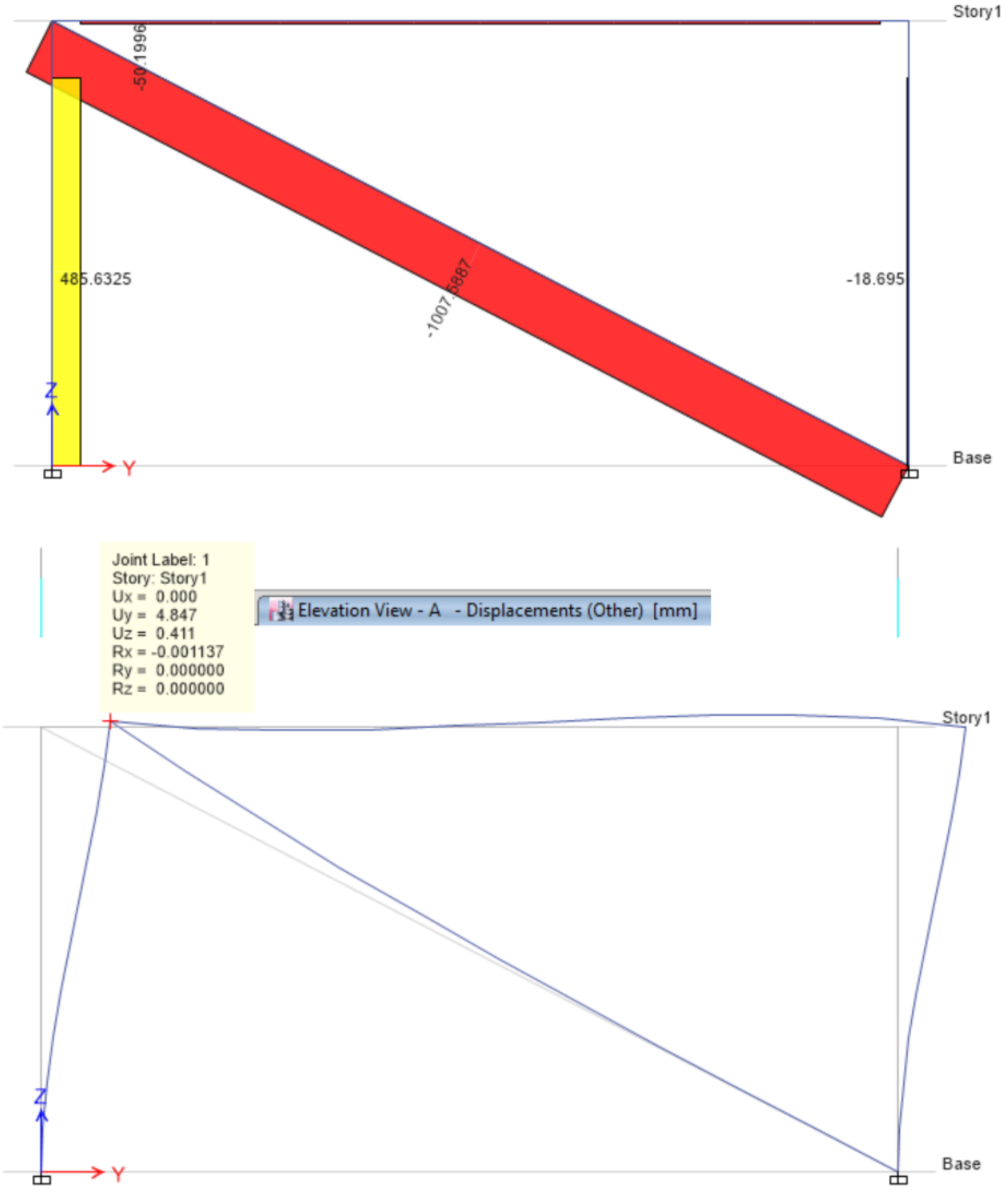

Figure A-39: Axial Force in kN, and joint displacements (ETABS)

Displacements shown in figure A-39 can be used in determining the axial deformation of the diagonal strut by drawing both the deformed and the nondeformed frame in 1:1 scale using AutoCAD. Figure A-40 shows a zoomed view for both deformed and nondeformed joint with a compression axial deformation of 0.0041 m.

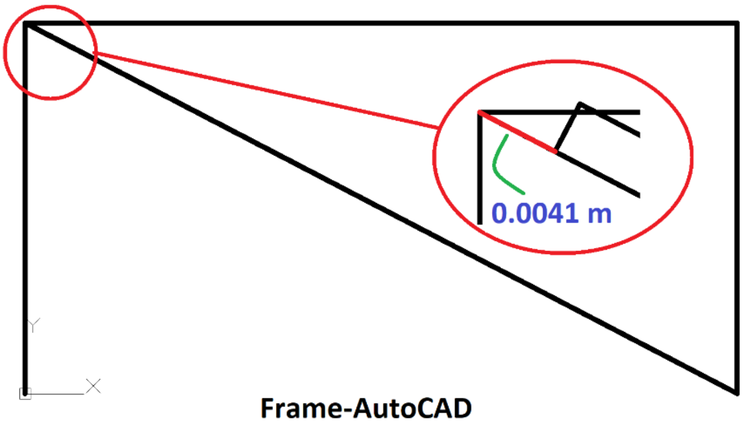

Figure A-40: Deformed and non-deformed frame (application of 1000 kN in x direction)

$$Axial\ Stiffness = \frac{1007}{0.0041} = 245609.75\frac{kN}{m}$$

Table A-46 shows comparison between manual computation and ETABS regarding the axial stiffness of the strut.

Table A-46: Comparison of diagonal contribution in the system stiffness (Manual Vs. ETABS)

Axial Stiffness of the Strut (ETABS VS. Manual)		
Stiffness (kN/m) – Manual	**Stiffness (kN/m) – ETABS**	**Difference**
2.452×10^5	2.456×10^5	0.16%

It is clear now that model with no strut has almost the same manual computed lateral stiffness, and it is also clear that the axial stiffness of the strut is almost same to manual results. Displacements as shown in figure A-41 are in two directions of both y and z. Axial stiffness of both column and beam is magnified by increasing the axial modifier to be 1000 instead of 1 as shown in figure A-41. These modifications are supposed to make model results closer to manual calculations.

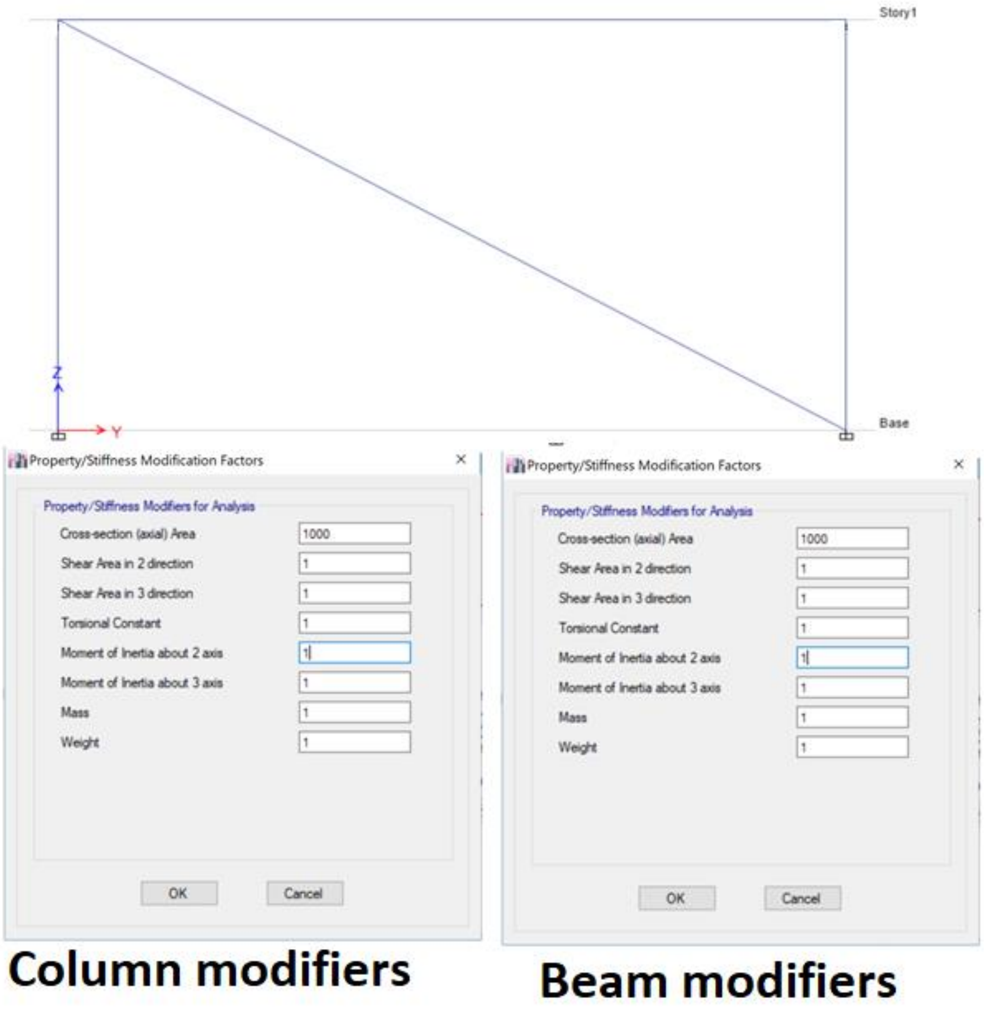

Figure A-41: Applied modifications on the 2D model

Figure A-42 shows the lateral stiffness of the structural system after the application of modifications.

	Story	Stiffness Y kN/m
▶	Story1	215405.928

Figure A-42: Lateral stiffness of the structural system after application of new assumptions on the ETABS model

Table A-47 compares modified ETABS model with manual calculations.

Table A-47: Comparison between manual value of lateral stiffness and ETABS value after applying assumptions on the model

Lateral Stiffness (kN/m) (Manual Vs. Modified model)		
Stiffness (kN/m) – Manual	**Stiffness (kN/m) – ETABS**	**Difference**
2.155×10^{5}	2.154×10^{5}	Almost zero

Based on this verification results of ETABS will be adopted for strut analysis.

جامعة النجاح الوطنية

كلية الدراسات العليا

أثر الجدران الخارجية الحاملة غير المسلحة المكونة من الخرسانة وحجر البناء على احتساب قيمة زمن التردد الأساسي

اعداد

محمد عمر محمود حلاحلة

اشراف

د. عبد الرزاق طوقان

د. منذر إبراهيم

قدمت هذه الأطروحة استكمالا لمتطلبات الحصول على درجة الماجستير في هندسة الإنشاءات بكلية الدراسات العليا في جامعة النجاح الوطنية، نابلس – فلسطين.

2019

أثر الجدران الخارجية الحاملة غير المسلحة المكونة من الخرسانة وحجر البناء على احتساب قيمة زمن التردد الأساسي

اعداد

محمد عمر حلاحلة

اشراف

د. عبد الرزاق طوقان

د. منذر ذياب إبراهيم

الملخص

ينتشر في فلسطين نمط البناء باستخدام التكسية الحجرية الطبيعية وعادةً ما تُنشأ هذه الجدران باستخدام طبقة من الخرسانة غير المسلحة، أو من الطوب المفرغ .

جرت العادة أن يتم إهمال هذه الجدران من التحليل الإنشائي، حيث تعتبر هذه الجدران جدراناً غير حاملةً، حيث تكون الفرضية المستخدمة في النمذجة اعتبار الإطارات والجدران المسلحة كعناصر إنشائية، ويتقصر تمثيل الجدران غير المسلحة على إضافة وزنها للنموذج الرياضي، دون إبداء أي مساهمة في مقاومة القوى الأفقية أو العمودية.

إن تجاهل تضمين هذه الجدران في عملية التحليل والتصميم يجعل التنبؤ بسلوك المنشآت محل شك، كما ويُنذر بخطورة تصرف المنشآت حين تعرضها لقوى الزلازل.

إن فهم سلوك المنشآت في الزلازل يعتمد بشكل رئيس على قيمة زمن التردد الأساسي. إن تطوير طرق نمذجة تعمل على رفع دقة التنبؤ بزمن التردد الأساسي خطوة أساسية ومهمة في الخطوات السليمة لتحليل وتصميم أي منشأ.

تهدف هذه الدراسة إلى اقتراح نموذج رياضي يمكن الوثوق به لتحسين دقة قيمة زمن التردد الأساسي التي يتم احتسابها، حيث إن المتعارف عليه في التحليل الإنشائي المستخدم في فلسطين هو إهمال هذه الجدران إنشائياً والتعامل معها بصفتها تساهم في الوزن فقط.

تهدف هذه الدراسة إلى تسليط الضوء على خطورة إهمال هذه الجدران في التحليل الإنشائي، وإعطاء توصية بضرورة نمذجتها باستخدام إحدى المعادلات المتاحة التي تستبدل الجدران بعنصر مكافئ، الأمر الذي من شأنه أن يرفع دقة التحليل الإنشائي وعليه يُقلل المخاطر المتوقعة عند حدوث الزلازل.